Preparation of Liposomes and Encapsulation of Bioactives Using Supercritical Carbon Dioxide

by

Lisha Zhao

A thesis submitted in partial fulfillment of the requirements for the degree of

Doctor of Philosophy

in

Food Science and Technology

Department of Agricultural, Food and Nutritional Science
University of Alberta

ABSTRACT

Liposomes are versatile vesicles of a phospholipid bilayer, which offer great protection for active compounds. Encapsulated compounds can be protected from unfavorable external conditions so that their chemical stability and bioavailability can be greatly enhanced. The supercritical carbon dioxide (SC-CO_2) technique has drawn great attention because of its unique advantages over the traditional preparation methods. To yield liposomes with improved characteristics, an improved SC-CO_2 method, which combined the processing advantages of two previously reported methods was developed for liposome preparation, which were then loaded with bioactives.

First, the effectiveness and fundamentals of a previously reported SC-CO_2 method was studied by equilibrating a soy lecithin aqueous suspension with high pressure CO_2. Unloaded liposomes were then formed via depressurization from the supercritical phase. The relative volumetric expansion of water upon equilibrium with CO_2 was 14.36%, 12.28% and 10.24% at 40°C, 50°C and 60°C, respectively. Liposomes had a particle size of 523±2 nm and a polydispersity index (PdI) of 0.226±0.01. Increased depressurization rate led to an improved homogeneity of vesicles, and liposomes could be stored for up to 4 weeks with limited size change (below 5%). The SC-CO_2 method displayed advantages of high stability and homogeneity for liposome preparation over the conventional thin film hydration (TFH) method.

Second, animproved SC-CO_2 method was developed, where unloaded liposomes were formed via depressurization from the liquid phase following two depressurization protocols: (I) depressurization at a constant rate, and (II) depressurization at a constant rate and pressure. The effects of processing and compositional parameters on the characteristics of liposomes were studied. Liposomes prepared by the improved SC-CO_2 method had a particle size of 265±4 nm

and 214±3 nm and PdI of 0.520±0.02 and 0.417±0.001 for protocols (I) and (II), respectively. Protocol (II) yielded smaller and more uniform particles. Liposomes were stable for up to 8 and 6 weeks for protocols (I) and (II), respectively. Elevated phospholipid levels resulted in smaller particle size with enhanced uniformity. Fatty acids with longer chain length in pure phospholipids resulted in a larger particle size while increased degree of unsaturation in the fatty acyl chains increased the asymmetry of vesicles. The improved supercritical method was more effective in liposome preparation than the TFH method for a reduced size and enhanced stability.

Next, lutein (hydrophobic) was encapsulated into liposomes by the improved SC-CO_2 method via the depressurization protocol (II). The effects of processing parameters and compositional parameters on the characteristics of liposomes were studied. Liposomes had a particle size of 155±1 nm, an encapsulation efficiency (EE) of 97.0±0.8% and a zeta potential of -61.7±0.6 mV. The higher pressure and depressurization rate promoted enhanced lutein encapsulation efficiency. The lutein concentration could significantly influence the morphology of vesicles along with size distribution and EE.

Finally, anthocyanin (hydrophilic) was encapsulated into liposomes by the improved SC-CO_2 method via the depressurization protocol (II). The effects of processing parameters and compositional parameters on the characteristics of liposomes were studied. The *in vitro* release of bioactives from liposomes was also investigated. Liposomes obtained had a particle size of 160±2 nm, EE of 52.2±2.1% and zeta potential of -41.3±1.2 mV. Increased pressure and depressurization rate resulted in reduced particle size and enhanced uniformity while high temperature increased the fluidity of the bilayer membrane. Elevated anthocyanin level increased the particle size with reduced uniformity while the elevated cholesterol concentration reduced the zeta potential of liposomes. Liposomes were stable for up to 3 weeks with a unimodal narrow

size distribution. The release of anthocyanin from the liposomes was slow with up to 35.9% in simulated gastric fluid while it was rapid in the simulated intestinal fluid due to liposome degradation by pancreatin.

In summary, the improved SC-CO_2 process was effective infinely dispersing the amphiphiles mixed with hydrophobic or hydrophilic bioactives suspended in an aqueous system into uniform nano/micro particles. The processing and compositional factors can be fine tuned to modulate the physicochemical properties of the liposomes obtained, depending on the targeted applications. This novel process is advantageous for potential scale-up of the production of micro/nano particles with desirable characteristics and shows great promise to encapsulate a variety of valuable bioactives for food, nutraceutical and medical applications.

PREFACE

This thesis contains original work done by Lisha Zhao and has been written according to the guidelines for a paper format thesis of the Faculty of Graduate Studies and Research at the University of Alberta. The concept and idea of this work originated from Lisha Zhao and her supervisor, Dr. Feral Temelli. The research was funded by a grant from the Natural Sciences and Engineering Research Council (NSERC) of Canada to Dr. Feral Temelli and scholarship support from Alberta Innovates Technology Futures and Ivy A. Thomson and William A. Thomson Graduate Scholarship to Lisha Zhao. The whole thesis is composed of seven chapters: Chapter 1 presents an introduction to this project and the objectives of the thesis. Chapter 2 is a literature review regarding the liposomes, their preparation, characterization and applications as a delivery system for lutein and anthocyanin.

Chapter 3 has been published as Lisha Zhao and Feral Temelli, "Preparation of liposomes using supercritical carbon dioxide via depressurization of the supercritical phase" in the *Journal of Food Engineering* 158 (2015) 104-112. In this chapter, Lisha Zhao was responsible for the experimental design and conducting the experiments, data analysis and writing the first draft of the manuscript. Dr. Temelli is the corresponding author and was responsible for the experimental design, data interpretation, correction and submission of the manuscript.

Chapter 4 has been published as Lisha Zhao and Feral Temelli, "Preparation of liposomes using a modified supercritical process via depressurization of liquid phase" in *The Journal of Supercritical Fluids* 100 (2015) 110-120. In this chapter, Lisha Zhao was responsible for designing and conducting the experiments, data analysis and writing the first draft of the manuscript. Dr. Temelli is the corresponding author and was responsible for theexperimental design, data interpretation, correction and submission of the manuscript.

Chapter 5 has been published as Lisha Zhao, Feral Temelli, Jonathan M. Curtis and Lingyun Chen. "Preparation of liposomes using supercritical carbon dioxide technology: Effects of phospholipids and sterols" in *Food Research International* 77 (2015) 63-72. In this chapter, Lisha Zhao was responsible for designing and conducting experiments, data analysis and writing the first draft of the manuscript. Dr. Temelli is the corresponding author and was responsible for advising experimental design, data interpretation, correction and submission of the manuscript. Dr. Jonathan M. Curtis was responsible for the determination of lecithin composition using hydrophilic interaction liquid chromatography liquid chromatography-tandem mass spectrometry (HILIC LC-MS/MS) and manuscript corrections. Dr. Lingyun Chen provided assistance with particle size determination using a Zetasizer Nano ZS instrument and manuscript corrections.

Chapter 6 is to be submitted for consideration for publication as Lisha Zhao, Feral Temelli, Jonathan M. Curtis and Lingyun Chen, "Characterization of lutein-loaded liposomes prepared via supercritical carbon dioxide". In this chapter, Lisha Zhao was responsible for designing and conducting experiments, data analysis and writing the first draft of the manuscript. Dr. Temelli is the corresponding author and was responsible for the experimental design, data interpretation, correction and submission of the manuscript. Dr. Jonathan M. Curtis provided assistance with the measurement of the phase transition behavior of all the phospholipid-based materials using differential scanning calorimetry (DSC) and manuscript corrections. Dr. Lingyun Chen provided assistance with particle size determination and manuscript corrections.

Chapter 7 has been accepted for publication as Lisha Zhao and Feral Temelli, "Preparation of anthocyanin-loaded liposomes using supercritical carbon dioxide" in *Innovative Food Science and Emerging Technologies* 39 (2017) 119-128. In this chapter, Lisha Zhao was responsible for designing and conducting experiments, data analysis and writing the first draft of the manuscript.

Dr. Temelli is the corresponding author and was responsible for advising experimental design, data interpretation, correction and submission of the manuscript.

Chapter 8 has been submitted for consideration for publication as Lisha Zhao, Feral Temelli and Lingyun Chen, "Encapsulation of anthocyanin in liposomes using supercritical carbon dioxide: Effects of anthocyanin and cholesterol concentrations" in the *Journal of Functional Foods*. In this chapter, Lisha Zhao was responsible for designing and conducting experiments, data analysis and writing the first draft of the manuscript. Dr. Temelli is the corresponding author and was responsible for theexperimental design, data interpretation, correction and submission of the manuscript. Dr. Lingyun Chen provided assistance with particle size determination, phospholipid-anthocyanin interaction measurement based on Fourier transform infrared spectroscopy (FTIR) and manuscript corrections.

This dissertation is dedicated to my beloved parents,
Nana Qi and Jichao Zhao

ACKNOWLEDGEMENTS

There are many people who have helped and supported me throughout my PhD study and who I am greatly grateful to. First and foremost, I would like to express my sincere gratitude to my supervisor Dr. Feral Temelli, who provided me with enormous support, encouragement and guidance during my whole PhD study. Her excellent supervision and patience enabled me to acquire considerable valuable experience and develop my abilities as an independent researcher with critical thinking, academic writing and presentation skills during my PhD study.

I would like to thank Dr. Jonathan Curtis and Dr. Lingyun Chen for being in my supervisory committee and all of their valuable feedback during my PhD program. Many thanks to Dr. Jonathan Curtis and Dr. Lingyun Chen for offering their versatile experimental apparatus, training and advice in my PhD program. Special thanks to Dr. Larry Unsworth from the Department of Chemical and Materials Engineering to be in my examining committee and Dr. Allan Paulson from the Department of Process Engineering and Applied Science of Dalhousie University as my external examiner, and all of their feedback for my PhD defense.

I would also like to express my sincere gratitude to my excellent colleagues and friends, Ehsan Jenab, Alex (Yixiang) Wang, Sarah (Jingqi) Yang, Yussef Esparza, Víctor Alvarez, Ricardo Tomas Do Couto, Cherry (Chen) Yang and Weijuan Huang for their help and suggestions in my experimental work. Special thanks to Dr. Yuanyuan Zhao for assisting with HILIC LC-MS/MS analysis and Ereddad Kharraz for assisting with DSC measurements. I am greatly grateful to Arlene Oatway in the Department of Biological Science who provided critical assistance with transmission electron microscopy (TEM) measurements. Special thanks to Nancy Zhang in NanoFAB, Wayne Moffat in the Department of Chemistry, Dr. Carlo Montemagno and Julie Qian in the National Institute for Nanotechnology, Woo Jung Cho in the

Department of Medical, Microbiology and Immunology and Xunjun Sun in the Department of Oncology for their kind assistance in the characterization of liposomes.

I am also grateful to the Natural Sciences and Engineering Research Council of Canada (NSERC) for financial support of my project and Alberta Innovates Technology Futures (AITF) and Ivy A. Thomson and William A. Thomson Graduate Scholarships to fund my PhD study. Special thanks to Jody Forslund for providing valuable information and advice for my scholarship applications.

Ultimately, I would like to thank my parents, Nana Qi and Jichao Zhao, for their unconditional love, support and encouragement throughout my PhD program, which give me continuous motivation, energy and courage to overcome any challenge in the pursuit of my career goal. Thanks to all of my friends located around the world for their encouragement, help and support, which are cherished by me as memories of good times we shared together.

TABLE OF CONTENTS

LIST OF TABLES

LIST OF FIGURES

LIST OF ABBREVIATIONS

AFM	Atomic force microscopy
ANOVA	Analysis of variance
BL	Bioactive loading
Cyro-TEM	Cryogenic transmission electron microscopy
DELOS	Depressurization of expanded liquid organic solution
DHA	Docosahexaenoic acid
DLS	Dynamic light scattering
DMPC	1,2-Dimyristoyl-sn-glycero-3-phosphatidylcholine
DOPC	1,2-Dioleoyl-sn-glycero-3-phosphatidylcholine
DPPC	1,2-Dipalmitoyl-3-phosphatidylcholine
DSC	Differential scanning calorimetry
DSPC	1,2-Distearoyl-sn-glycero-3-phosphatidylcholine
EE	Encapsulation efficency
ELS	Electrophoretic light scattering
ESG	Esterified steryl glucosides
FTIR	Fourier transform infrared spectroscopy
GUV	Giant unilamellar vesicle
HILIC	Hydrophilic interaction chromatography
HPLC	High performance liquid chromatography
ISCRPE	Improved supercritical reverse phase evaporation
LC-MS/MS	Liquid chromatography-tandem mass spectrometry
LDL	Low density lipoprotein
LUV	Large unilamellar vesicle
MLV	Multilamellar vesicle
MVV	Multivesicular vesicle
P	Critical packing parameter
PA	Phosphatidic acid
PC	Phosphatidylcholine
PdI	Polydispersity index
PE	Phosphatidylethanolamine
PI	Phosphatidylinositol
PS	Phosphatidylserine
PTA	Phosphotungstic acid
RESOLV	Rapid expansion of supercritical solution into a liquid solvent

SAS	Supercritical antisolvent
SC-CO_2	Supercritical carbon dioxide
SCRPE	Supercritical reverse phase evaporation
SD	Standard deviation
SG	Steryl glucosides
SGF	Simulated gastric fluid
SIF	Simulated intestinal fluid
SPE	Solid phase extraction
STEM	Scanning transmission electron microscopy
SuperLip	Supercritical assisted liposome formation
SUV	Small unilamellar vesicle
TEM	Transmission electron microscopy
TFH	Thin film hydration
T_m	Phase transition temperature
V_0	Phase volume prior to CO_2 pressurization
V_P	Phase volume after CO_2 pressurization
XRD	X-ray diffraction
ΔH	Transition enthalpy
$\Delta V\%$	Relative volumetric expansion

CHAPTER 1 - INTRODUCTION AND THESIS OBJECTIVES

Liposomes are artifical colloidal vesicles composed of one or more phospholipid bilayers with important applications for pharmaceuticals and nutraceuticals. Liposomes can be used to encapsulate valuable hydrophilic and hydrophobic components for a number of benefits. Liposomes can form a barrier around their encapsulated components which is resistant to adverse interactions with some gastric enzymes, pH, chemical interactions as well as free radicals. By encapsulation, high-value ingredients can be protected from external conditions so that their stability, absorption and performance can be greatly enhanced (Laridi et al., 2003). Liposomes are widely employed in the pharmaceutical industry, and they have drawn increasing attention in food, nutraceutical and nutritional applications for their unique features. Recently, liposomes have been studied for the delivery of flavors, colors, nutrients and antimicrobials for food applications (Mozafari, Johnson, Hatziantoniou, & Demetzos, 2008).

Traditional preparation methods to yield liposomes include thin film hydration (TFH), ethanol injection, reverse phase evaporation and detergent depletion methods (Meure, Foster, & Dehghani, 2008). However, they usually result in undesirable characteristics such as organic solvent residues, difficulty with scale-up, heterogeneous size distribution as well as low stability and reproducibility. To overcome these drawbacks, supercritical carbon dioxide (SC-CO_2) technology has been used in liposome preparation as an innovative alternative. The SC-CO_2 technology uses CO_2 under temperature and pressure conditions above its critical point (31°C, 74 bar) to replace traditional organic solvents for liposome preparation and has recently drawn increasing interest over traditional processing techniques based on its novel processing features, improved homogenization quality, enhanced product safety and promise for industrial applications.

Although different approaches have been used to produce liposomes using SC-CO_2, several disadvantages, such as the use of organic solvents, large particle size and heterogeneous size distribution, still remain to be resolved. For liposomes used in the medical and nutraceutical applications, desirable characteristics include controllable size down to the nanometer range, narrow size distribution, high encapsulation efficiency, consistent shape and lamellarity as well as long term stability. Therefore, there is a need to improve liposomal preparation using SC-CO_2 in an effort to yield liposomes with excellent characteristics, which forms the basis for thisresearch. Despite their shortcomings, two previously reported supercritical methods (Cano-Sarabia et al., 2008; Otake et al., 2006) have merits. Cano-Sarabia et al. (2008) designed a depressurization of expanded liquid organic solution (DELOS) process and achieved liposomes with small particle size (167 nm) and high uniformity. Otake et al. (2006) used an improved supercritical reverse phase evaporation (ISCRPE) method and obtained liposomes completely free of organic solvents. Thus, the possibility of combining these merits into one process, which may yield high quality liposomes with enhanced desirable characteristics, is of great interest. The improved SC-CO_2 method developed in this research, was based on a modification of these two methods, combining the advantages of both techniques, for improved liposome preparation. In an effort to optimize this improved SC-CO_2 method, three different depressurization protocols were tested, including depressurization from (I) the supercritical phase at a constant depressurization rate, (II) the liquid phase at a constant depressurization rate, and (III) the liquid phase at constant pressure and depressurization rate. Next, the unloaded liposomes were fabricated and characterized, followed by the preparation of liposomes loaded with bioactives. To test the liposomal encapsulation, a hydrophobic bioactive compound (lutein) and a hydrophilic one (anthocyanin) were selected as model compounds. Lutein is a powerful antioxidant, lowering the

risks of heart disease and cancer with poor aqueous solubility and stability (Zhao, Cheng, Jiang, Yao, & Han, 2014). Anthocyanin is a valuable flavonoid with health benefits but sensitive to the neutral pH in the intestinal tract (Keppler & Humpf, 2005). Thus, the encapsulation of these biaoctives with liposomes aims to achieve enhanced stability under the gastrointestinal conditions and efficacy and health benefits through food; however, there is a lack of information in the literature in this regard. Better understanding of the fundamentals and liposomal behavior achieved by this innovative technique will contribute to the development of novel bioactive encapsulation systems for enhanced protection and functionality with potential applications in a variety of food and other products. Cholesterol is used in traditional liposome formulations to minimize the leakage of an encapsulated bioactive through the phospholipid bilayer. Although the amount of cholesterol added is relatively small, phytosterols were used as a replacement to minimize the adverse effects associated with cholesterol intake, with the expectation that phytosterol may have similar functions to cholesterol, such as reducing the bilayer permeability and lowering the bioactive leakage.

It was hypothesized that high quality liposomes can be produced using the improved SC-CO_2 method to encapsulate hydrophobic and hydrophilic bioactives. The specific hypotheses were: (a) physicochemical properties of unloaded liposomes can be manipulated by controlling the processing and compositional parameters employed using the improved SC-CO_2 method, and (b) lutein and anthocyanin can be loaded into liposomes via this method, resulting in liposomes with desirable characteristics.

The overall objectives of this research were: (a) to develop an improved SC-CO_2 process for liposome preparation and to study the fundamentals associated with it, and (b) to investigate the

encapsulation of a hydrophobic and a hydrophilic bioactive compound into liposomes and characterize them. The specific objectives were:

(1) To investigate the preparation of unloaded liposomes using a SC-CO_2 method with depressurization protocol I and to evaluate the effects of processing parameters (pressure, depressurization rate and temperature) on the characteristics of liposomes (Chapter 3),

(2) To investigate the preparation of unloaded liposomes using a SC-CO_2 method with depressurization protocols II and III and to evaluate the effects of processing parameters (pressure, depressurization rate and temperature) on the characteristics of liposomes (Chapter 4),

(3) To investigate the preparation of unloaded liposomes using a SC-CO_2 method with the optimized depressurization protocol and to evaluate the effects of phospholipid type and concentration and sterol type and concentration on the characteristics of liposomes (Chapter 5),

(4) To investigate the preparation of lutein-loaded liposomes using the improved SC-CO_2 method and to evaluate the effects of pressure, depressurization rate, temperature and lutein-to-lipid ratio on the characteristics of liposomes (Chapter 6), and

(5) To investigate the preparation of anthocyanin-loaded liposomes using the improved SC-CO_2 method and to evaluate the effects of pressure, depressurization rate, temperature, cholesterol concentration and anthocyanin concentration on the characteristics of liposomes (Chapters 7 and 8).

CHAPTER 2 – LITERATURE REVIEW

2.1. Introduction

Many medical and bioactive agents suffer from a few disadvantages, including low bioavailability, fast clearance and high toxicity. In order to overcome these drawbacks, there is an increasing demand to develop more effective drug and bioactive delivery systems, which offers enhancement of stability and bioavailability while minimizing their side effects and toxicity. Liposomes have shown great potential as versatile delivery vehicles to protect sensitive components. Since their discovery by Bangham in the 1960s (Bangham, Standish, & Watkins, 1965), liposomes have been studied in depth, and they continue to constitute a field of intense research. Liposomes are valued for their biological and technological advantages, and are considered to be the most successful drug and bioactive delivery system known to date (Bozzuto & Molinari, 2015). In addition to their diverse medical applications, liposomes have also drawn significant interest in the agricultural, food, nutrition and cosmetic fields.

2.1.1. Structure of liposomes

Liposomes are colloidal spherical phospholipid vesicles used to deliver drug, nutraceutical and bioactive ingredients, with the particle size ranging from 20 nm to several micrometers (Marrink & Mark, 2003). In the presence of water, phospholipids can organize themselves into a spherical capsule to minimize unfavorable interactions between their hydrophobic tails and the aqueous phase, with their polar head groups oriented outward and exposed to the aqueous phase while the non-polar tails are inward, interacting with one another (van Meer, Voelker, & Feigenson, 2008). This orientation clearly separates the liposome into a phospholipid bilayer enclosing an aqueous core (Fig. 2.1), which can be used for the encapsulation of different components. Hydrophobic interactions are behind the formation of these lipid bilayers, and van

der Waals forces keep the long hydrocarbon tails together, thus strengthening this architecture (Bozzuto & Molinari, 2015). Due to its amphiphilicity, hydrophobic components are able to be incorporated into the phospholipid bilayer membrane while hydrophilic components are entrapped within its aqueous core.

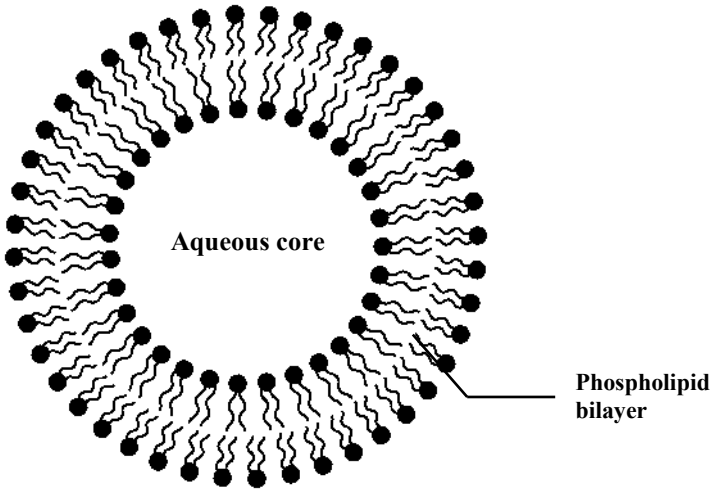

Figure 2.1: A schematic representation of a unilamellar liposome.

Liposomes can be divided into several categories (Fig. 2.2) including (a) small unilamellar vesicles (SUV) (20-100 nm), (b) large unilamellar vesicles (LUV) (100-1000 nm), (c) giant unilamellar vesicles (GUV) (>1000 nm), (d) multilamellar vesicles (MLV) (>500 nm), and (e) multivesicular vesicles (MVV) (>1000 nm) based on their size and lamellarity (Laouini et al., 2012). They can also be classified in terms of their composition and function: (a) conventional liposomes, (b) pH-sensitive liposomes, (c) cationic liposomes, (d) immunoliposomes and (e) long-circulating liposomes. Among these vesicles, unilamellar vesicles are mostly utilized in research due to their well characterized membrane and readily regulated properties. Although unilamellar liposomes are most commonly used for the encapsulation of bioactives,

multilamellar and multivesicular vesicles are also prepared to achieve higher payload and controlled release of encapsulated agents.

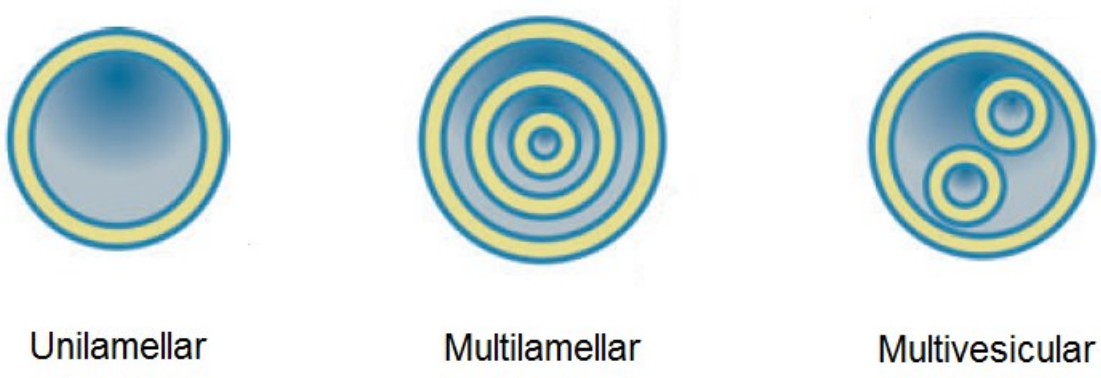

Figure 2.2: Schematic representation of different types of liposome vesicles.

2.1.2. Composition of liposomes

The components to form liposomes are phospholipids, which can be primarily derived from egg yolk and soybeans (Burling & Graverholt, 2008). Phospholipids are amphiphilic surfactants, with hydrophilic phosphate head and hydrophobic fatty acyl tails attached to the glycerol backbone. The schematic structure of several common phospholipid classes yielding liposomes are shown in Fig. 2.3, which include phosphatidylcholine (PC), phosphatidylethanolamine (PE), phosphatidylserine (PS), phosphatidic acid (PA) and phosphatidylinositol (PI), depending on the variation in the head group. Phospholipids can also vary in the chain length and degree of saturation of fatty acyl chains, which closely influence bilayer packing, membrane fluidity and phase transition behaviors. Liposomal vesicles can be formed by pure or mixed lipid systems. Although pure lipid classes are generally preferred for a desirable preparation, mixed lipid systems are of great interest for regulation of interfacial properties and bilayer interactions for improved functionality (Almgren, 2000; Khan & Marques, 1999). Studies on the use of mixed lipid compositions for liposome formulation are limited and need further investigation. Thus, soy

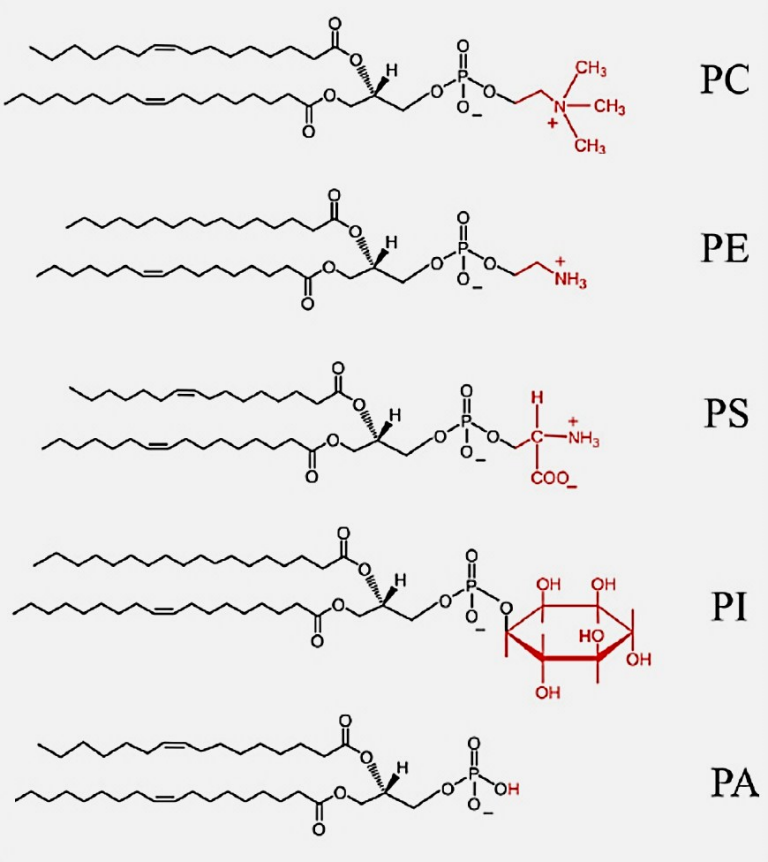

Figure 2.3: Schematic representation of chemical structures of phospholipids. PC: phosphatidylcholine, PE: phosphatidylethanolamine, PG: phosphatidylglycerol, PS: phosphatidylserine, PI: phosphatidylinositol, PA: phosphatidic acid.

lecithin (a mixture of PC, PE, PI and PA) was selected as the major material for liposome formation in this research. Each phospholipid type has an individual packing parameter (the geometry of amphiphiles), which can dictate the morphology and size of the resulting liposomes. The head group manipulates the surface charge of vesicles and influence the zeta potential and in turn the stability of liposomes (Seelig, MacDonald, & Scherer, 1987). Liposome physicochemical properties such as size, geometry and surface charge can also be modulated by the head group, temperature, degree of unsaturation of fatty acyls, pH, encapsulated agents and ionic strength (Li et al., 2015).

Besides phospholipids, cholesterol is usually added into liposome formulations (Fig. 2.4).

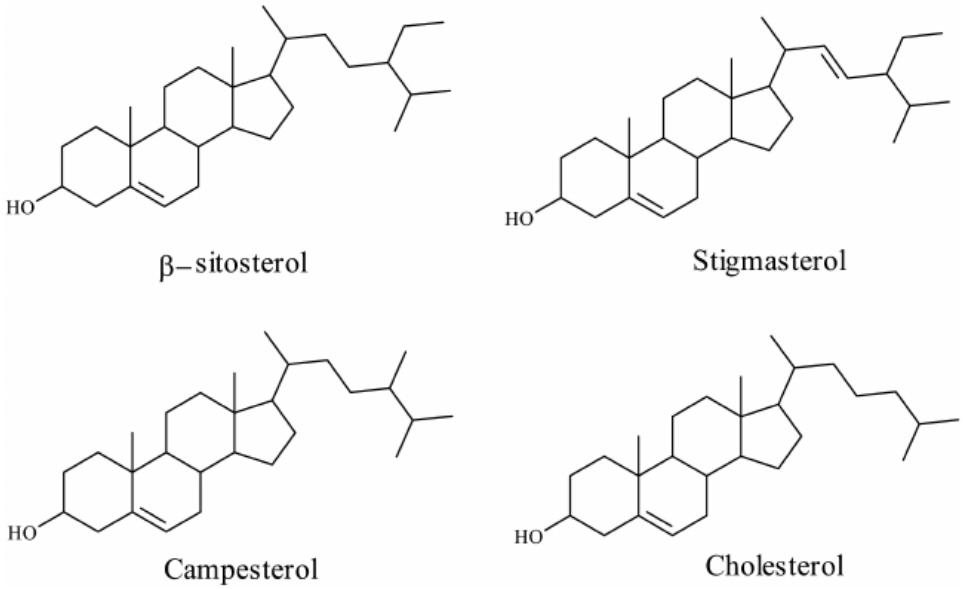

Figure 2.4: Schematic representation of chemical structures of cholesterol and common photosterols.

Cholesterol is an amphiphilic molecule primarily derived from animals. For its incorporation, cholesterol can be oriented with its sterol ring structure inserted into the hydrophobic region of the bilayer whereas the hydroxyl group would be interacting with the phosphate head via hydrogen bonding and facing toward the aqueous phase (Chan, Chen, Chiu, & Lu, 2004; Hąc-Wydro, Wydro, Dynarowicz-Łątka, & Paluch, 2009). The addition of cholesterol into liposomes can fill the gaps within lipid bilayers created by imperfect packing and thereby reduce leakage of encapsulated biaoctives. Also, it reduces the membrane permeability and increases their *in vivo* and *in vitro* stability, since the presence of cholesterol induces a dense packing of phospholipids and modulates membrane fluidity (Bozzuto & Molinari, 2015). Cholesterol incorporated into the bilayer also reduces the surface charge of liposomes as a neutral species and hinders the binding affinity among the cations in the buffer solution and the phospholipid head groups (Ding, Palaiokostas, Wang, & Orsi, 2015). Although cholesterol serves as an important component in the plasma lipoprotein and steroid hormones, the increased risk of atherogenesis and

cardiovascular diseases associated with hypercholesterolaemia has raised health concerns and led to recommendations to restrict cholesterol intake by health professionals.

In order to minimize the adverse effects associated with high cholesterol intake, phytosterols have received increasing attention for their health benefits (Fig. 2.4). Phytosterols are plant-derived compounds that are similar in structure but show the possibility of lowering or inhibiting the absorption of cholesterol (Chan et al., 2004). For instance, daily consumption of β-sitosterol can lower plasma levels of low-density lipoprotein (LDL) cholesterol and function as a hypocholesterolaemic agent (Zák, Zeman, Vítková, Hrabák, & Tvrzická, 1990). As well, US Food and Drug Administration and Health Canada have agreed that the intake of two servings of phytosterols or phytostanol with at least 0.8 g in a low fat diet is able to reduce the risk of coronary heart disease (Maki et al., 2012). Thus, the use of plant-derived sterol/stanol capsules offers a promising alternative for a LDL cholesterol lowering effect. Hwang, Tsai and Hsu (2010) used β-sitosterol and stigmasterol as a substitute for cholesterol in liposomes loaded with antihypertensive oligopeptides and obtained a similar EE for phytosterol-containing liposomes compared to cholesterol containing ones. Alexander, Lopez, Fang and Corredig (2012) used a mixture of β-sitosterol, stigmasterol, and campesterol to replace cholesterol in the preparation of liposome loaded with Vitamin C and found there was no significant difference in the encapsulation efficiency (EE) between the cholesterol- and the phytosterol-containing liposomes. Although reports on the use of phytosterols in liposomes are limited, phytosterols show great potential to replace cholesterol and perform similar functions in liposomes such as reducing drug leakage and improving the packing of bilayers.

2.1.3. Liposomal advantages and disadvantages

Liposomes have a number of advantages as successful encapsulation vehicles and bioactive carriers. They have good biocompatibility, biodegradability, low toxicity and non-immunogenicity. Liposomes can be utilized to encapsulate a variety of bioactives with the following merits: (a) improve the water dispersibility of hydrophobic components and enhance their bioavailability after oral administration; (b) protect encapsulated components from unfavorable conditions such as light, heat, pH, oxidation, hydrolysis or chemical reactions; (c) target the delivery of an encapsulated agent to a specific location and reduce its side effects and toxicity; and (d) control the circulation in the body via modulation of their particle size and release profiles by surface modifications. Liposomes are also widely used as biomembrane models to simulate cells and encapsulation carriers. On the other hand, liposomes also have several drawbacks in contrast to other nanocarrier candidates. First, liposomes formed by natural lecithin with unsaturated fatty acid chains can undergo oxidation and should be stored under nitrogen. Secondly, liposomes may be partially disintegrated in the intestinal tract by lipases, thus limiting prolonged payload activity and their oral administration applications (Li, Paulson, & Gill, 2015). The payload of water-soluble ingredients in liposomes is generally low (usually around 10-20%) and thereby results in bioactive loss compared to other types of nanoparticles. Compared to liposomes, other carriers like niosome, which have a longer hydrophilic portion in their amphiphile molecule can carry a higher payload (Pham, Jaafar-Maalej, Charcosset, & Fessi, 2012). In addition, liposomes are prone to aggregation and fusion to reorganize into larger vesicles, which may lead to the leakage of entrapped materials (Akbarzadeh et al., 2013). Since liposomes are usually prepared in a suspension form, the freezing and thawing as well as the dehydration and rehydration of liposomes can result in altered liposomal properties in terms of their

size and encapsulation efficiency due to the crystallization of ice and collapse of the aqueous core, and therefore leading to increased challenges for their storage stability.

2.2. Preparation of liposomes

2.2.1. Conventional preparation methods

Many different methods have been developed to manufacture liposomes. The physicochemical characteristics of liposomes like particle size, lamellarity as well as payload content can be adjusted relying on the amount of energy input and the processing techniques (Mozafari et al., 2008). Mechanical treatment such as agitation, homogenization, extrusion and sonication are usually employed during conventional preparation for targeted characteristics like particle size, lamellarity and homogeneity (Lasic, 1999). Conventional methods to prepare liposomes include thin film hydration (TFH), ethanol injection, reverse phase evaporation and detergent depletion methods.

2.2.1.1 Thin film hydration

Thin film hydration (TFH) is one of most widely used techniques, originally proposed by Bangham for liposome preparation (Bangham et al., 1965). It involves the dissolution of the phospholipids in an organic solvent (mostly chloroform), evaporation of the solvent to form a thin film layer, followed by the dispersion of the dry lipid film in an aqueous phase. The method yields MLVs with a broad size distribution and serves as the basis for the SUVs after sonication. The TFH method may be ideal for encapsulation of hydrophobic bioactives, however, its EE of hydrophilic bioactives is relatively low (around 10-20%). A relatively low volume of entrapped aqueous space is found per mole of lipid, thereby restricting the ability to encapsulate a high amount of bioactives. This is because in MLVs, most of the lipids are participating in forming the internal lamellae, and the close proximity of the adjacent bilayers restricts the internal water space finally achieved (Szoka and Papahadjopoulos, 1978). This highly reduced internal aqueous

volume within liposome vesicles of MLVs greatly decreases the EE of hydrophilic agents. It also requires additional processing steps such as sonication or extrusion to reduce the particle size and increase particle uniformity. A major drawback of the TFH method is the difficulty in scale up. TFH is a commonly used approach due to its simple and rapid nature at the laboratory scale for encapsulation and comparison purposes. Therefore, the TFH method is selected to compare with the improved SC-CO_2 method in this research.

2.2.1.2 Ethanol injection

The ethanol injection method was the first alternative method to TFH proposed by Batzri and Korn (1973). In this process, an ethanol/lipid solution is injected at a specific rate through a fine needle into an aqueous medium containing bioactives, followed by the solubilization of ethanol in the water and formation of liposomes due to the hydrophobic interaction between fatty acyl chains of lipids. The ethanol injection method can produce small liposomes with a narrow size distribution in a single step and modulate the particle size via the regulation of the ethanol injection rate and volume ratio of organic solvent to water, without further processing operations. However, the EE for the hydrophilic compound is low, liposomes with different lamellas may be generated and a post-processing step is needed to remove residual organic solvent. The lipid concentration in ethanol may be restricted by the lipid solubility. This method is not suitable for encapsulation of ethanol-sensitive components (Charcosset, Juban, Valour, Urbaniak, & Fessi, 2006). The ethanol injection method overcomes one drawback of the TFH method as it can be scaled up for industrial production of liposomes.

2.2.1.3 Reverse phase evaporation

Reverse phase evaporation was developed by Szoka and Papahadjopoulos (1978), which produces liposomes based on the “inverted micelles”. It involves the formation of a water-in-oil

emulsion by mixing a small amount of water into the lipid organic solution, slowly evaporating the organic solvent under reduced pressure to form a temporary water-in-lipid gel state, which then collapses to form liposomes. The reverse phase evaporation method can generate droplets stabilized by a phospholipid monolayer (inverted micelles) during the process and thus can form a large enclosed aqueous core surrounded by the bilayers of liposomes. Therefore, this method results in a high EE and can be used to replace TFH and ethanol injection methods for encapsulation of hydrophilic bioactives. However, it usually employs more than one type of organic solvent and readily results in residues of organic solvents during the rotary evaporation step. It can yield heterogeneous vesicles mixed with different lamellas and may not be suitable for the encapsulation of bioactives sensitive to organic solvents.

2.2.1.4 Detergent depletion

The detergent depletion method was developed by Milsmann, Schwendener and Weder (1978). It involves the formation of mixed micelles of phospholipid-detergent molecules in the aqueous medium and then removal of detergent by controlled dialysis to form liposomes. During the dialysis step, small surfactant molecules flow out of the dialysis membrane and phospholipids within micelles will approach one another to form bilayers of liposomes, avoiding the exposure to aqueous phase. The detergent depletion method can generate SUVs with high homogeneity and modulate the liposome size by adjusting the lipid:detergent ratio (Zumbuehl & Weder, 1981). However, this method is time consuming to form liposomes (> 20 h) compared to the other methods and the residues of surfactants may remain in the final product. The encapsulated agents can be exposed to the detergents so it may not be suitable for the encapsulation of detergent-sensitive components. In addition, the interactions between detergents and encapsulated agents must be carefully considered to prevent bioactive loss.

2.2.2. Recent developments in liposome preparation methods

Although traditional methods can be used for liposome preparation, they usually have a few drawbacks such as requiring post-processing operations, difficulty in scale-up and residues of organic solvents. To overcome these disadvantages and improve liposome preparation, some emerging techniques have been recently developed, which include dual asymmetric centrifugation (Hirsch, Ziroli, Helm, & Massing, 2009), membrane contactor technology (Pham et al., 2012), freeze drying double emulsion (Wang et al., 2006), cross-flow filtration technology (Peschka, Purmann, & Schubert, 1998) and microfluidic mixing methods (Yu, Lee, & Lee, 2009). Compared to the traditional methods, dramatic progress has been made in efficient mixing and reduction of particle size by these innovative methods and scale-up of production with relative ease. However, usage of organic solvents and surfactants has not been completely avoided. In this regard, supercritical carbon dioxide techniques have shown merits, which are described further below.

2.2.3. Supercritical carbon dioxide-based liposome preparation methods

2.2.3.1. Introduction to supercritical carbon dioxide

The supercritical carbon dioxide (SC-CO_2) technology employs CO_2 as a processing medium at the temperature and pressure conditions above its critical point (31.1°C; 74 bar), especially for processing of high-value products. Following high pressure processing, CO_2 is released upon depressurization and high quality products can be readily achieved free of organic solvents. SC-CO_2 has a relatively low critical temperature, which facilitates the processing of thermally labile bioactives and prevents heat-related damage. SC-CO_2 offers an anaerobic atmosphere and prevents the oxidative damage of active biomolecules (Lee, Lee, Choi, & Hur, 2015). Its tunability of physiochemical properties, high diffusivity, low interfacial tension and

viscosity compared to those of traditional solvents also facilitates efficient processing of naturally derived materials (Johnston & Shah, 2004).

For liposome production, several supercritical methods (Beh, Mammucari, & Foster, 2012), such as the rapid expansion of supercritical solution into a liquid solvent (RESOLV) (Wen et al., 2011), supercritical anti-solvent (SAS) (Lesoin, Crampon, Boutin, & Badens, 2011), depressurization of expanded liquid organic solution (DELOS) (Cano-Sarabia et al., 2008; Elizondo et al., 2012) as well as supercritical reverse phase evaporation (SCRPE) (Otake, Imura, Sakai, & Abe, 2001), its improved version (ISCRPE) (Otake et al., 2006) and supercritical assisted liposome formation (SuperLip) (Campardelli et al., 2016) have been designed. Among all of the SC-CO_2 methods, DELOS and ISCRPE methods have been adopted as the basis for the improved process developed in this thesis and are therefore discussed in more detail.

2.2.3.2. DELOS method

The DELOS method is one readily scalable SC-CO_2 method developed by Ventosa, Sala, Veciana, Torres, and Llibre (2001), which has been applied in the preparation of a few nano- and micro-particles, such as quatsomes, liposomes (Cabrera et al., 2013) and vesicles of cholesterol and surfactants (Elizondo et al., 2012). It uses dense phase CO_2 as a cosolvent in the organic solvent and generates a highly expanded liquid phase equilibrated with CO_2, which is then depressurized into an aqueous phase to form liposomes. The DELOS process was found to yield small vesicles with a narrow size distribution (PdI $\leq$ 0.2) compared to the TFH method (Cano-Sarabia et al., 2008). In DELOS, an abrupt and rapid depressurization from the liquid phase generates efficient dispersion and very fine droplets, which gives rise to the high homogeneity of particles, even without further processing or the addition of surfactants. In this regard, the DELOS method demonstrates a unique advantage of achieving high uniformity of liposomes

over most traditional methods, which greatly rely on the addition of surfactants. However, considering the low solubility of phospholipids in SC-CO_2, DELOS relies on the use of CO_2-expanded liquid organic solvents to solubilize phospholipids and hence results in solvent residues in the final liposome products.

2.2.3.3. ISCRPE method

The ISCRPE method is a SC-CO_2 method first reported by Otake et al. (2006). In 2001, Otake and his colleagues developed the SCRPE method (Otake et al., 2001), which involves the formation of a phospholipid/ethanol/SC-CO_2 mixture under pressure first and then mixing it with an aqueous phase to form liposomes. However, an organic solvent (ethanol) was still present in the liposomes. Afterwards, Otake et al. (2006) developed the ISCRPE method as an improved version of SCRPE. The ISCRPE method was designed to pressurize a heterogeneous phospholipid aqueous suspension first and then depressurize it from the supercritical phase to transform the crude mixture into liposomes. This method used glucose as a model hydrophilic compound and demonstrated higher stability and encapsulation efficiency compared to the traditional TFH method. Large unilamellar liposomes with a higher encapsulation of hydrophilic components were achieved. The ISCRPE method is a valuable and novel method, which forms liposomes in a single step but completely avoids the usage of organic solvents and surfactants. This is a major advantage considering that most of the traditional and innovative methods require further operations to eliminate traces of residual solvents. Thus, this method was selected as one of the reference method in this research to achieve a higher level of safety in food and nutraceutical applications.

2.3. Physicochemical characteristics of liposomes

The physicochemical properties of liposomes are of great significance for the bioactive encapsulation, delivery and metabolic processes. These properties can be evaluated using different techniques.

2.3.1. Particle size and size distribution

Particle size and size distribution are important parameters in the characterization and applications of liposomes, which are related to the metabolic pathway, localization and their interaction with cells (Shang, Nienhaus, & Nienhaus, 2014). Particle size specification is also crucial in the transportation and circulation in the body for drug delivery purposes. For oral administration, particle mobility and diffusion rate can be decreased with increasing particle size in the intestinal mucus (Yildiz, McKelvey, Marsac, & Carrier, 2015). For example, nanoparticles with a diameter of 100 nm were taken up in the gastrointestinal tract by 15-250 folds higher than 1000 nm particles (Desai, Labhasetwar, & Amidon, 1996). Ideally, a particle size of less than 300 nm is advisable for intestinal transport (Das & Chaudhury, 2011) while particle size not exceeding 200 nm can be used for long circulation (Moghimi, Hunter, & Murray, 2001). Also, these two parameters can affect the aggregation and fusion of particles and therefore are highly associated with the liposome shelf life and stability (Jesorka & Orwar, 2008).

The dynamic light scattering (DLS) technique is the most widely applied method for the determination of mean particle size of liposomes in a suspension. DLS is a simple and rapid method where particle size is calculated according to the Stokes-Einstein equation of Brownian motion (Kaszuba, McKnight, Connah, McNeil-Watson, & Nobbmann, 2008). It provides the mean hydrodynamic diameter of particles, which is usually larger than their real size. DLS also offers the size distribution through the polydispersity index (PdI) value calculated upon the

cumulants analysis of the intensity autocorrelation function of dynamic light scattering (Kaszuba et al., 2008), which is arbitrarily scaled from 0 to 1. PdI values below 0.3 are usually considered as monodisperse, while those greater than 0.7 are considered to be highly polydisperse (Gibis, Rahn, & Weiss, 2013). This method has been applied to determine the particle size and size distribution of liposomes encapsulating a variety of bioactives, such as nisin (Colas et al., 2007), β-carotene (Tan et al., 2014), vitamin E (Kamezaki et al., 2016), curcumin (Hasan et al., 2014), tea polyphenols (Gülseren, Guri, & Corredig, 2012) and resveratrol (Vanaja, Wahl, Bukarica, & Heinle, 2013).

Apart from DLS, several microscopy techniques such as transmission electron microscopy (TEM), freeze fracture TEM, and cryo-TEM, can also be applied to characterize the particle size based on the view of liposomal appearance (Ruozi et al., 2011). TEM and cryo-TEM can provide high resolution images of liposomal morphology and information on the true particle size instead of the hydrodynamic size (Ruozi et al., 2011). However, these two techniques usually display a small number of particles, which may not be representative of the bulk particle system. Size exclusion chromatography can also be used to determine the hydrodynamic diameters by separation and resolution of liposomes via a gel column packed with porous materials (Jesorka & Orwar, 2008). The process of separation is based on the elution of large particles first followed by the smaller particles. However, these methods are usually employed to complement the DLS technique since they are relatively expensive and time consuming compared to the DLS method.

2.3.2. Morphology

The morphology of liposomes can be characterized by TEM, cryo-TEM and atomic force microscopy (AFM). TEM and AFM can provide accurate information on the surface, shape and appearance of liposomes in either single or bulk forms while the cryo-TEM and freeze fracture

TEM can be used to investigate the lamellarity and cross sectional morphology of liposomes (Yaghmur, Azmi, Moghimi, & Helvig, 2015). Traditional TEM is a versatile and rapid approach to assess the morphology of liposomes at high magnification (as high as 150,000x). It involves the deposition of particles onto a carbon-coated copper grid, removal of the liquid and negatively staining the vesicles for direct imaging. However, since its sample preparation requires dehydration of liposomes from the liquid phase, TEM can generate artifacts, like vesicular shrinkage or distortion and result in damaged vesicles mixed with intact ones (Laouini et al., 2012). Cryo-TEM can be used without such a drawback but TEM is still widely used, considering that it is relatively inexpensive and easier to operate. The traditional TEM has been used to study the morphology of liposomes loaded with nisin (Laridi et al., 2003), catechin (Rashidinejad, Birch, Sun-Waterhouse, & Everett, 2014), casein hydrolysates (Yokota, Moraes, & Pinho, 2012) and lactoferrin (Liu, Ye, Liu, Liu, & Singh, 2013).

Cryo-TEM is an advanced technique, allowing visualization of the organization of supramolecular assemblies with very good resolution and minimum sample damage. It usually involves the vitrification of a thin liposome suspension film and then storing and imaging the specimens under liquid nitrogen. Therefore, specimens are well preserved in their native state. Since the liposomal temperature is brought down to -183°C at an ultrafast rate, specimens are embedded in vitreous (amorphous) ice, avoiding any damage arising from the formation of ice crystals. Cryo-TEM has been shown to be effective in the assessment of full morphological features, like shape and lamellarity of liposomes, which can also be applied to confirm the records obtained from other techniques like TEM. Cryo-TEM is relatively more expensive and requires a high level of expertise in sample handling and controlling the growth of ice crystals during the measurement. Cryo-TEM has been used to evaluate liposomes loaded with β-carotene

(Fernandez et al., 2015), vincristine (Zhigaltsev et al., 2005), doxorubicin (Chiu et al., 2005) and quercetin (Castangia et al., 2014).

AFM can provide the three-dimensional profile like shape or surface of liposomes without removing them from their native liquid environment (Ruozi et al., 2011). Thus, liposomes can be measured with less damage compared to the traditional TEM technique. However, AFM may not be used for visualizing inside structure and lamellarity of vesicles since the AFM is more suitable to assess the surface features (Egawa & Furusawa, 1999; Palmer, Wingert, & Nickels, 2003). The elongated incubation time can modify the liposomal shapes due to reorganization of phospholipids (Bhuvana & Dharuman, 2014). Beside these three techniques, freeze fracture TEM can also offer information on the liposomal morphology but it is not used commonly owing to the relatively low contrast.

2.3.3. Zeta potential

The zeta potential is a critical parameter highly associated with the stability of liposomes. Around a charged particle surface, there is a Stern layer where the ions are strongly bound to the particle and a diffuse layer where they are less firmly bound (Elizondo et al., 2011). As the particle moves, two layers move with the charged particle as a whole. Zeta potential is defined as the electric potential in the interfacial double layer at the slipping plane to the bulk liquid (Hunter, Midmore, & Zhang, 2001). Zeta potential is usually measured by electrophoresis, which involves applying an electric field to the liposome suspension and then calculating the electrophoretic mobility of the nanoparticles, moving at a velocity related to their zeta potential. Zeta potential is an important index to indicate the overall surface charge that a lipid vesicle acquires in a particular medium (Corvo et al., 2016). The surface charge of liposomes mainly results from the ionization of surface groups as well as the adsorption of charged species onto the surface

(Elizondo et al., 2011). For the ionization effect, the dissociation of acidic groups in the phospholipids can give a negative charge on the liposome surface, whereas basic groups will lead to a positive charge. For the adsorption effect, ions may be specifically adsorbed onto the particle surface, which contribute to a positively or a negatively charged surface (Laouini et al., 2012). Zeta potential can be used to predict particle stability during their storage, and particles with a zeta potential value greater than 30 mV or less than -30 mV are considered to be stable (Monteiro, Martins, Reis, & Neves, 2014). High absolute zeta potential values suggest that sufficient repulsion force is present between the particles to avoid aggregation and thus result in good stability.

2.3.4. Encapsulation efficiency and bioactive loading

The encapsulation efficiency (EE) is a critical parameter to indicate the capacity of liposomes to capture bioactives. It is usually defined as the ratio of entrapped bioactives to the total amount of bioactives added into the preparation. The bioactive loading (BL) is defined as the ratio of entrapped bioactive to the total lipid content. A higher EE and BL is desirable in liposome formulations as an increased payload of bioactives can increase their potential usage, enhance the bioactive efficacy, and reduce the loss of payloads and toxicity that may be associated with the non-encapsulated components (Wallace, Li, Nation, & Boyd, 2012). To evaluate EE and BL, the loaded nanoparticles must be separated from the non-encapsulated active ingredients. Dialysis with an appropriate cut-off membrane, ultracentrifugation, ultrafiltration and size exclusion chromatography can be employed for this purpose (Ricci et al., 2006; Wallace et al., 2012; Wang et al., 2009). After separation from the free bioactives, bioactive-loaded liposomes are disintegrated using a selected organic solvent (methanol or ethanol) to release the encapsulated bioactives. The bioactive content in the two phases can be

quantified by using spectrophotometry, fluorescence spectroscopy or high performance liquid chromatography (HPLC). The EE and BL in a liposome depend on the polarity of the bioactive, liposomal properties, bioactive interactions with the lipid bilayers and the bioactive loading method (Kulkarni, Betageri, & Singh, 1995). Both EE and BL play an essential role for an efficient delivery of bioactives at a certain dosage.

2.3.5. Phase transition behavior

Differential scanning calorimetry (DSC) can be employed as a standard technique to monitor the phase transition behavior of bilayer membranes (Elizondo et al., 2011). Upon heating, phospholipids can absorb energy and transform from a rigid gel phase into a liquid-crystalline state (Fig. 2.5) beside the melting process. DSC thermograms are usually represented as heat flow versus temperature and provide the thermal profile such as phase transition temperature (T_m) and the transition enthalpy (ΔH) associated with the gel to liquid-crystalline phase transition. This behavior is an indication of the cooperative melting of the hydrocarbon chains in lipid bilayers, excluding their phosphate heads (Jacobson & Papahadjopoulos, 1975). Below the T_m, lipid bilayers present a highly ordered and rigid phase where the mobility of fatty acyl chains is highly restricted. However, as the temperature increases above T_m, energy input can disrupt the interactions between the hydrocarbon chains and allow them to change into a disordered and fluid state (Tarahovsky, Kim, Yagolnik, & Muzafarov, 2014). Phase transition temperature is highly associated with the hydrocarbon chain length, degree of saturation and

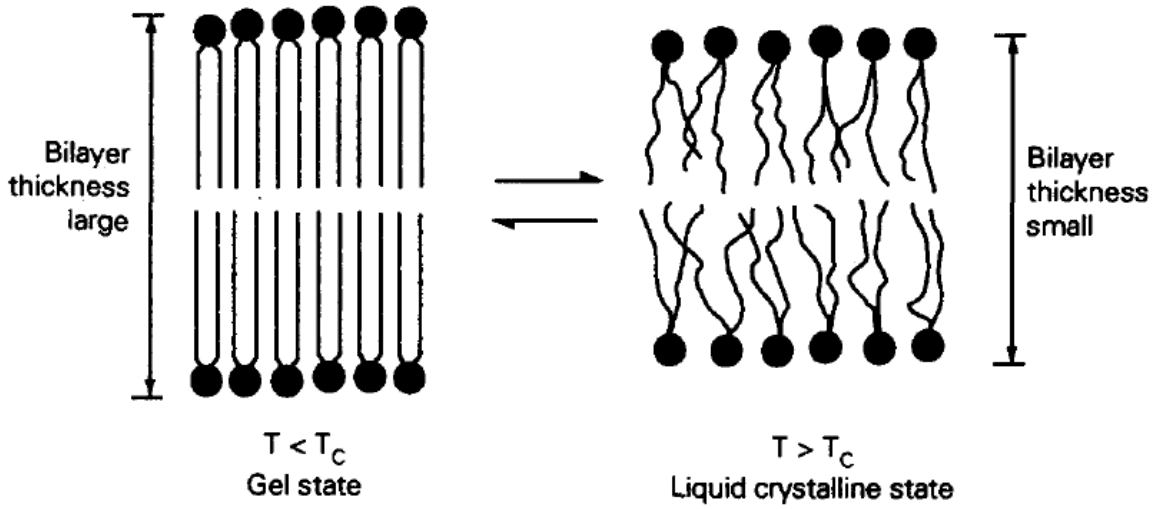

Figure 2.5: Schematic representation of gel to liquid-crystalline phase transition of lipid bilayers. Source: McEihaney (1976), reprinted with permission from Academic Press.

their packing order of materials (Jacobson & Papahadjopoulos, 1975). For pure phospholipids, the phase transition behavior usually occurs in a narrow temperature range. The phosphatidylcholines have been well studied and their phase transition temperatures were reported as -17°C, 55°C, 41°C and 24°C for 1,2-dioleoyl-sn-glycero-3-phosphatidylcholine (DOPC), 1,2-distearoyl-sn-glycero-3-phosphatidylcholine (DSPC), 1,2-dipalmitoyl-sn-glycero-3-phosphatidylcholine (DPPC) and 1,2-dimyristoyl-sn-glycero-3-phosphatidylcholine (DMPC), respectively (Eze, 1991; Kučerka, Nieh, & Katsaras, 2011). Embedding hydrophobic bioactive compounds into the bilayer membranes can have pronounced effects on the phase transition behavior. Depending on the nature and arrangement of the bioactives, they may disrupt the T_m or strengthen the hydrophobic interactions, and create a more tightly packed bilayer phase to increase the T_m (Bhattacharya & Haldar, 2000; Hianik, 1999). Generally, elevated bioactive concentration can suppress the phase transition temperature due to the disruption of the gel phase bilayers (Bothun, 2008). The DSC thermograms can be used to study the lipid arrangement,

bioactive distribution and their interactions between the bilayers. DSC has been applied to study the phase transition of liposomes embedded with carvacrol and thymol (Liolios, Gortzi, Lalas, Tsaknis, & Chinou, 2009), vitamin E (Rovoli, Gortzi, Lalas, & Kontopidis, 2014) and β-carotene (Gruszecki & Strzałka, 2005). Further work is needed to understand the impact of other bioactives on liposome phase transition. Besides phase transition, DSC can also be applied to evaluate other thermal phase transformations such as the melting, crystallization, oxidation and decomposition of materials.

2.3.6. Structural features and lipid-bioactive interactions

There are a few possible non-covalent interactions available between phospholipids and bioactives. Hydrophobic compounds usually interact with lipids via hydrophobic and van der Waals interactions while the hydrophilic drug and bioactive molecules can interact with the phosphate head groups via electrostatic interaction and hydrogen bonding (Maghraby, Williams, & Barry, 2005; Bruno et al., 2013). Amphiphilic compounds interact with bilayers via some or all of the interactions mentioned above, depending on their structural features. These interactions, which are closely associated with their structural features, are of great significance in the modulation of the properties of liposomes such as particle size, encapsulation efficiency, morphology and bilayer behavior.

The structural features, functional groups and possible lipid-bioactive interactions within the liposomes can be evaluated using Fourier transform infrared spectroscopy (FTIR). FTIR can generate spectra on all regions of the liposomes without introducing perturbing extrinsic probes and thereby yield accurate information on the structure and lipid arrangement (Lewis & McElhaney, 1998). The FTIR spectra are usually presented in terms of infrared intensity versus wavelength number. FTIR spectra can be used to interpret the interactions between phospholipid

bilayers and bioactives as well as organizational changes in the particles. For phospholipids, the C=O stretching absorption band has been shown to be a summation of at least two major components that are usually centered near 1740cm^{-1} and near 1725 cm^{-1}, while the P=O stretching frequency for the phosphate group is typically observed near 1230 cm^{-1} (Lewis & McElhaney, 1998). The bands at around 1068 cm^{-1} and 1050 cm^{-1} usually refer to two C–O–P stretching modes of the phosphodiester moiety ($C_{glycerol}$–O–(P)) and (C_{head}–O–(P)) present in phosphodiester compounds (Garidel, Blume, Hübner, 2000). The O-H absorption band is generally located at around 3200-3600 cm^{-1}. Generally, a peak shift in O-H stretching band indicates the formation of hydrogen bonding between molecules. For the phospholipids, the peak changes or frequency shift at the absorption range of P=O and C-O-P may suggest a structural change of bilayers due to the modified interactions between lipids with encapsulated bioactives (Pohle et al., 2001).

2.3.7. Crystallinity

X-ray diffraction plays a significant role in the measurement of the crystalline nature of lipids. It can be used to interpret the phase behaviors such as phase transition and fluidity and to predict distribution of the hydrophobic or amphiphilic bioactives in between the bilayers. The principle involves the detection of the reflection of an incident X-ray beam when applied to a crystal plane. It has been used to measure the particles and generate a unique diffraction pattern of materials in terms of the diffracted ray intensity versus angles. XRD can also be used to identify crystals or mixtures (polymorphism) as each individual component can be present in different crystalline states and arrangements. XRD can assess materials in a non-destructive manner and thus the same material may be used for other measurements.

Compared to the other readily dried nanoparticles, reports on the use of XRD for liposome characterization are limited and need further investigation. Preparation of fine dehydrated lipid vesicles without disturbing their original packing and order is a major challenge. Vesicles should be dried in a gentle manner prior to measurement. To date, the best protocol seems to be the one reported by Cavalcanti, Konovalov, and Haas (2007) who applied the liposome suspension onto a glass holder and dried them in an environment of controlled relative humidity (84%). XRD can be used in combination with DSC to better interpret the molecular distribution, arrangement and phase change prior to and after the bioactive loading. Generally, a strong and sharp peak suggests a well ordered crystalline state while a depressed and wide peak in the diffractogram suggests a poor crystalline structure or amorphous nature of the particles. Generally, poor crystallinity profile suggests a relatively low phase transition temperature and high fluidity due to disordered states of lipids whereas the high crystallinity suggests the opposite (Anderson et al., 2007). If the raw materials show a highly ordered state while the encapsulated particles do not, it is highly possible that the bioactive compounds are finely distributed in between the lipid molecules and disrupt the original ordered state of bilayers (Jose et al., 2014; Guo, Zhang, Zhao, Zhu, & Feng, 2015).

2.3.8. *In vitro* release of bioactives

The release rate of encapsulated components in the gastrointestinal tract is another critical parameter closely associated with the stability and absorption of encapsulated bioactives in the oral administration process. To analyze this, *in vitro* simulated gastric fluid (SGF) and simulated intestinal fluid (SIF) can be prepared for the study of enzymatic decomposition of lipid-based formulations, where enzymes and salts are added to maintain an appropriate composition of the digestive fluids. Reports on liposomal behavior in the gastrointestinal tract are controversial and

show low reproducibility, depending on the encapsulated agent (Cansell, Nacka, & Combe, 2003; Chia-Ming & Weiner, 1987). On one hand, liposome encapsulation has been suggested to offer protection for the bioactives in the gastrointestinal tract (Patel & Ryman, 1976) and facilitate the gastrointestinal transport of a number of agents (Kim, Kim, & Lee, 2013). For liposome uptake, liposomes with bioactives can be absorbed by fusion or endocytosis with mucosa cells in the gastrointestinal tract, thereby facilitating transport of valuable molecules, which have poor permeability through the gastrointestinal mucosa in their free state (Andrieux et al., 2009; Cansell et al., 2003). On the other hand, the intactness of liposomes, which promote enhanced chemical stability of encapsulated agents undergoing enzymatic or pH attack in the digestive tract was also questioned (Liu et al., 2013). Since liposomes may be partially digested by the phospholipases and bile salts present in the intestinal fluid, they may not have high stability as oral drug carriers. It has been reported that the surface modification of liposomes may be an effective way to improve the *in vitro* and *in vivo* stability of liposomes, with a surface coating such as poloxamer, polysorbate 80, carboxymethyl chitosan, or dextran derivatives for oral administration purpose (Iwanaga et al., 1999; Takeuchi, Matsui, Yamamoto, & Kawashima, 2003). The *in vitro* release rate of liposomes can be influenced by the lipid composition, temperature, enzymes, pH, ionic strength, EE and interactions with bioactives (Anderson & Omri, 2004; Cipolla et al., 2014; Shibata, Izutsu, Yomota, Okuda, & Goda, 2015).

2.3.9. Storage stability

The stability of liposomes can be determined using physical, chemical and biological approaches. Liposomes tend to fuse or aggregate into larger vesicles, which is favorable from a thermodynamic aspect. The particle size, size distribution and turbidity can be used to evaluate the physical stability of liposomes throughout storage (Zuidam, Gouw, Barenholz, & Crommelin,

1995). Apart from the zeta potential described above, the physical stability of liposomes is greatly influenced by the preparation method and phospholipid concentration. A higher shear applied in liposome formation, such as with sonication or extrusion, can enhance physical stability (Rasti, Jinap, Mozafari, & Yazid, 2012) while an increased lipid concentration usually leads to a contrary result. On the other hand, The EE, BL and phospholipid content can be determined to assess the chemical stability of liposomes. Chemical stability is usually associated with the liposome composition, temperature, aqueous medium and storage conditions (Allen Zhang & Pawelchak, 2000; Grit & Crommelin, 1993). Bioactives, especially non-encapsulated compounds sensitive to external conditions, may undergo degradation and change in their chemical structures during storage. Phospholipids, comprised of unsaturated fatty acids derived from natural sources may suffer from oxidation and hydrolysis. These reactions can lead to permeability changes and bioactive leakage within the liposome bilayers. The biological stability refers to the stability of liposomes in biological fluids like plasma. Reports on this aspect are limited, which depends on the presence of special agents like proteins that can interact with liposomes, and influence the circulation pathway of liposomes.

2.4. Applications of liposomes

Liposomes are versatile vesicles offering a variety of diverse applications. The most successful application of liposomes is their use in the pharmaceutical industry as a potent drug carrier in cancer treatment and gene therapy (Allen & Cullis, 2013). Drug efficacy can be greatly improved by liposome encapsulation, and their side effects can be minimized. In addition, drugs with poor aqueous solubility can be embedded in the liposome bilayers to achieve enhanced absorption and bioavailability. For example, insulin (Patel & Ryman, 1976) and cysteamine (Bhuvana & Dharuman, 2014) have been encapsulated into liposomes for protection from

enzymatic degradation, while doxorubicin (Molavi et al., 2013), anthracycline (Alberts et al., 2004) and clofazimine (Mehta, 1996) have been encapsulated for improved efficacy and reduced toxicity to the human body. Liposomes can also be used as a model system to investigate the conformation, phase behavior, permeability, fusion of membranes and other metabolic aspects in basic science (Bangham, Hill, & Miller, 1974; Pignatello, Musumeci, Basile, Carbone, & Puglisi, 2011).

In addition to the medical applications, liposomes can also be utilized in food science and natural health product areas with many merits (summarized in Table 2.1). For instance, liposomes loaded with enzymes have been applied in fermentation processes due to their sustainable release property (Rao, Chawan, & Veeramachaneni, 1994) and antimicrobials encapsulated in liposomes, like bacteriocin and nisin have been applied in cheese (Malheiros, Sant'Anna, Barbosa, Brandelli, & Franco, 2012), milk (Laridi et al., 2003) and meat (Nieto-Lozano, Reguera-Useros, Peláez-Martínez, & Hardisson de la Torre, 2006). As well, antioxidants like vitamin E and polyphenols (Fang & Bhandari, 2010) encapsulated in liposomes have been used to protect them from oxidation, and improve their quality. Liposomes are also applied for the protection of valuable bioactives in food and natural health product industries to enhance the functionality of products and achieve desirable health benefits. For example, liposomes loaded with vitamin C ("Dr. Mercola premium supplements: Liposomal Vitamin C"), docosahexaenoic acid (DHA) and CoQ10 (Empirical labs: Liposomal DHA and CoQ10) have been commercialized to enhance their bioavailability in the body.

In this research, lutein and anthocyanin were selected as model bioactives of hydrophobic and hydrophilic nature, respectively, since the literature lacks information on their

Table 2.1: Liposomes utilized in the encapsulation of different bioactives for food and natural health product applications.

Bioactive	Particle size and EE*	Purposes	References
Vitamin E	164 nm, 84%	Protect from oxidation and heat treatment	Zhao et al. (2011)
ω-3 Fatty acids	87 nm, 52%	Protect from oxidation and decrease the odors of volatile compounds	Hadian, Sahari, Moghimi, and Barzegar
Lycopene	67 nm, 94%	Protect from oxidative damage	Tan et al. (2014)
β-Carotene	110 nm, 90%	Controlled release in the food system	Thompson, Couchoud, and Singh (2009)
Tea polyphenol	160 nm, 60%	Protect from light and oxygen	Lu, Li, and Jiang (2011)
Coenzyme Q10	118 nm, 95%	Protect from oxidation and improve its absorption	Xia, Xu, Zhang, and Zhong (2007)
Bacteriocin	160 nm, 95%	Protect from Maillard reaction	Sant'Anna, Malheiros, and Brandelli (2011)
Nisin Z	725 nm, 47%	Reduce nisin affinity to food ingredients, eliminate interference with starter growth	Laridi et al. (2003)
Cyprosin	12.7%	Controlled release to achieve improved fermentation in cheese	Picon, Serrano, Gaya, Medina, and Nuñez
Grape seed polyphenol	86.5 nm, 88%	Controlled release of bioactives and preserve aqueous products	Gibis, Ruedt, and Weiss (2016)
Hibiscus extract	46 nm, 72%	Protect from oxidation	Gibis, Zeeb, and Weiss (2014)
Quercetin	220 nm, 82%	Enhance water dispersibility, eliminate bitterness of quercetin	Frenzel, Krolak, Wagner, and Steffen-
Eugenol	210 nm, 68%	Protect essential oil from light and oxidation	Sebaaly, Greige-Gerges, Stainmesse, Fessi, and
ω-3 Fatty acids	409 nm, 92%	Yogurt fortification, eliminate fish odor	Ghorbanzade, Jafari, Akhavan, and Hadavi
Catechin	139 nm, 75%	Protect cheese from oxidation	Rashidinejad et al. (2014)
Clove oil	156 nm, 20%	Controlled release of bioactive, inhibit the growth of *Staphylococcus aureus* in tofu	Cui, Zhao, and Lin (2015)

*EE: encapsulation efficiency.

encapsulation in liposomes. The main aim is to protect lutein and anthocyanin from unfavorable conditions and achieve improved chemical stability by their encapsulation into liposomes using the SC-CO_2 technique. The encapsulation of these two bioactives and their advantages are discussed in more detail in the following sections.

2.4.1. Encapsulation of lutein

The encapsulation of lutein for enhanced structural integrity and efficacy is of great significance. Lutein is a plant-based carotenoid antioxidant compound that plays a vital role in maintaining eye function (Fig. 2.6). Lutein works to prevent age-related macular degeneration (Olmedilla, Granado, Blanco, Vaquero, & Cajigal, 2001), cataract (Moeller et al., 2006), and retinitis pigmentosa (Eliot L. Berson et al., 2010) and also to reduce the risk of cardiovascular disease (Omenn et al., 1996), stroke (Polidori et al., 2002) and lung cancer (Ito et al., 2003). Lutein cannot be synthesized by the human body and thus requires replenishment from the diet. Despite so many benefits, the usage of lutein is hampered by its poor water solubility and high hydrophobicity. In addition, it is susceptible to rapid degradation that is associated with the reactivity of conjugated double bonds on exposure to light, oxygen and temperature. The incorporation of lutein into liposomes is expected to preserve its activity, improve its aqueous dispersibility and enhance its *in vivo* behavior for improved efficacy and bioavailability.

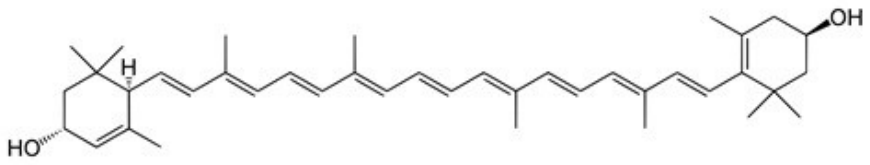

Figure 2.6: Chemical structure of lutein.

To date, there have been only a few reports on the characterization of liposomes loaded with lutein and their *in vitro* behavior. Tan et al. (2013) obtained lutein-loaded liposomes that had a mean diameter of 83.5 nm via the ethanol injection method with an EE of 92%. Xia, Hu, Jin, Zhao, and Liang (2012) prepared lutein-loaded proliposomes (lipid powder that can be hydrated to form liposomes) via the supercritical anti-solvent method with a mean diameter of 200 nm and an EE of 90%. Lutein incorporation into liposomes might modulate the degree of crystallinity, membrane fluidity and conformational order of liposomal bilayers (Tan et al., 2013). The incorporation of carotenoid compounds is suggested to have an influence on the liposomal morphology, particle size distribution and *in vitro* release profiles (Xia et al., 2015). In addition, a high payload may be achieved by adjusting the lutein-to-lipid ratio and other processing parameters. There are no studies available about lutein-loaded liposomes obtained using the improved SC-CO_2 method targeted in this research. Thus, their physiochemical features may be of great interest for novel food and natural health product applications.

2.4.2. Encapsulation of anthocyanins

The encapsulation of anthocyanins into liposomes is of great importance to protect them from adverse conditions and maintain their stability and efficacy. Anthocyanins are powerful flavonoid antioxidants, which give the colors of red, blue and purple in different varieties of flowers, fruits and vegetables. Anthocyanins have received growing attention as a natural colorant in food, nutraceutical and cosmetic formulations not only due to their extensive range of colors but also their health benefits. Anthocyanins have been shown to offer health benefits, including reducing the risk of cardiovascular disease, control of obesity and diabetes as well as improvement of visual and brain functions (Tsuda, 2012). However, their high reactivity renders them susceptible to degradation due to factors such as light, heat, oxygen and relatively basic pH

in the gastrointestinal tract. The chemical structure of anthocyanins depend critically on the pH of the aqueous medium, which varies from flavylium cation to chalcone (Yoshida, Mori, & Kondo, 2009). Anthocyanins usually exist in a mixture of different forms in equilibrium with one dominant form being present at each pH condition (Welch, Wu, & Simon, 2008). The chemical structure of anthocyanin at various pH levels is presented in Fig. 2.7.

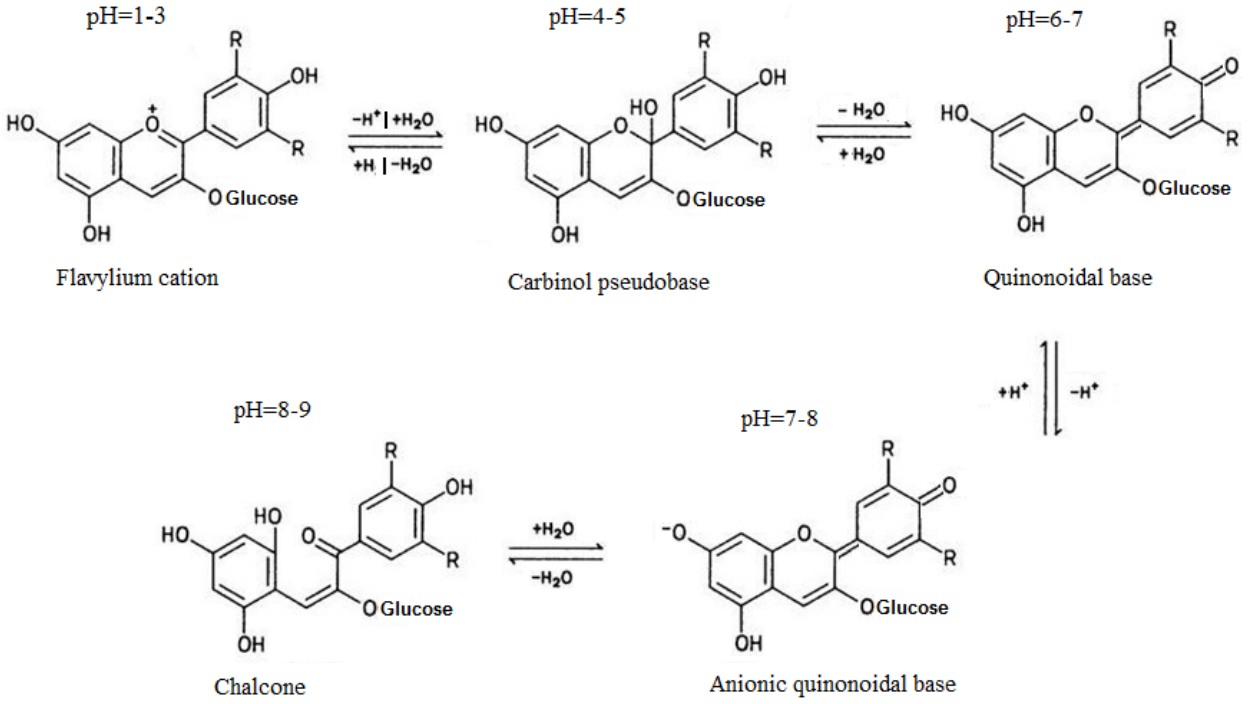

Figure 2.7: Chemical structures of anthocyanin in response to pH.

Several studies have reported anthocyanin encapsulation into liposomes using the traditional methods. Hwang, Kuo, Lin, and Kao (2013) prepared liposomes loaded with anthocyanin using the reverse phase evaporation method and obtained a particle size of 158 nm and EE of 55%. Gibis et al. (2014) prepared liposomes loaded with hibiscus anthocyanin with high speed homogenization combined with a microfluidic technique and achieved a particle size of 46 nm and EE of 72%. Bryła, Lewandowicz, and Juzwa (2015) prepared liposomes loaded with

elderberry anthocyanins by the thin film hydration method and obtained a particle size of 378 nm and EE of 69%. The encapsulation of anthocyanin in liposomes has been shown to effectively reduce the oxidation of phospholipids as well as the other sensitive molecules in food systems (Cavalcanti, Santos, & Meireles, 2011; Ossman, Fabre, & Trouillas, 2016). The encapsulation of anthocyanin can be used in functional foods for enhanced health benefits (Fang & Bhandari, 2010). However, the physiochemical properties of anthocyanin-loaded liposomes such as phase transition behavior, crystallinity and morphology have not been completely elucidated. Since a hydrophobic portion exists in the anthocyanin molecules, a partitioning of this bioactive into the bilayer membrane may occur during encapsulation (Ossman et al., 2016) and increase the complexity of anthocyanin behavior. The elucidation of fundamentals of anthocyanin-loaded liposomes is critical to predict the behavior and feasibility when they are used in food and natural health product applications.

2.5. Summary

Liposomes are valuable phospholipid vesicles with a number of medical, nutraceutical and food applications. Liposomes can protect sensitive but beneficial ingredients from unfavorable conditions so that their stability and bioavailability can be greatly improved. Traditional methods can yield liposomes but have several drawbacks while significant progress has been made with some innovative methods to improve liposomal characteristics. The SC-CO_2 technique shows great potential to utilize high pressure CO_2 for nanoparticle formation. Among all of the SC-CO_2 methods, the DELOS and ISCRPE methods are of great importance with unique advantages and their combination in the processing aspect is promising to generate liposomes with desirable characteristics. Liposomes can be characterized in terms of their physical, chemical and biological properties. Lutein and anthocyanin are selected as model bioactive compounds, which

can be stabilized using liposomal encapsulation by the SC-CO_2 method. The fundamental understanding of these two types of liposomes is essential for the prediction of their behaviors and applications in natural health products and food systems.

CHAPTER 3 – PREPARATION OF UNLOADED LIPOSOMES USING SUPERCRITICAL CARBON DIOXIDE VIA DEPRESSURIZATION OF SUPERCRITICAL PHASE[1]

3.1. Introduction

Recently, production of nanoparticles, which are utilized as carriers to deliver a number of health benefiting bioactive components has gained increasing attention. Liposomes offer superior advantages over competitor polymer-based nanoparticles and have been considered as an effective vesicular system to deliver bioactive compounds (Fenske, Chonn, & Cullis, 2008). Liposomes are spherical self-assembled phospholipid vesicles that can be used to protect high-value components against degradation in harsh environmental conditions and, therefore, stabilized for higher bioavailability and efficacy (Fahr & Liu, 2007). Liposomes can offer a versatile and different way of encapsulation, depending on the properties of the bioactives, where hydrophobic agents are incorporated in between the phospholipid fatty acyl chains and hydrophilic agents are entrapped in the aqueous core while encapsulation of amphiphilic agents depends on their partitioning between the lipid and aqueous phases (Kulkarni, Betageri, & Singh, 1995). Liposomes play an important role in pharmaceutical, food and natural health product related applications.

Although there are a few conventional methods that can be used to generate liposomes, the supercritical carbon dioxide (SC-CO_2) technique has drawn great interest as a promising alternative because it has great potential to overcome some drawbacks of conventional methods.

[1]A version of this chapter has been published: Zhao, L., & Temelli, F. (2015). Preparation of liposomes using supercritical carbon dioxide via depressurization of the supercritical phase. *Journal of Food Engineering, 158*, 104-112.

Obtaining products free of organic solvent residues upon release of CO_2 into the gas state is important for enhanced safety, especially for applications in the agricultural, food and medical fields. Despite the above advantages, investigation of the preparation of liposomes using SC-CO_2 technology has been relatively limited compared to the conventional methods, considering the requirements for specific training and high pressure equipment. However, the SC-CO_2 method can provide novel and promising perspectives for liposome preparation, which is worthy of further study in both fundamental and practical terms. In addition, the characteristics of liposomes can be regulated by adjusting the processing parameters of SC-CO_2, which has the potential to be developed into a large-scale and continuous process in contrast to the conventional methods. Among several SC-CO_2-based methods, Otake et al. (2006) developed the improved supercritical reverse phase evaporation (ISCRPE) method and successfully produced glucose-encapsulated liposomes with several desirable advantages. This method not only generated unilamellar vesicles in a single and rapid step, but also improved the encapsulation efficiency (EE) of hydrophilic compounds over conventional methods. Moreover, the usage of organic solvent or surfactant was avoided. Since the focus of Otake et al. (2006) was on encapsulating glucose in the liposome as a model compound, information on the fundamental aspects of the liposome formation without the interactions from any encapsulated compound is lacking. Investigation of the formation of unloaded liposomes is essential to better interpret phospholipid behavior under high pressure CO_2 and during depressurization as well as the effect of key processing parameters on liposome characteristics. Based on such fundamentals, it would be possible to optimize and control the process better.

Development of an effective process to form liposomes also requires a good understanding of the phase behavior under high pressure, including CO_2 solubility in water and density and

volumetric expansion of the aqueous phase. Although the first two parameters have been evaluated previously (Ferrentino, Calix, Poletto, Ferrari, & Balaban, 2012), limited data are available on the volumetric expansion of water or phospholipid suspension. The volumetric expansion dictates the change in liquid volume upon equilibration with high pressure CO_2 and thus, is essential for process and equipment design.

The main objective of this study was to investigate the processing of liposomes using the ISCRPE method of Otake et al. (2006) by depressurization of the supercritical phase. The specific objectives were to investigate the volumetric expansion of water and phospholipid suspension in equilibrium with high pressure CO_2 and to evaluate the effects of the key processing parameters (pressure, depressurization rate and temperature) on the characteristics (particle size distribution, zeta potential, morphology and stability) of the liposomal vesicles obtained with soy lecithin. Furthermore, liposomes prepared using SC-CO_2 were compared to those obtained by the traditional thin film hydration (TFH) method in terms of their quality.

3.2. Materials and methods

3.2.1. Materials

Soy lecithin obtained from Fisher Scientific (Ottawa, ON, Canada) was used for liposome preparation. Liquid CO_2 (purity of 99.99%) supplied by Praxair Canada (Mississauga, ON, Canada) was used in all high pressure CO_2 processing. Water purified by Milli-Q advantage a10 ultrapure water purification system (EMD Millipore, Billerica, MA, USA) was used in all experiments.

3.2.2. Preparation of phospholipid suspension

Fresh phospholipid suspension was prepared as the starting material for liposome preparation. Soy lecithin (1.33 g, molecular weight of 677.92 g/mole as specified by the supplier)

was dispersed in 100 mL Milli-Q water with continuous agitation for 30 min. The final concentration of soy lecithin was controlled at 20 mM. The crude suspension was sealed under nitrogen, stored at 4°C and used within one week.

3.2.3. Experimental apparatus

A schematic diagram of the experimental apparatus used for the volumetric expansion measurement and liposome preparation (Phase Equilibria Apparatus, SITEC-Sieber Engineering AG, Maur/Zurich, Switzerland) is presented in Fig. 3.1. The apparatus mainly consisted of a 10 mL high pressure view cell connected to an ISCO 500D syringe pump (Teledyne Isco, Lincoln, NE, USA). A heating jacket filled with circulating water connected to a water bath (Model 260, Thermo Fisher Scientific Inc., Waltham, MA, USA) was used to regulate the cell temperature. A micrometering valve F installed at the exit from the upper portion of the cell was used to depressurize samples. Phase visualization was achieved through the sapphire windows installed at mid-level on the side of the high pressure vessel. A microscope with a video camera (MD800E, AmScope, Iscope Corp., Chino, CA, USA) was used to record the phase behavior inside the cell.

3.2.4. Phase behavior and volumetric expansion

The volumetric expansion of water and phospholipid suspension in equilibrium with high pressure CO_2 was measured according to the protocol of Jenab and Temelli (2012). A stainless steel frame with a microscopic glass scale (NE41 Graticules, Pyser-SGI Ltd., Kent, UK) was placed inside the cell. A teflon-coated magnetic bar was placed in the center of the base of steel frame to mix the cell contents thoroughly. First, a calibration curve was established. Different volumes of Milli-Q water were pipetted and equilibrated in the vessel until the set temperature was reached. The corresponding reading on the microscopic scale for each volume of water added was recorded from the camera image. Next, volumetric expansion measurement at

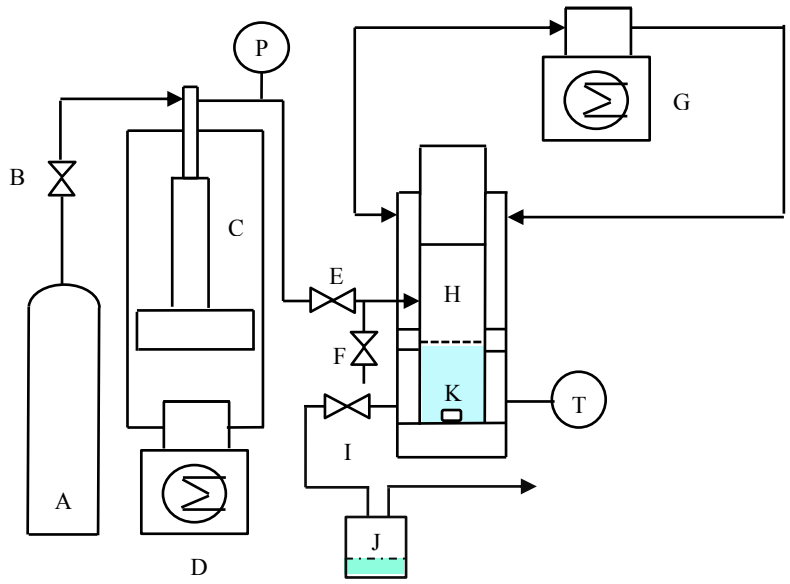

Figure 3.1: Schematic flow diagram of SC-CO_2 system. (A) CO_2 tank; (B) (E) (I) on/off valves; (C) ISCO syringe pump; (D) refrigeration bath; (G) water bath; (H) high pressure view cell; (F) micrometering valve; (J) sample vial; (K) magnetic stirrer; (P) pressure gauge; (T) thermocouple.

different pressures and temperatures was performed. After placing 3.5 mL Milli-Q water into the vessel, the vessel was gently flushed with CO_2 and equilibrated at the set temperature and atmospheric pressure until the level was stabilized on the microscopic scale and recorded. The vessel was then pressurized with CO_2 at each set pressure and mixed for 2 h until the level was stabilized and recorded again. The volumes corresponding to the water levels measured at atmospheric (V_0) and high pressures (V_P) were obtained from the calibration curve. The relative volumetric expansion ($\Delta V\%$) was calculated according to Eq. 3.1:

$$\Delta V\% = \frac{V_P - V_0}{V_0} \tag{3.1}$$

The volumetric expansion of the phospholipid suspension was measured in a similar manner. All the levels of liquid phase in equilibrium with CO_2 were measured at 40°C, 50°C and 60°C from 0 to 300 bar for the determination of relative volumetric expansion.

3.2.5. Preparation of liposomes by SC-CO_2

Liposomes were prepared according to Otake et al. (2006) with some modification. Phopholipid suspension (6 mL) was sealed inside the high pressure vessel. The vessel with contents was gently flushed with CO_2 to remove the air trapped inside and equilibrated to reach the set temperature at atmospheric pressure. Then, the vessel was pressurized with CO_2 to the set pressure. A magnetic stirrer at the bottom was used for thorough mixing of the cell contents for 1 h. Cell content was then depressurized by releasing CO_2 from the upper supercritical phase through a micrometering valve. To achieve a targeted constant depressurization rate, preliminary tests were performed. The specific position on the scale of the micrometering valve corresponding to a certain depressurization rate was recorded. This valve position was then applied during liposome preparation to achieve the desired depressurization rate. The sample was depressurized through the micrometering valve F at a constant rate to form the liposomes (Fig. 3.1). After depressurization to the atmospheric pressure, the cell cap was opened and liposome suspension was collected from the top opening of the cell for further analysis. Different experimental conditions employed for liposome formation within the experimental design were summarized in Table 3.1.

Table 3.1: Processing conditions used to form liposomes by the SC-CO_2 method.

Factors	**Levels**	**Constant parameters**
Pressure (bar)	60, 80, 100, 150, 200, 250, 300	40°C, 60 bar/min
Depressurization rate (bar/min)	10, 20, 40, 60, 90, 120	40°C, 200 bar
Temperature (°C)	40, 45, 50, 55, 60, 65	300 bar, 60 bar/min

3.2.6. Preparation of liposomes by TFH

Liposomes were also prepared by the TFH method (Bangham et al., 1965) for comparison. Soy lecithin (54.23 mg) was dissolved in chloroform (3 mL) with continuous agitation for 5 min using a magnetic stirrer. Then, chloroform was slowly removed by evaporation under a gentle stream of nitrogen to form a homogeneous thin film of phospholipid at the round bottom of the flask. Milli-Q water (4 mL) was added and held at 50°C in a water bath for 10 min for hydration of the thin film, followed by 1 min vortex agitation to thoroughly disperse the phospholipid and form multilamellar vesicles. Vesicle suspension was then sonicated for 5 min using an ultrasonic sonication bath (Model FS30H, Fisher Scientific, Ottawa, ON, Canada) to form liposomes. The final concentration of soy lecithin in water suspension was controlled at 20 mM.

3.2.7. Particle size distribution

The mean size and size distribution of unloaded liposomes were measured by a Zetasizer Nano ZS instrument (Model ZEN3500, Malvern Instruments, Worcestershire, UK) using the Dynamic Light Scattering (DLS) technique. The sample was measured at ambient conditions using a laser wavelength of 535 nm and scattering angle of 173°.

3.2.8. Zeta potential

The surface charge of liposomes was measured using the same instrument as above by the Electrophoretic Light Scattering (ELS) technique. The zeta cell was cleaned and dried before use. Sample was loaded into the zeta cell avoiding any bubbles. The laser power and electric field were controlled at 60 mW and 25 V/cm, respectively. Zeta potential was measured at 25°C with a laser scattering angle of 13°.

3.2.9. Morphology

The morphology was evaluated via transmission electron microscopy (TEM) technique. One drop of liposome suspension was pipetted onto a 300 mesh formvar-carbon (01753-F, Ted Pella, Redding, CA, USA) coated copper grid, and then adhered on the grid for 10 min. The grid was blot dried and negatively stained using phosphotungstic acid (PTA) at 2% (w/v) for 10 s. After blotting dry, the sample was examined using a FEI Morgagni 268 electron microscope (FEI, Hillsboro, OR, USA) at 80 kV. The instrument was equipped with an Orius® SC1000 CCD Camera (Gatan, Pleasanton, CA, USA) for observation and imaging.

3.2.10. Storage stability

The storage stability of liposomes was followed visually for up to 8 weeks and particle size distribution was measured weekly for up to 8 weeks. Liposome suspensions were sealed under nitrogen atmosphere with Parafilm M sealing film (Fisher Scientific, Ottawa, ON, Canada) and stored in the dark at ambient temperature (23°C). Particle size of liposomes was measured as described above.

3.2.11. Statistical analysis

At each condition, liposomal samples were prepared in triplicate. The particle size, size distribution, zeta potential and stability of each sample were analyzed in triplicate. Data analysis was performed using Minitab statistics software 16 (Minitab Inc., State College, PA, USA) and reported as the mean ± standard deviation (SD). One-way analysis of variance (ANOVA) was conducted and significant differences between means were obtained by Tukey's multiple comparison test at a significance level of $p<0.05$.

3.3. Results and discussion

3.3.1. Volumetric expansion

To obtain uniform liposome vesicles, sufficient amount of CO_2 should be accumulated in between the phospholipid bilayers, which would subsequently lead to uniform dispersion of phospholipid molecules upon depressurization before they reorganize into vesicles. The volume of the liquid phase expands due to the solubilization of CO_2 at a given temperature and pressure. Thus, the volumetric expansion can be used as an indication of the extent of CO_2 present in the liquid phase and whether phospholipid molecules can be well dispersed to form a uniform vesicular system. Thus, prior to liposome preparation, it was necessary to evaluate the volumetric expansion and phase behavior of water + CO_2 and phospholipid suspension + CO_2 systems under different pressures.

The volumetric expansion of pure water in equilibrium with CO_2 at different pressures was presented in Fig. 3.2. With an increase in pressure from ambient level to 300 bar, relative volumetric expansion of water increased up to 14.4%, 12.3% and 10.2% at 40°C, 50°C and 60°C, respectively. At each temperature, relative volumetric expansion increased steadily up to 100-150 bar and then reached a plateau. According to CO_2 solubility data in water (Dodds, Stutzman, & Sollami, 1956; Ferrentino et al., 2012), CO_2 solubility increased with pressure, introducing more CO_2 into the water phase, thus raising the water volume. Temperature had a significant effect ($p<0.05$) on the relative volumetric expansion of water at each pressure. With an increase in temperature from 40°C to 60°C, relative volumetric expansion decreased. This trend was also consistent with the CO_2 solubility data (Dodds et al., 1956; Ferrentino et al., 2012), since less amount of CO_2 was solubilized in the water phase as the temperature rose and thus decreased the relative volumetric expansion. There is limited data available on the volumetric expansion of

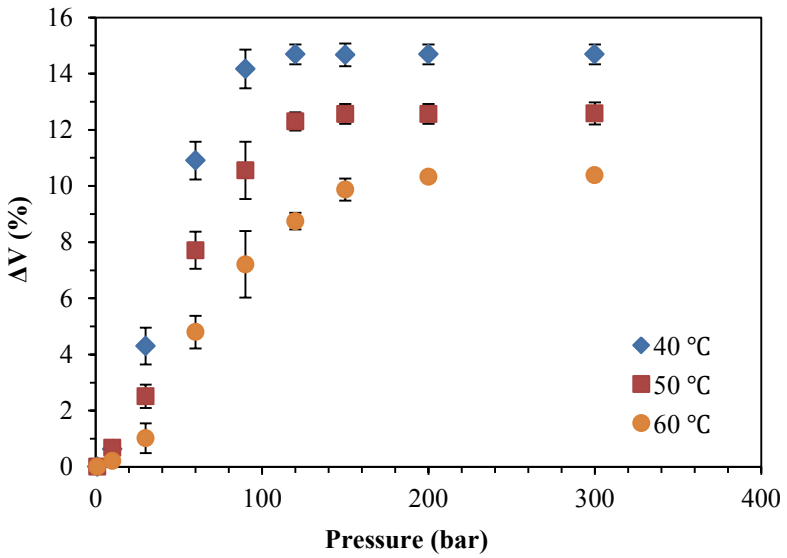

Figure 3.2: Relative volumetric expansion (ΔV%) of water in equilibrium with CO_2 as a function of pressure at different temperatures.

aqueous solutions in equilibrium with high pressure CO_2 whereas most of the studies focused on the investigation of lipid products, like fish oil (Seifried & Temelli, 2009), corn oil (Tegetmeier, Dittmar, Fredenhagen, & Eggers, 2000), canola oil (Jenab & Temelli, 2012) and cocoa butter (Calvignac, Rodier, Letourneau, Almeida dos Santos Pedro, & Fages, 2010). The overall trends obtained in this study were in agreement with those reported for lipid systems. The trend was also in agreement with that reported by Tegetmeier et al. (2000) for the relative volumetric expansion of water in contact with CO_2 up to 300 bar as 6.8% and 6.2% at 20°C and 40°C, respectively. They reported that temperature had a minor effect on the relative volumetric expansion in the 20-40°C range; however, a significant effect of temperature was found in this study in the range of 40-60°C. A relatively larger value (14.4%) for volumetric expansion was obtained in this research at 40°C.

Compared to this and other studies (Seifried and Temelli, 2009; Jenab and Temelli, 2012), where volumetric expansion reached a plateau around 100 bar for most isotherms, volumetric

expansion curves of oils reported by Tegetmeier et al. (2000) were still increasing even up to 300 bar. Since the method of mixing and the time to reach equilibrium with CO_2 were not provided and the approach to measure the liquid level was different, it is not possible to clearly elucidate the difference in volumetric expansion results obtained in this study and by Tegetmeier et al. (2000).

Microscopic images displaying the phase behaviors of water and phospholipid suspension in equilibrium with CO_2 at ambient and high pressures were shown in Fig. 3.3. Water in equilibrium with CO_2 was a transparent uniform system and its volume expanded as the pressure was elevated. In contrast, the light was not transmitted through the phospholipid suspension, thus, the meniscus of the liquid could not be detected from the camera image (Figs. 3.3 (g), (h)). Due to the surface tension of liquid, especially in the presence of surface active phospholipid molecules, the thickness of the depression interfered with the reading and the corresponding scale readings could not be obtained accurately.

3.3.2. Effect of pressure on liposome formation

The effect of pressure on the mean diameter and polydispersity index (PdI) of liposomes was shown in Fig. 3.4. Pressure had a significant effect ($p < 0.05$) on the particle size of liposomes. With an increase in pressure from 60 to 300 bar, particle size of liposomes was reduced from 553±5 nm to 523±2 nm. This indicated that a higher pressure of SC-CO_2 was favorable for the formation of smaller vesicles. The PdI of liposomes was also evaluated. Pressure also had a significant effect ($p<0.05$) on the uniformity of liposomes. With an increase in pressure, PdI was reduced from 0.278±0.011 to 0.226±0.009. PdI displays the size distribution of a vesicular system and values lower than 0.3 are attributed to a narrow size distribution and formation of a homogeneous colloidal system (Furneri, Fresta, Puglisi, & Tempera, 2000).

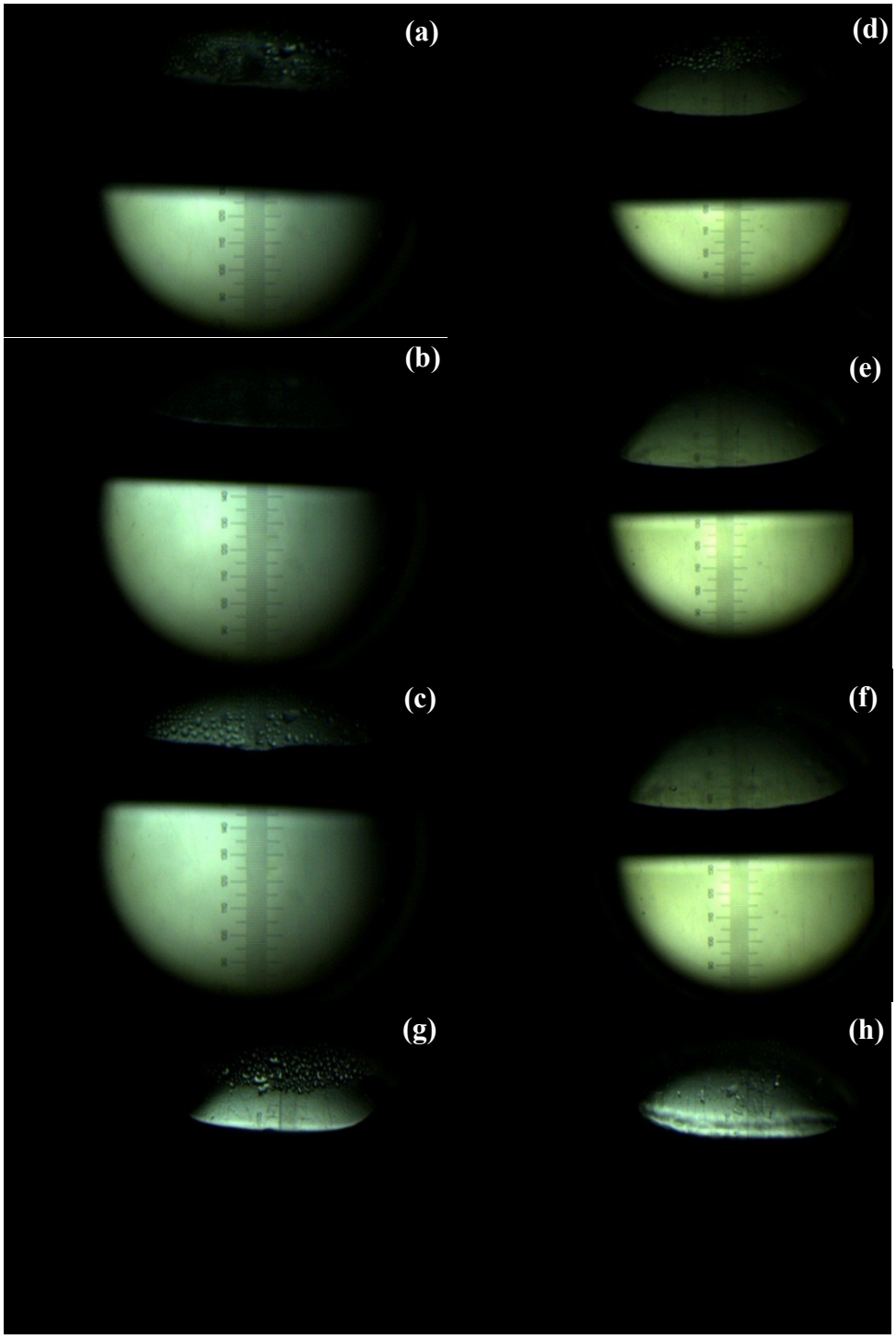

Figure 3.3: Microscopic images of phase behavior of water (a-f) and phospholipid suspension (g-h) in equilibrium with CO_2 at elevated pressure at (a-c) 40°C and (d-f) 60°C. (a)(d)(g) 1 bar, (b)(e) 90 bar, (c)(f) (h) 150 bar.

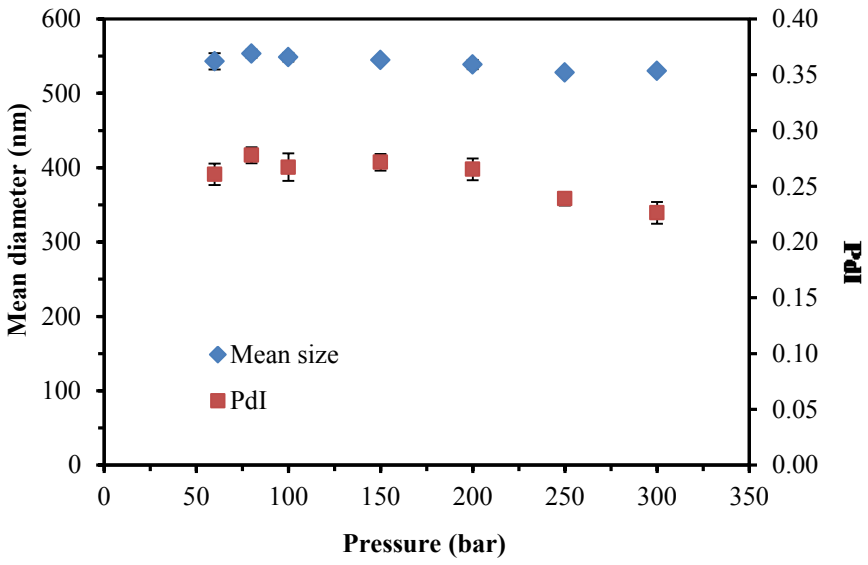

Figure 3.4: Effect of pressure on mean diameter and polydispersity index (PdI) of liposomes obtained using SC-CO_2 technology at 40°C and 60 bar/min.

The PdI value of below 0.3 suggested that the liposomes obtained had limited variation in particle size. The possible mechanism of liposome formation by SC-CO_2 technology has not been investigated in detail. However, based on the interpretation of the current results obtained with the system being depressurized from the top, CO_2 may be released from the liquid phase into the supercritical phase to compensate for the pressure difference, as CO_2 in the supercritical phase was gradually released from the exit line connected to the top portion of the vessel. Elevated pressure increases the amount of CO_2 accumulated within the phospholipid bilayers, which leads to scatter and breakup of the phospholipid bilayers into discrete molecules during depressurization. High pressure promotes better dispersion of the phospholipid molecules before they reorganize into liposomes and allows the formation of small vesicles. At each time point, a similar amount of CO_2 was solubilized and available for dispersion of phospholipid bilayers throughout each portion of the liquid phase. During depressurization, CO_2 was released uniformly from every portion of the liquid phase and led to low PdI and narrow size distribution

of liposomes. At a higher pressure, with more CO_2 accumulating within the bilayers, depressurization of the system takes longer. Therefore, a higher pressure yielded improved uniformity of liposomes. Size distribution curves of liposomes at different processing pressures were displayed in Fig. 3.5. As the pressure increased, a higher and narrower peak was obtained for particle size distribution, resulting in a lower PdI value. At least 200 bar was recommended to form small particles while 300 bar was recommended for high uniformity.

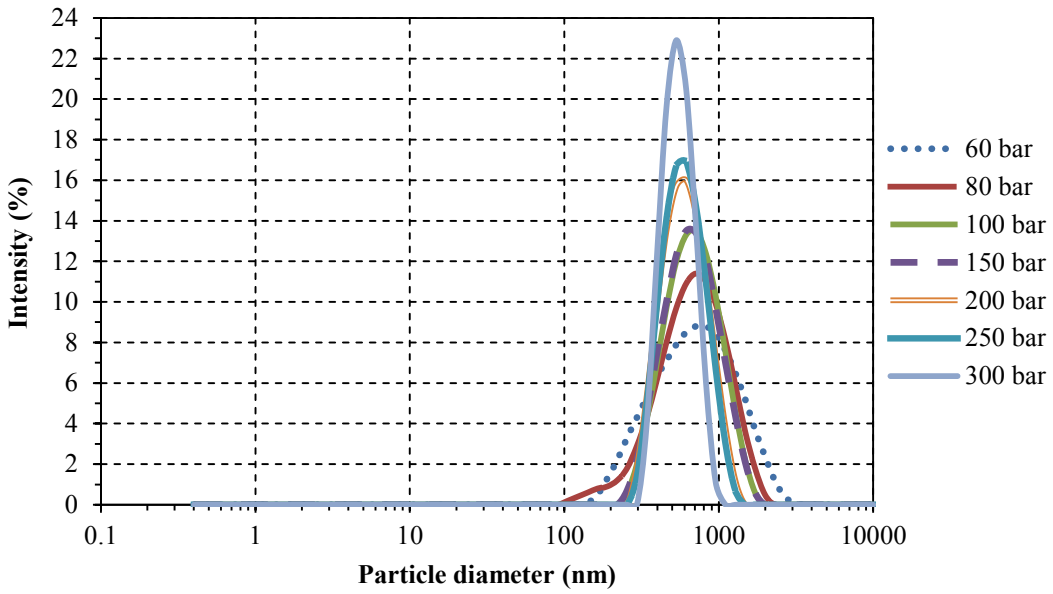

Figure 3.5: Size distribution of liposomes at different processing pressures using SC-CO_2 technology at 40°C and 60 bar/min.

3.3.3. Effect of depressurization rate on liposome formation

The effect of depressurization rate on liposome preparation was shown in Fig. 3.6. As the depressurization rate increased, particle size stayed constant without significant change ($p > 0.05$). This conclusion was in agreement with that of Otake et al. (2006), who used a similar method to prepare and evaluate the effect of depressurization rate on the particle size of liposomes loaded with glucose. With regard to the effect of pressure and depressurization rate on

liposome formation, it may be concluded that particle size depended mainly on the amount of CO_2 dissolved instead of the release rate of CO_2 in the liquid phase. However, depressurization rate had a significant effect on PdI of liposomes ($p<0.05$) obtained in this study. Overall, PdI was reduced from 0.290±0.003 to 0.198±0.016 at a higher depressurization rate. A low depressurization rate may not be sufficient to disperse phospholipid molecules thoroughly enough to enhance the uniformity of liposomes. Depressurization rate is an important parameter during the liposome formation process using SC-CO_2 and should be controlled with care. Fast depressurization rate yielded enhanced uniformity and may be more advantageous for liposome preparation. Slow depressurization usually causes a prolonged release of CO_2 from bilayers and may impair the dispersion of phospholipids. Depressurization rate of 120 bar/min was recommended to obtain a high homogeneity.

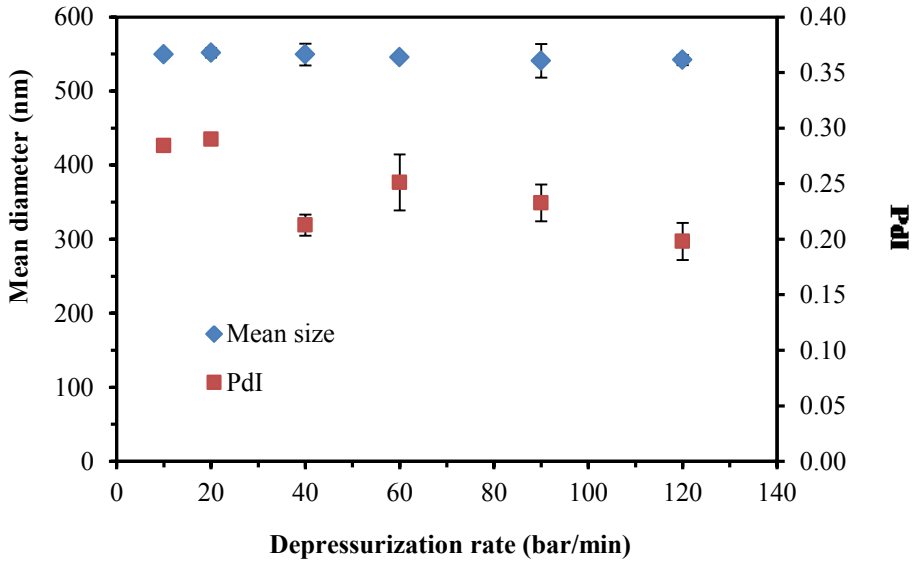

Figure 3.6: Effect of depressurization rate on mean diameter and polydispersity index (PdI) of liposomes obtained using SC-CO_2 at 40°C and 200 bar.

3.3.4. Effect of temperature on liposome formation

The effect of temperature on the mean diameter and PdI of liposomes was presented in Fig. 3.7. Temperature had a significant effect ($p < 0.05$) on the particle size of liposomes. As temperature increased, particle size dropped to 495±6 nm at 50°C and then increased to 535±6 nm. The trend of temperature effect can be ascribed to two opposing aspects. Elevated temperature can input energy and disrupt the van der Waals interactions between phospholipid molecules, thus, enhancing the mobility and fluidity of phospholipid bilayers (Quinn, 1981). This aspect contributes to the formation of smaller and more uniform vesicles (Kalepu, Manthina, & Padavala, 2013). On the other hand, elevated temperature leads to a reduced solubility of CO_2 in water and therefore weakens the dispersion of phospholipid molecules as less CO_2 would be present within the bilayers (Ferrentino et al., 2012), which results in the formation of larger vesicles. Thus, the decrease in particle size in the lower temperature range may be dominated by

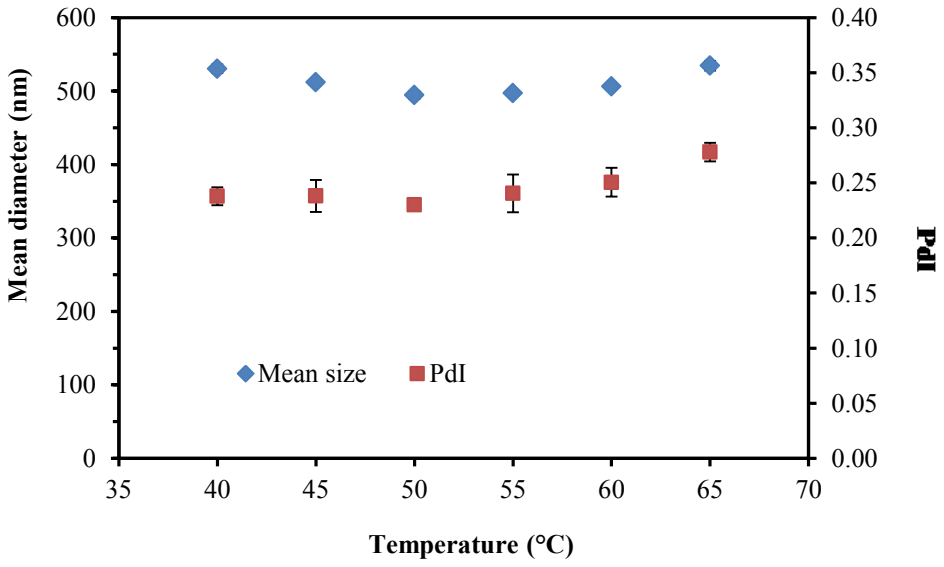

Figure 3.7: Effect of temperature on mean diameter and polydispersity index (PdI) of liposomes obtained using SC-CO_2 at 200 bar and 60 bar/min.

enhanced fluidity of bilayers whereas the increase in particle size in the higher temperature range was mainly controlled by reduced solubility of CO_2. Temperature also had a significant effect ($p<0.05$) on the PdI of liposomes. Uniformity of liposomes remained constant from 40°C to 60°C and then started to increase. This may be attributed to the reduced solubility of CO_2 in between the bilayers, as a small amount of CO_2 may not be sufficient to thoroughly separate the phospholipid molecules. A temperature of 50°C was recommended for smaller size and better uniformity of liposomes.

3.3.5. Morphology of liposomes

The TEM images with regard to internal (a-d) and external (e-f) structures for the discrete liposomes prepared at different pressures were shown in Fig. 3.8. The external and internal images were defined since they are captured simultaneously by the TEM measurement. Liposomes may distribute at different levels in the thin layer of the specimen. When the electron beam was applied, most of liposomes stay intact while a small amount of liposomal vesicles on the surface layer of the specimen could be fractured by the electron beam. Thus, it was possible to capture the external and cross-sectional morphology simultaneously. The external images showed the surface morphology of liposomes, like shape or clusters attached to vesicles, while the internal images reflected the cross-sectional characteristics of liposomes, like shape, intactness or inclusions. Based on the internal images, as the pressure increased, more spherical vesicles could be obtained. Liposomes prepared at the low pressure range showed more irregularity and asymmetry in their appearance while liposomes obtained at the higher pressure range (100-300 bar) displayed spherical shape. Hence, at least 100 bar was recommended for liposome preparation to achieve a spherical morphology. Higher pressure leads to thorough dispersion of phospholipid molecules due to increased solubility of CO_2, which may be

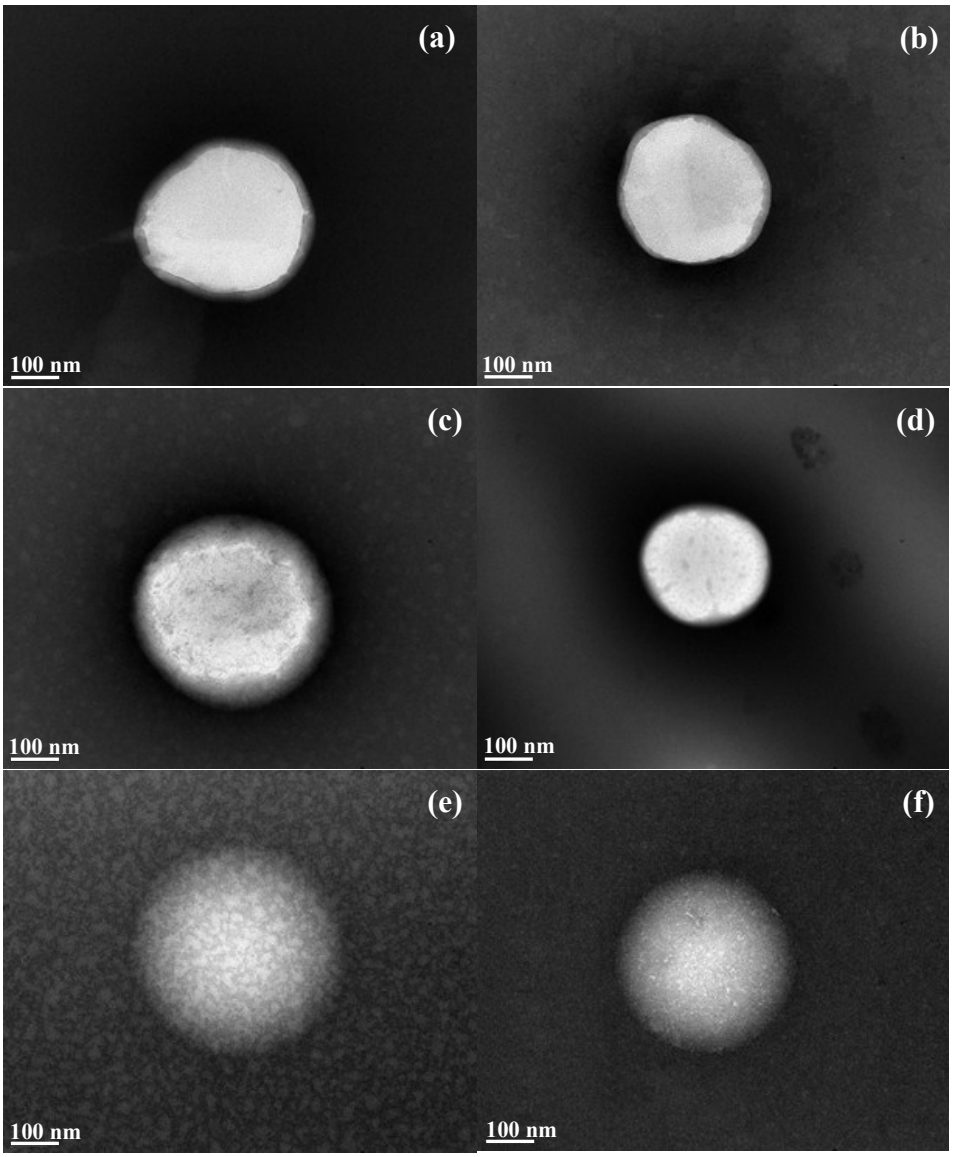

Figure 3.8: Transmission electron microscopy (TEM) images of internal (a-d) and external (e-f) structures of discrete liposomes prepared by SC-CO_2 technology at 40°C and 60 bar/min at different pressures**:** (a) 60 bar, (b) 80 bar, (c)(e) 100 bar, (d)(f) 300 bar.

beneficial for the formation of a spherical shape. Internal images also demonstrated that vesicles prepared at different pressures using SC-CO_2 were intact without leakage (no dye entered so only brightness detected), even though no cholesterol was added, as is typically done in conventional processes (Justo & Moraes, 2011). This may indicate that during depressurization, the SC-CO_2

method could yield stable liposomes without destruction or deformation of vesicles, which was also common in conventional preparation methods. The external images at 100 bar and 300 bar displayed perfectly spherical vesicles and distinct surface, verifying the shapes concluded based on internal images. The morphology of bulk vesicles at 300 bar and two different depressurization rates was shown in Fig. 3.9. Both images showed liposomes with spherical shapes without leakage in the bulk vesicular system. Liposomes prepared at the depressurization rate of 20 bar/min showed relatively high heterogeneity while those at 120 bar/min displayed pronounced homogeneity, which confirmed the trend of depressurization rate on the PdI in Fig. 3.6.

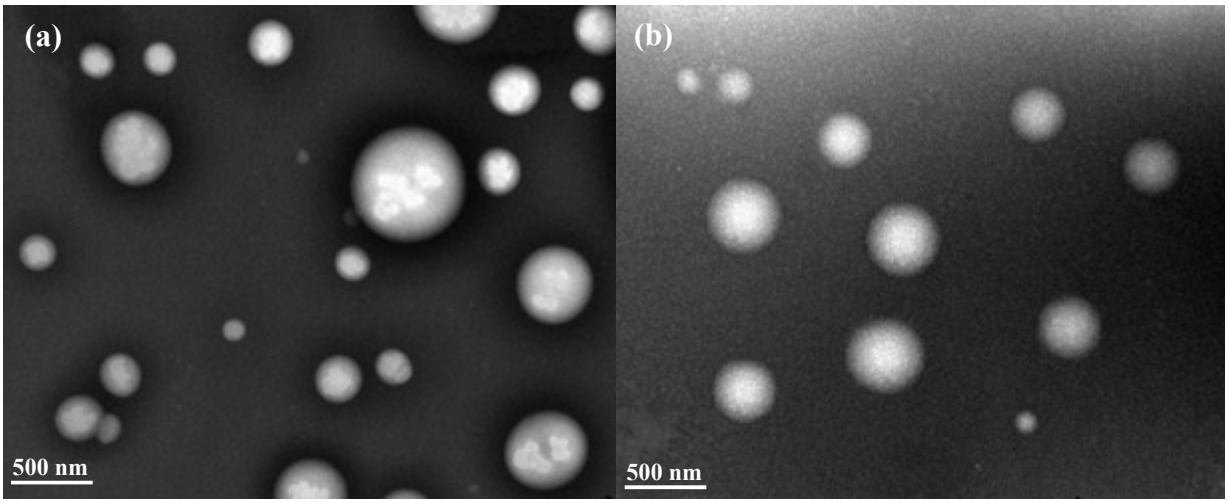

Figure 3.9: Transmission electron microscopy (TEM) images of bulk liposomes prepared by SC-CO_2 at 50°C and 300 bar at different depressurization rates: (a) 20 bar/min, (b) 120 bar/min.

3.3.6. Storage stability of liposomes

The change in particle size and images of liposomes throughout storage time were shown in Figs. 3.10 and 3.11, respectively. For all the processing pressures tested, liposomes prepared using SC-CO_2 remained stable for up to 4 weeks with minimal change in particle size (below

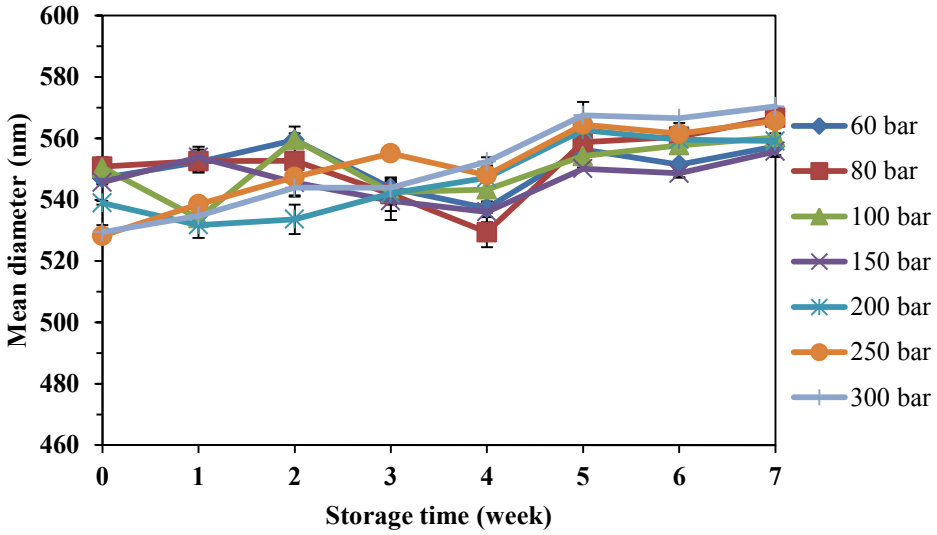

Figure 3.10: Storage stability of liposomes prepared at different pressure using SC-CO_2 technology at 40°C and 60 bar/min. Storage condition: light proof, ambient temperature (25°C) under nitrogen.

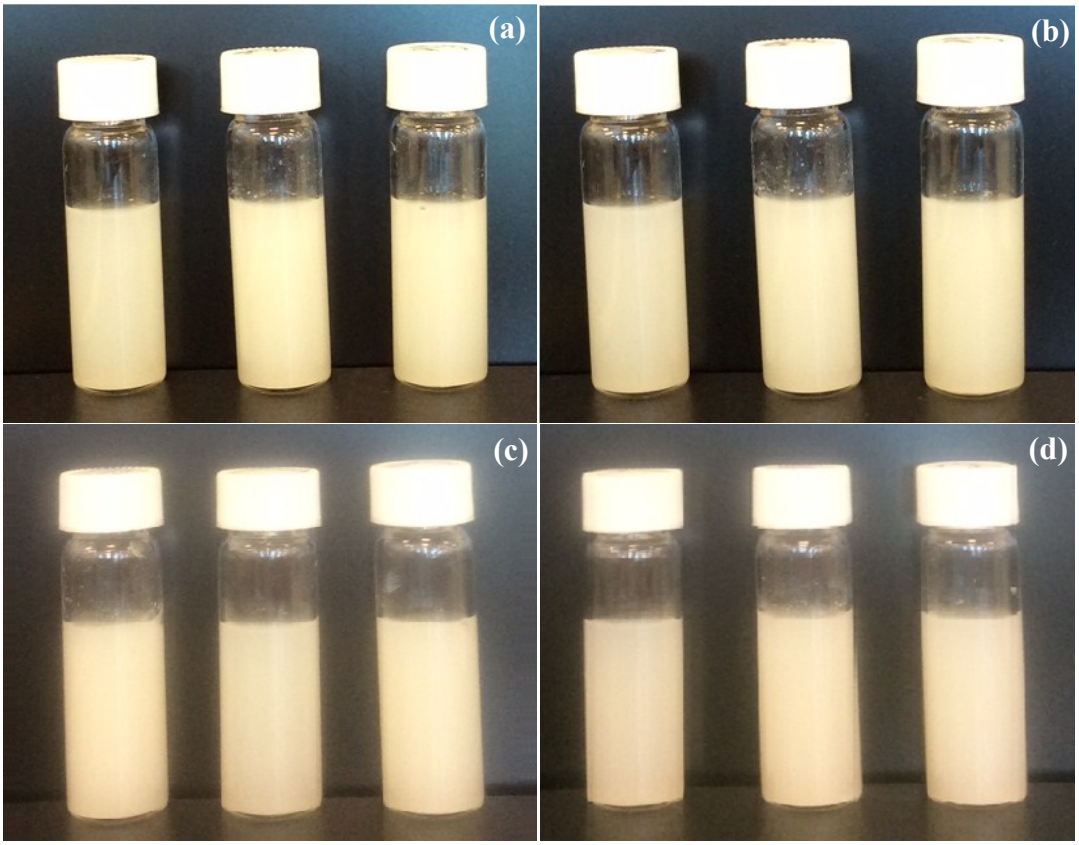

Figure 3.11: Storage stability of liposomes prepared using SC-CO_2 at 40°C, 200 bar and 60 bar/min. Storage time: (a) Fresh; (b) 4 weeks; (c) 6 weeks; (d) 8 weeks.

5%). Low pressure range (60-150 bar) gave higher stability of liposomes than the high pressure range (200-300 bar). For instance, at 5 weeks of storage, particle size of liposomes prepared at 80 bar increased by 1.5% while that of liposomes obtained at 300 bar increased by 7.2%. Images of liposomes during storage demonstrated no phase separation or particle deposition for up to 8 weeks, which indicated superior stability of this vesicular system over those prepared by conventional methods. The zeta potential of liposomes was measured and a relatively high value of -70.17±0.75 mV was found for liposomes prepared at 200 bar and 40°C. Particles with a zeta potential value greater than 30 mV or less than -30 mV are generally considered to be stable (Hunter et al., 2001). The value obtained indicated that a relatively high repulsive interaction existed between liposomes to prevent their aggregation, thus accounting for a longer stability during storage (Laouini et al., 2012).

3.3.7. Comparison of liposomes obtained by different methods

Liposomes were also produced using the conventional method of TFH for comparison. Liposomes prepared by the TFH method had a mean diameter of 474±14 nm and a PdI of 0.370±0.121. Thus, compared to the supercritical method of preparation, the TFH method yielded liposomes with a relatively smaller particle size but higher heterogeneity. The micrographic image of liposomes showed various morphology and relatively high heterogeneity in the vesicles prepared via TFH (Fig. 3.12). Considerable leakage in the vesicles was detected for conventional preparation, which indicated that the particles had some degree of deformation or destruction. Compared with the bulk liposomes obtained by the SC-CO_2 method (Fig. 3.9), the difference was quite pronounced.

These findings demonstrated that the supercritical technology was superior to the conventional TFH method, considering that it could yield spherical and stable liposomes, even

without the addition of cholesterol or a surfactant, which is commonly used in conventional techniques. These results provide the basis for the encapsulation of hydrophobic and hydrophilic food-derived bioactives into liposomes using the SC-CO_2 method. Hydrophilic compounds, like polyphenols, water-soluble vitamins and minerals can be protected from extreme food processing conditions. Hydrophobic compounds, like carotenoids, phytosterols and fatty acids, can be dispersed in water-based beverages with ease. This is advantageous and promising for the encapsulation of high-value components into a variety of food products with enhanced nutritional value and for additional health benefits. Plus, the scaling up of liposome production using this technique can be easily achieved.

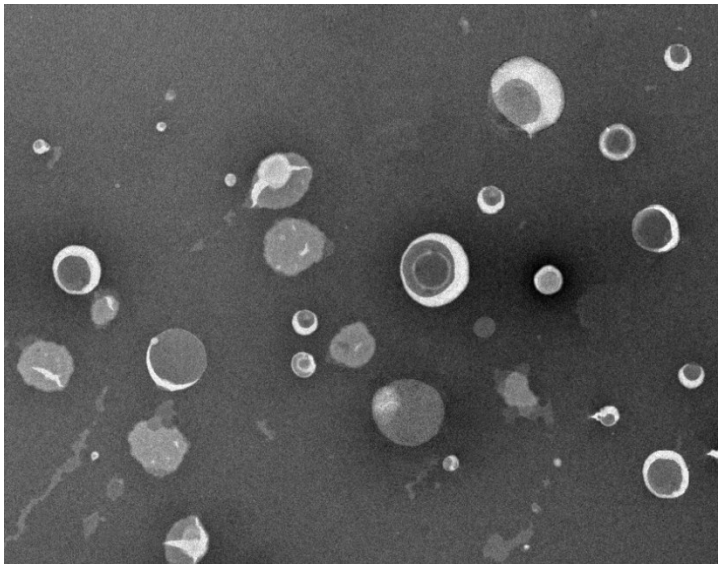

Figure 3.12: Transmission electron microscopy (TEM) images of bulk liposomes prepared by thin film hydration method at 50°C.

3.4. Conclusions

The effects of pressure, depressurization rate and temperature on the liposome preparation using SC-CO_2 technology were investigated, employing the route of depressurization of the supercritical phase. Sufficient dispersion of phospholipid molecules prior to their reorganization

to form vesicles is crucial for the SC-CO_2 processing. Pressure of 200 bar, depressurization rate of 120 bar/min and temperature of 50°C were recommended to prepare high quality liposomes. Higher pressure contributed to the formation of smaller vesicles while higher depressurization rate boosted the homogeneity of vesicles. Pressure of at least 100 bar was recommended to achieve a spherical morphology. Due to the high zeta potential, liposomes displayed relatively high stability for up to 4 weeks during storage. SC-CO_2 technology shows advantages over the conventional TFH preparation method and offers great promise as a potential carrier, encapsulating a variety of valuable compounds.

CHAPTER 4 – PREPARATION OF UNLOADED LIPOSOMES USING SUPERCRITICAL CARBON DIOXIDE VIA DEPRESSURIZATION OF LIQUID PHASE[2]

4.1. Introduction

Development of delivery systems by encapsulating valuable pharmaceutical or bioactive components has become a major focus of recent research with promising perspectives (de Melo, Danh, Mammucari, & Foster, 2014). Liposomes are powerful delivery systems, which can efficiently transport active components for enhanced therapeutic efficiency (Freitas, Merkle, & Gander, 2005). Liposomes are one type of versatile and biodegradable vesicles, allowing encapsulation of hydrophilic and hydrophobic components, offering great protection of active ingredients. As described in Chapter 2, the drawbacks associated with the conventional preparation methods of liposomes such as residues of organic solvents, high energy cost and multi-step operations limit their applications in specific areas with increased processing costs. Thus, development of an innovative preparation approach to overcome some of the above disadvantages but yield desirable characteristics is needed. Supercritical carbon dioxide (SC-CO_2) technology offers promising perspectives in liposome preparation as an alternative to conventional techniques. With depressurization and release of CO_2, no solvent residue remains in the liposome products avoiding such concerns. Plus, a mild operation temperature just above the critical temperature (31°C) is ideal for processing and encapsulation of thermolabile compounds.

Several methods using supercritical fluids have been developed to produce liposomes, such

[2]A version of this chapter has been published: Zhao, L., & Temelli, F. (2015). Preparation of liposomes using a modified supercritical process via depressurization of liquid phase. *The Journal of Supercritical Fluids, 100*, 110-120.

as the rapid expansion of supercritical solution into a liquid solvent (RESOLV) (Wen et al., 2011), supercritical anti-solvent (SAS) (Lesoin, Crampon, Boutin, & Badens, 2011), depressurization of expanded liquid organic solution (DELOS) (Cabrera et al., 2013; Cano-Sarabia et al., 2008) as well as supercritical reverse phase evaporation (SCRPE) (Otake et al., 2001) and its improved version (ISCRPE) (Otake et al., 2006). Although much progress has been made, several challenges, primarily the usage of organic solvent or surfactant (RESOLV and DELOS), relatively large liposome size (SCRPE, ISCRPE), relatively heterogeneous size distribution and morphology (SCRPE), and multistep preparation (SAS), still remain to be resolved in supercritical preparation approaches. Among these methods, two processes are of great interest to generate excellent characteristics. For the ISCRPE method (Otake et al., 2006), a sample of phospholipids dispersed in pure water was saturated with CO_2 under pressure and depressurized from the top supercritical phase, which was advantageous because it was free of organic solvent and surfactant. For the DELOS method (Cano-Sarabia et al., 2008), a sample solubilized in an organic solvent and saturated with pressurized CO_2 was depressurized from the bottom expanded liquid phase with a large pressure drop from 100 bar to ambient pressure at a high depressurization rate, which was advantageous for obtaining small liposome size and uniformity. Therefore, there is potential to develop an improved process combining the advantages of the ISCRPE and DELOS techniques by employing a similar phospholipid in water suspension as in ISCRPE and a depressurization protocol as in DELOS, for improved liposomal characteristics.

The main objective of this study was to develop an improved SC-CO_2 technique for the formation of liposomes. The specific objective was to evaluate the influence of the major processing parameters (pressure, depressurization rate, temperature and depressurization protocol)

on the liposomal characteristics (particle size distribution, zeta potential, morphology and stability). Furthermore, the quality of liposomes prepared with the SC-CO_2 method was compared to that obtained with the traditional thin film hydration (TFH) method.

4.2. Materials and methods

4.2.1. Materials

Soy lecithin (Fisher Scientific, Ottawa, ON, Canada) was used for liposome formation. Liquid CO_2 (Praxair Canada, Mississauga, ON, Canada) with a purity of 99.99% was used for the process to prepare liposomes. Water purified by a Milli-Q® advantage a10 ultrapure water purification system (EMD Millipore, Billerica, MA, USA) was used in all experiments.

4.2.2. Preparation of phospholipid suspension

The preparation of crude phospholipid suspension was performed in a similar manner as described in Section 3.2.2.

4.2.3. Preparation of liposomes using SC-CO_2

The experimental apparatus for liposome preparation (Fig. 4.1) was similar to that described in Section 3.2.3, except it was modified by switching the micrometering valve and on/off valve at positions F and I. In this case, the micrometering valve was used to depressurize the high pressure mixture from the liquid phase. The unloaded liposomes were produced in a batch mode. Soy lecithin suspension (6 mL) was placed inside the high pressure view cell. The liquid level as well as the condition of the suspension during the pressurization and mixing process could be observed through the sapphire windows and the camera attached to the system. After sealing the top with a lid, the vessel was gently flushed with CO_2 to remove the air trapped inside. The vessel was equilibrated until the set temperature was reached and then pressurized with CO_2 up to the required pressure. A magnetic stirrer at the bottom of the cell was used for thorough

mixing of the cell contents at 550 rpm for 1 h to reach equilibrium. CO_2-expanded liquid phase was then depressurized through a micrometering valve at position I (Fig. 4.1). To achieve a targeted constant depressurization rate, preliminary tests were performed and the specific position on the scale of the micrometering valve corresponding to a certain depressurization rate was recorded. This valve position was then applied during liposome preparation to achieve the desired depressurization rate. In this system, liposomes were formed through depressurization of

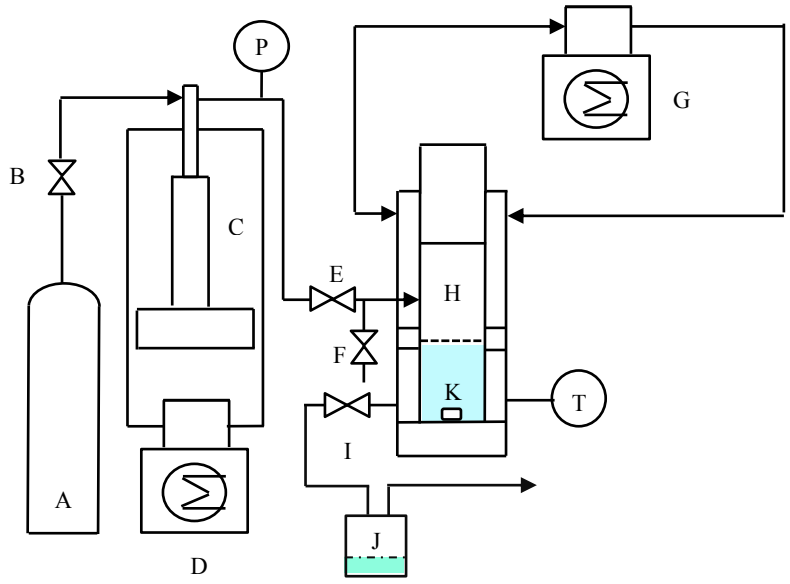

Figure 4.1: Schematic flow diagram of SC-CO_2 system. (A) CO_2 tank; (B) (E) (F) on/off valves; (C) ISCO syringe pump; (D) refrigeration bath; (G) water bath; (H) high pressure view cell; (I) micrometering valve; (J) sample vial; (K) magnetic stirrer; (P) pressure gauge; (T) thermocouple.

the CO_2-expanded liquid phospholipid suspension phase using two different protocols: (I) at a constant depressurization rate and (II) at constant depressurization rate while also maintaining the pressure inside the cell constant. For Protocol (I), valves E and F were closed and the sample was depressurized through the micrometering valve I, while for Protocol (II), valve F was closed, but more CO_2 was introduced into the cell to maintain constant pressure by keeping valve E open and the sample was depressurized similarly through the micrometering valve I (Fig. 4.1).

Liposome suspension was collected in vial J for further analysis. For the experimental design, the effect of processing parameters (pressure, depressurization rate and temperature) on liposome formation by the improved supercritical method was investigated. The experimental conditions employed were summarized in Table 4.1.

The configuration of the high pressure vessel in the high pressure unit is such that the depressurization valve I outlet is located on the side close to the bottom. Thus, a small amount of liquid (~1 mL) is left in the vessel after the liquid phase is depressurized through valve I. In the earlier sets of experiments (effects of pressure and depressurization rate), the residual liquid in the vessel was combined with the liquid collected through valve I; therefore, the analysis results reflect the combined sample. However, upon further analysis of the two liquid portions separately, it became apparent that the small amount of liquid left in the vessel had a larger particle size (~1 μm) compared to the liquid collected through valve I since the depressurization mechanisms of the two liquid portions are different. Therefore, in the later sets of experiments (effect of temperature), the small portion left behind in the vessel was discarded and only the portion collected through valve I was analyzed and reported.

Table 4.1: Processing conditions of SC-CO_2 method.

Factors	**Levels**	**Constant parameters**
Pressure (bar)	60, 80, 100, 150, 175, 200,	40°C, 60 bar/min
Depressurization rate (bar/min)	10, 20, 40, 60, 90, 120	40°C, 200 bar
Temperature (°C)	40, 45, 50, 55, 60, 65	300 bar, 60 bar/min

4.2.4. Preparation of liposomes by TFH

The preparation of liposomes by the TFH method was conducted in a similar manner as described in Section 3.2.6.

4.2.5. Particle size distribution

The determination of mean size and size distribution of unloaded liposomes was performed in a similar manner as described in Section 3.2.7.

4.2.6. Zeta potential

The determination of zeta potential of unloaded liposomes was performed in a similar manner as described in Section 3.2.8.

4.2.7. Morphology

The general morphology of unloaded liposomes via the TEM technique was performed in a similar manner as described in Section 3.2.9. In addition, the morphology and lamellarity of liposomes were also evaluated using cryogenic transmission electron microscopy (cryo-TEM). A 5 μL sample was placed on a copper grid coated with a carbon holey film. After adhering for 1 min, the grid was gently blotted to obtain a thin film (100-300 nm) of liquid. The grid was plunged into liquid ethane (-180°C) for vitrification and transferred into liquid nitrogen (-196°C). The vitrified sample placed in liquid nitrogen was transferred for examination under a JEM-2200FS transmission and scanning transmission electron microscope (TEM/STEM) (JEOL USA, Inc., Peabody, MA, USA). The operating temperature was -181°C, and the acceleration voltage was controlled at 200 kV. Images of the liposomes within holes were observed and recorded by an ultrascan 1000 TEM CCD camera (Gatan Inc., Pleasanton, CA, USA).

4.2.8. Storage stability

The storage stability of unloaded liposomes was measured for up to 8 weeks in a similar manner as described in Section 3.2.10.

4.2.9. Statistical analysis

At each processing condition, liposome samples were prepared in triplicate. The mean particle size, size distribution, zeta potential and stability of each sample were also analyzed in triplicate. Data analysis was performed using Minitab statistics software 16 (Minitab Inc., State College, PA, USA) and reported as the mean ± standard deviation (SD). One-way (preparation method) and two-way (pressure, depressurization rate, temperature with the depressurization protocol, individually) analyses of variance (ANOVA) were conducted and significant differences between means were obtained by Tukey's multiple comparison test at a significance level of $p < 0.05$.

4.3. Results and discussion

4.3.1. Possible mechanism of liposome formation

One possible mechanism of liposome formation by the improved supercritical method was proposed in Fig. 4.2. The formation of liposomes was achieved through pressurization and depressurization steps, which led to a “dispersing effect” by CO_2 release upon depressurization. At ambient conditions, phospholipid molecules exist primarily in the form of a bilayer or curvature when dispersed in water (Templeton & Lasic, 1999). After pressurization, CO_2 molecules solubilize in water rapidly and establish equilibrium with water to form carbonic acid, where a considerable amount of CO_2 molecules would still be present in the unhydrated state (Erkmen, 2012). Unhydrated CO_2 can diffuse and accumulate in between the hydrophobic fatty acyl chains of phospholipids and between the phospholipid monolayers, thus, expanding the

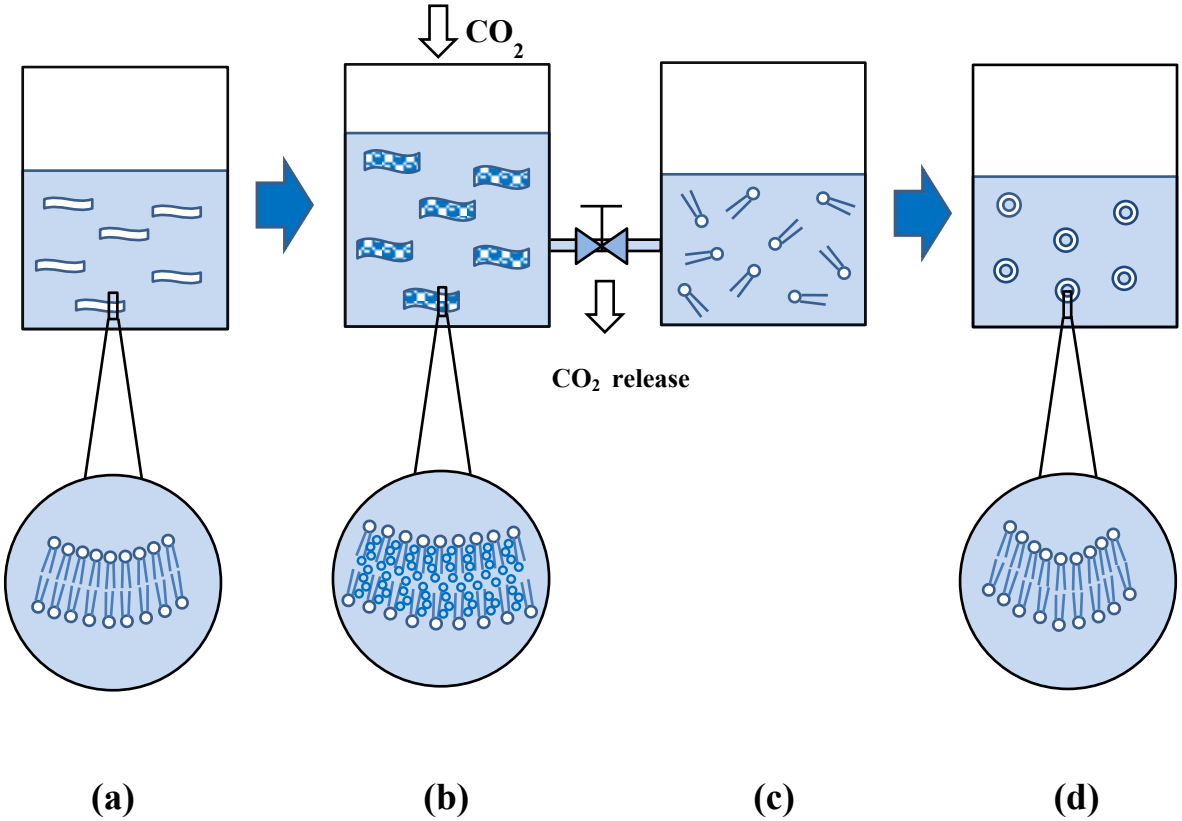

Figure 4.2: Schematic mechanism of liposome formation by the improved supercritical method: (a) phospholipid curvatures present at ambient condition, (b) formation of expanded phospholipid bilayers after pressurization and equilibration with CO_2, (c) formation of instantaneous dispersion of discrete phospholipid molecules during depressurization of CO_2, (d) formation of liposome vesicles due to hydrophobic interaction after depressurization.

length and thickness of the bilayer (Kamihira, Taniguchi, & Kobayashi, 1987). Upon depressurization, CO_2 molecules would be released rapidly from between the fatty acyl chains and break up the curvatures into separated phospholipids, which would form an instantaneous dispersion of discrete phospholipid molecules. The extent of this break up would depend on pressure and depressurization rate as discussed later. Due to hydrophobic interactions, separated phospholipid molecules would reassemble spontaneously into a spherical bilayer to form liposomes. The break up effect of phospholipids by this pressurization-depressurization process may be similar to that in conventional homogenization. However, due to the phase transition of

CO_2 during depressurization as it is released from the liquid phase to gas phase, heat is removed from the phospholipid suspension, resulting in a temperature drop in the liposome suspension as opposed to the introduction of heat into the system in the case of conventional homogenization. This cooling effect may be favorable for encapsulation of thermally labile compounds into liposomes. The above proposed mechanism seems plausible to explain the liposome formation process. Lesoin, Boutin, Crampon, and Badens (2011) reported the behavior of CO_2/water/surfactant tertiary system under supercritical conditions, but the real behavior may vary according to surfactant type and its packing characteristics. Verification of the proposed mechanism is needed based on the characterization of the physico-chemical fundamentals of the system, which is beyond the scope of the current study. In this study, the mechanism depicted in Fig. 4.2 was adopted to explain the effects of the different processing parameters.

4.3.2. Effect of pressure on liposome formation

The size distribution curves of liposomes obtained with both protocols at 80, 200 and 300 bar were shown in Fig. 4.3. Protocol (II) showed advantages over protocol (I) and yielded a more uniform size distribution, especially at higher pressures. Although the liposomes obtained displayed a bimodal size distribution at all pressures, the mean particle diameter was used for comparison between different processing conditions and polydispersity index was used to assess the overall uniformity of particles. The effects of pressure on particle size and polydispersity index (PdI) of liposomes obtained by the depressurization protocols (I) and (II) were shown in Figs. 4.4 (a) and (b), respectively. Particle size refers to the mean hydrodynamic diameter of liposomes calculated based on the Stokes-Einstein equation of Brownian motion (Wengeler & Nirschl, 2007). With an increase in pressure, the particle size of liposomes was reduced significantly ($p<0.05$) for both protocols. From 60 to 300 bar, particle size was reduced from

326±4 nm to 265±4 nm and 307±9 nm to 214±3 nm for protocols (I) and (II), respectively. According to the CO_2 solubility data in water (Dodds et al., 1956; Ferrentino et al., 2012), elevated pressure increased CO_2 solubility in the liquid phase and thus introduced more unhydrated CO_2, which would accumulate in between the phospholipid bilayers and scatter phospholipid molecules upon depressurization. This is favorable for better dispersion of phospholipids due to an elevated dispersion force and weakened interactions between fatty acyl chains. Uniform phospholipid dispersion may allow discrete phospholipid molecules to rearrange

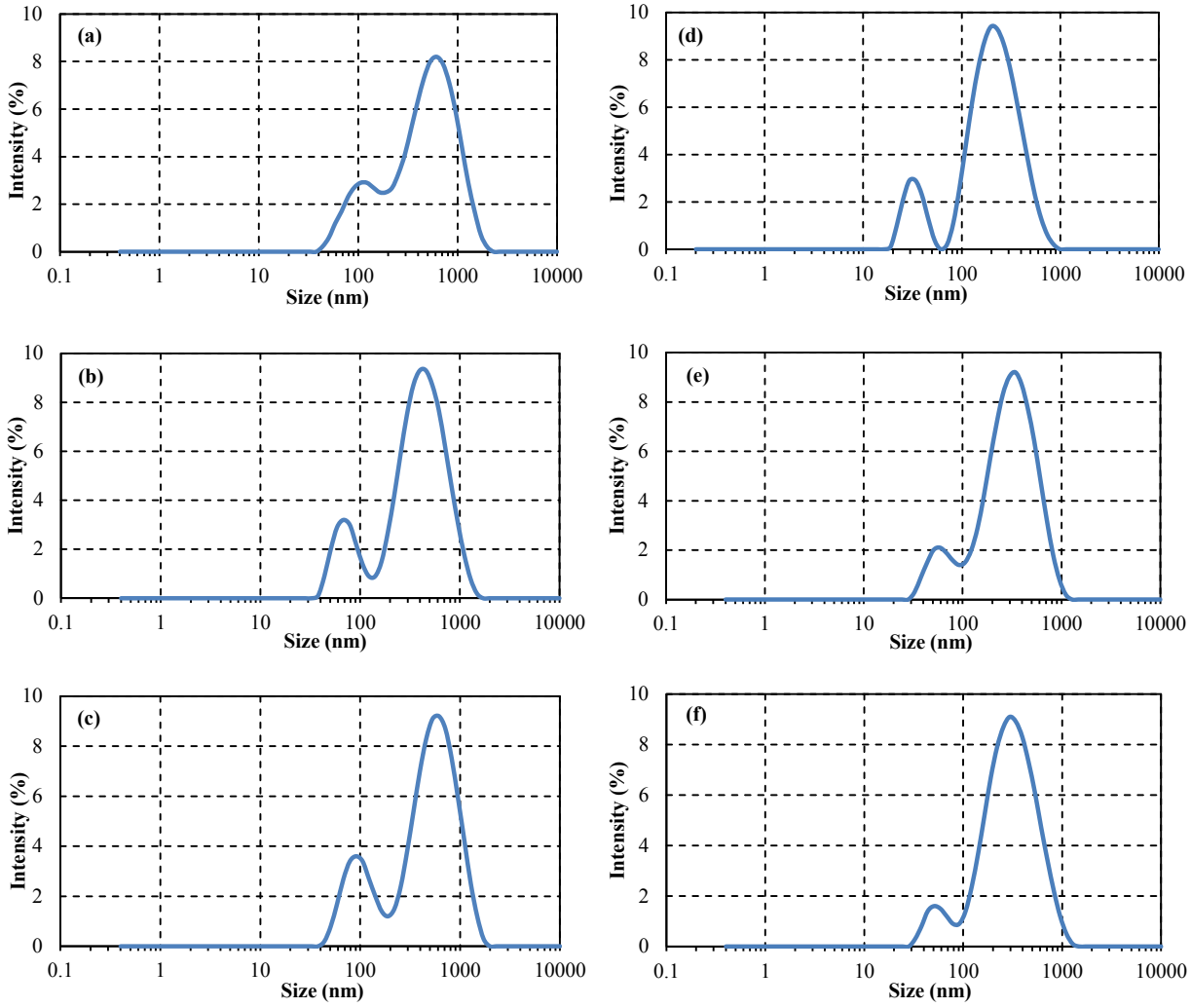

Figure 4.3: Size distribution of liposomes obtained at different pressures using depressurization protocol (I) (a-c) and protocol (II) (d-f): (a)(d) 80 bar, (b)(e) 200 bar, (c)(f) 300 bar.

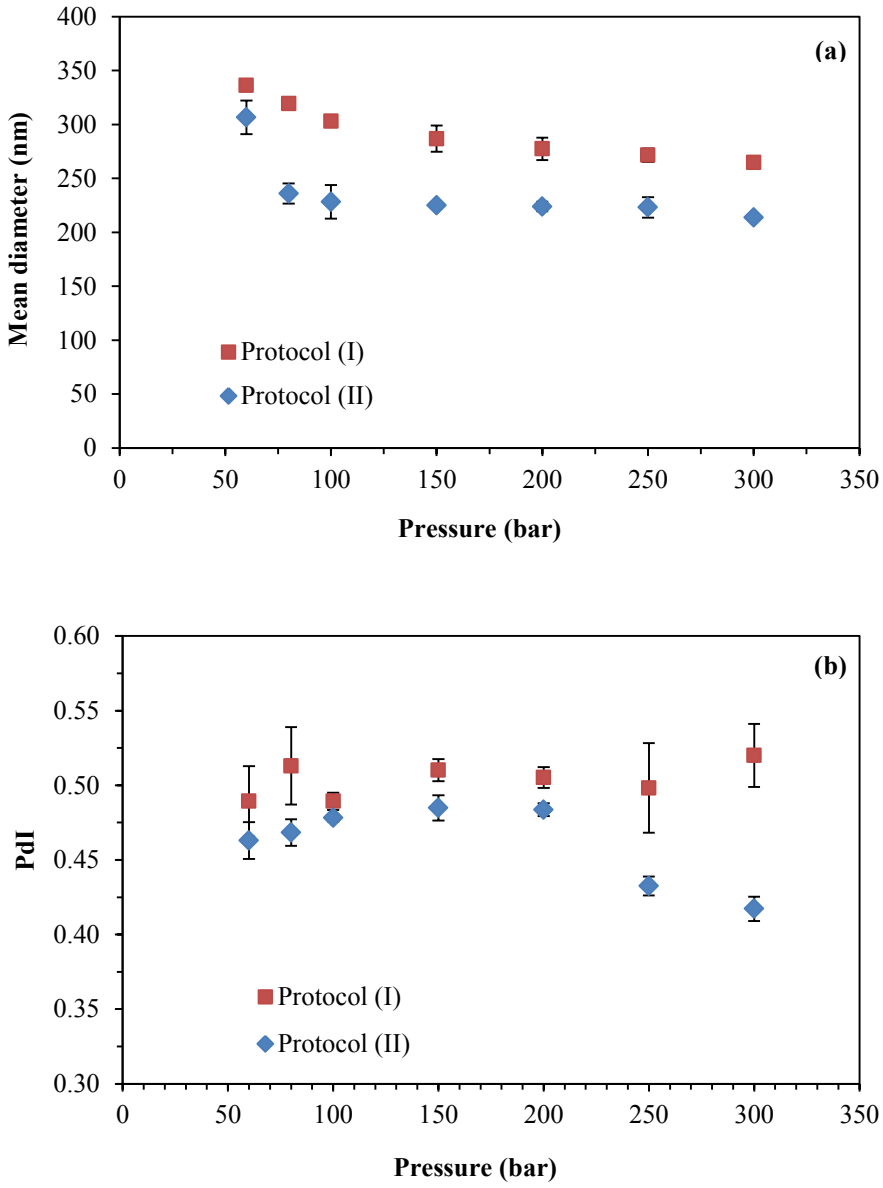

Figure 4.4: Effect of pressure on (a) particle size and (b) polydispersity index (PdI) of liposomes obtained using depressurization protocols (I) and (II) at 40°C and 60 bar/min.

into small vesicles of liposomes. For both protocols shown in Fig. 4.4 (a), compared to the higher pressure range, a larger decrease in particle size was achieved at the low pressure range (60 to 100 bar), since a larger increase in CO_2 solubility in water was shown within this pressure range in contrast to higher pressures (Dodds et al., 1956). Protocol (II) produced smaller particles than

protocol (I) due to the constant pressure maintained within the cell and bilayers during the depressurization of the liquid phase and thus CO_2 dissolved in liquid water was not released into the gas phase within the view cell throughout the depressurization step.

The PdI of liposomes was also evaluated. PdI values below 0.2 are usually considered monodisperse, while those greater than 0.7 are considered highly polydisperse. With an increase in pressure, there was no significant change ($p > 0.05$) in PdI for protocol (I), whereas for protocol (II) the PdI increased significantly ($p < 0.05$), from 0.463±0.012 to 0.484±0.008 at 60 to 200 bar and then dropped to 0.417±0.008. PdI data indicated that the improved supercritical method at these conditions yielded relatively heterogeneous size distribution of liposomes and the uniformity of liposomes should be improved further. However, the fact that the residual sample in the vessel was combined with the sample collected through the depressurization valve in these set of samples would have contributed to the heterogeneity observed in the results. Protocol (II) yielded a smaller PdI value than protocol (I) ($p < 0.05$), indicating a more uniform size distribution of liposomes. In summary, a pressure of at least 150 bar and 100 bar, respectively, is recommended to form relatively small particles for protocols (I) and (II).

4.3.3. Effect of depressurization rate on liposome formation

The effects of depressurization rate on the particle size and PdI of liposomes obtained by depressurization protocols (I) and (II) were presented in Figs. 4.5 (a) and (b), respectively. With an increase in the depressurization rate at 200 bar, particle size of liposomes was reduced significantly ($p < 0.05$) for both protocols. From 10 to 40 bar/min, particle size was reduced from 343±7 nm to 287±2 nm and 249±2 nm to 231±1 nm for protocols (I) and (II), respectively, and then remained constant. Relatively smaller particle size could be achieved when the depressurization rate was above 40 bar/min. A similar trend of particle size was obtained with

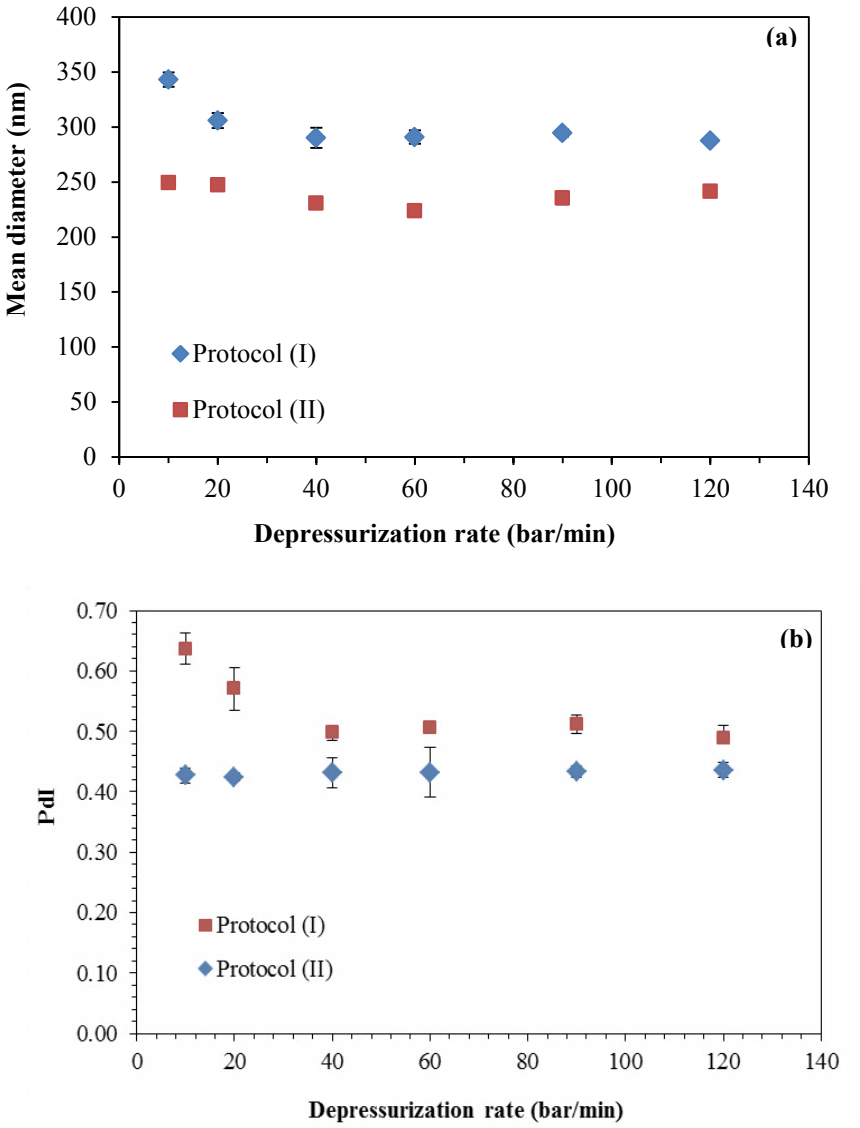

Figure 4.5: Effect of depressurization rate on (a) particle size and (b) polydispersity index (PdI) of liposomes obtained using depressurization protocols (I) and (II) at 40°C and 200 bar.

size stayed constant regardless of the depressurization rate (data not shown). This may indicate that at a high pressure (200-300 bar) and higher depressurization rate, the formation of liposomes may primarily depend on the amount of CO_2 solubilized in the bilayer and interacting with the fatty acyl chains of phospholipids instead of the release rate. In contrast, low depressurization rate, even at a high pressure, may not be as sufficient as the higher rate to separate the phospholipid bilayers into discrete molecules before reassembly into liposomes, and therefore

leading to a larger size. With the increased depressurization rate, the PdI of liposomes had a significant change ($p < 0.05$) for protocol (I), which was reduced from 0.637±0.003 to 0.492±0.004 nm with an increase in depressurization rate from 10 to 40 bar/min and then remained constant. For protocol (II), there was no change in PdI ($p>0.05$) with depressurization rate. The reason for this difference between the two protocols may be similar to that for particle size. A low depressurization rate may not be sufficient to separate the phospholipid bilayers thoroughly so that the uniformity of liposomes was reduced. Overall, at least 40 bar/min was recommended for liposome formation.

4.3.4. Effect of temperature on liposome formation

The effects of temperature on the particle size and PdI of liposomes obtained by depressurization protocols (I) and (II) were presented in Figs. 4.6 (a) and (b), respectively. With an increase in temperature, particle size first decreased and then increased ($p<0.05$) for both protocols, but this trend was somewhat more pronounced for protocol (II). This trend can be attributed to a combined effect of two opposing factors. First, increased temperature can contribute to higher mobility and flexibility of phospholipids, leading to a disordered state and thus, resulting in a higher fluidity of bilayers (Leonenko, Finot, Ma, Dahms, & Cramb). This may be favorable for the formation of smaller, more stable and more uniform vesicles (Gibson, 2007). Meanwhile, increased temperature resulted in a reduced solubility of CO_2 and therefore weakened the dispersion effect of CO_2 due to less CO_2 being solubilized within the bilayers (Dodds et al., 1956), which led to the formation of larger particles. Therefore, the decrease in particle size in the lower temperature range was attributed to the enhanced fluidity of bilayers while the increase in particle size in the higher temperature range was mainly controlled by reduced solubility of CO_2. On the other hand, PdI remained constant from 40 to 50°C and

increased at a higher temperature using protocol (II) ($p<0.05$) while there was no significant change in PdI using protocol (I) ($p>0.05$). The increased PdI value obtained using protocol (II) was ascribed to the dominant effect of reduced solubility of CO_2 over enhanced fluidity at a higher temperature, which contributed to weakened dispersion and more heterogeneous size distribution of liposomes.

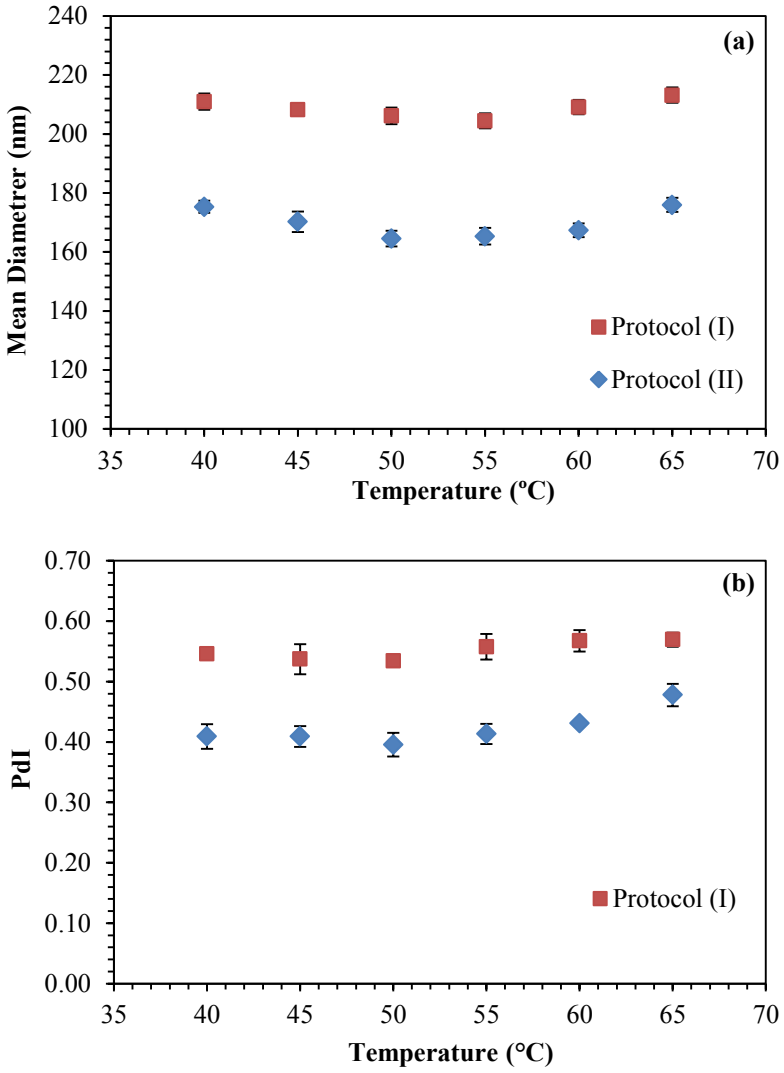

Figure 4.6: Effect of temperature on (a) particle size and (b) polydispersity index (PdI) of liposomes obtained using depressurization protocols (I) and (II) at 300 bar and 60 bar/min.

Comparison of the particle size of liposomes obtained at the same conditions of 40°C, 300 bar and 60 bar/min depressurization rate between the two sets of samples depicted in Figs. 4.6(a) and 4.4(a) highlight that liposomes in the sample collected through valve I alone were smaller (Fig. 4.6(a)) than those when the sample was combined with the residual liquid left in the vessel (Fig. 4.4(a)). Further detailed analysis of the residual sample confirmed that liposome characteristics (particle size: ~1 μm; PdI: ~0.4-0.5) (full data not shown) are different from those of the sample collected through valve I. This is due to the different depressurization mechanisms of the sample collected through valve I versus the residue left in the vessel, as was discussed in more detail in Chapter 3.

4.3.5. Morphology of liposomes

The traditional TEM images of discrete and bulk liposomes prepared by the improved SC-CO_2 method were shown in Figs. 4.7 and 4.8, respectively. Fig. 4.7 demonstrated that spherical or near-spherical nanovesicles were achieved by this method. For both depressurization protocols, vesicles prepared at 60 bar showed more irregularity and asymmetry in the bilayer (Figs. 4.7(a), (d)). The black region inside the liposomes indicated the dye entering the vesicles. In contrast, vesicles prepared at pressures $\geq$100 bar displayed a spherical and stable shape. The images suggested that low pressure may not be effective enough to form a spherical and stable shape. Due to the irregularity and asymmetry in the vesicle morphology, uneven curvature stress may be exerted on the phospholipid bilayers (Yang, Guo, Li, & Hui, 1997). Thus, vesicles became vulnerable to rupture and leakage and exhibited reduced stability. However, higher pressure could facilitate better dispersion of phospholipids into individual phospholipid molecules (Fig. 4.2), which would allow them to reassemble into a more symmetrical and spherical vesicle. Therefore, a relatively higher pressure (at least 100 bar) may be required to

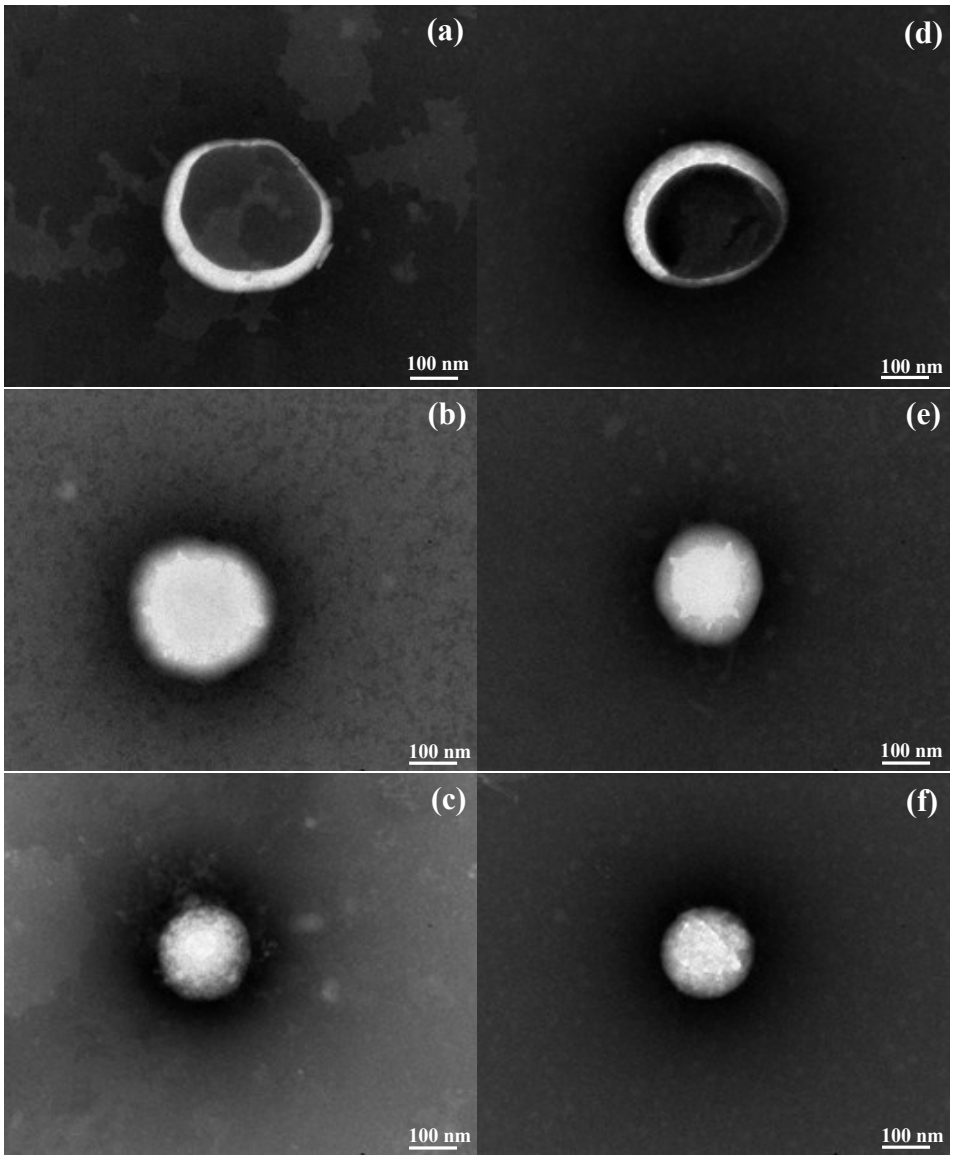

Figure 4.7: Transmission electron microscopy (TEM) images of discrete liposomes prepared by the improved SC-CO_2 method at 40°C and 60 bar/min at different pressures using depressurization protocol (I) (a-c) and protocol (II) (d-f): (a)(d) 60 bar, (b)(e) 100 bar, (c)(f) 300 bar.

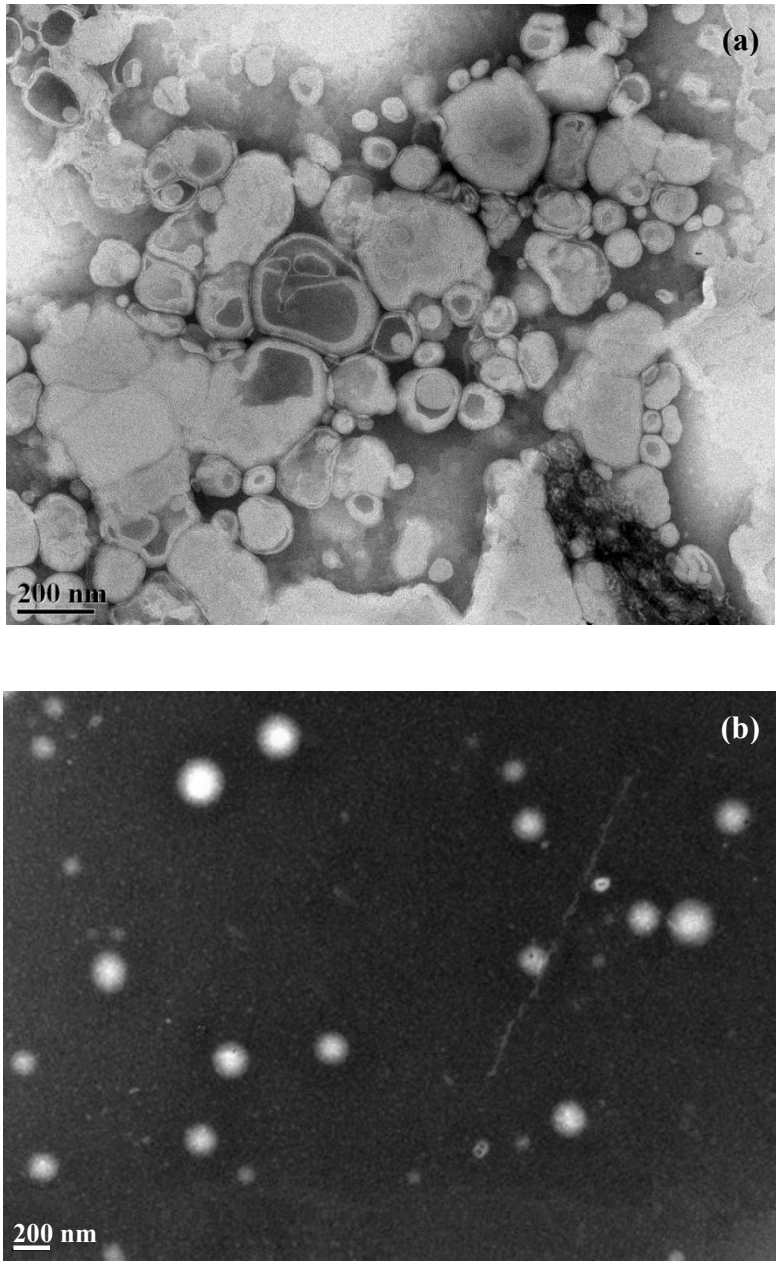

Figure 4.8: Transmission electron microscopy (TEM) images of bulk liposomes prepared by the improved supercritical method at 40°C and 300 bar at different depressurization rates: (a) Heterogeneous vesicles formed at 10 bar/min using protocol (I), (b) relatively uniform vesicles formed at 60 bar/min using protocol (II).

form spherical liposomes. Fig. 4.8 exhibited two extreme conditions in liposome morphology. The low depressurization rate (10 bar/min) of protocol (I) tended to form a relatively heterogeneous vesicle system (Fig. 4.8(a)) while a high depressurization rate (60 bar/min) of protocol (II) contributed to a relatively uniform vesicle system (Fig. 4.8(b)), again due to better dispersion of phospholipids upon depressurization at a higher rate. These findings were in good agreement with the effect of depressurization rate on particle size and PdI depicted in Fig. 4.5.

The cryo-TEM images of liposomes prepared by protocols (I) and (II) were shown in Figs.4.9 (a) and (b), respectively, to verify the conventional TEM images. Some degradation of particles was apparent in these images. This was due to the fact that the particles were deposited into the holes of the carbon film in the grid and sequentially vitrified in a vertical manner; therefore, large particles dropped to the bottom due to the gravitational force. Liposomes displayed primarily unilamellar spherical vesicles by protocol (I) at 300 bar and 60 bar/min (Fig. 4.9(a)); however, a small number of liposomes with bilamellar or multilamellar vesicles were also present. In contrast, liposomes prepared by protocol (II) showed a larger proportion of unilamellar spherical vesicles, with higher uniformity and rarely multilamellar shapes (Fig. 4.9 (b)). This indicated that protocol (II) provided an improved method of liposome preparation. These findings were consistent with the data shown in Fig. 4.4.

4.3.6. Storage stability of liposomes

The stability of liposomes prepared by the improved SC-CO_2 method at all pressures was evaluated based on weekly particle size measurements. As shown in Fig. 4.10, the liposomes prepared by protocols (I) and (II) were stable at ambient conditions for up to 8 and 6 weeks, respectively, where the change in particle size was $<5\%$. Zeta potential of the liposomes was also measured. Zeta potential is an important index to predict the stability of particles and

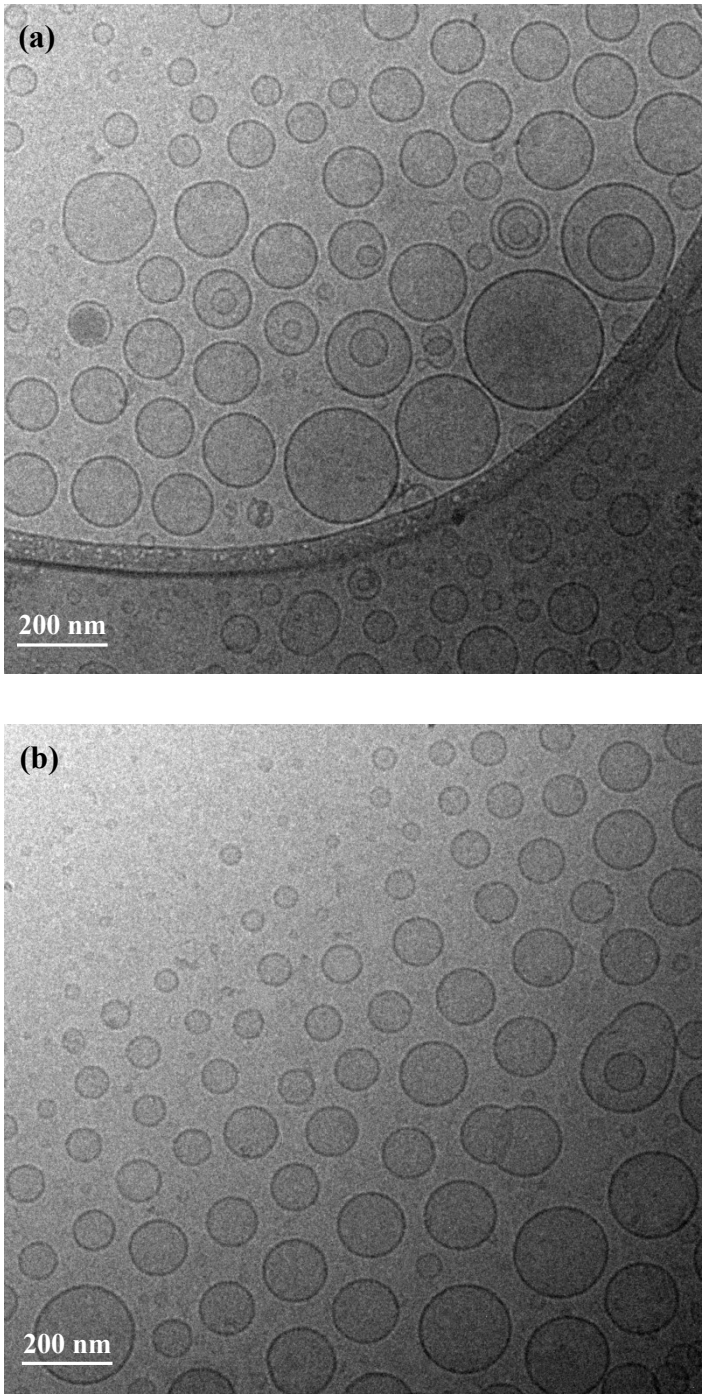

Figure 4.9: Cryogenic transmission electron microscopy (cryo-TEM) images of liposomes prepared by the improved SC-CO_2 method at 40°C, 300 bar and 60 bar/min using depressurization protocols (I) (a) and (II) (b). The circle arc at the bottom of image (a) reflects the edge of a hole in the carbon film on the grid.

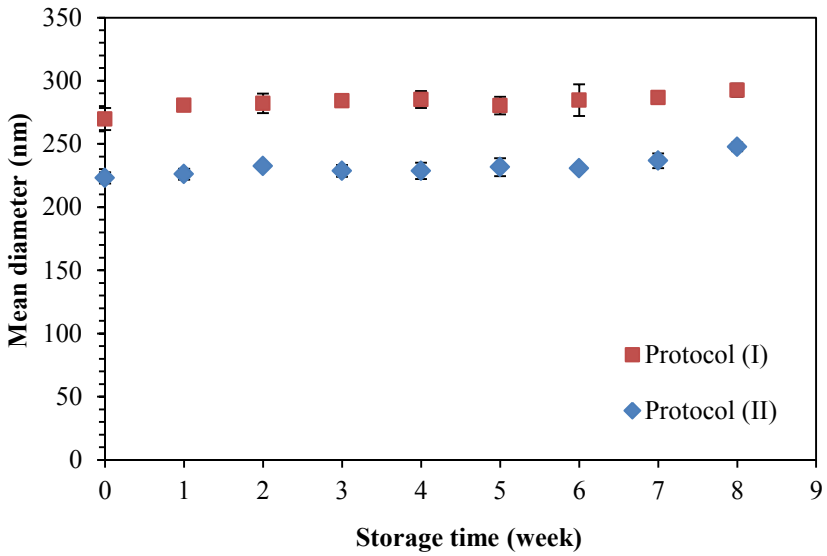

Figure 4.10: Storage stability of liposomes prepared by protocol (I) and (II) as a function of time. The supercritical preparation condition: 300 bar, 40°C and 60 bar/min. Storage condition: 25°C, under nitrogen and light proof.

indicates the overall charge of a particle in the dispersion medium (Laouini et al., 2012). Particles with a zeta potential value greater than 30 mV or less than -30 mV are considered to be stable (Hunter et al., 2001). High zeta potential values suggest that enough repulsion force is present between particles to avoid aggregation and thus result in long-term stability (Yang et al., 1997). In this study, relatively large values, -66.68±0.98 and -50.9±4.98, were found for liposomes obtained by protocols (I) and (II), respectively, which contributed to the stability of the dispersions. The large zeta potential value of liposomes was attributed to its composition of phospholipids. Soy lecithin used in this study is a natural mixture of phosphatidylcholine (PC), phosphatidylethanolamine (PE), phosphatidylinositol (PI) and phosphatidic acid (PA). Although PC and PE are zwitterionic molecules, PI and PA carry one negative charge at the pH of the liposome suspension (pH 6.5). Liposomes of protocol (I) had a zeta potential greater than that of protocol (II) ($p<0.05$), leading to their stability over a longer period of time. In addition to the

large zeta potential, the cooling effect induced by the release of CO_2 upon depressurization may also contribute to such high stability during storage. Release of CO_2 from the liquid to gas phase causes a temperature drop in the liquid phase (around 15°C after the suspension was depressurized), which may lead to partial phase transition of phospholipid molecules from the liquid crystalline phase to gel phase (Fig. 2.5) after the liposome is formed (Jacobson & Papahadjopoulos, 1975). This may reduce the fluidity of the phospholipid bilayer and improve its rigidity against fusion for a more stable system.

4.3.7. Comparison of liposomes obtained by different methods

Liposomes were also produced from soy lecithin using the conventional TFH method for comparison. The particle size of liposomes obtained by different methods and raw lecithin suspension was shown in Fig. 4.11. Although all preparation methods reduced the particle size significantly compared to that of the raw lecithin suspension, the supercritical method resulted in the formation of smaller particles and a more uniform system than those obtained by the conventional TFH method. The TEM images of raw lecithin and liposomes obtained by TFH and supercritical method were presented in Fig. 4.12. Unprocessed lecithin showed large size, heterogeneous distribution and varied morphology of phospholipid aggregates. TFH improved its homogeneity and formed multilamellar, near spherical vesicles; however, vesicles exhibited irregular thickness of bilayer, which may reduce its membrane stability and lead to considerable leakage. In contrast, the improved supercritical method formed small unilamellar and spherical vesicles with more uniform distribution without leakage. Therefore, this method was more effective for liposome formation than the conventional TFH method. Moreover, protocol (II) was more effective in liposome preparation than protocol (I), in terms of particle size and uniformity, owing to improved dispersion of discrete phospholipid molecules during the depressurization

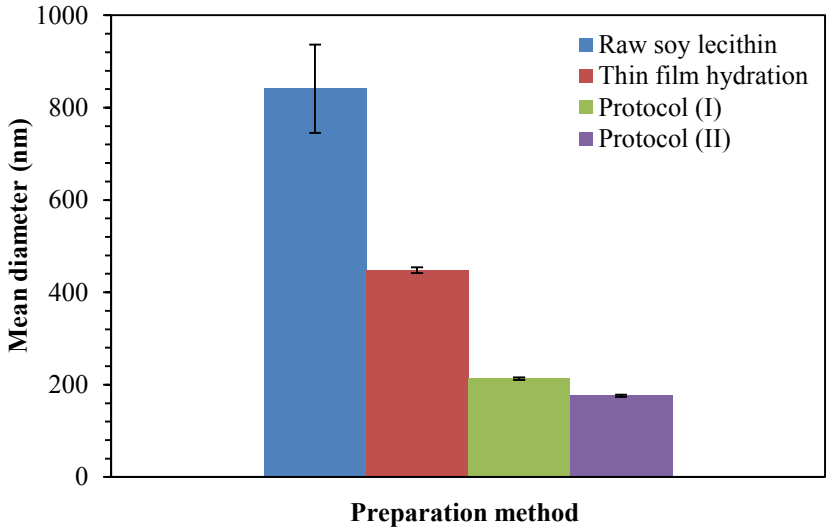

Figure 4.11: Particle size of raw material and liposomes formed by different preparation methods. Thin film hydration: 40°C, improved supercritical method: 300 bar, 40°C, 60 bar/min.

step. Also, protocol (II) was found to be more reproducible than protocol (I) in replicates prepared under similar conditions. Liposomes of protocol (I) had a higher stability during storage over those of protocol (II) due to its larger zeta potential. During depressurization, an instantaneous and large pressure drop (ΔP) to ambient pressure experienced by the liquid phase can be favorable for the formation of small and uniform vesicles. In addition, during protocol (II), CO_2 was introduced into the vessel during the depressurization step to maintain constant pressure inside the vessel. In contrast, without CO_2 addition to keep the pressure constant during protocol (I), some of the CO_2 solubilized in the liquid phase would be released to the gaseous phase inside the vessel and the liquid phase would experience a gradual decrease in pressure. This would lead to more variation in the vesicular system and less dispersion for the sample removed later during depressurization. Thus, for supercritical preparation, protocol (II) with constant pressure showed superior formation of liposomes over protocol (I).

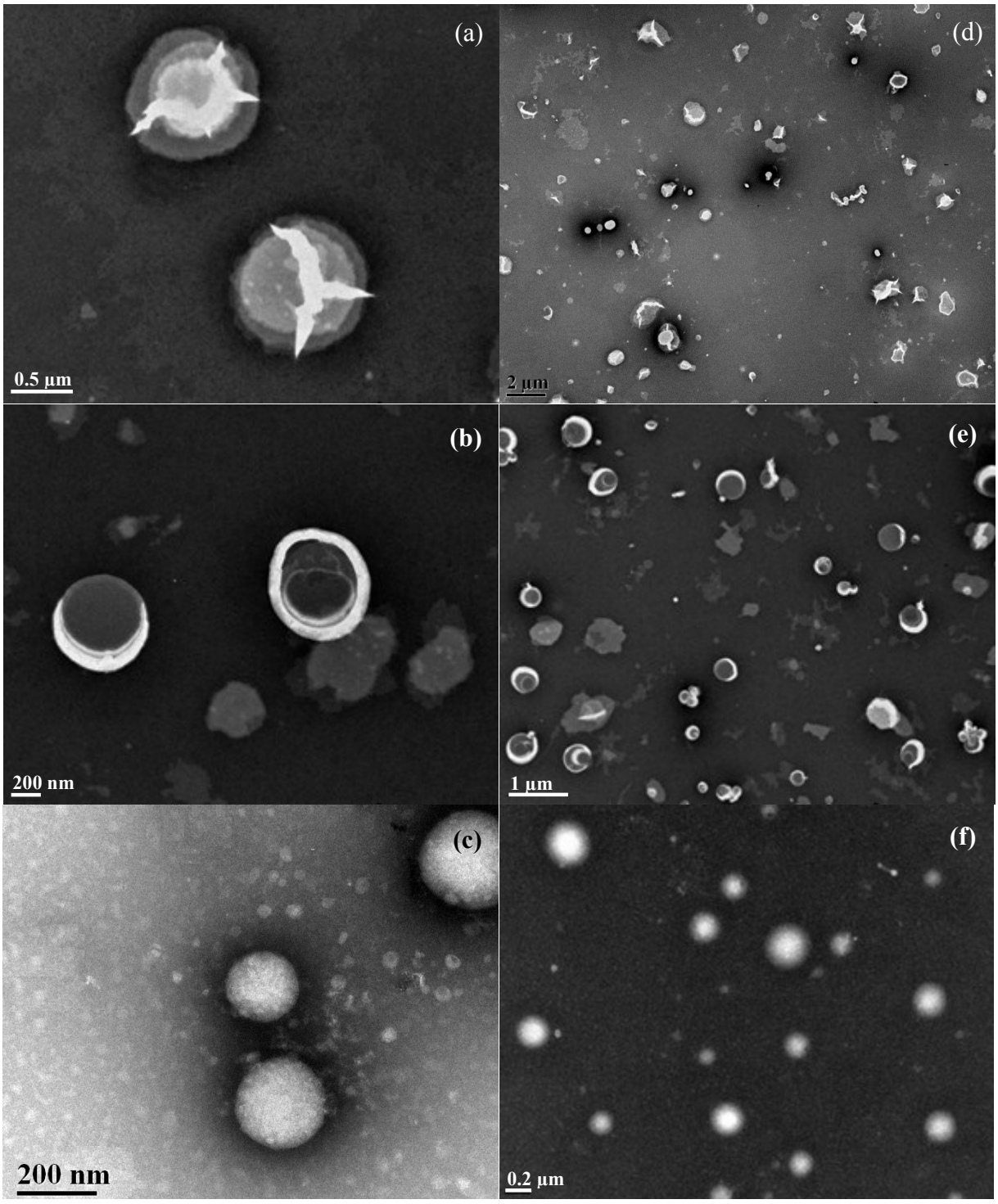

Figure 4.12: Transmission electron microscopy images of (a)(b) unprocessed soy lecithin and liposomes prepared by (b)(e) thin film hydration and (c)(f) improved SC-CO_2 method. (a-c) discrete liposome, (d-e) bulk vesicle system. Supercritical preparation conditions: protocol (II), 300 bar, 60 bar/min, 40°C.

To the best of the author's knowledge, there are no other reports available in the literature on this improved SC-CO_2 method. Therefore, liposomes prepared using this method were compared to those reported for ISCRPE and DELOS methods. ISCRPE used phospholipid suspension in water as the raw material but the supercritical phase was depressurized instead of the liquid phase as was done in this study. Otake et al. (2006) used this method and yielded a larger size (1350 nm) of liposomes with reduced stability (4 weeks) than the liposomes obtained with the two protocols (280 nm and 224 nm for protocol (I) and (II)) employed in this study at 200 bar. In Chapter 3, a larger particle size of 523±2 nm was achieved for the liposomes prepared using the ISCRPE method. In the DELOS process, phospholipid solution in an organic solvent was depressurized into an aqueous phase and liposomes were obtained via a constant ΔP and faster depressurization rate (5 mL/s). DELOS yielded liposomes with a smaller size (138 nm) and a slightly higher uniformity (PdI=0.4) than the improved SC-CO_2 method (228 nm and PdI=0.47) at 100 bar (Elizondo et al., 2012). However, the DELOS method introduces organic solvent and surfactant to assist liposome formation. At a fast depressurization rate, a low temperature below the phase transition temperature of materials may be reached and if no surfactant is added, a suspension of crystalline materials can be formed instead of vesicles. In contrast, the improved SC-CO_2 method developed in this study is completely free of organic solvent or surfactant. Plus, liposomes were prepared with soy lecithin in this process, compared with pure phosphatidylcholine used in these other two studies (Elizondo et al., 2012; Otake et al., 2006). Thus, the improved SC-CO_2 method is considered as an effective process, free of organic solvent or surfactant, to produce unilamellar liposomes with relatively small size and high storage stability.

4.4. Conclusions

The effects of pressure, depressurization rate, temperature and protocol on the liposome preparation using an improved SC-CO_2 method were investigated. While increased pressure was favorable for the formation of smaller vesicles, liposomes prepared at ≥ 100 bar displayed a spherical and stable shape. Depressurization rate above 40 bar/min resulted in particles with a higher uniformity. The amount of unhydrated CO_2 dissolved in the phospholipid bilayer is crucial to obtain a small particle size while release rate from between the bilayers may affect size distribution to a greater extent. Liposomes prepared by this method were stable for up to 8 and 6 weeks for protocols (I) and (II), respectively, with a high zeta potential value. Protocol (II) yielded smaller and more uniform particles while protocol (I) gave higher storage stability. Without surfactant addition, the improved SC-CO_2 method showed superior advantages of small size, relatively narrow distribution and enhanced stability of unilamellar vesicles. This improved supercritical process shows great potential for encapsulation of valuable compounds related to nutraceutical, functional food, pharmaceutical and cosmetic applications.

CHAPTER 5 – PREPARATION OF LIPOSOMES USING SUPERCRITICAL CARBON DIOXIDE: EFFECTS OF PHOSPHOLIPIDS AND STEROLS[3]

5.1. Introduction

Recently, the use of different micro- and nano-encapsulation techniques for the production of functional food ingredients has gained increasing attention (Sanguansri & Augustin, 2006). Liposomes have been shown to have a number of advantages as encapsulation systems to deliver high value components. Encapsulation may improve the *in vivo* absorption of hydrophobic components, which are insoluble in the aqueous phase (Zvonar, Berginc, Kristl, & Gašperlin, 2010). Encapsulation can result in the controlled release of flavor and antimicrobial compounds to improve food quality (Augustin & Hemar, 2009). Encapsulation can also enhance the stability and bioavailability of compounds by protection from degradation induced by unfavorable conditions and treatments applied during food processing or storage (Fahr & Liu, 2007). In addition, they can also be isolated from undesirable interactions such as pH, hydrolysis, or enzymatic reactions in the gastrointestinal tract (Augustin & Sanguansri, 2012).

Liposomes can be prepared by several traditional methods for medical and other applications. However, some drawbacks usually exist in these techniques; thus, the search for a cost-effective alternative to prepare liposomes without these drawbacks is ongoing. Supercritical carbon dioxide (SC-CO_2) technology offers a promising approach to replace the current reliance on organic solvents. It is also suitable for large scale production of materials in the food industry due to the relative ease of scale up.

---

[3]A version of this chapter has been published: Zhao, L., Temelli, F., Curtis, J. M., & Chen, L. (2015). Preparation of liposomes using supercritical carbon dioxide technology: Effects of phospholipids and sterols. *Food Research International, 77*, 63-72.

In Chapters 3 and 4, a single step preparation via a SC-CO_2 process, which took advantage of different aspects of previously reported approaches (Cano-Sarabia et al., 2008; Otake et al., 2006) without the addition of organic solvent or surfactant, was developed. Effects of pressure, depressurization rate, depressurization protocol and temperature on liposome preparation were evaluated and 300 bar, 60 bar/min and depressurization at a constant rate and pressure were selected in Chapter 4. To further elucidate this method, investigation of the effects of other parameters critical for liposome preparation was necessary. The phospholipid composition is of great importance to liposome formation. Each phospholipid type has an individual critical packing parameter (the geometry of amphiphiles), which can dictate the morphology and size of resulting liposomes. The head group manipulates the surface charge of vesicles and influences the zeta potential and stability of liposomes (Seelig et al., 1987). Chain length and degree of saturation determine the phase transition temperature of phospholipids (the temperature at which there is a change from an ordered gel phase to a disordered liquid crystalline phase as shown in Fig. 2.5), which closely affects mobility and fluidity as well as packing style (Vlaia, Coneac, Olariu, Vlaia, & Lupuleasa, 2016).

Sterols are usually added during liposome preparation since they fill the gaps within bilayers and reduce leakage created by imperfect packing. The addition of sterol to liposomes can modulate membrane fluidity and promote stability of phospholipid bilayers (Chen, Han, Cai, & Tang, 2010). Even though cholesterol has been commonly used in traditional liposome formulations, the literature shows limited information on the performance of phytosterols in liposomes. Phytosterols are plant-derived steroid compounds, which function similarly to cholesterol but have been shown to lower plasma cholesterol and triacylglyceride levels and reduce the risk of a number of diseases (QuÍlez, GarcÍa-Lorda, & Salas-Salvadó, 2003). Thus, it

is desirable to use phytosterol instead of cholesterol and to assess its function in liposome formation. Therefore, the objective of this study is to evaluate the effect of the compositional parameters (phospholipid concentration, phospholipid type, sterol concentration and sterol type) on the liposomal characteristics (particle size, uniformity, zeta potential and morphology). The properties of liposomes prepared using the SC-CO_2 method were compared to those obtained by the traditional thin film hydration (TFH) method.

5.2. Materials and methods

5.2.1. Materials

Soy lecithin purchased from Fisher Scientific (Ottawa, ON, Canada) was used for liposome preparation. Cholesterol (99%), β-sitosterol (97%), stigmasterol (95%) and 6-ketocholestanol (95%) were obtained from Sigma-Aldrich (Oakville, ON, Canada). 1,2-Dimyristoyl-sn-glycero-3-phosphatidylcholine (DMPC), 1,2-dipalmitoyl-3-phosphatidylcholine (DPPC) and 1,2-distearoyl-sn-glycero-3-phosphatidylcholine (DSPC) and 1,2-dioleoyl-sn-glycero-3-phosphatidylcholine (DOPC) with purity > 99% were purchased from Avanti Polar Lipids (Alabaster, AL, USA). Liquid CO_2 (purity of 99.99%) supplied by Praxair Canada (Mississauga, ON, Canada) was used in all high pressure CO_2 processing. Water purified by Milli-Q® ultrapure water purification system (EMD Millipore, Billerica, MA, USA) was used in all experiments.

5.2.2. Preparation of phospholipid suspension

The preparation of crude phospholipid suspension was performed in a similar manner as described in Section 3.2.2. Different levels of sterols (10-50%, mole % of the total number of moles of lecithin and sterol) were used for the evaluation of the sterol concentration effect.

5.2.3. Preparation of liposomes by SC-CO_2

A schematic diagram of the apparatus (Phase equilibria apparatus, SITEC-Sieber Engineering AG, Maur/Zurich, Switzerland) used for liposome formation was provided in Fig. 4.1 and the preparation of liposomes was performed in a similar manner as described in Section 4.2.3. Liposomes were formed through depressurization of the CO_2-expanded liquid phospholipid suspension phase at constant depressurization rate and pressure. The liposome suspension was collected in a vial for further analysis. All of the experimental conditions employed to study the effects of phospholipid type and concentration and sterol type and concentration were summarized in Table 5.1. The effect of phospholipid type was studied at 65°C (a temperature above the phase transition temperatures of all the phospholipid types investigated) to guarantee liposome formation.

Table 5.1: Processing conditions of liposome preparation using supercritical CO_2.

Factors	**Levels**	**Processing parameters**
Phospholipid concentration (mM)	5, 10, 15, 20, 25, 30	300 bar, 60 bar/min at 40, 45, 50 °C
Phospholipid type	DOPC, DMPC, DPPC, DSPC, soy lecithin	65°C, 300 bar and 60 bar/min
Molar concentration of sterol (mole%)	0, 10, 20, 30, 40, 50	50°C, 300 bar and 60 bar/min
Sterol type	cholesterol, β-sitosterol, stigmasterol, 6-ketocholestanol	50°C, 300 bar and 60 bar/min

5.2.4. Preparation of liposomes by TFH

The preparation of liposomes by the TFH method was performed in a similar manner as described in Section 3.2.6.

5.2.5. Characterization of lecithin composition

The lipid classes in soy lecithin were fractionated using the solid phase extraction (SPE) method. A SPE cartridge packed with silica (Supelclean™ ENVI-Carb™, Sigma-Aldrich, Oakville, ON, Canada) was conditioned with chloroform and then 2 mL of soy lecithin in chloroform was applied onto the cartridge. The cartridge was eluted in order with chloroform, acetone/methanol (9:1, v/v) and methanol to recover neutral lipids, glycolipids, and phospholipids, respectively. Solvents in the three fractions collected were evaporated carefully under nitrogen and the lipid residues were weighed.

The composition of the phospholipid fraction in soy lecithin was determined by hydrophilic interaction chromatography liquid chromatography-tandem mass spectrometry (HILIC LC-MS/MS) method as described by Xiong et al. (2012). Samples were analyzed using an Agilent 1200 series HPLC system equipped with a 3200 QTRAP mass spectrometer (AB SCIEX; Concord, ON, Canada). Separation was carried out on a HILIC column (2.7 μm; 150 × 2.1 mm) (Sigma, St. Louis, MO, USA) operating at 25°C. The mobile phase was a mixture of acetonitrile/ammonium formate (AF) in water (10 mM, pH 3.0) with the following gradient: 0–0.1 min, 8% AF; 0.1–10 min, from 8% to 30% AF; 10–17 min, 95% AF and elution flow rate of 400 μL/min (20 to 27 min) and 200 μL/min (rest).

5.2.6. Particle size distribution

The particle size distribution of liposomes was measured in a similar manner as described in Section 3.2.7.

5.2.7. Zeta potential

The zeta potential of liposomes was performed in a similar manner as described in Section 3.2.8.

5.2.8. Morphology

The general morphology of unloaded liposomes via the TEM technique was performed in a similar manner as described in Section 3.2.9.

5.2.9. Statistical analysis

At each processing condition, liposome samples were prepared in triplicate. The mean particle size, size distribution, zeta potential and stability of each sample were also analyzed in triplicate. Data analysis was performed using Minitab statistics software 16 (Minitab Inc., State College, PA, USA) and reported as the mean ± standard deviation (SD). One-way (phospholipid type, sterol concentration, sterol type) and two-way (phospholipid concentration and temperature) analyses of variance (ANOVA) were conducted and significant differences between means were obtained by Tukey's multiple comparison test at a significance level of $p < 0.05$.

5.3. Results and discussion

5.3.1. Characterization of lecithin composition

Prior to liposome formation, the composition of soy lecithin was characterized via SPE followed by HILIC LC–MS/MS methods. The SPE process was used to separate the lipid classes of triacylglycerides, glycolipids and polar lipids (mainly phospholipids) while HILIC LC-MS/MS was used to determine the profile of polar lipids. The soy lecithin used was a complex mixture of phospholipids (67.8%), glycolipids (14.3%), neutral lipids (12.5%) and others (5.4%). In the HILIC LC-MS/MS chromatogram (Fig. 5.1), the phospholipid classes were resolved into individual peaks based on the head group polarities. Phosphatidylcholine (PC), phosphatidylethanolamine (PE) and phosphatidylinositol (PI) were detected as the major phospholipid components in soy lecithin with contents of 20.9%, 26.2% and 14.3%, respectively,

together with 6.4% of phosphatidic acid (PA). These results for soy lecithin are in agreement with those of Erdahl, Stolyhwo, and Privett (1973).

5.3.2. Effect of phospholipid concentration on liposome formation

The effect of soy lecithin concentration on the mean diameter, polydispersity index (PdI) and zeta potential of liposomes was shown in Fig. 5.2. There was a relatively small change in particle size with an increase in lecithin concentration. At 50°C, liposomes at 30 mM showed the smallest particle size (146±1 nm). Particles obtained at temperatures of 40°C and 45°C had similar sizes ($p>0.05$) but there was a significant ($p<0.05$) drop when the temperature was increased to 50°C (Fig. 5.2a). As the phospholipid concentration increased, more phospholipid molecules might be available to act as surfactants that stabilize and favor the formation of smaller vesicles. This trend is in agreement with that reported by Shahi, Sonwane, Zadbuke, and Tadwee (2013). The increased concentration of amphiphilic molecules per unit volume may contribute to the increase in particle size while decrease in the mean size at higher concentrations

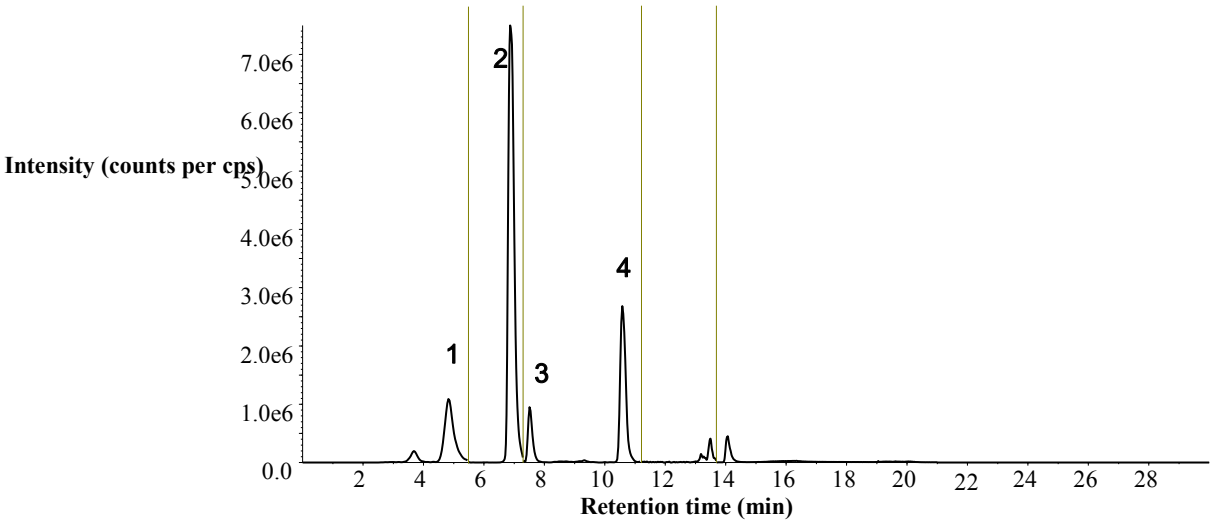

Figure 5.1: HPLC profile of crude soy lecithin used for liposome preparation. Peaks in the LC-MS/MS chromatogram: 1. PI, 2. PE, 3. PA, 4. PC. Conditions are as described in section 5.2.5.

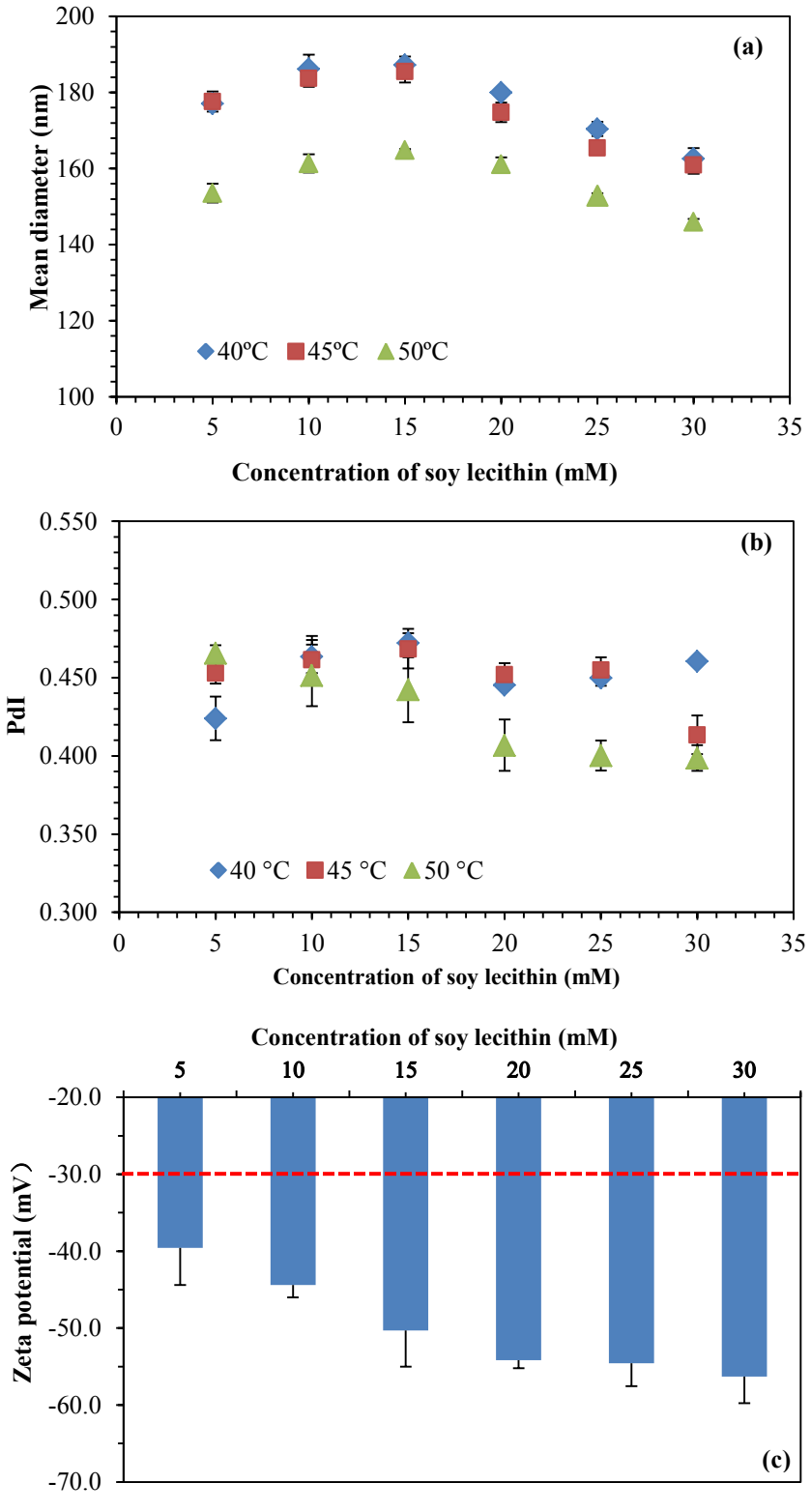

Figure 5.2: Effect of soy lecithin concentration on (a) mean diameter, (b) PdI and (c) zeta potential (50°C) of liposomes prepared by SC-CO_2 at 300 bar and 60 bar/min.

may be related to the complex composition of soy lecithin. Phospholipid molecules may rearrange into smaller vesicles based on a single phospholipid type to minimize the hydrophobic interaction and create improved packing of amphiphiles (Mannock, Lewis, McMullen, & McElhaney, 2010).

The PdI was reduced to 0.398±0.008 at the higher temperature (50°C) (Fig. 5.2b). This indicated that the higher lecithin concentration favored better particle uniformity at the higher temperature. The mobility and flexibility of phospholipids increase with temperature, which leads to enhanced fluidity of the bilayer and results in the formation of smaller and more uniform vesicles (Woodbury, 2012; Zook & Vreeland, 2010). At 50°C, zeta potential was decreased from -39.7±4.7 mV to -56.3±3.4 mV with an increase in lecithin concentration, due to the increased concentration of charged components in soy lecithin. All of the zeta potential values smaller than -30 mV suggested that liposomes prepared by the SC-CO_2 method had high stability since large charge repulsion can effectively prevent aggregation of vesicles. Overall, 30 mM and 50°C gave the smallest diameter and PdI of vesicles.

5.3.3. Effect of phospholipid type on liposome formation

The effect of phospholipid type on the mean diameter, PdI and zeta potential of liposomes was shown in Fig. 5.3. Fatty acyl chain length and degree of saturation had significant effects on particle size ($p<0.05$). The increase in particle size from DMPC (C14:0) to DSPC (C18:0) can be attributed to two factors: packing parameter and phase transition temperature. Phospholipids with a short fatty acyl chain length have a lowered packing parameter (DSPC>DPPC>DMPC) (Lichtenberg & Barenholz, 2006), resulting in increased fluidity, which is favorable for the formation of highly curved aggregates (Zhang, 2003). DMPC, DPPC, DSPC and DOPC have different phase transition temperatures of 23.6°C, 41.3°C, 54.5°C and -16.5°C, respectively

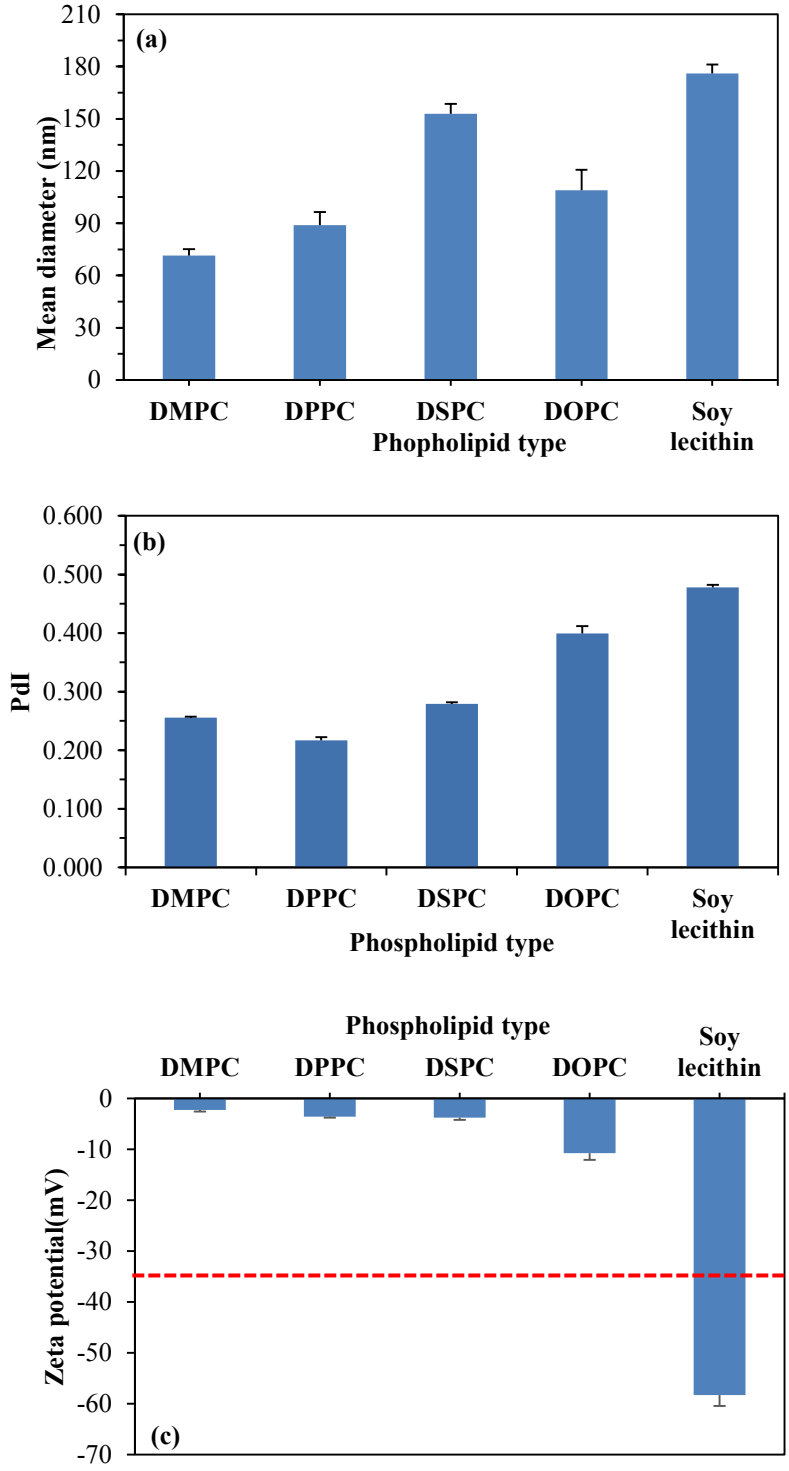

Figure 5.3: Effect of phospholipid type at the concentration of 20 mM on (a) mean diameter, (b) PdI and (c) zeta potential of liposomes prepared by SC-CO_2 at 65°C, 300 bar and 60 bar/min.

(Liu & Conboy, 2004; Ulrich, Sami, & Watts, 1994). Saturated phospholipids with a short chain length led to a relatively low phase transition temperature, which enhanced the fluidity of bilayer and resulted in a small size (Smith & Dea, 2013). DOPC has the highest packing parameter (saturated PC: P<1; DOPC: P~1) (Nomura, Mizutani, Kurita, Watanabe, & Akiyoshi, 2005), but lowest phase transition temperature, which accounted for the smaller size of liposomes (Fig. 5.3a). Pure phospholipids yielded a smaller size and higher uniformity compared to the mixture present in soy lecithin (Fig. 5.3 a, b). Single phospholipid species eliminated imperfect packing caused by different chain lengths and head groups present in soy lecithin and contributed to smaller size and enhanced uniformity. Furthermore, glycolipids present in the soy lecithin also influence the particle size and uniformity of liposomes. Glycolipids in soy lecithin are mainly composed of steryl glucosides (SG, 17.2%), esterified steryl glucosides (ESG, 36%) and cerebrosides (37%) (Nguyen et al., 2014). Inclusion of glycolipids, especially SG and ESG, into phospholipid bilayers increased the particle size. Since SG and ESG have a similar sterol distribution attached to a sugar group (or esterified sugar group) as found in the sterols, it was expected that they would also have a similar influence on the packing of the phospholipid bilayer.

Soy lecithin exhibited a remarkably high absolute zeta potential value (-58.3±2.17 mV) among all the phospholipid types. This would be expected to result in excellent liposome stability due to the larger repulsion among vesicles. The large zeta potential was attributed to the charged phospholipids present in lecithin. In contrast to PC and PE, which are zwitterionic components of soy lecithin, PI and PA carry one net negative charge at the pH (6.0~6.5) of liposome suspension. Hence, the higher content of PI and PA derived from soy lecithin resulted in a larger absolute value of zeta potential compared to the pure phospholipids studied. Liposomes prepared by pure phospholipids had absolute zeta potential values much lower than

30 mV (e.g. -3.55±0.42 mV for DPPC); therefore, they are not expected to be stable during storage and extra surfactant assistance may be needed to enhance their storage stability.

5.3.4. Effect of sterol concentration on liposome formation

The effect of β-sitosterol molar concentration on the mean diameter, PdI and zeta potential of liposomes was shown in Fig. 5.4. With the sterol concentration elevated from 10% to 50%, particle size of liposomes increased from 147±9 nm to 246±7 nm. Sterol has a shorter hydrocarbon moiety compared to the fatty acyl chains of phospholipids and usually interacts with the portions of hydrocarbon chains close to the head group. At a low concentration, the sterol molecules separate the hydrophobic fatty acyl chains and hence weaken the hydrophobic interactions, thus increasing the fluidity of bilayer and promoting small vesicles (Demel & De Kruyff, 1976; Wong, 2009). In contrast, at high concentrations, sterols strengthen the packing of bilayers due to increased interactions, resulting in reduced fluidity and larger size (Coderch et al., 2000; Marsh & Smith, 1973). PdI increased from 0.406±0.016 to 0.514±0.018 as the sterol concentration increased, which indicates that a high level of sterol may lead to mixed amphiphile types and increase the heterogeneity of the vesicular system. The increased level of sterol reduced the net charge on the vesicular surface ($p<0.05$) and suggested that the charge reduction was caused by partial charged phospholipids being replaced by neutral β-sitosterol. The large absolute zeta potential value (>30 mV) suggests high stability that is beneficial for long term storage. Sterol interacts with the head group of phospholipids via hydrogen bonding and their inclusion reinforces hydrophobic interaction with fatty acyl chains and reduces the electrostatic repulsion among head groups, which further helps to stabilize the bilayers (Bhattacharya & Haldar, 2000). Their inclusion may also change the lipid ordering and bilayer thickness. These results were in good agreement with others (Lee et al., 2005; Sparks et al., 1993), who obtained

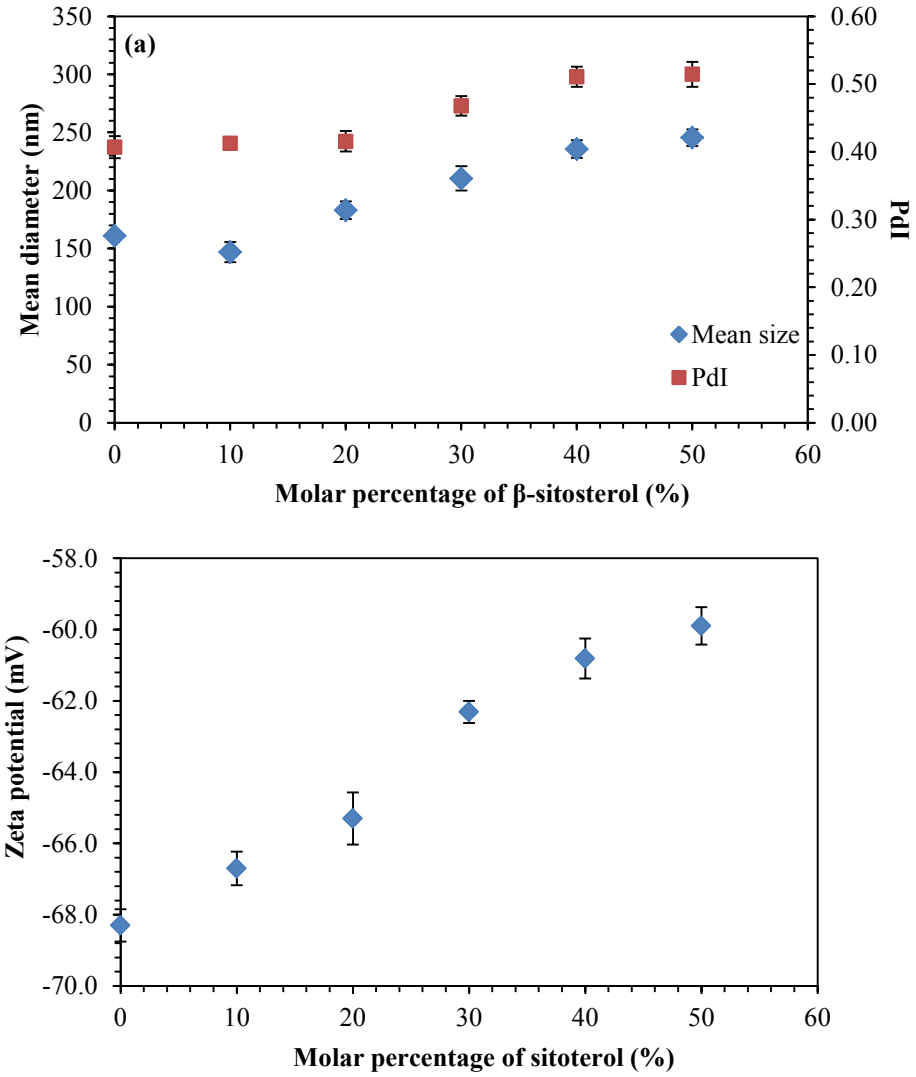

Figure 5.4: Effect of β-sitosterol concentration on (a) mean diameter and PdI and (b) zeta potential of liposomes prepared by SC-CO_2 at 50°C, 300 bar and 60 bar/min.

liposomes using conventional preparation methods.

5.3.5. Effect of sterol type on liposome formation

The effect of different types of sterol on the mean diameter and PdI of liposomes was shown in Fig. 5.5. Particle size and PdI of liposomes varied with the sterol type ($p<0.05$). The phytosterols, stigmasterol and β-sitosterol yielded a smaller size (210±4 nm) and PdI (0.447±0.02) than cholesterol (241±8 nm and 0.475±0.02). This indicated the possibility of using

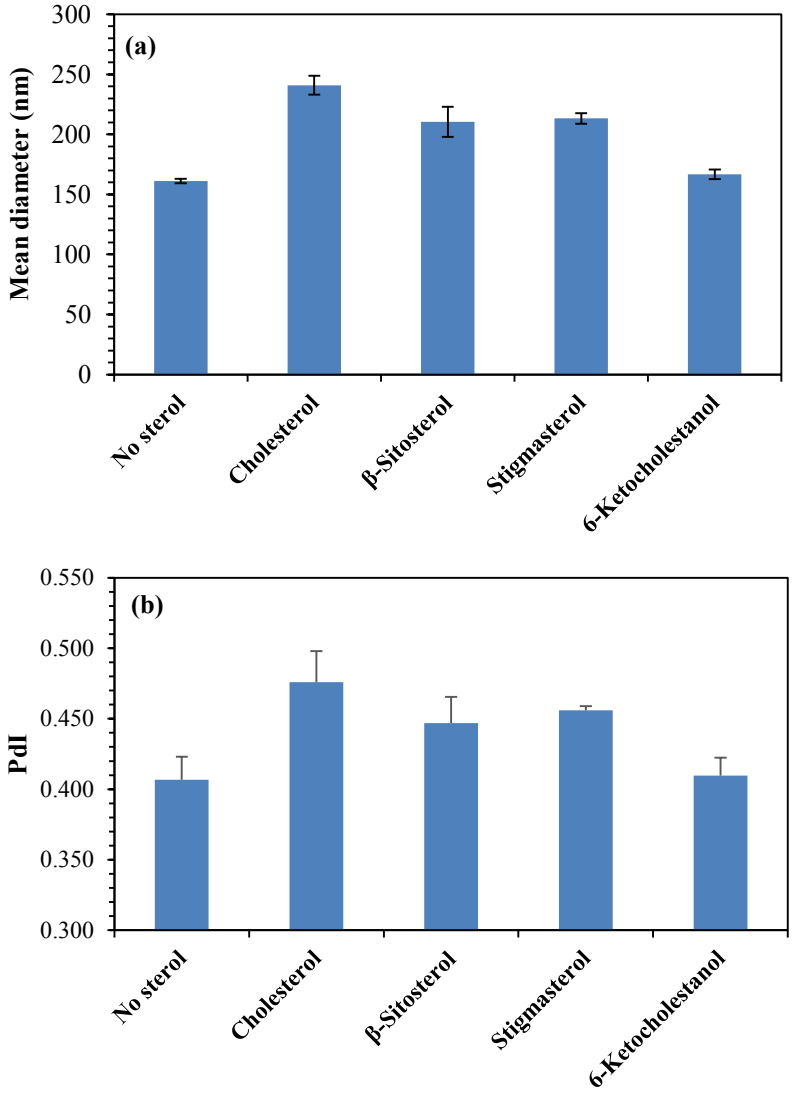

Figure 5.5: Effect of sterol type with 20 mM soy lecithin on (a) mean diameter, (b) PdI of liposomes prepared by SC-CO_2 at 20%, 50°C, 300 bar and 60 bar/min.

phytosterols and their advantages to replace cholesterol. The particle size and PdI of liposomes can be affected by the packing and organization of sterol type when incorporated into the bilayer membranes. Although the orientation of cholesterol has been studied greatly, there are limited reports on the arrangement of phytosterols in the bilayers and their comparison. However, it was reported that phytosterols always contain one or two carbon substituents with variable

stereochemistry at the C-24 position on the sterol side chain and are less effective in ordering the lipid bilayers, in contrast with cholesterol (Kamal & Raghunathan, 2012). Thus, the reduction in particle size due to the phytosterol addition may have resulted from the enhanced disruption of phospholipid bilayers and formation of a more disordered state in the bilayer membranes based on extra carbon substituents present in phytosterols compared to cholesterol (Kamal & Raghunathan, 2012). Liposomes prepared with 6-ketocholestanol had the smallest particle size and PdI values compared to the other sterol types. 6-Ketocholestanol has a keto group and a large dipole moment compared to the other sterols, which may change the fluidity and lead to the improved packing of the phospholipid bilayer. The zeta potential remained constant ($p>0.05$) at -65.1±0.8 mV for all sterol types.

5.3.6. Morphology of liposomes

The morphology of discrete and bulk liposomes prepared using the SC-CO_2 process at all conditions was evaluated via TEM technique. Morphology is a critical parameter to assess the shape, size, uniformity and the intactness of liposomal vesicles. It also indicates membrane rigidity, phase transition and curvature packing of phospholipids (Canelas, Herlihy, & DeSimone, 2009). Since any fluctuation in the curvature may lead to leakage of encapsulated agents and affect the retention rate of bioactives, ideal liposomes should be small, uniform and spherical vesicles without any deformation or leakage on the surface for better encapsulation and controlled release purposes (Champion, Katare, & Mitragotri, 2007). Liposomes of lecithin displayed spherical and near-spherical shapes under different concentrations (Fig. 5.6), with seldom deformation, which is beneficial for encapsulation. Liposomes prepared at low concentrations (5-10 mM) had more spherical shape than those at the high concentration range, which suggested a better packing of phospholipid molecules. The high phospholipid content in

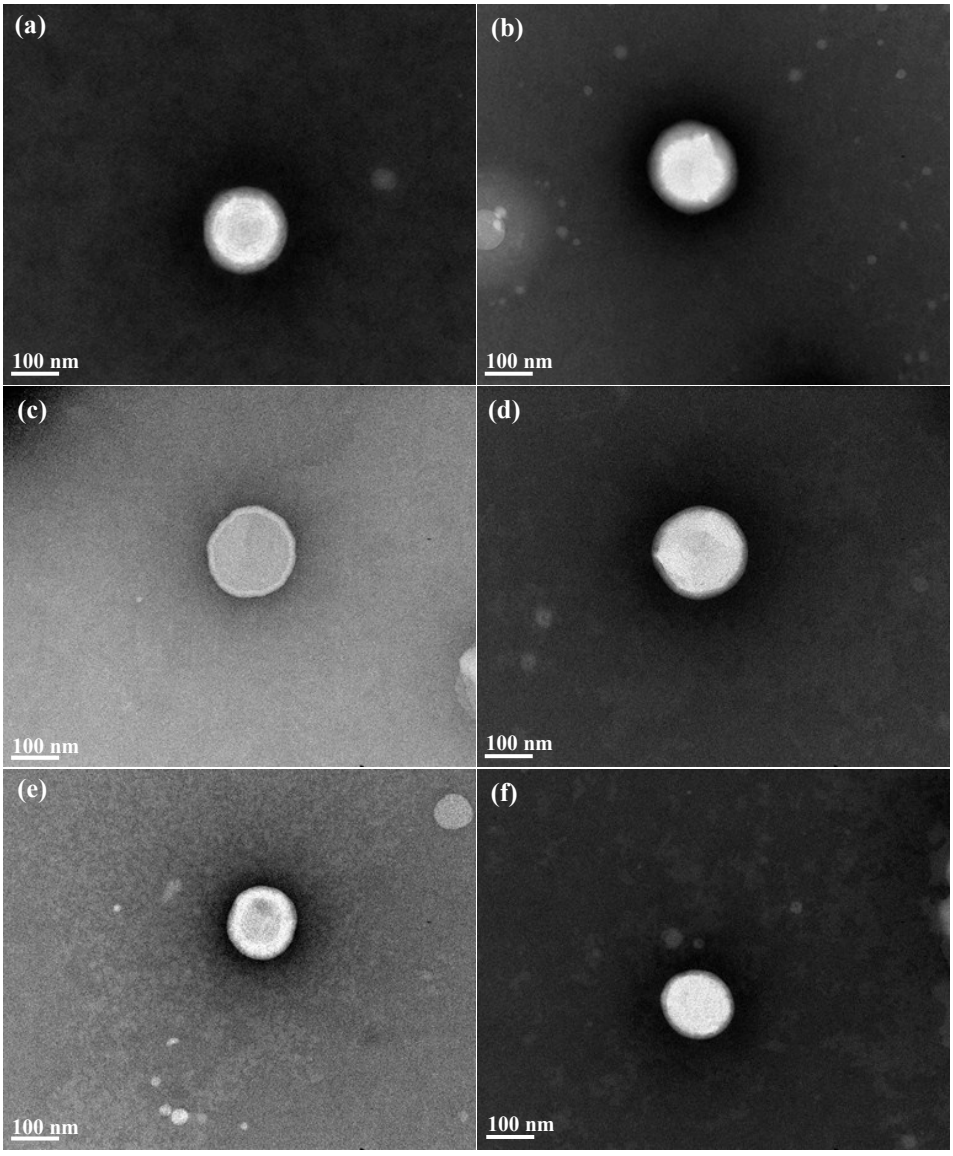

Figure 5.6: TEM images of liposomes prepared by the SC-CO_2 method at 50°C and 60 bar/min at different soy lecithin concentrations: (a) 5 mM, (b) 10 mM, (c) 15 mM, (d) 20 mM, (e) 25 mM, (f) 30 mM.

the aqueous suspension may result in dense packing and more fluctuation of the membrane. The mechanism of liposome formation using SC-CO_2 was proposed in Chapter 4 (Section 4.3.1). The findings here suggest that at a specific pressure, CO_2 solubilized in a diluted lecithin suspension might result in enhanced dispersion of phospholipid molecules upon depressurization, which

allows discrete phospholipids to reorganize into a better packing arrangement and more symmetrical vesicle. The brightness detected inside of vesicles (no dye entered) indicated liposomes prepared using the SC-CO_2 method were intact without leakage, even without any sterol addition. This is favorable for the encapsulation and controlled release of hydrophilic compounds. Due to their structural similarity to sterols, glycolipids present in soy lecithin are expected to strengthen the hydrophobic interactions and weaken the electrostatic repulsion of head groups among phospholipid monomers, which may play a similar role as sterols in stabilizing the bilayers and preventing leakage. This finding may offer the possibility of adding glycolipids into liposome formulations to adjust the phase transition and packing properties related to bilayer membranes, which requires further research.

In terms of the different types of pure phospholipids, unsaturated DOPC caused more asymmetry in the vesicles and did not yield liposomes as spherical as the other saturated phospholipids (Fig. 5.7). With a packing parameter larger than those for saturated phospholipids, it is harder for DOPC to pack into vesicular structures. In addition, DPPC and DSPC offered more spherical and symmetrical vesicles compared to DMPC (Fig. 5.7), which may be attributed to the increased hydrocarbon chain-CO_2 interaction induced by the longer chains. These hydrocarbon-CO_2 interactions include quadruple-induced dipole and van der Waals interactions with the hydrocarbon chains of phospholipids. An increased fatty acyl chain length can lead to more CO_2 being embedded in between the hydrocarbon chains, thus resulting in enhanced dispersion of phospholipid molecules upon depressurization. Thus, enhanced symmetry in liposomes prepared with DPPC or DSPC shows more advantages for encapsulation and delivery of drugs and bioactives.

The morphology of liposomes with various sterol concentrations were shown in Fig. 5.8.

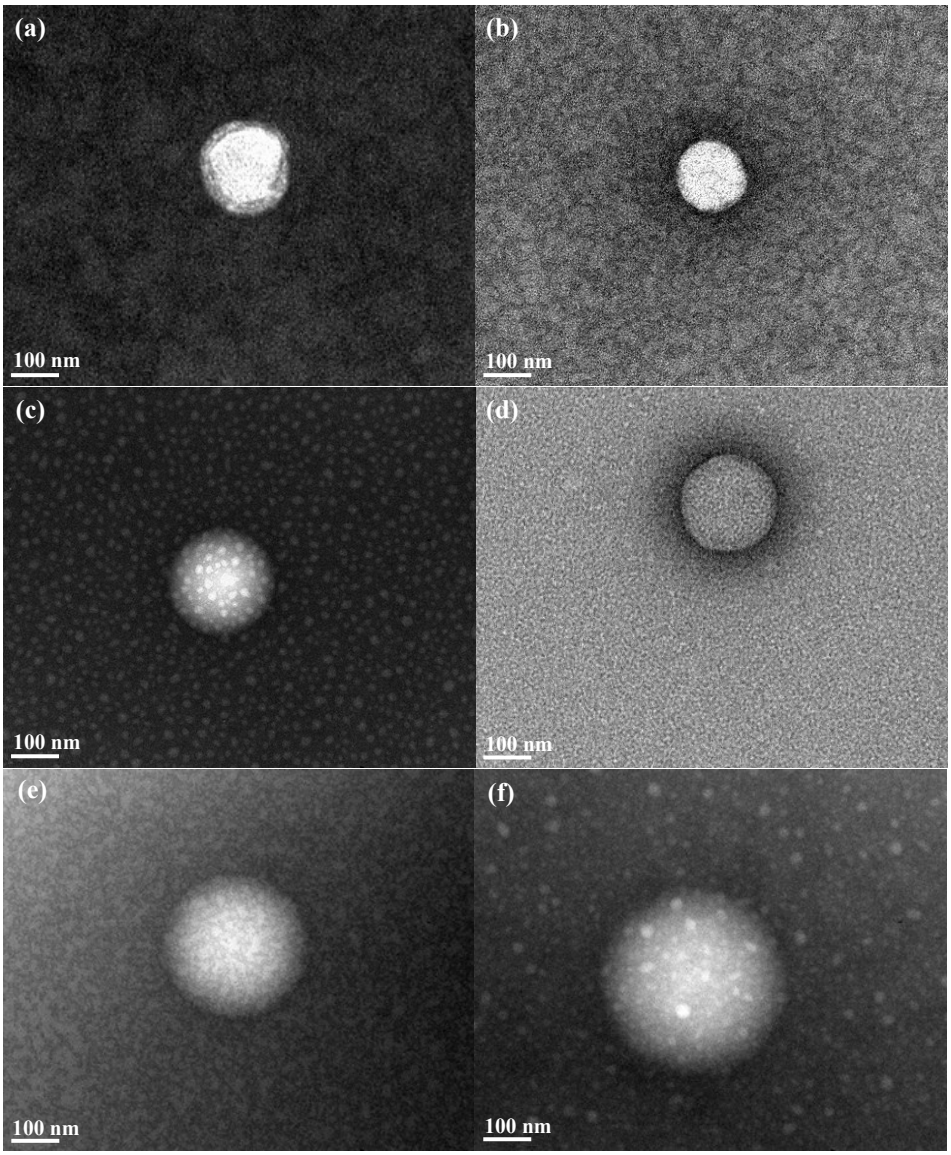

Figure 5.7: TEM images of liposomes prepared by SC-CO_2 technology at 65°C, 300 bar and 60 bar/min using different types of phospholipids:**.** (a) DOPC, (b) DMPC, (c) DPPC, (d) DSPC. Liposomes prepared by TFH method using (e) DMPC and (f) DSPC.

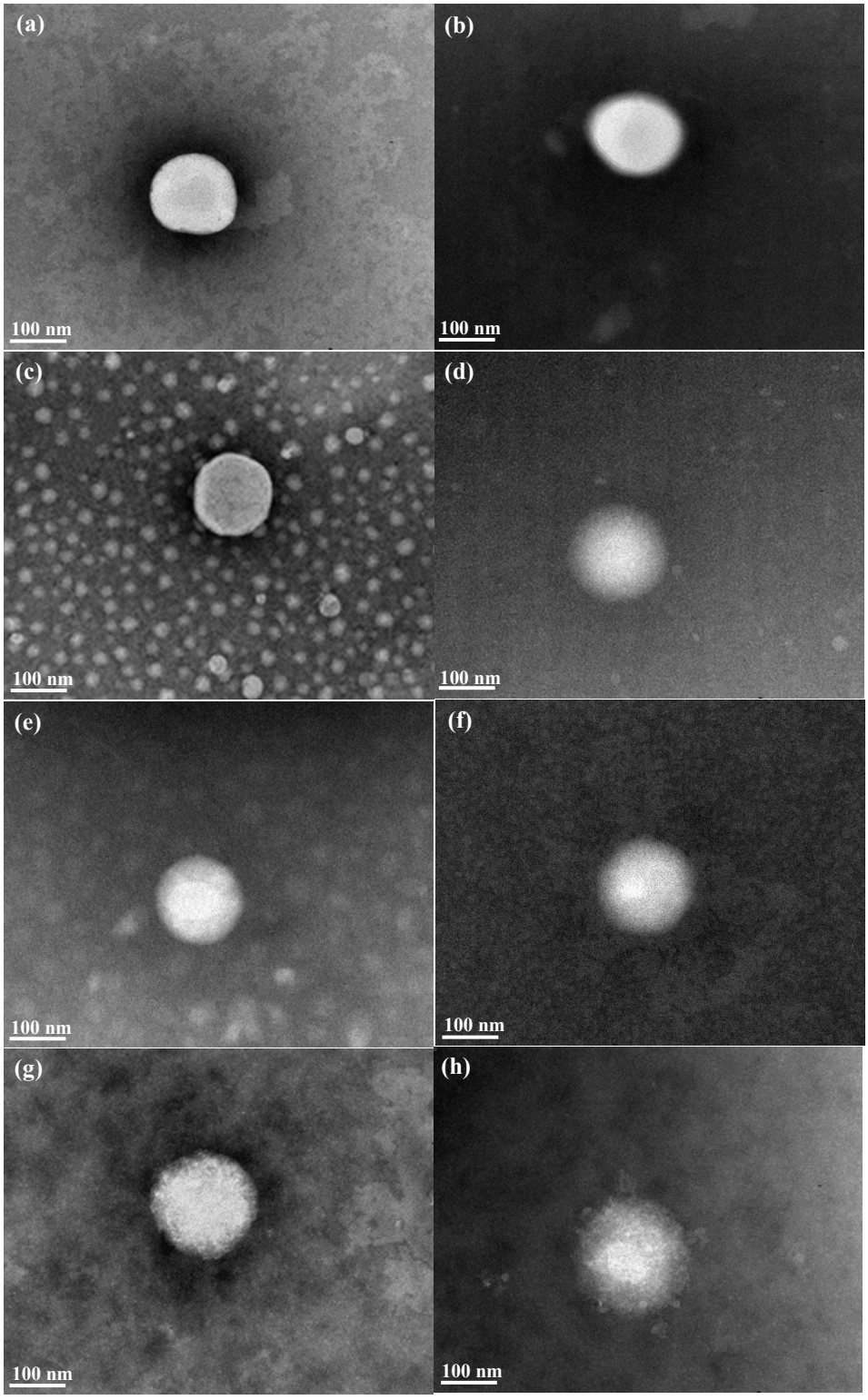

Figure 5.8: TEM images of liposomes with different sterol types (20%) and concentrations (β-sitosterol) prepared using the SC-CO_2 method at 65°C, 300 bar and 60 bar/min: (a) Cholesterol, (b) stigmasterol, (c) β-sitosterol, (d) 6-ketocholestanol. (e) 10%, (f) 20%, (g) 40%, (h) 50%.

Since the sterol embedded within the bilayers is a shorter molecule compared to phospholipids, this diversity in structure may change the packing of molecules and lead to more irregularity in the vesicles (Fig. 5.8 (a-d)). However, 6-ketocholestanol has a higher polarity in its structure, which resulted in a more symmetrical vesicular shape with better packing. The morphology of liposomes obtained at different β-sitosterol concentrations was also investigated (Fig. 5.8 (e-h)). Liposomes obtained at the low concentrations (10-20%) showed a spherical and distinct shape, which was not the case for those obtained at higher concentrations. Sterol has a larger packing parameter (P>1) compared to those of the phospholipids (Nomura et al., 2005), which suggests that high sterol concentrations increase the difficulty of packing the mixed amphiphiles into vesicles.

5.3.7. Comparison with the TFH method

Liposomes prepared by the SC-CO_2 method using soy lecithin and pure phospholipids were compared to those obtained by the TFH method (Figs. 5.9 and 5.10). Overall, liposomes prepared by the TFH method had a relatively larger size and PdI compared to those prepared by the SC-CO_2 method. At 20% β-sitosterol with lecithin, liposomes obtained by TFH had a particle size of 297±14 nm and PdI of 0.533±0.03, compared to 193±7 nm and 0.447±0.018 by the SC-CO_2 method. For liposomes of pure phospholipids (DMPC and DSPC), TFH yielded spherical morphology with relatively perfect packing and high uniformity, which were comparable to those obtained by the SC-CO_2 method (Fig. 5.7 and 5.9). This indicated the formation of well packed lipid bilayers in liposomes and the effectiveness of both techniques based on the pure phospholipid formulation. However, a significant difference in the morphology was detected when liposomes were prepared using soy lecithin. With sterol addition, both methods yielded intact vesicles without leakage, but SC-CO_2 yielded more spherical vesicles with relatively high

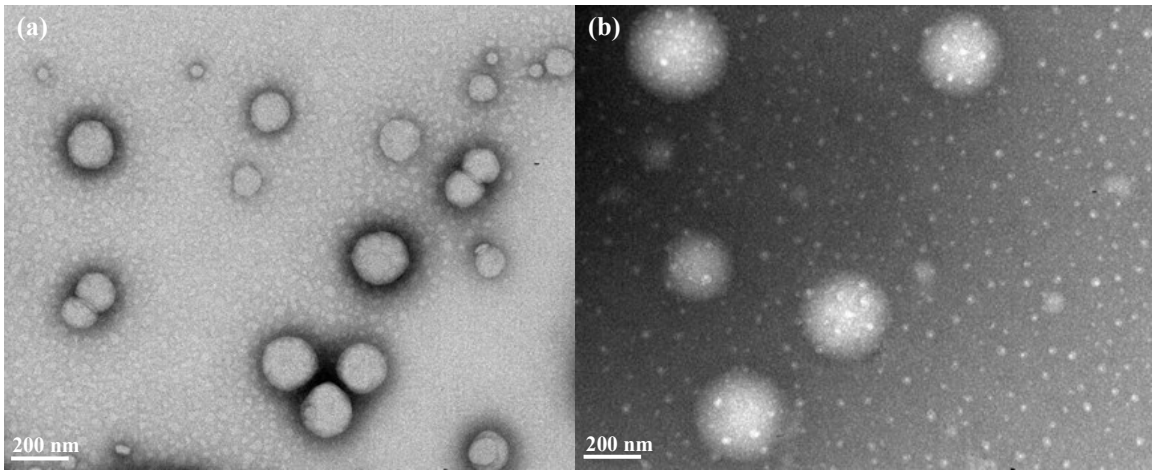

Figure 5.9: TEM images of bulk liposomes prepared by (a) SC-CO_2 at 300 bar and 60 bar/min and (b) TFH using DSPC at 65°C.

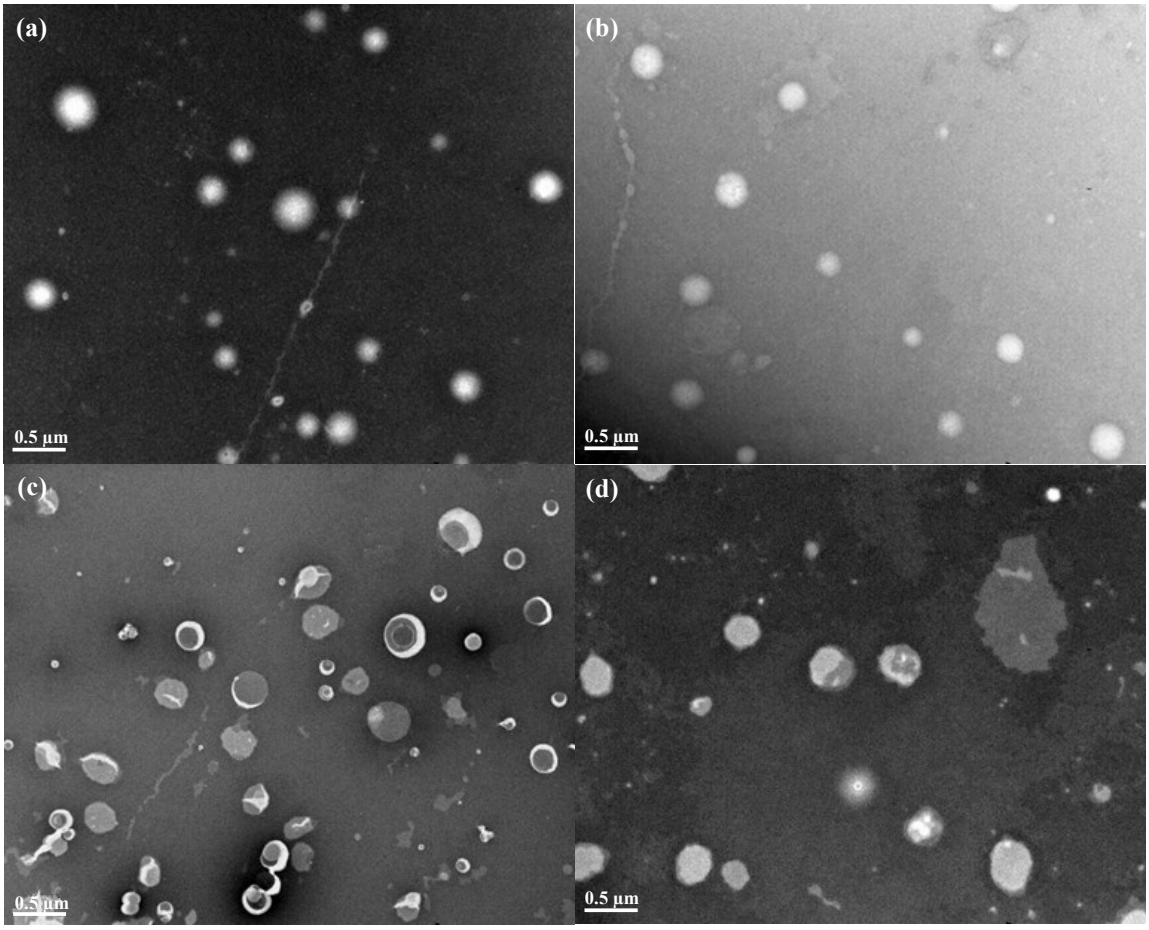

Figure 5.10: TEM images of bulk liposomes prepared by (a-b) SC-CO_2 method (300 bar and 60 bar/min) and (c-d) TFH method using soy lecithin at 50°C**.** (a)(c) Liposomes without sterol, (b)(d) liposomes with 20% β-sitosterol.

uniformity over the traditional TFH method. Without sterols, liposomes prepared by the TFH method exhibited relatively high heterogeneity, including increased asymmetry, irregular thickness in vesicles and considerable leakage (Fig. 5.10). In contrast, liposomes prepared using SC-CO_2 exhibited a high level of intactness and good uniformity without leakage, even when no sterol was added. This might offer a promising way to reduce the usage of sterols in liposome formulations while eliminating organic solvent usage. During SC-CO_2 processing, CO_2 molecules were dissolved into bilayers and resulted in better dispersion of phospholipids. In addition, the phase transition temperature of the bilayer membrane is expected to be depressed when a considerable amount of CO_2 is dissolved in between the bilayers. In previous studies (Ciftci & Temelli, 2014; Jenab & Temelli, 2011), it was shown that the melting point and viscosity of lipids saturated with CO_2 under high pressure were depressed, which indicates that CO_2 solubilized in between the phospholipid bilayers might serve as a spacer and lubricant to change its physicochemical properties. However, the change in the phase transition temperature of phospholipids upon saturation with CO_2 needs to be studied further. Such changes, especially the potential depression of phase transition temperature would modify the packing behavior of phospholipids under high pressure and might offer unique advantages for liposome preparation compared to the traditional preparation methods, which do not involve CO_2 interaction. Overall, these findings indicated that under the conditions employed, the SC-CO_2 method resulted in the preparation of superior liposomes, including small size and relatively narrow size distribution, enhanced stability and intactness of vesicles over the traditional TFH method.

5.4. Conclusions

The effects of phospholipid type, phospholipid concentration, sterol type and sterol concentration on the preparation of liposomes using the SC-CO_2 method were investigated. High

soy lecithin concentrations led to the formation of smaller size and higher uniformity while low concentrations gave a more spherical morphology for encapsulation purposes. Pure phospholipids with long fatty acid chain lengths formed larger vesicles with a spherical shape, while phospholipids with unsaturated fatty acyl chains resulted in increased asymmetry. Liposomes of soy lecithin gave the highest absolute zeta potential, owing to the presence of charged PA and PI. Addition of sterols reduced the absolute zeta potential. Phytosterols yielded liposomes with a smaller size and PdI compared to cholesterol. High β-sitosterol concentration yielded liposomes with a large size, reduced uniformity and decreased zeta potential. The selection of optimal conditions was based on size, PdI, zeta potential and morphology. A temperature of 50°C was selected due to smaller size of liposomes. Although 30 mM of soy lecithin gave the smallest diameter and PdI of vesicles, it resulted in more irregularity in morphology. Thus, 25 mM of lecithin was recommended as optimal phospholipid concentration. Similarly, 20% of β-sitosterol was selected as optimal sterol concentration due to better morphology. 6-Ketocholestanol was selected as optimal sterol type owing to its excellent liposome characteristics among all the sterol types investigated. The SC-CO_2 method resulted in superior preparation of liposomes over the traditional TFH method, including small size, relatively high uniformity and enhanced stability of spherical shape while offering improved physicochemical properties of bilayer membranes and the possibility of reducing the usage of sterols.

CHAPTER 6 – PREPARATION OF LUTEIN-LOADED LIPOSOMES USING SUPERCRITICAL CARBON DIOXIDE[4]

6.1. Introduction

Lutein is a plant-based carotenoid antioxidant that plays a vital role in maintaining eye function. Lutein works to prevent age-related macular degeneration (Olmedilla et al., 2001), cataract (Moeller et al., 2006) and retinitis pigmentosa (Berson, Rosner, Sandberg, & et al., 2004) and also to reduce the risk of cardiovascular disease (Omenn et al., 1996), stroke (Polidori et al., 2002) and lung cancer (Ito et al., 2003). Lutein cannot be synthesized by the human body and thus requires replenishment from the diet. However, its use is hampered by its poor solubility when added into food systems, due to its high hydrophobicity. In addition, it is susceptible to rapid degradation that is associated with the reactivity of conjugated double bonds on exposure to light, oxygen and temperature. The incorporation of lutein into nanocarriers like liposomes may preserve its activity, improve its aqueous dispersibility and enhance its absorption. Liposomes have shown great promise as a carrier for the stabilization and delivery of nutraceuticals in food systems. As a self-assembled vesicle comprised of a bilayer of phospholipids enclosing an aqueous core, liposomes create a physical barrier and protect encapsulated bioactives from degradation due to external unfavorable conditions during food processing (Kraft, Freeling, Wang, & Ho, 2014). They may also improve the bioavailability of poorly aqueous soluble or rapidly metabolized agents. Their biocompatibility and non-immunogenicity have resulted in recognition of liposomes in medicinal formulations for their unique advantages and recently, are of growing interest in the food, nutraceutical and nutritional

[4]A version of this chapter is to be submitted for consideration for publication: Zhao, L., Temelli, F., Curtis, J. M., & Chen, L. (2016). Preparation of lutein-loaded liposomes using supercritical carbon dioxide.

applications (Marsanasco, Márquez, Wagner, del V. Alonso, & Chiaramoni, 2011). For food and natural health product applications, liposomes have been studied as delivery vehicles to encapsulate curcumin (Takahashi, Uechi, Takara, Asikin, & Wada, 2009), resveratrol (Isailović et al., 2013), vitamins (Marsanasco et al., 2011), quercetin (Liu et al., 2013) and others.

To date there have been few reports of liposomes loaded with lutein for protection purposes. Tan et al. (2013) obtained lutein-loaded liposomes via the ethanol injection method with an encapsulation efficiency (EE) of 92.0% and a mean diameter of 83.5 nm. Xia et al. (2012) prepared lutein-loaded proliposomes via the supercritical anti-solvent method with a mean diameter of 200 nm and an EE of 90.0%. Lutein incorporation into liposomes might modulate the degree of crystallinity (Xia et al., 2012), membrane fluidity and conformational order (Tan et al., 2013) of liposomal bilayers.

The conventional preparation methods of liposomes, such as thin film hydration (TFH), usually have drawbacks associated with organic solvent/surfactant residues, heterogeneous size distributions, high energy consumption and low storage stability of the resulting liposomes. In order to improve liposome preparation, a single-step supercritical carbon dioxide (SC-CO_2) process, which combined the merits of two different supercritical methods (Cano-Sarabia et al., 2008; Otake et al., 2006) was developed in previous studies. Unloaded liposomes were prepared and the effects of pressure, depressurization rate, temperature (Chapter 4) and liposomal composition (phospholipid and sterol type and concentration) (Chapter 5) on their characteristics were investigated. The liposomes obtained were superior to those prepared by the TFH method since they were free of organic solvent and had small particle sizes, enhanced vesicular intactness and high storage stabilities. Thus, the next test is to use this SC-CO_2 method to encapsulate bioactive components into liposomes. Lutein was selected as the model hydrophobic

bioactive compound for this purpose and this study was designed to better understand the fundamental aspects of lutein incorporation into liposomes in terms of the lutein-phospholipid interactions and the physicochemical behavior of such multicomponent vesicles. It is known that lutein incorporation into liposomes, especially at high molar concentrations, can affect the physical properties of the bilayer membrane, including the phase transition temperature, degree of order as well as packing parameters, lipid fluidity, polarity and the hydrophobicity of bilayer membranes (Pham, Jaafar-Maalej, Charcosset, & Fessi, 2012). Thus, the objective of this study is to evaluate the effects of pressure, depressurization rate, temperature and lutein-to-lipid ratio on the properties of the resulting liposomes. These properties include the particle size distribution, zeta potential, encapsulation efficiency, bioactive loading, morphology, phase transition and crystallinity. Even though the effects of pressure, depressurization rate and temperature on the formation of unloaded liposomes were evaluated previously in Chapter 4, it is important to investigate if similar trends prevail in the presence of lutein.

6.2. Materials and methods

6.2.1. Materials

Soy lecithin obtained from Fisher Scientific (Ottawa, ON, Canada) was used for liposome preparation. Lutein (80%) was purchased from Hangzhou Ningsi Bio-tech (Hangzhou, China). Ethanol (99.8%) and petroleum ether (95%) were obtained from Sigma-Aldrich (Oakville, ON, Canada) and liquid CO_2 (purity of 99.99%) was supplied by Praxair Canada (Mississauga, ON, Canada). Water purified by a Milli-Q® ultrapure water purification system (EMD Millipore, Billerica, MA, USA) was used in all experiments.

6.2.2. Preparation of phospholipid/lutein suspension

The phospholipid suspension was prepared fresh for each liposome preparation. Soy lecithin (1.33 g, MW: 677.92 g/mole as specified by the supplier) was dispersed in 100 mL Milli-Q water with continuous agitation for 30 min using a magnetic stirrer at 1200 rpm. The final concentration of phospholipids was controlled at 20 mM. Lutein (MW: 568.87 g/mole) was slowly added to obtain different lutein concentrations (0.5-20, mole % of total number of moles of lecithin and lutein) and mixed with phospholipids thoroughly at 1200 rpm in the dark for 1 h. The crude phospholipid/lutein suspension was stored under nitrogen in the dark at 4°C and used within one week.

6.2.3. Preparation of liposomes using SC-CO_2

The preparation of lutein-loaded liposomes was performed in a similar manner as described in Section 4.2.3. Crude phospholipid/lutein suspension (6 mL) was sealed in a high pressure vessel. Liposomes were formed upon depressurization of the CO_2-expanded liquid phospholipid suspension at constant depressurization rate and pressure. Different levels of pressure, depressurization rate, temperature and lutein-to-lipid ratio were tested as summarized in Table 6.1.

Table 6.1. Processing conditions for liposome preparation using the SC-CO_2 method.

Factors	Levels	Processing parameters
Pressure (bar)	30, 60, 80, 100, 150, 200, 250, 300	50°C, 1% and 90 bar/min
Depressurization rate (bar/min)	20, 40, 60, 90, 120, 150, 200	50°C, 1% and 300 bar
Temperature (°C)	40, 45, 50, 55, 60, 65	1%, 300 bar and 90 bar/min
Lutein concentration (mole %)	0.5, 1, 2, 5, 10, 20	50°C, 300 bar and 90 bar/min

6.2.4. Particle size distribution

The particle size and size distribution of lutein-loaded liposomes was measured in a similar manner as described in Section 3.2.7.

6.2.5. Zeta potential

The zeta potential of lutein-loaded liposomes was measured in a similar manner as described in Section 3.2.8.

6.2.6. Encapsulation efficiency and bioactive loading

The EE was determined by quantification of free and encapsulated lutein. Free lutein content (μg) in the aqueous phase was measured according to Tan et al. (2013) with modification. Lutein-loaded liposomes (0.5 mL) were mixed with petroleum ether (3 mL) and centrifuged at 2000 rpm for 5 min to separate the upper phase. This protocol was repeated and the two supernatants were combined. The absorbance of total supernatant was measured in a semi-micro quartz cuvette (Hellma 6040-UV, Hellma Analytics, Müllheim, Germany) using a UV-Visible spectrophotometer (Jenway 6305, Bibby Scientific Limited, Staffordshire, UK). Prior to the absorbance measurement, a full spectrum scan of lutein in petroleum ether was performed and the peak wavelength was determined as 442 nm. A calibration curve of absorbance versus lutein concentration was established to determine the concentration of free lutein (μg/mL). The free lutein content (μg) was calculated via the free lutein concentration (μg/mL) in petroleum ether times its volume (mL) for the supernatant obtained.

The encapsulated lutein content (μg) in the liposomal phase was measured according to Lang (1990) with some modification. The lower phase of liposome dispersion obtained after the phase separation in the above procedure was mixed with ethanol (6 mL) by vortexing for 3 min until liposomes were completely disintegrated. The liquid mixture was filtered to separate the

aqueous ethanol-containing lutein/phospholipids from the insoluble phospholipids (<4% of total, w/w). The absorbance of lutein in the phospholipid/water/ethanol solution was then measured in a similar manner to that described above. A full UV/visible spectrum of lutein in the phospholipid/water/ethanol solution was obtained and the peak wavelength was detected at 447 nm. Using this wavelength, a calibration curve of absorbance versus lutein concentration was plotted to determine the concentration of encapsulated lutein (μg/mL). The encapsulated lutein content (μg) was calculated from the encapsulated lutein concentration (g/mL) in the phospholipid/water/ethanol solution times its total volume (mL). The bioactive loading (BL) of liposomes was obtained by dividing the encapsulated lutein content (μg) by the total lipid content (μg), calculated based on the lecithin concentration times the volume of suspension used. The EE and BL of liposomes were determined according to Eqs. (6.1) and (6.2), respectively.

$$\text{EE (\%)} = \frac{\text{Encapsulated lutein content (μg)}}{\text{Encapsulated lutein content (μg)} + \text{Free lutein content (μg)}} \times 100\% \qquad (6.1)$$

$$\text{BL (\%)} = \frac{\text{Encapsulated lutein content (μg)}}{\text{Total lipid content (μg)}} \times 100\% \qquad (6.2)$$

6.2.7. Morphology

The surface and cross-sectional appearance as well as lamellarity of liposomes were evaluated using conventional transmission electron microscopy (TEM) and cryogenic transmission electron microscopy (cryo-TEM) as previously described in Section 4.2.7.

6.2.8. Phase transition behavior

In preparation for differential scanning calorimetry (DSC) measurement, soy lecithin, lutein and their physical mixtures (5%, 10% and 20% (mole %) lutein mixed with lecithin) in granular form were pressed at 13,300 N (3,000 lb_f) into a thin film using a hydraulic press (Carver Hydraulic Unit-model#3912, Wabash, IN, USA) to improve the uniformity. The liposomal

suspension (2.5 mL) was concentrated by ultrafiltration using a membrane concentrator (Vivaspin® 6, MWCO 10,000, Vivaproducts, Littleton, MA, USA) at 4,000×g at 4°C for 4.5 h. Lipid residues were kept under nitrogen at 4°C overnight to evaporate the water completely. DSC measurements were carried out using a DSC Q100 unit (TA Instruments, New Castle, DE, USA). Approximately 5 mg of the sample was sealed in a zero aluminum hermetic pan (TA Instruments, New Castle, DE, USA) with an empty pan serving as the reference. Prior to measurement, the lipid sample was heated to 200°C at 20°C/min to erase thermal history and then cooled down to 0°C at a cooling rate of 10°C/min. Samples were then heated from 0°C to 200°C at a scanning rate of 5°C/min. All DSC measurements were carried out under a dry nitrogen atmosphere. DSC data were analyzed using Universal Analysis 2000 software (TA Instruments, New Castle, DE, USA).

6.2.9. Crystallinity

Soy lecithin, lutein and their physical mixtures (5%, 10% and 20% (mole %) lutein mixed with lecithin) were pressed in a similar manner as in DSC measurements described above. Liposomes were pretreated according to Cavalcanti, Konovalov and Haas (2007) with modification. A liposomal suspension (3 mL) was placed into the well (diameter: 240 mm; depth: 0.5 mm) of a glass holder and dried under controlled relative humidity (76%) at 4°C. The X-ray diffraction (XRD) patterns of soy lecithin, lutein, their mixtures and liposomes were determined using an X-ray diffractometer (Bruker D8-discover, Bruker AXS, Madison, WI, USA) equipped with proportional Lynx Eye Detector. Cu Kα radiation (λ = 1.5405 Å, nickel filter) was generated at 40 mA and 40 kV. Data were collected as a function of X-ray intensity versus 2θ in the range from 5° to 50° at a scanning rate of 5°/min. The XRD data were analyzed by MDI Jade 7.0 software (Materials Data Inc., Livermore, CA, USA).

6.2.10. Statistical analysis

At each processing condition (Table 6.1), liposome samples were prepared in duplicate. The particle size distribution, zeta potential, encapsulation efficiency, bioactive loading, phase transition and crystallinity of each liposome and other lipid samples were measured in triplicate. Data analysis was performed using Minitab statistics software 16 (Minitab Inc., State College, PA, USA) and reported as the mean ± standard deviation (SD). One-way analysis of variance (ANOVA) was conducted and significant differences between means were obtained by Tukey's multiple comparison test at a significance level of $p < 0.05$.

6.3. Results and discussion

6.3.1. Effect of pressure on liposome formation

The effect of pressure on the particle size, PdI, EE and BL of liposomes was shown in Fig. 6.1. The particle size of liposomes significantly increased ($p<0.05$) with pressure up to 150 bar before it dropped to 162±2 nm. At 50°C, liposomes prepared at 150 bar had the largest size (195±2 nm). PdI showed a relatively small decrease as the pressure increased. EE and BL showed a significant increase ($p<0.05$) with pressure, reaching up to 82.9±2.2% and 0.69±0.02%, respectively, at 300 bar with 1% of lutein added (mole %, equals 0.84% (w/w)). Pressure dictates the amount of CO_2 solubilized in the aqueous suspension. With more pressure, the amount of CO_2 solubilized in the aqueous suspension increases (Dodds et al., 1956) and consequently more unhydrated CO_2 molecules are introduced into the phospholipid bilayers (Isenschmid, Marison, & von Stockar, 1995). This leads to weakened interactions among the hydrocarbon moieties and uniform instantaneous dispersion of phospholipids upon depressurization, which may allow better dispersion of phospholipids into monomers before reaggregation into vesicles. Also, the affinity of CO_2 with lipophilic lutein (dipole-dipole and dipole-induced dipole interactions)

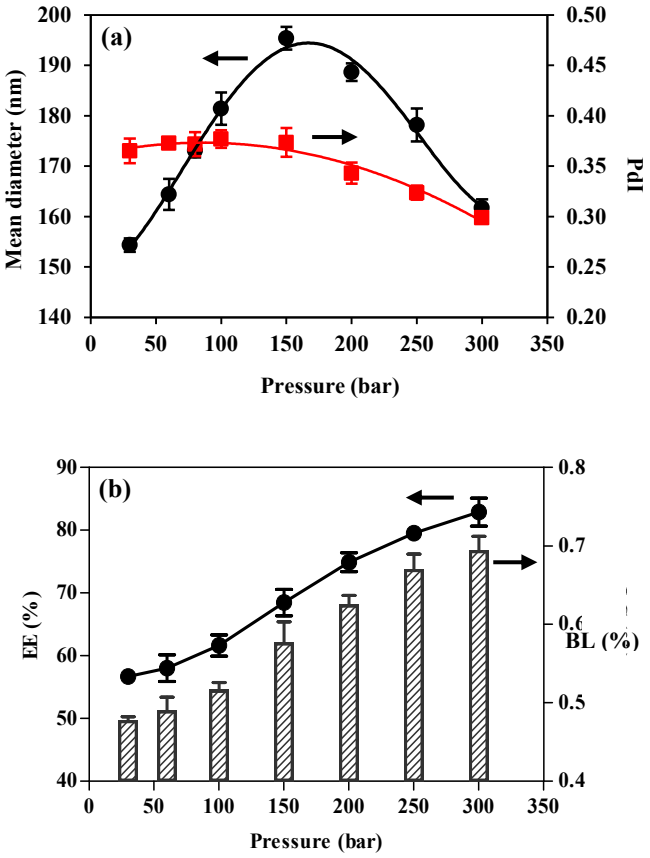

Figure 6.1: Effect of pressure on (a) mean diameter and polydispersity index (PdI) and (b) encapsulation efficiency (EE) and bioactive loading (BL) of liposomes prepared with 1% lutein at 50°C and 90 bar/min.

encourages CO_2 incorporation in between the lutein oligomers/aggregates (Cygnarowicz, Maxwell, & Seider, 1990; Vagi et al., 2007). However, data on CO_2 solubility in the lutein crystals dispersed in the aqueous phase are lacking. Based on the experimental observations , the number of lutein crystals visible in the crude suspension was significantly reduced after the CO_2 treatments. Thus, it was hypothesized that the rapid release of CO_2 leads to the formation of instantaneous lutein monomers upon depressurization and strong scattering for better encapsulation. Thus, pressure can have two opposing effects on vesicular size. On one hand, it promotes more lutein incorporation into liposomes to form larger vesicles. Lutein monomers fill the gaps and eliminate the imperfect packing created by the unsaturated fatty acids of

phospholipids within the bilayers, so that the hydrophobic interactions between lutein and phospholipids strengthen the ordering of alkyl chains of phospholipids and reduce the fluidity and mobility of the membrane (Wisniewska & Subczynski, 1998; Wisniewska et al., 2006). On the other hand, CO_2 at higher pressure forces dispersion of bilayers in the suspension into individual molecules upon depressurization and leads to the formation of smaller vesicles. The increase in particle size in the lower pressure range may be dominated by increased lutein incorporation whereas the decrease in particle size in the higher pressure range was mainly controlled by enhanced dispersion. Pressure levels higher than 300 bar were not evaluated in this study and require further investigation because higher pressures may be expected to generate smaller particles. Based on the present findings, 300 bar was selected as the optimal pressure for liposome formation to study the other parameters.

6.3.2. Effect of depressurization rate on liposome formation

The effect of depressurization rate on the mean diameter, PdI, EE and BL of liposomes is shown in Fig. 6.2. Particle size significantly increased ($p<0.05$) with depressurization rates of up to 120 bar/min, above which it started to decrease. PdI showed a decrease ($p<0.05$) with elevated depressurization rate, indicating improved uniformity of vesicles. Depressurization rate had a strong impact ($p<0.05$) on EE and BL, which reached up to 97.1±0.8% and 0.81±0.01%, respectively, at 200 bar/min. When the amount of solubilized CO_2 is fixed due to a constant temperature and pressure, a low depressurization rate brings about a slow diffusion of CO_2 molecules out of the hydrophobic aggregates. As a result, there is little disruption of the original assemblies, like little separation of the phospholipid and lutein aggregates into discrete

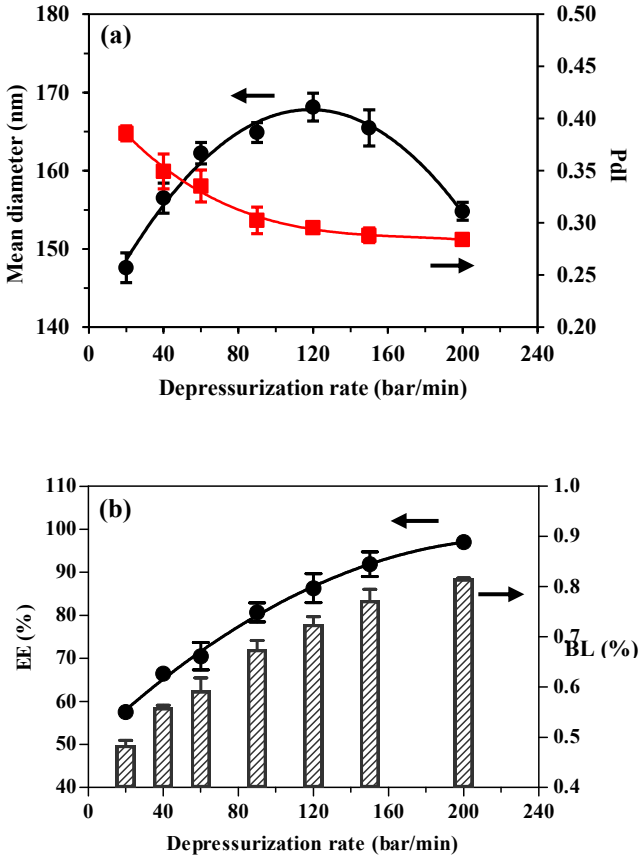

Figure 6.2: Effect of depressurization rate on (a) mean diameter and PdI and (b) EE and BL of liposomes prepared with 1% lutein at 50°C and 300 bar.

molecules upon depressurization prior to their reaggregation into vesicles. In contrast, a faster release of CO_2 at high depressurization rates generated a strong disruption of these assemblies and improved instantaneous dispersion. Such strong scattering behavior is favorable for the formation of: (a) highly dispersed phospholipid monomers, which quickly reassemble into small and uniform vesicles, and (b) CO_2-dispersed lutein monomers, which are easily assembled and incorporated into the phospholipid vesicles via hydrophobic interactions.

The data of Figs. 6.1 and 6.2 suggest that the particle size distribution and lutein encapsulation in liposomes depend on the amount of CO_2 initially solubilized in the bilayers as well as the release rate of CO_2 from the liquid phase. This finding is promising for regulating

these two processing parameters in order to achieve a desirable particle size, uniformity and bioactive loading in liposomes. Although 200 bar/min appears to be the best depressurization rate for maximized lutein encapsulation, such a high CO_2 release rate may be more challenging to scale up, considering the Joule-Thomson effect (Burnett, 1923). In addition, considering the morphology and stability of vesicles (as discussed in section 6.3.6), 90 or 120 bar/min may be more practical for the purpose of larger scale liposome production.

6.3.3. Effect of temperature on liposome formation

The effect of temperature on the mean diameter, PdI, EE and BL of liposomes is shown in Fig. 6.3. As the temperature was increased, particle size reached a minimum at 50°C, whereas the PdI stayed constant. The highest level of EE and BL was achieved at 65°C, which would improve the payload of these particles. Temperature has a significant impact on the physical properties of the aqueous suspension, including its CO_2 solubility, density and volumetric expansion. Temperature also affects the properties of bilayer membranes, including the degree of order, fluidity, permeability and lutein solubility. High temperature is favorable for lutein encapsulation since it assists in breaking up interactions (primarily hydrophobic interactions and van der Waals forces) between the alkyl chains of phospholipids. As a result, increasing temperature enhances the fluidity, disorder and permeability of bilayers (Gruszecki & Strzałka, 2005). In the absence of literature data on the effect of temperature on the solubility of carotenoids within the phospholipid membranes, it is anticipated that high temperatures may increase the solubility of lutein monomers, resulting in a higher lutein partitioning in the bilayer membrane. On the other hand, higher temperatures reduce the CO_2 solubility in the aqueous suspension (Dodds et al., 1956) and therefore weaken the dispersion of lutein and bilayer aggregates due to the lower amounts of CO_2 being solubilized within them. This leads to the

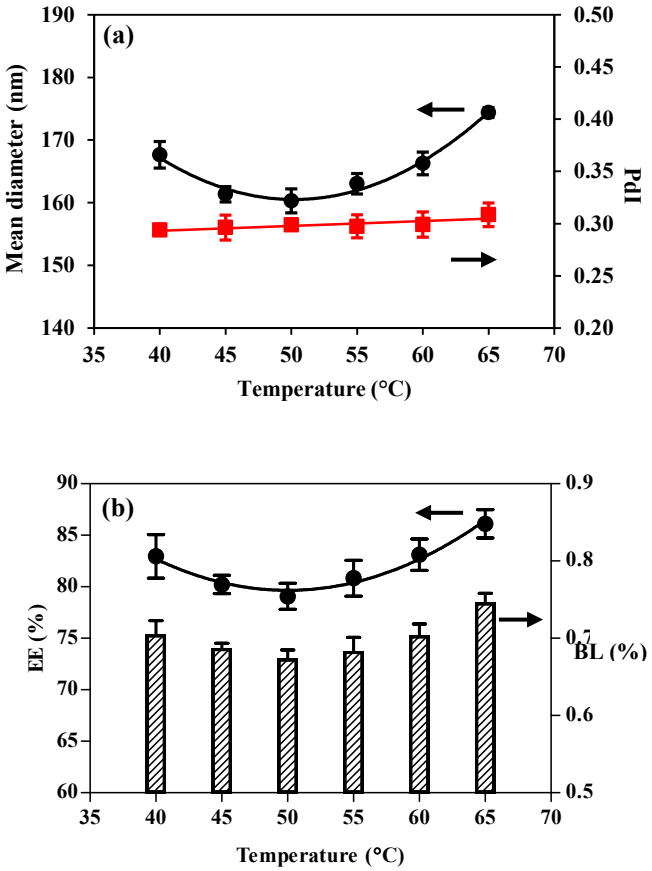

Figure 6.3: Effect of temperature on (a) mean diameter and PdI and (b) EE and BL of liposomes prepared with 1% lutein at 300 bar and 90 bar/min.

formation of larger vesicles. Although 65°C seems to be the best temperature in view of the higher EE achieved and the desirable morphology of liposomes generated as discussed later, 50°C was selected as the optimal processing temperature, considering the increased thermal degradation of lutein at temperatures ≥ 60°C (Ahmad, Asenstorfer, Soriano, & Mares, 2013).

6.3.4. Effect of lutein concentration on liposome formation

The effect of the lutein concentration on the characteristics of liposomes is shown in Fig. 6.4. Both particle size and PdI exhibited an increasing trend with increasing lutein concentration. These findings are in agreement with the results of Tan et al. (2013). Size distribution curves became broader at elevated lutein addition levels, with unimodal distribution switching to

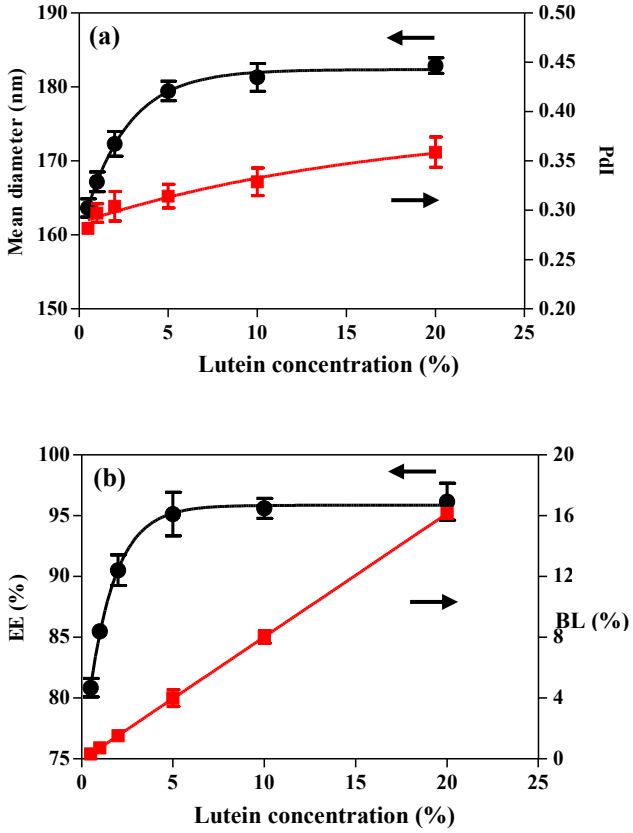

Figure 6.4: Effect of lutein concentration (mole %) on (a) mean diameter and PdI and (b) EE and BL of liposomes prepared at 50°C, 300 bar and 90 bar/min.

bimodal mode at the highest lutein levels (data not shown). This is also reflected in the increasing PdI values shown in Fig. 6.4(a). Increased lutein level enhanced the heterogeneity in the mixed phospholipid and lutein species used to form the vesicles, which may reduce the uniformity of the liposomal system. Furthermore, a higher level of lutein addition may result in an increased number of free lutein aggregates suspended in the aqueous medium. On the other hand, with the increased level of lutein addition, the EE of liposomes increased sharply up to the lutein concentration of 5% and then reached a plateau of 96.2±1.5%. This trend suggests that at 20 mM of soy lecithin, a lutein addition of up to 17% molar concentration can be mostly encapsulated into the vesicles under the current conditions. High lutein levels may modify the

physical properties of bilayers after initial lutein encapsulation (Shafaa, Diehl, & Socaciu, 2007). The higher lutein incorporation can result in an increased thickness and a decreased phase transition temperature of the phospholipid membrane (Wisniewska et al., 2006). In addition, a higher proportion of lutein incorporated into the vesicles promotes an increased number of hydrophobic lutein molecules to be buried in between the phospholipid membranes, hence reducing its contact with the aqueous phase and increasing the hydrophobicity of bilayer membranes. Encapsulated lutein molecules are present in the liposomal bilayer via their solubilization as monomers or incorporation as small aggregates (dimer, oligomer, etc.) in the liposomal membrane (Pintea, Diehl, Momeu, Aberle, & Socaciu, 2005). Higher levels of lutein encapsulation introduces an increased hydrophobic portion into the phospholipid bilayers and alters lipid packing geometry, thus resulting in an increased packing parameter of bilayers and a larger particle size. This aspect was reflected in the previous finding involving the change in particle size with the higher lutein addition.

6.3.5. Zeta potential

The zeta potential is of great significance to denote the surface charge of a particle in the dispersion (Laouini et al., 2012) and particles with an absolute zeta potential value of greater than 30 mV are considered to be stable (Hunter et al., 2001). At a lutein concentration of 1%, the zeta potential of liposomes remained constant at -55.9±0.83 ($p>0.5$) as the pressure, depressurization rate and temperature were changed (data not shown). However, an elevated lutein content significantly increased ($p<0.5$) the value of negative charge on the liposomal surface from -54.5±0.34 mV to -61.7±0.56 mV (Fig. 6.5). These high zeta potential values, arising from the presence of charged phospholipid species (phosphatidylinositol, phosphatidylglycerol and phosphatidic acid) in soy lecithin as described in Chapter 5, suggest

that large repulsive interactions exist between liposomes, which avoid vesicular aggregation, resulting in enhanced stability. Contrary to the expectation that elevated lutein content as a neutral species may reduce the surface charge of liposomes, the zeta potential values shown in Fig. 6.5 exhibited the opposite trend. Lutein is oriented via hydrogen bonding with mainly the carbonyl group on the fatty acyl chain and slightly with the phosphate head (Pasenkiewicz-Gierula, Baczynski, Murzyn, & Markiewicz, 2012). Increased lutein incorporation is expected to enlarge the space between the charged phospholipids and lead to an enhanced exposure of phosphate head groups to the aqueous medium. This enhanced surface hydration in the phosphate heads may favor the ionized state in phosphate heads for acquisition of higher charge (Disalvo et al., 2008). The observed trend of zeta potential is in good agreement with the findings of Tan et al. (2013).

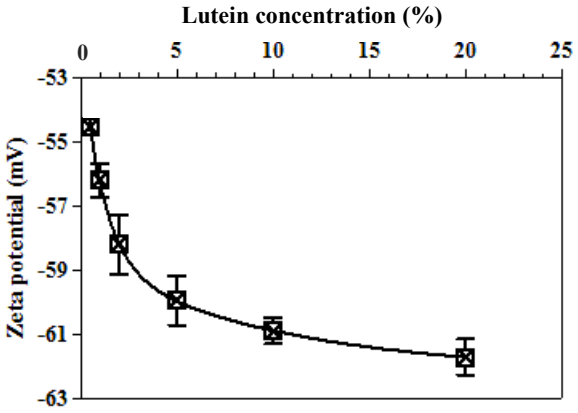

Figure 6.5: Zeta potential of liposomes as a function of lutein concentration prepared at 50°C, 300 bar and 90 bar/min.

6.3.6. Morphology of liposomes

The morphology of single liposomes as influenced by the pressure, depressurization rate and temperature was evaluated using a conventional TEM technique (Figs. 6.6-6.8). Morphology, which demonstrates the shape, size, uniformity and the intactness of liposomal vesicles, is of key

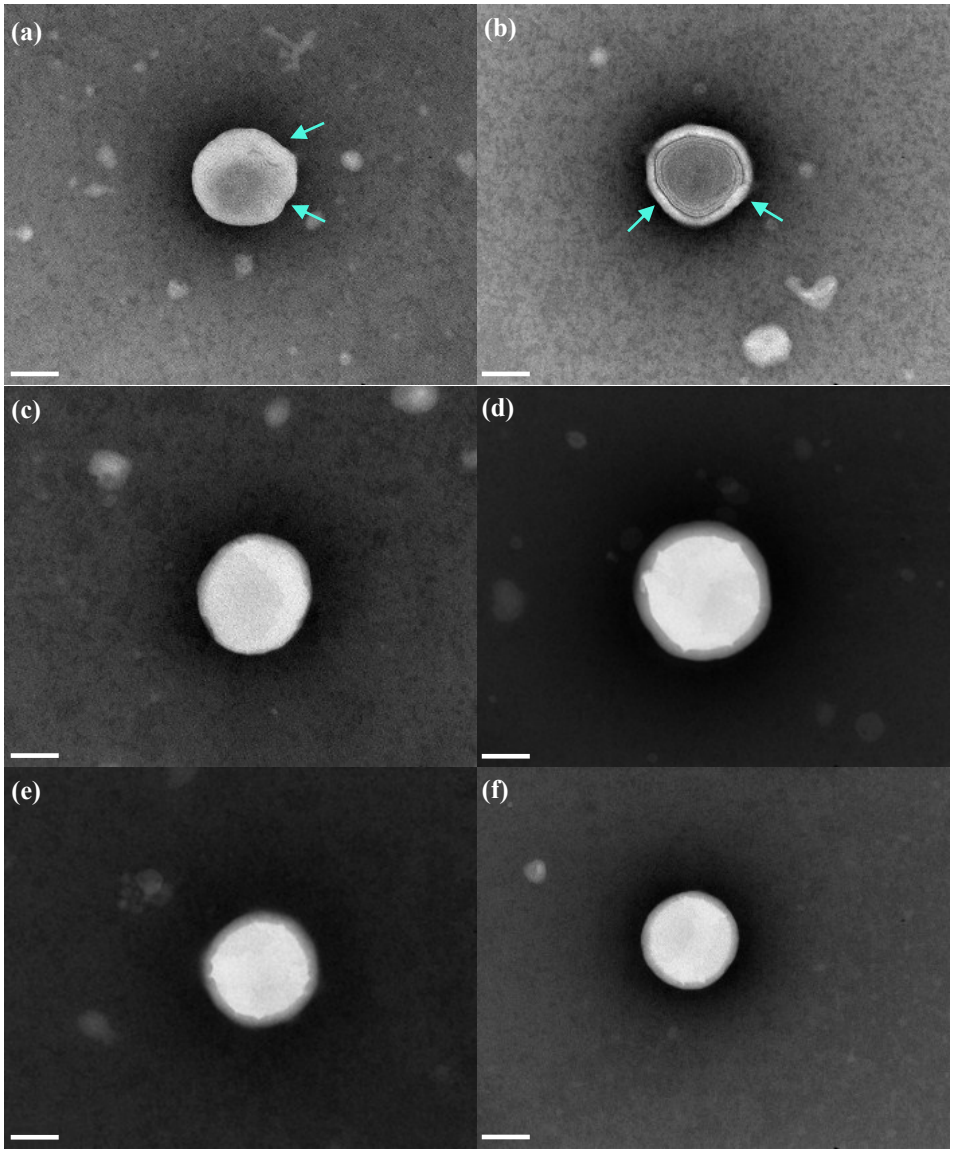

Figure 6.6: TEM images of single liposomes prepared with 1% lutein at 50°C and 90 bar/min at different pressures: (a) 30 bar, (b) 100 bar, (c) 150 bar, (d) 200 bar, (e) 250 bar, (f) 300 bar. Scale bars in TEM images (a)-(f) represent 100 nm. Arrows indicate irregularity induced by imperfect packing of phospholipid molecules on liposomal surface.

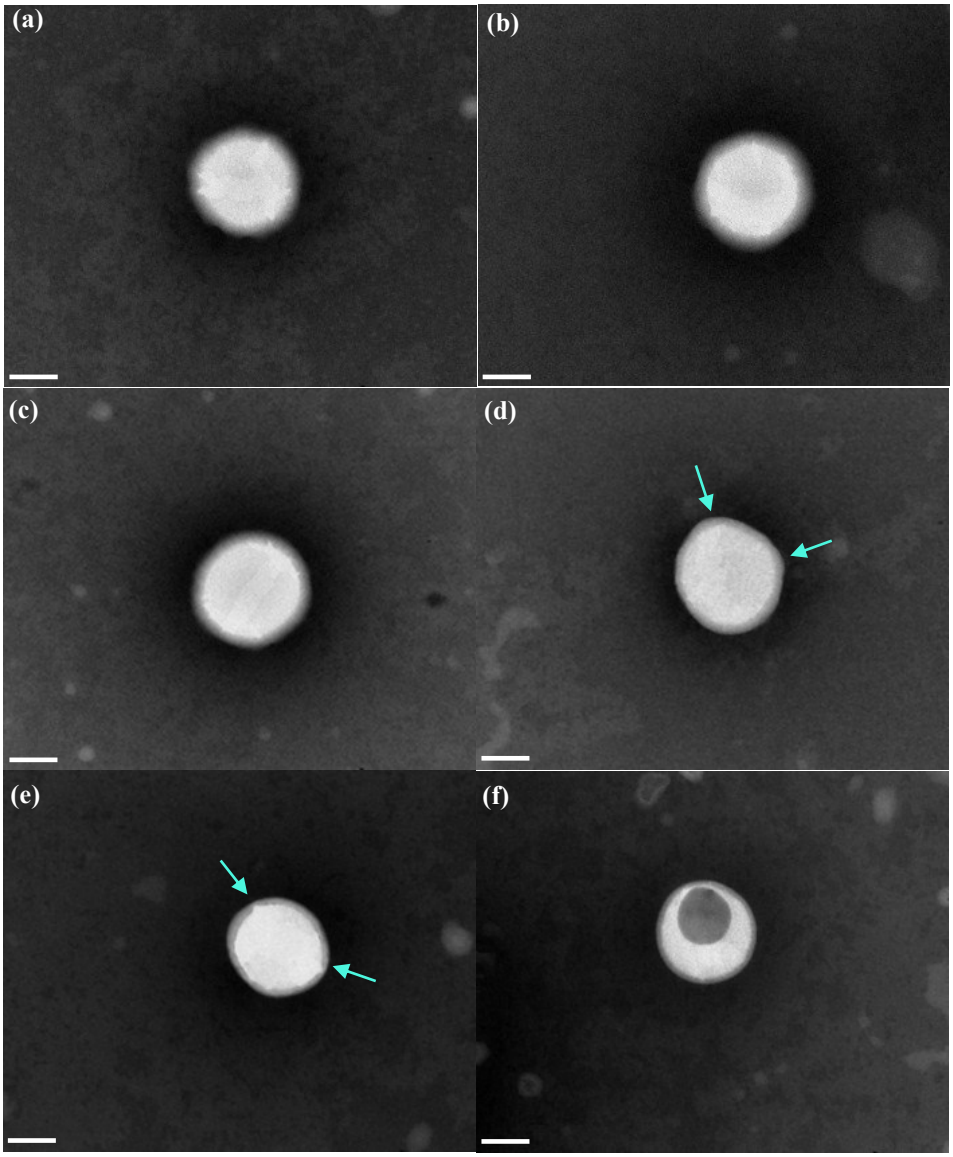

Figure 6.7: TEM images of single liposomes prepared with 1% lutein at 50°C and 300 bar at different depressurization rates: (a) 20 bar/min, (b) 40 bar/min, (c) 60 bar/min, (d) 120 bar/min, (e) 150 bar/min, (f) 200 bar/min. Scale bars in TEM images (a)-(f) represent 100 nm. Arrows indicate irregularity induced by imperfect packing of phospholipid molecules on liposomal surface.

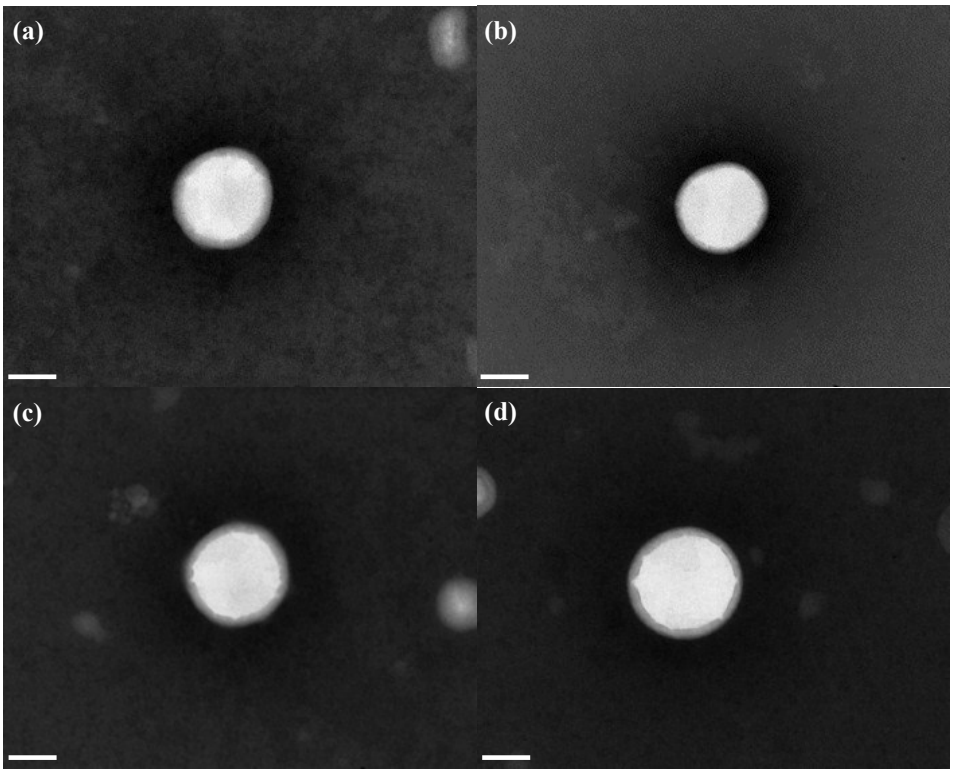

Figure 6.8: TEM images of single liposomes prepared with 1% lutein at 300 bar and 90 bar/min at different temperatures: (a) 40°C, (b) 45°C, (c) 60°C, (d) 65°C. Scale bars in TEM images (a)-(d) represent 100 nm.

importance to manipulate liposome properties in drug and nutraceutical delivery applications (Henry, 2005). It can also be an indication of membrane rigidity, phase transitions and the packing of phospholipids (Canelas et al., 2009). An ideal liposome is small and spherical with a uniform size distribution and without any roughness or rupture on the liposomal surface generated by imperfect packing. The latter would cause deformation and rupture in the bilayer membranes, leading to leakage of encapsulated agents through them (Champion et al., 2007). TEM images showing single liposomes prepared by the SC-CO_2 method displayed diversity, ranging from spherical to near-cubic vesicles, depending on the processing conditions (1 out of 30 morphological images was selected to typically represent a single vesicle at each condition). Liposomes prepared at low pressures (60-100 bar) showed more irregularity in the membrane

and leakage in the vesicles while liposomes obtained at high pressures displayed enhanced sphericity and intactness (Fig. 6.6). These findings are in agreement with the results of PdI and EE (Fig. 6.1). Higher pressure encourages a thorough dispersion of phospholipid and lutein aggregates into monomers and promotes more uniformly distributed lutein incorporation into liposomes. Moreover, increased encapsulation of lutein fills the gaps created by the imperfect packing of phospholipids and thus improves the intactness of vesicles. Liposomes maintained the spherical state and smoothness in the curvature at depressurization rates of up to 120 bar/min and intactness up to 150 bar/min (Fig. 6.7). A higher temperature range (50-65ºC) yielded liposomes with more uniform packing and spherical shape (Fig. 6.8), which may be attributed to the improved fluidity of membranes derived with an elevated energy input. Liposomes showed improved spherical shape as the lutein concentration increased to 2% and remained spherical (≤10%) whereas they transformed into near-squared shape at the ratio of 20% (Fig. 6.9). The surface appearance of liposomes was also captured in the TEM images. Unloaded liposomes displayed a relatively smooth surface (Fig. 6.9(g)) whereas the 20% lutein-loaded liposomes (Fig. 6.9(h)) illustrated a squared appearance with irregularity in the surface due to component diversity. Lutein incorporation disrupts the original packing of bilayers since it interacts with phospholipid fatty acyl chains via van der Walls forces and with the phosphate head groups via hydrogen bonding, which increases the diversity of bilayer species and leads to altered arrangement of bilayers. This suggests that a high level of lutein incorporation might create an expanded membrane packed with lutein and phospholipid molecules and thus lead to asymmetry and deformation. Overall, 300 bar, 120 bar/min, 5% lutein and 65°C were found to give the optimal morphology.

The morphology of crude lecithin suspension, crude lecithin-lutein suspension as well as

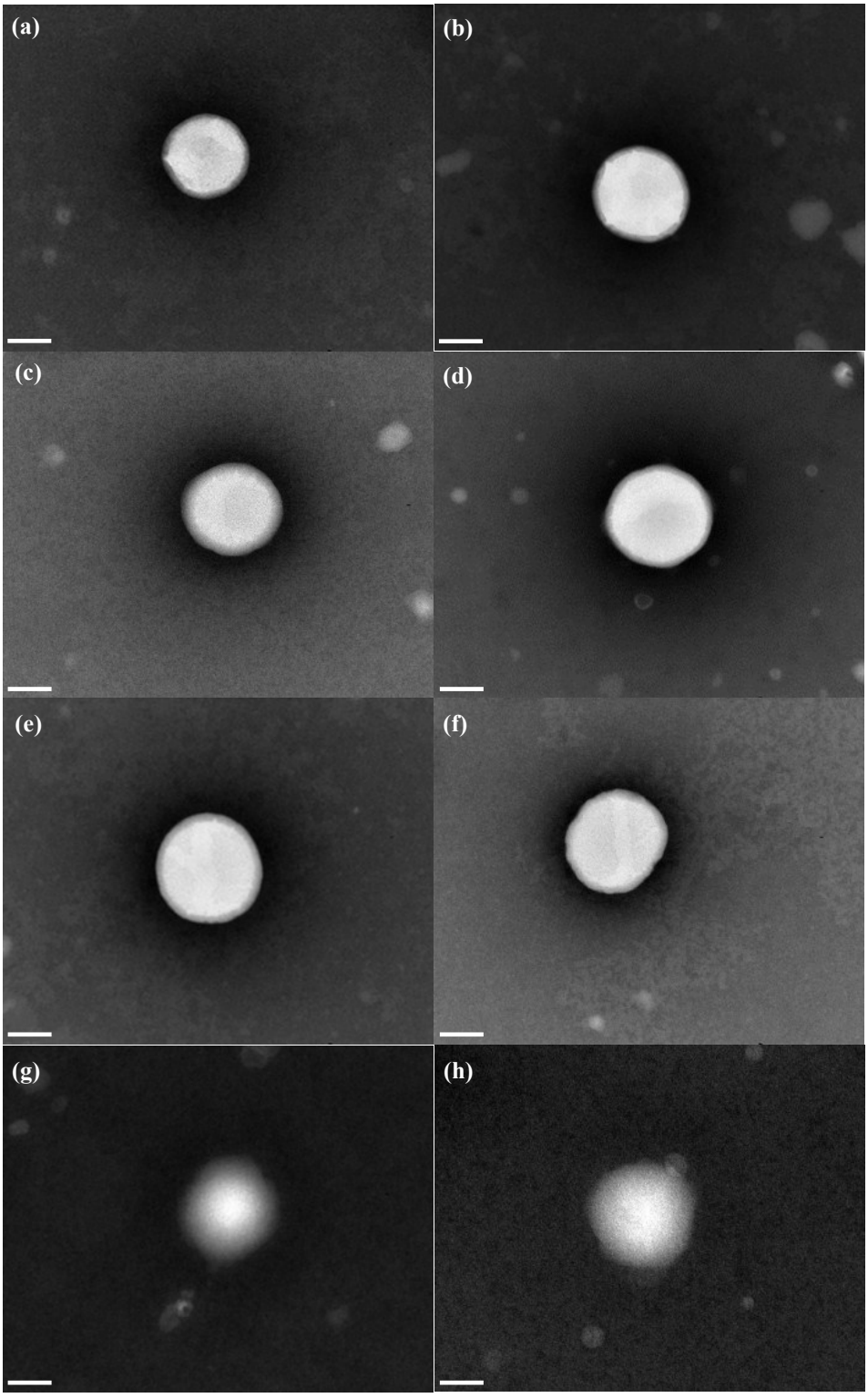

Figure 6.9: TEM images of internal and external structures of liposomes loaded with lutein at different lutein concentrations (mole %) prepared at 300 bar, 90 bar/min and 50°C. Internal structure: (a) 0%, (b) 0.5%, (c) 2%, (d) 5%, (e) 10%, (f) 20%; external structure: (g) 0%, (h) 20%.

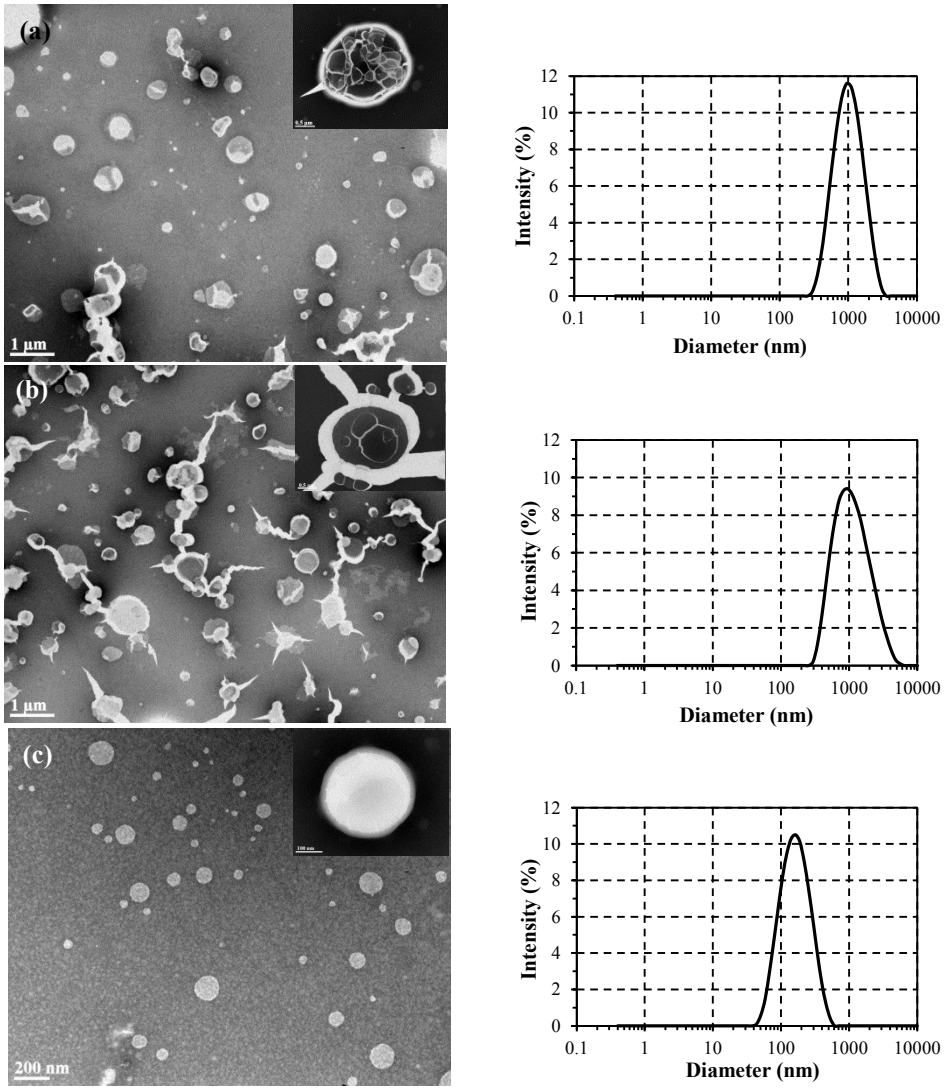

Figure 6.10: TEM images and size distribution of (a) crude lecithin suspension, (b) crude lecithin with 5% lutein suspension, and (c) bulk liposomes loaded with 5% lutein prepared using SC-CO_2 at 300 bar, 90 bar/min and 50°C.

bulk liposomes is illustrated in Fig. 6.10 to demonstrate the effectiveness of the SC-CO_2 method. Lecithin and lecithin-lutein suspensions (Figs. 6.10(a) and (b)) had large phospholipid aggregates (mean diameter of 774±46 nm and 826±57 nm, respectively) with a variety of shapes. Single aggregates in the crude suspension showed a variety of organized multivesicular systems mixed

rarely with small vesicles (data not shown). In contrast with the high heterogeneity of shapes in the crude suspensions, liposomes (Fig. 6.10(c)) displayed small and uniformly spherical shapes in the bulk vesicular system after SC-CO_2 processing. Fig. 6.10(c) clearly indicates the effectiveness of utilizing the SC-CO_2 method for liposome production.

The morphology and lamellarity of liposomes were further examined by cryo-TEM (Fig. 6.11). Based on 500 vesicles captured in 40 cryo-TEM images, liposomes obtained using SC-CO_2 exhibited primarily unilamellar spherical vesicles (87.1%); however, a small proportion of liposomes had bivesicular (8.7%) or bilamellar (4.2%) shapes. Such vesicles may be formed when the two nearby domains of phospholipids were scattered upon depressurization and reassembled via the outer layer encompassing the inner one depending on the original localization of the two aggregates.

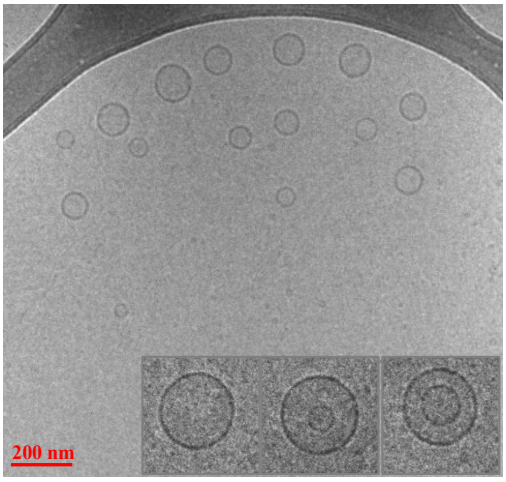

Figure 6.11: Cryogenic TEM image of morphology and lamellarity of liposomes prepared with 5% lutein by the SC-CO_2 method at 300 bar, 90 bar/min and 50°C.

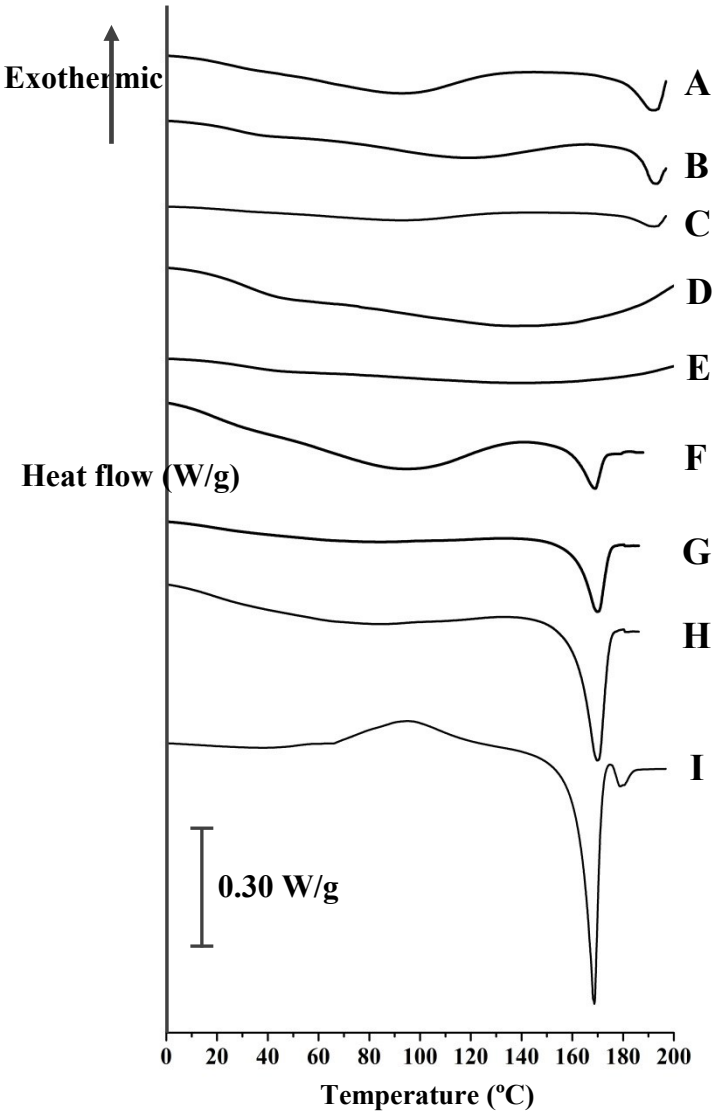

Figure 6.12: DSC thermograms of lecithin and lutein before and after SC-CO_2 treatment at 300 bar, 90 bar/min and 50°C: (A) lecithin; (B) unloaded liposomes (0% lutein); (C) liposomes with 5% lutein; (D) liposomes with 10% lutein; (E) liposomes with 20% lutein; (F) physical mixture of lecithin and 5% lutein; (G) physical mixture of lecithin and 10% lutein; (H) physical mixture of lecithin and 20% lutein; and (I) lutein.

6.3.7. Differential scanning calorimetry

The DSC thermograms of lecithin and lutein before and after SC-CO_2 treatment were shown in Fig. 6.12. Lecithin showed a highly broad endothemic peak (92ºC) during phase transition,

which suggested poor crystallinity (Fig. 6.12 A). Soy lecithin contains four phospholipid species with a variety of fatty acyl chains (van Nieuwenhuyzen & Tomás, 2008), which resulted in high heterogeneity and limited effective packing of phospholipids into crystals. Unloaded liposomes composed of the same components illustrated similar phase transition behavior as lecithin but the peak shifted to 116ºC (Fig. 6.12 B). Lutein thermograms exhibited a sharp narrow peak at 169°C (Fig. 6.12 I), indicating that pure lutein had good uniformity and crystallinity, which contributed to highly cooperative endothermic phase transition with a relatively large enthalpy compared with other multicomponent systems. The physical mixtures of lutein and lecithin also exhibited sharp endothermic peaks at the same phase transition temperature of 169ºC as the lutein concentration increased (Fig. 6.12 F, G, H), which indicated amplified lutein signals in the mixture. In contrast with the physical mixtures of lecithin and lutein, presenting lutein phase transition signals, liposomes loaded with lutein (5-20%) had no distinct phase transition peaks for soy lecithin or lutein in the DSC thermograms (Fig. 6.12 C, D, E). This may be attributed to the simultaneous disruption of lutein and phospholipid arrangements after liposome formation. The absence of the lutein signal at 169°C demonstrates the loss of lutein crystallinity due to the thorough disruption of lutein crystals into smaller units (monomers, dimers or oligomers) after being loaded into liposomes, thereby destroying the original specific crystalline arrangement of lutein. Lutein incorporation also interferes with the original packing of phospholipids, increasing the fluidity of bilayer membranes and thereby further widens the phase transition signal of phospholipids. In addition, with the disruption of the original arrangements, reorganization and interactions between phospholipids and lutein, liposomal bilayers were mostly present in a loosely packed amorphous state. These findings are in good agreement with those of Kostecka-Gugała et al. (2003) and Hu, Lin, Liu, Li and Zhao (2012). It seems that physical mixing of

lutein and lecithin components have no pronounced influence on the integrity of lutein crystals and lecithin aggregates while liposomal incorporation can significantly alter the molecular arrangement and yield a highly distinct phase transition.

6.3.8. X-ray diffraction

XRD patterns of lecithin, with or without lutein addition, and liposomes are presented in Fig. 6.13. Lutein has several resolved and sharp peaks in the diffraction pattern (Fig. 6.13 A) and good crystallinity yielded by mixed crystals whereas the physical mixtures of lecithin with different ratios of lutein showed reduced peaks and depressed degree of crystallinity (Fig. 6.13 B, C, D). Lecithin also exhibits some crystalline state prior to SC-CO_2 treatment since it had a wide and distinct peak at around 2θ of 20.7°. The elevated lutein signal shown at similar angles in proportion to increased lutein addition in the diffractogram indicated increased lutein crystals in the physical mixture, which may be attributed to the formation of polymorphs as reported previously (Bose & Michniak-Kohn, 2013; Cavalcanti et al., 2007). These data suggest that the physical mixing operation brings about little and limited disruption of lecithin and lutein crystals. However, when compared with these curves (A-E), liposomal diffractograms (Figs. 6.13 F, G, H, I) exhibited a very poor crystallinity no matter how much lutein was added. The absence of lutein and lecithin signals implied a complete disruption of lutein crystals upon its rearrangement and incorporation into the bilayers of liposomes. In contrast with the results obtained for the physical mixtures and lutein, lutein-loaded liposomes showed a significantly modified lutein distribution into the lipid components of soy lecithin. These data corroborate the DSC results (Fig. 6.12) for the same materials. These data are in good agreement with those obtained by Zhao, Cheng, Jiang, Yao and Han (2014).

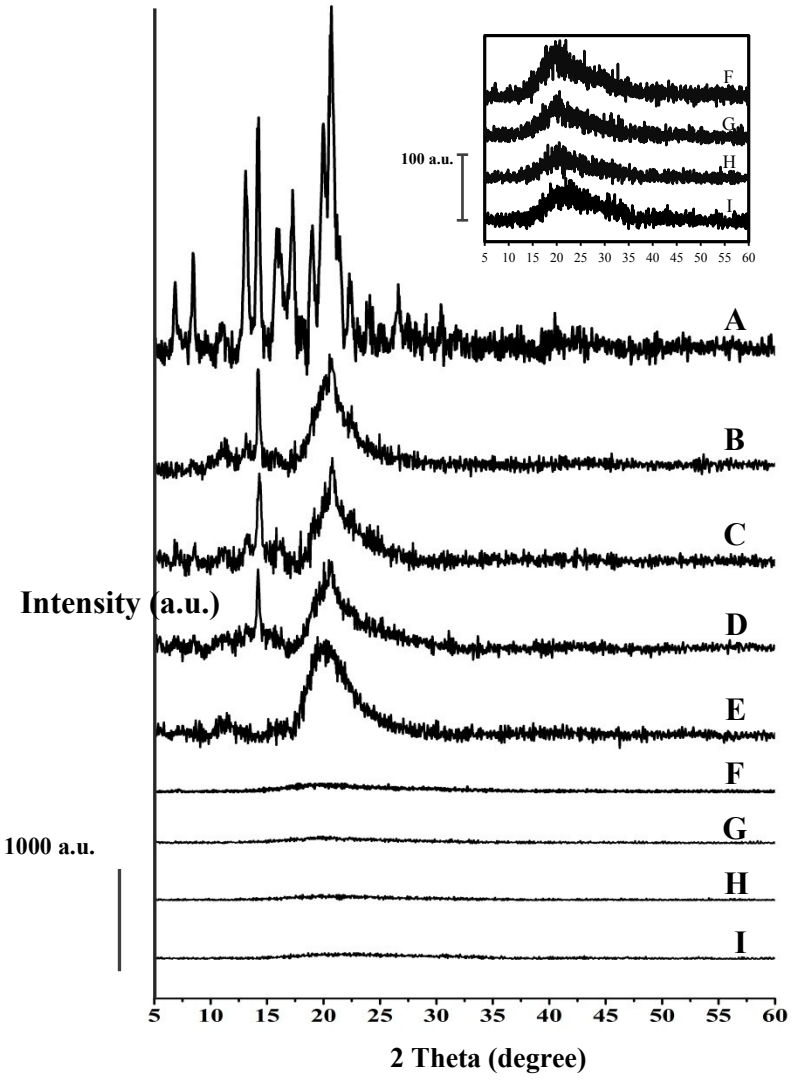

Figure 6.13: XRD diagrams of lecithin and lutein before and after SC-CO_2 treatment at 300 bar, 90 bar/min and 50°C: (A) lutein; (B) physical mixture of lecithin and 20% lutein; (C) physical mixture of lecithin and 10% lutein; (D) physical mixture of lecithin and 5% lutein; (E) lecithin; (F) liposomes with 20% lutein; (G) liposomes with 10% lutein; (H) liposomes with 5% lutein; and (I) unloaded liposomes.

6.3.9. Proposed mechanism of liposome formation

A possible mechanism for the formation of unloaded liposomes using the SC-CO_2 method was proposed in Chapter 4 (Section 4.3.1, Fig. 4.2). In this study, the previous elucidation for unloaded liposomes was adapted with some modification, considering the lutein addition. Overall, the formation of lutein-loaded liposomes was achieved via pressurization and depressurization steps, which brought about a "dispersion and disruption effect" by the rapid release of CO_2 from the aqueous medium upon depressurization. The overall mechanism (Fig. 6.14) can be considered as having four major steps:

(A) At ambient pressure and temperature, phospholipids were present primarily in the form of bilayers with curvature, forming spontaneously in the aqueous medium, whereas lutein was mainly present in the form of aggregates of dimers or oligomers.

(B) After pressurization with CO_2, high pressure promoted the solubilization of CO_2 molecules and equilibrium was established with water, resulting in the formation of carbonic acid but a portion of CO_2 remaining in the unhydrated state (Erkmen, 2012). Unhydrated CO_2 can diffuse and get partially localized in between the hydrophobic fatty acyl chains of phospholipids (or phospholipid leaflets) as well as in the lutein aggregates (Garcia-Gonzalez et al., 2007; Isenschmid et al., 1995). The high affinity between CO_2 and the bilayer membrane was previously confirmed by Spilimbergo, Elvassore and Bertucco (2002), who determined the solubility of CO_2 in the phospholipids using a model cell membrane system. Accumulation of CO_2 in the lipophilic polymers encouraged disordering (Jones & Greenfield, 1982) and reorganization among phospholipids and lutein monomers (Garcia-Gonzalez et al., 2007) and thereby the expansion of the length and thickness of the bilayers and lutein aggregates (Kamihira et al., 1987). An equilibrium among CO_2, water,

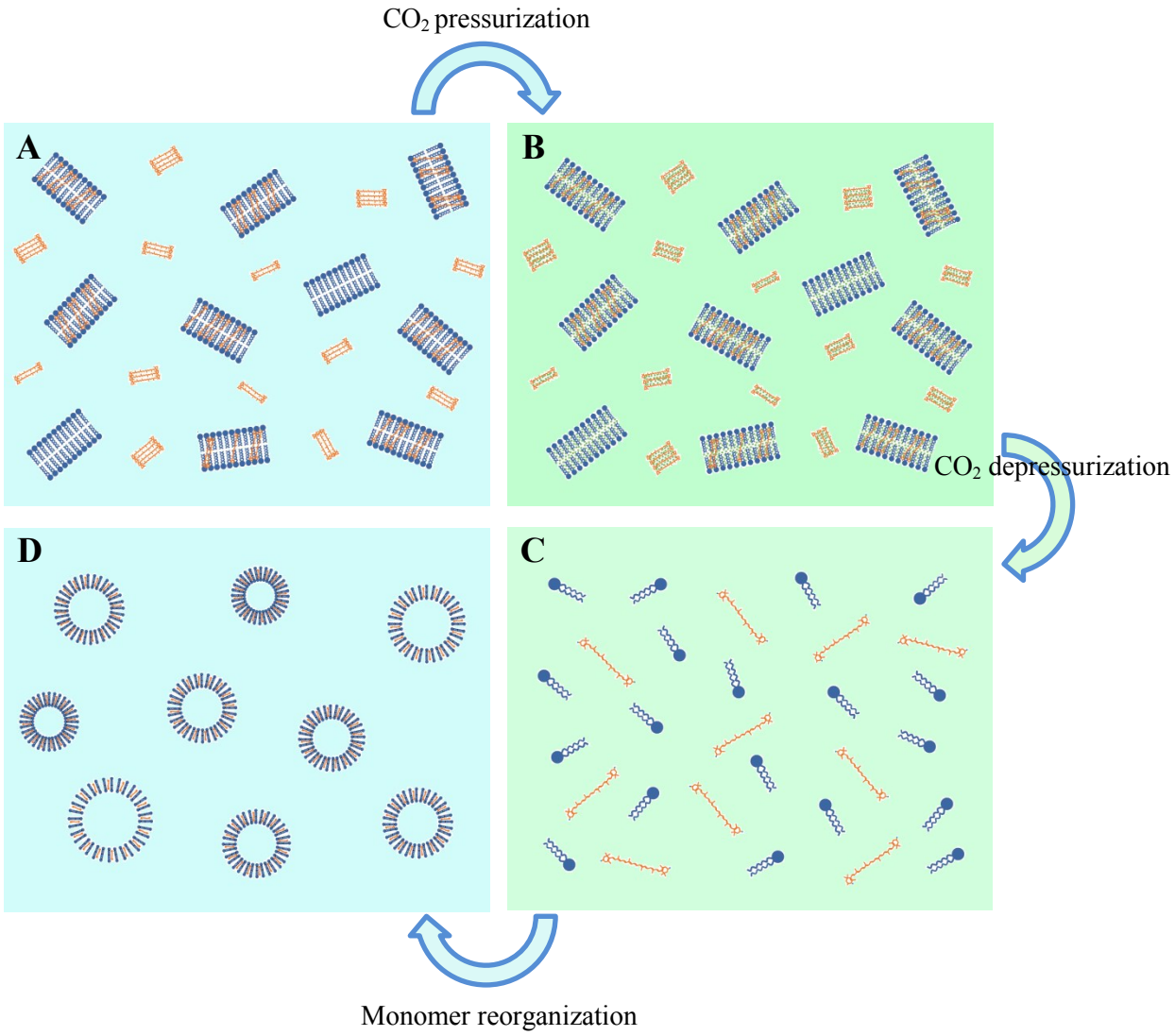

Figure 6.14: Schematic illustration of proposed mechanism of lutein-loaded liposome formation by the SC-CO_2 method: (A) Aqueous suspension of phospholipid bilayers and lutein aggregates at ambient conditions, (B) CO_2-expanded phospholipid bilayers and lutein aggregates in equilibrium with high pressure CO_2, (C) Instantaneous solution of discrete phospholipid and lutein molecules formed during depressurization of CO_2, (D) Lutein-loaded liposome dispersion at ambient conditions.

phospholipids and lutein was established.

(C) Upon depressurization, CO_2 molecules are released in a dramatically rapid manner from the phospholipid bilayers and lutein aggregates, forcing these to be dispersed into a short-lived discrete monomer state, resulting in an instantaneous aqueous solution of discrete phospholipid and lutein molecules.

(D) After formation of the instantaneous solution, the temporarily separated phospholipid and lutein monomers reorganize due to hydrophobic and van der Waals interactions and finally pack into lutein-loaded liposomes. In these liposomes, lutein molecules span the bilayers with their hydrophilic groups anchored in the two opposite polar heads of the phospholipids (Gruszecki & Strzałka, 2005). Thus, lutein adopts localization by two hydroxyl groups interacting with the phosphate groups of lecithin on both ends and the polyene chain interacting with the fatty acyl chains in between (Gruszecki & Strzałka, 2005; Tan et al., 2013).

The effect of the break-up of aggregates during depressurization on the liposomal characteristics would predominantly depend on the pressure and depressurization rate, as discussed previously in Chapter 4. It was inferred that the disruption effect of the pressurization–depressurization step on the phospholipids may be similar to that in the conventional homogenization of these materials, which breaks up bulk bilayers and form smaller vesicles. However, due to the phase transition of CO_2 during depressurization as it is released from the liquid phase to the gas phase, heat is absorbed and extracted from the phospholipid-lutein suspension, resulting in a rapid temperature drop as opposed to the heat accumulation in conventional homogenization. This cooling effect is favorable for the stabilization of thermally

labile bioactive compounds during encapsulation into liposomes for functional food and nutritional applications.

6.4. Conclusions

Lutein-loaded liposomes were prepared by an improved SC-CO_2 method. They were characterized by their particle size distribution, encapsulation efficiency, bioactive loading, zeta potential, morphology, phase transition and crystallinity. Ultimately, liposomes with a particle size of 155±1 nm, EE of 97.0±0.82% and zeta potential of -61.7±0.55 mV were obtained. An elevated pressure and depressurization rate encouraged a higher encapsulation efficiency of lutein due to the enhanced dispersion of lecithin and lutein. High temperature (>50°C) was favorable for lutein encapsulation due to breaking up of interactions. The lutein concentration showed a significant effect on the morphology of vesicles, as well as size distribution and EE. DSC and XRD results implied that a significantly modified phase transition and loss of crystallinity occurred upon the redistribution of lutein into the liposomes. The SC-CO_2 method resulted in liposomes with superior characteristics that were highly associated with CO_2 dispersion during processing. This offers possibilities for the homogenization of amphiphilic molecules using dense phase CO_2 and further for fine-tuning their physicochemical properties via control of pressure and depressurization rate.

CHAPTER 7 – PREPARATION OF ANTHOCYANIN-LOADED LIPOSOMES USING SUPERCRITICAL CARBON DIOXIDE: EFFECTS OF PROCESSING PARAMETERS[5]

7.1. Introduction

Nowadays, development of an efficient, reproducible, environmentally friendly and readily scalable process to yield liposomes with desirable characteristics like small particle size, high homogeneity and high encapsulation efficiency is of great industrial interest (Cano-Sarabia et al., 2008). Supercritical carbon dioxide (SC-CO_2) is a promising technique to process amphiphilic aggregates into nano-forms with unique features. The SC-CO_2 technique offers great potential for scale up based on excellent solvating power similar to liquid organic solvents during processing of materials. In addition, the tunability of its density, high diffusivity, low interfacial tension and viscosity provide advantages which cannot be easily achieved in traditional solvent-based methods.

Among the unit operations involving SC-CO_2, formation of liposomes and other nano-sized carrier forms from heterogeneous material systems for encapsulation and delivery purposes has gained great importance. Liposomes are valuable phospholipid assemblies, which are being used as encapsulation vehicles to deliver hydrophilic and hydrophobic ingredients (Cabrera et al., 2013). Liposomes offer unique features to protect active compounds from a number of unfavorable conditions for enhanced efficacy (Bozzuto & Molinari, 2015) and are also suitable for a number of versatile applications with respect to the models of cell membranes, reaction vessels and delivery systems (Elizondo et al., 2012).

[5]A version of this chapter has been accepted for publication: Zhao, L., Temelli, F. (2016). Preparation of anthocyanin-loaded liposomes using an improved supercritical carbon dioxide method. *Innovative Food Science and Emerging Technologies, 39*, 119-128.

In Chapters 4 and 5, an improved SC-CO_2 process, combining the advantages of two previously reported supercritical methods (Cano-Sarabia et al., 2008; Otake et al., 2006), was developed to produce liposomes with desirable characteristics. The performance of unloaded liposomes was firstly studied and the impact of processing and compositional parameters was assessed. Then, a hydrophobic bioactive compound (lutein) was encapsulated into liposomes using this technique and their encapsulation behaviors and characteristics were studied (Chapter 6). To further assess the effectiveness of this SC-CO_2 method, the next step is to encapsulate a hydrophilic compound into liposomes and compare their characteristics with those obtained by the traditional thin film hydration (TFH) method. Anthocyanin was selected as the model hydrophilic component for encapsulation into liposomes.

Anthocyanin is a powerful flavonoid antioxidant, which gives the colors of red, blue and purple in different varieties of flowers, fruits and vegetables. Anthocyanin has received growing attention as a natural colorant in food, natural health product and cosmetic formulations not only due to its extensive range of colors but also its health benefits. Anthocyanin has been shown to offer health benefits, including reducing the risk of cardiovascular disease, control of obesity and diabetes as well as improvement of visual and brain functions (Tsuda, 2012). However, its high reactivity renders it susceptible to degradation due to factors such as light, heat, oxygen and relatively basic pH in the gastrointestinal tract. Thus, encapsulation of anthocyanin in liposomes is of great importance to protect anthocyanin from these adverse conditions and maintain its stability and efficacy. A small amount of cholesterol is incorporated into liposome membranes to improve the packing of phospholipids, reduce the membrane permeability and prevent the leakage of anthocyanins from liposomes (Bozzuto & Molinari, 2015). The objective of this study was to evaluate the effects of pressure, depressurization rate, and temperature on the

characteristics of liposomes, including particle size distribution, morphology, encapsulation efficiency, bioactive loading and stability. In addition, liposomes loaded with anthocyanin generated by the SC-CO_2 method were compared to those prepared by the traditional TFH method.

7.2. Materials and methods

7.2.1. Materials

Soy lecithin obtained from Fisher Scientific (Ottawa, ON, Canada) was used for liposome preparation. Anthocyanin (76%) from bilberry (*Vaccinium myrtillus*) was purchased from Hangzhou Ningsi Bio-tech (Hangzhou, China). Sodium citrate dehydrate (99%), citric acid monohydrate (99%), cholesterol (99%), ethanol (99.8%) and methanol (99.9%) were purchased from Sigma-Aldrich (Oakville, ON, Canada). Liquid CO_2 (purity of 99.99%) supplied by Praxair Canada (Mississauga, ON, Canada) was used in all high pressure CO_2 processing. Water purified by Milli-Q® ultrapure water purification system (EMD Millipore, Billerica, MA, USA) was used in all experiments.

7.2.2. Preparation of crude suspension

Crude lecithin/anthocyanin/cholesterol suspension was prepared fresh for liposome preparation. Anthocyanin from the bilberry (*Vaccinium myrtillus*) (MW: 466 g/mole) at 10% (mole % of the total number of moles of lecithin, cholesterol and anthocyanin) was dissolved in 100 mL sodium citrate buffer (pH 3.5) in a dark environment. The pH of the suspension used for liposome formation was controlled at pH of 3.5 for two reasons. Firstly, stability of anthocyanins can be maintained at this pH. Secondly, phospholipids can have sufficient dissociation in the phosphate head groups to main their packing parameters within the range of 0.5-1.0, which is favorable for liposome formation (more acidic pH condition reduced the head group area and

may lead to the formation of inverse hexagonal phase (Cullis, & De Kruyff, 1976)). Then, soy lecithin (1.33 g, MW: 677.92 g/mole) was dispersed into the anthocyanin solution with continuous agitation for 30 min using a magnetic stirrer at 1200 rpm. The final concentration of phospholipids was controlled at 20 mM. Cholesterol at 20% (mole %) level was slowly added and thoroughly mixed with the lecithin/anthocyanin suspension at 1200 rpm in the dark for 1 h. The crude lecithin/anthocyanin/cholesterol suspension was stored under nitrogen and dark at 4°C and used within one week.

7.2.3. Preparation of liposomes by SC-CO_2

The preparation of anthocyanin-loaded liposomes was performed in a similar manner as described in Section 4.2.3. Crude lecithin/anthocyanin/cholesterol suspension (6 mL) was sealed in a high pressure vessel. Liposomes were formed upon depressurization of the CO_2-expanded liquid phospholipid suspension phase at constant depressurization rate and pressure. Different levels of pressure, depressurization rate and temperature were evaluated as summarized in Table 7.1.

Table 7.1: Processing conditions for liposome preparation using the SC-CO_2 method.

Factors	Levels	Processing parameters
Pressure (bar)	60, 100, 150, 200, 250, 300	50°C, 90 bar/min, 10% anthocyanin and 20% cholesterol
Depressurization rate (bar/min)	10, 20, 40, 60, 90, 120, 150, 200	50°C, 300 bar, 10% anthocyanin and 20% cholesterol
Temperature (°C)	40, 45, 50, 55, 60, 65	300 bar, 90 bar/min, 10% anthocyanin and 20% cholesterol

7.2.4. Preparation of liposomes by TFH

The preparation of liposomes by the TFH method was performed in a similar manner as described in Section 3.2.6.

7.2.5. Particle size distribution

The particle size and size distribution of anthocyanin-loaded liposomes was measured in a similar manner as described in Section 3.2.7.

7.2.6. Zeta potential

The zeta potential of lutein-loaded liposomes was measured in a similar manner as described in Section 3.2.8.

7.2.7. Encapsulation efficiency and bioactive loading

Encapsulation efficiency of liposomes was determined according to Panwar, Pandey, Lakhera, and Singh (2010) with modification. Liposomes were subjected to ultracentrifugation at 50,000×g for 30 min at 4°C in an Optima Max-XP ultracentrifuge (Beckman Coulter, Fullerton, CA, USA) to obtain phase separation. The pellets were washed twice with 1 mL sodium citrate buffer (pH 3.5) and centrifuged again for 30 min. For the free anthocyanin determination, the upper phase was separated and diluted by the sodium citrate buffer (1:1). For encapsulated anthocyanin determination, 6 mL of acidic methanol (1% HCl, w/v) was added to the lower phase and subjected to vortex mixing for 1 min. Prior to absorbance measurement, full spectrum scanning of bilberry anthocyanin in the buffer and acidic methanol was performed and the peak wavelengths were detected as 522 nm and 529 nm, respectively. Calibration curves of absorbance versus anthocyanin concentration were established to determine the concentration of anthocyanin (μg/mL) in both phases. The absorbance of anthocyanin in the upper and lower phases was determined at 522 and 529 nm, respectively. The EE and BL were calculated according to Eqs. (7.1) and (7.2), respectively:

$$\text{EE (\%)} = \frac{\text{Loaded anthocyanin content (μg)}}{\text{Loaded anthocyanin content (μg)} + \text{Free anthocyanin content (μg)}} \times 100\% \qquad (7.1)$$

$$\text{BL (\%)} = \frac{\text{Loaded anthocyanin content (μg)}}{\text{Total lipid content (μg)}} \times 100\% \quad (7.2)$$

7.2.8. Morphology

The morphology of liposomes was evaluated using conventional transmission electron microscopy (TEM) and cryogenic transmission electron microscopy (cryo-TEM). For assessment of general morphology, TEM was performed using a FEI Morgagni 268 electron microscope (FEI, Hillsboro, OR, USA) at 80 kV equipped with an Orius® SC1000 CCD Camera (Gatan, Pleasanton, CA, USA) as described in Section 3.2.9. Cryo-TEM was used to assess morphology and lamellarity. The sample (5 μL) was placed on a glow-discharged formvar carbon-coated grid (200 mesh, Ted Pella, Inc., Redding, CA, USA). After adhering for 15 s, the grid was gently blotted to obtain a thin film of liquid. A thin film of liposomes was immediately plunge-frozen using liquid ethane and then stored in liquid nitrogen for observation. Liposomes were observed in liquid nitrogen using a JEM-2100 TEM (JEOL USA, Inc., Peabody, MA, USA) at -170°C and 200 kV and recorded by an Orius SC1000 CCD camera (Gatan Inc., Pleasanton, CA, USA).

7.2.9. Storage stability

Liposomes were sealed under nitrogen in a glass vial and wrapped with parafilm M sealing film around the cap (Fisher Scientific, Ottawa, ON, Canada). Sealed liposome vials were wrapped with aluminum foil and stored in the dark at 4°C. The storage stability of liposomes was assessed by evaluating their particle size distribution weekly for up to 5 weeks with the particle size distribution measured as above.

7.2.10. Statistical analysis

Liposomes were prepared in triplicate at each processing condition (Table 7.1). Particle size distribution, zeta potential, encapsulation efficiency and bioactive loading of each liposome and other lipid sample were measured in triplicate. Data analysis was performed using Minitab

statistics software 16 (Minitab Inc., State College, PA, USA) and reported as the mean ± standard deviation (SD). One-way analysis of variance (ANOVA) was conducted and significant differences between means were obtained by Tukey's multiple comparison test at a significance level of $p < 0.05$.

7.3. Results and discussion

7.3.1. Effect of pressure on liposome formation

The effect of pressure on the particle size, polydispersity index (PdI), EE and BL of liposomes was shown in Fig. 7.1. Particle size of liposomes refers to their mean hydrodynamic diameter calculated based on the Stokes-Einstein equation of Brownian motion. As the pressure was elevated, the particle size of liposomes significantly decreased ($p<0.05$) from 238±4 nm to 160±2 nm (Fig. 7.1(a)). PdI is calculated based on the cumulants analysis of the intensity autocorrelation function of dynamic light scattering. PdI values below 0.2 are usually considered to be monodisperse, whereas indices less than 0.3 are considered as ideal and indicate a narrow size distribution of particles (Meledandri, Ninjbadgar, & Brougham, 2011). PdI also displayed a significant decrease ($p<0.05$) with pressure, from 0.384±0.032 to 0.262±0.013 (Fig. 7.1(a)). The size distribution curves (Fig. 7.2) indicated that liposomes prepared by the SC-CO_2 method at 100-300 bar all exhibited a unimodal distribution, and higher pressure was favorable for a narrower size distribution. The particle size and PdI data suggested that the higher pressure could improve the particle characteristics with reduced particle size and enhanced homogeneity of liposomes. Pressure dictates the solubility of CO_2 in the liquid phase and elevated pressure increases the solubility of CO_2 as well as the amount of unhydrated CO_2 accumulated in between the phospholipid bilayers (Duan & Sun, 2003). As described later in Section 7.3.6 to propose a mechanism for liposome formation, increased CO_2 accumulation leads to weakened interactions

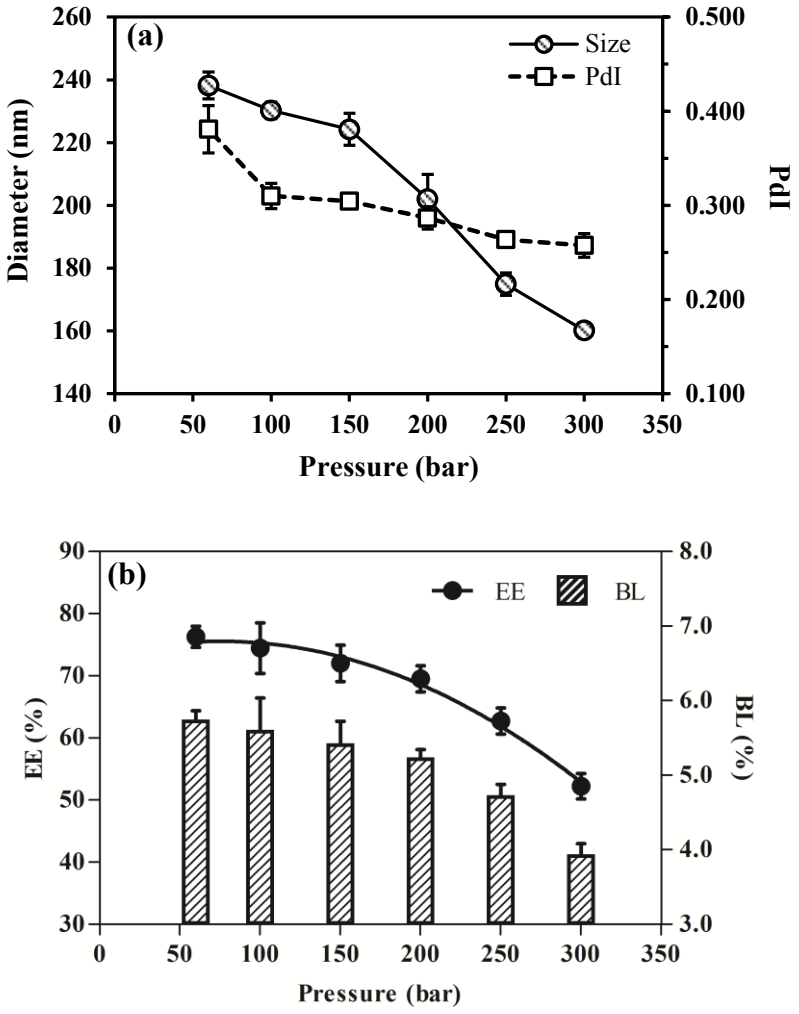

Figure 7.1: Effect of pressure on (a) mean diameter and polydispersity index (PdI) and (b) encapsulation efficiency (EE) and bioactive loading (BL) of anthocyanin-loaded liposomes prepared with 10% anthocyanin and 20% cholesterol at 90 bar/min and 50°C by the SC-CO_2 method.

among the fatty acyl moieties and thereby a better dispersion of phospholipids into monomers instantaneously upon depressurization before they reassemble into vesicles of smaller size and higher uniformity.

The EE and BL showed a similar trend, with a significant decrease ($p<0.05$) with increased pressure to 52.2 ± 2.1% and 4.39 ± 0.18%, respectively, at 300 bar (Fig. 7.1(b)). The EE and BL are closely associated with the entrapped aqueous volume in the core of liposomes. A large

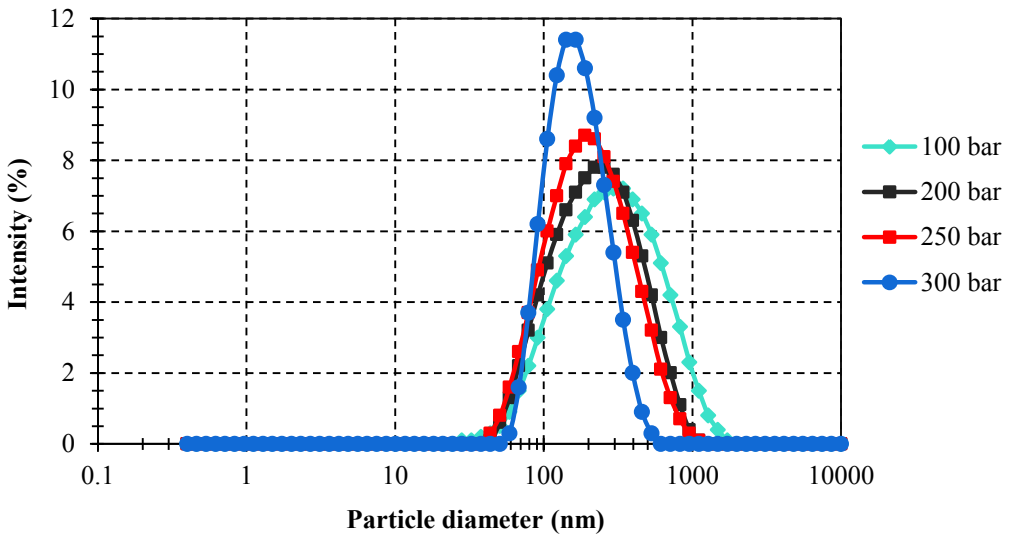

Figure 7.2: Size distribution of anthocyanin-loaded liposomes prepared at different pressures with 10% anthocyanin and 20% cholesterol at 90 bar/min and 50°C by the SC-CO_2 method.

liposomal size surrounding a large internal aqueous volume leads to a higher EE and BL of hydrophilic bioactives. Although it was found that a larger EE and BL were achieved at a low pressure range, a high pressure is preferred for liposome preparation considering the homogeneity and morphology.

The EE obtained for the anthocyanin encapsulation was higher than those reported for other hydrophilic compounds (Nii & Ishii, 2005; Otake et al., 2006). Such a high level of encapsulation may result from the partial partitioning of anthocyanin into the liposomal bilayers, which impacts membrane fluidity (Arora, Byrem, Nair, & Strasburg, 2000; Bonarska-Kujawa, Pruchnik, & Kleszczyńska, 2012). Although anthocyanin is usually classified as a hydrophilic molecule with a number of hydroxyl groups attached, it also contains aromatic rings (partially hydrophobic) (Fig. 2.6). Due to this special structure, the characteristics such as encapsulation efficiency and particle size of anthocyanin-loaded liposomes have shown differences from those of liposomes loaded with traditional hydrophilic drugs. This partitioning into the fatty acyl

region of lipid bilayers in addition to interacting at the lipid-water interface would enhance the particle size and encapsulation efficiency. In terms of a detailed chemical structure, bilberry anthocyanin is present as the glycosides of polyhydroxy and polymethoxy derivatives of 2-phenyl-benzopyrylium (Welch et al., 2008). The molecular structure of anthocyanin was described in Section 2.4.2 as affected by pH (Fig. 2.6). Anthocyanin can exhibit various colors due to structural transformation as pH changes, like flavylium cation as red at pH of 1-3, carbinol pseudobase as colorless at pH of 4-5 and anionic quinonoidal base as blue at pH of 7-8, among which the flavylium cation is considered to be the most stable (Brat, Tourniaire, & Amiot-Carlin, 2008). Anthocyanin is usually present as a mixture of different forms in equilibrium with one form being dominant at each pH condition (Welch et al., 2008). Compared to the pH 3.5 of the anthocyanin-lecithin suspension prepared at ambient condition in this study, increased pressure leads to a pH reduction (pH may drop to 2.8 at 300 bar and 50°C) due to enhanced CO_2 solubilization in the aqueous phase and formation of carbonic acid (Balaban et al., 1991). This may result in the formation of an increased level of flavylium cation of anthocyanin as well as a reduced number of negatively charged phospholipids, resulting from altered dissociation at more acidic conditions. Therefore, the stability of anthocyanin will be enhanced during SC-CO_2 processing, which is a unique advantage of the SC-CO_2 process. In addition, EE and BL may also be influenced by the electrostatic interactions between the positively charged pyridine ring of anthocyanin and the negatively charged phosphate head group of phospholipids. Although the low pressure range (≤100 bar) resulted in a higher encapsulation of anthocyanin (Fig. 7.1(b)), 200 bar was selected as the optimal pressure for liposome formation considering a balance in vesicular uniformity and EE as well as morphology (as discussed in Section 7.3.4).

7.3.2. Effect of depressurization rate on liposome formation

The effect of depressurization rate on the particle size, PdI, EE and BL of liposomes was shown in Fig. 7.3. Particle size and PdI showed a significant decrease ($p<0.05$) as the depressurization rate increased and then remained constant at 157±1 nm and 0.260±0.012, respectively (Fig. 7.3(a)). This indicated that smaller vesicles with higher uniformity were generated with increased depressurization rate. With the amount of CO_2 solubilized in the liquid phase being fixed at a constant pressure and temperature, a low depressurization rate induces a slow release of CO_2 trapped between the fatty acyl chains of phospholipids, which is unfavorable for the separation of phospholipid bilayers into discrete molecules upon depressurization. On the contrary, a faster release of CO_2 at high depressurization rates brings about a scattering of these assemblies and thereby generates a homogeneous instantaneous dispersion with highly scattered phospholipids prior to their reassembly into vesicles. The EE and BL of anthocyanin-loaded liposomes both displayed a significant decrease from 75.5 ± 2.8% to 50.2 ± 1.1% and from 5.54 ± 0.37% to 3.78 ± 0.08% (Fig. 7.3(b)), respectively, with increased depressurization rate of CO_2, which is in good agreement with the trend of particle size and thus the internal aqueous volume of liposomes. It is possible that the encapsulated anthocyanin may partially bind to the liposome membrane surface through the electrostatic interaction between the flavylium cation and the negatively charged phospholipids, which may lead to structural changes in the phosphate head groups (Bonarska-Kujawa et al., 2014). Besides, with several hydroxyl groups attached, encapsulated anthocyanin in liposomes may interact with phospholipids or cholesterol via hydrogen bonding, which is favorable for the purpose of encapsulation (Kopeć, Telenius, & Khandelia, 2013). Overall, although 200 bar/min seems to be the best depressurization rate for optimal characteristics, such a high CO_2 release rate may be more challenging to scale up,

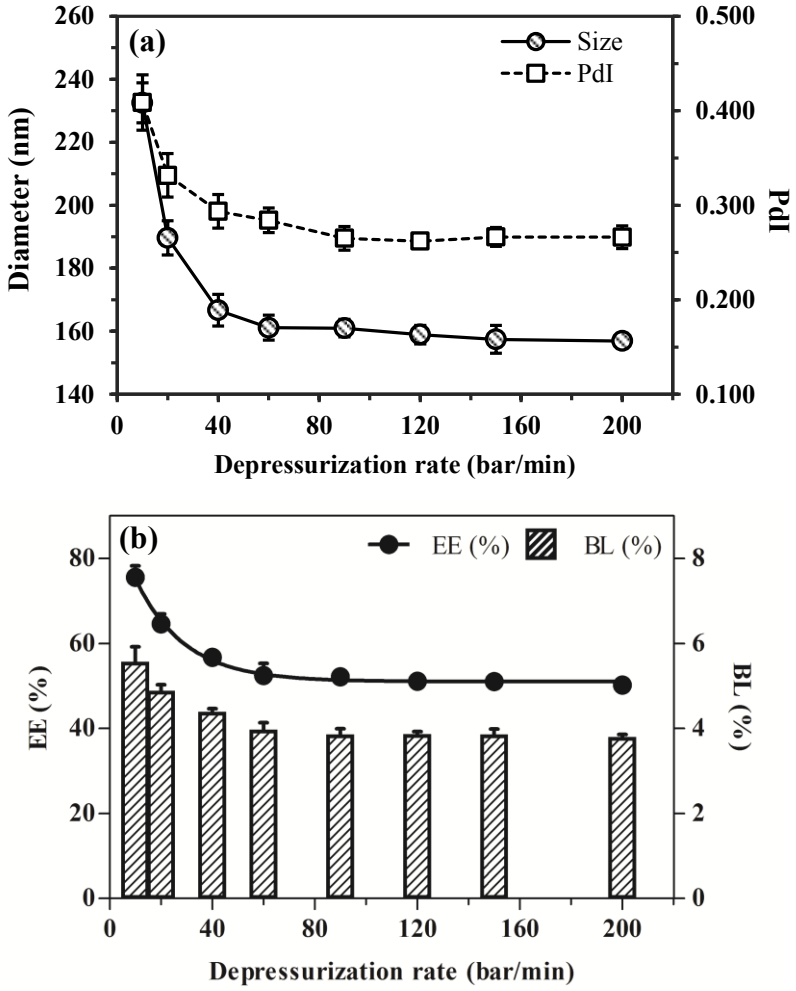

Figure 7.3: Effect of depressurization rate on (a) mean diameter and polydispersity index (PdI) and (b) encapsulation efficiency (EE) and bioactive loading (BL) of anthocyanin-loaded liposomes prepared with 10% anthocyanin and 20% cholesterol at 300 bar and 50°C by the SC-CO_2 method.

considering the Joule-Thomson effect. Considering this aspect along with the morphology of vesicles (as discussed in Section 7.3.4), 90 or 120 bar/min may be more practical for scale up purposes.

7.3.3. Effect of temperature on liposome formation

The particle size of liposomes decreased and then increased ($p<0.05$) while PdI decreased to a small extent ($p<0.05$) with a temperature increase from 40 to 65°C (Fig. 7.4(a)). Temperature

can have two opposing effects on liposome characteristics. Higher temperature can disrupt van der Waals interactions between the phospholipid molecules due to the enhanced energy input and thereby improve the fluidity of phospholipid bilayers (Mansilla, Cybulski, Albanesi, & de Mendoza, 2004). In addition, high energy input may also break up the partial interactions of anthocyanin with phospholipids or cholesterol. This can result in the formation of smaller vesicles (Venkataram, Awni, Jordan, & Rahman, 1990). On the other hand, higher temperature reduces the solubility of CO_2 in the liquid phase (Weiss, 1974) and weakens the dispersion of phospholipid molecules upon depressurization owing to a lowered amount of CO_2 within the bilayers, which results in the formation of larger vesicles. Hence, the decrease in particle size in the lower temperature range may be dominated by the enhanced fluidity of bilayers, whereas the increase in particle size in the higher temperature range was mainly controlled by the reduced solubility of CO_2.

The EE and BL exhibited a similar trend to that of the particle size ($p<0.05$), which again confirmed the fact that smaller particles resulted in lower EE and BL. Although all parameters investigated had significant impacts, temperature seemed to result in a relatively smaller change in particle size compared to pressure and depressurization rate. Besides, considering the fact that high temperature results in the degradation of anthocyanin and lowered antioxidant activity and associated health benefits (Moldovan, David, Chişbora, & Cimpoiu, 2012), a relatively low temperature is preferred to minimize the degradation of bioactives. It has been reported that anthocyanin degrades at a relatively faster rate at temperatures above 30°C (Buckow, Kastell, Terefe, & Versteeg, 2010; Ramasamy, Mazlan, Ramli, Rasidi, & Manickam, 2016). Considering all the effects on the size, uniformity and morphology, a temperature of 50°C was recommended

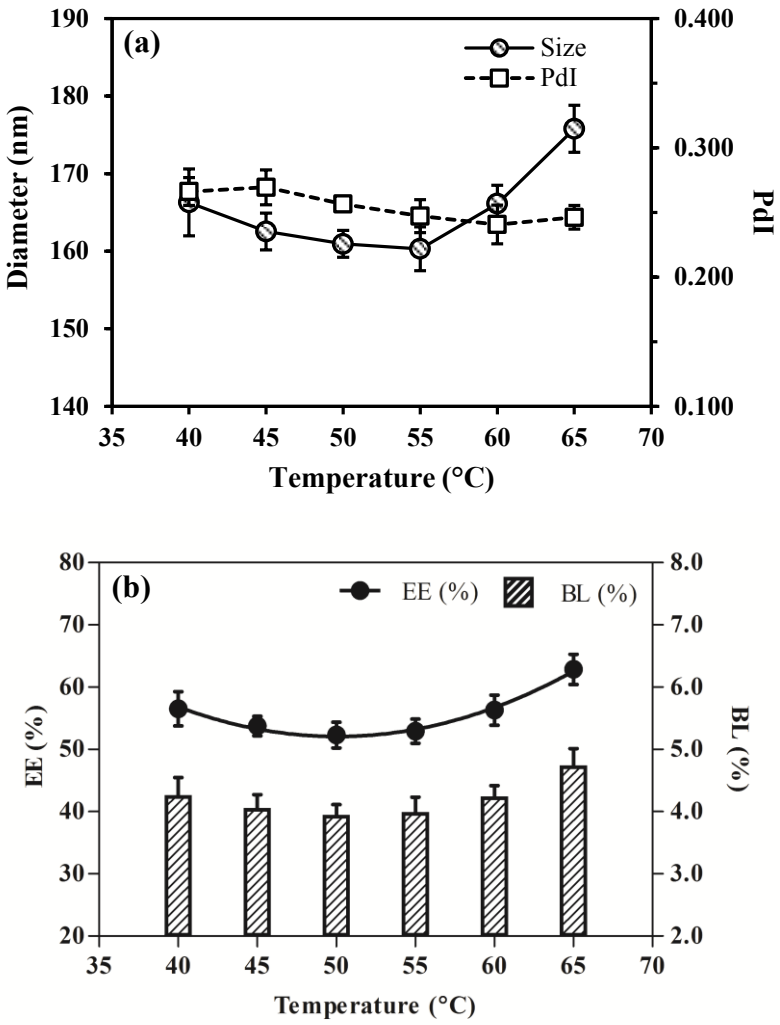

Figure 7.4: Effect of temperature on (a) mean diameter and polydispersity index (PdI) and (b) encapsulation efficiency (EE) and bioactive loading (BL) of anthocyanin-loaded liposomes prepared with 10% anthocyanin and 20% cholesterol at 300 bar and 90 bar/min by the SC-CO_2 method.

for liposome formation.

7.3.4. Morphology of liposomes

The morphology of liposomes prepared at various processing conditions was displayed in Figs. 7.5-7.8. The TEM images of liposomes prepared at the low pressure range (below 100 bar) presented more irregularity and asymmetry in the vesicles but they switched to a more spherical appearance at higher pressures (Fig. 7.5). Pressure of 300 bar yielded optimal vesicular

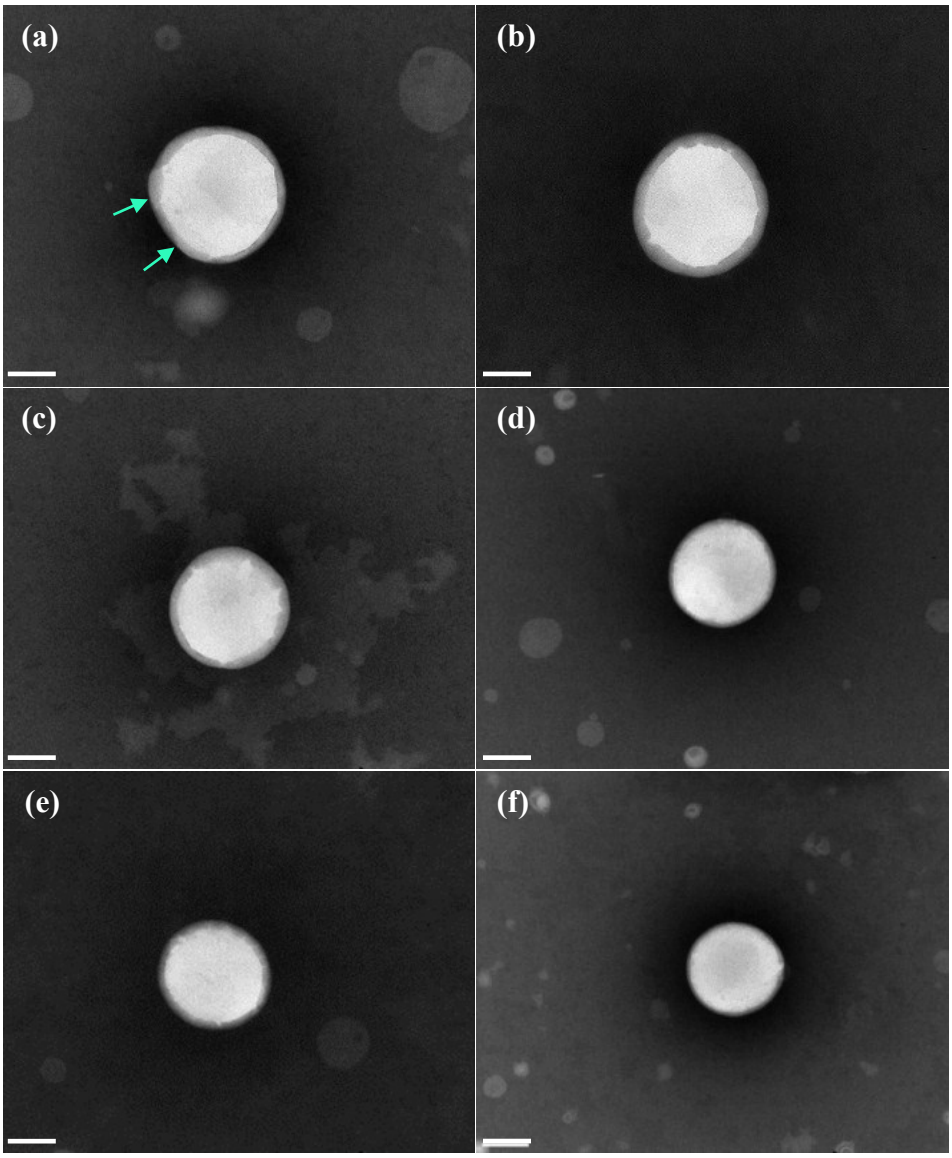

Figure 7.5: TEM images of single anthocyanin-loaded liposomes prepared with 10% anthocyanin and 20% cholesterol at 50°C and 90 bar/min at different pressures: (a) 60 bar, (b) 80 bar, (c) 100 bar, (d) 200 bar, (e) 250 bar, (f) 300 bar. Scale bars in TEM images (a)-(f) represent 100 nm. Arrows indicate irregularity on liposomal surface induced by imperfect packing of phospholipid molecules.

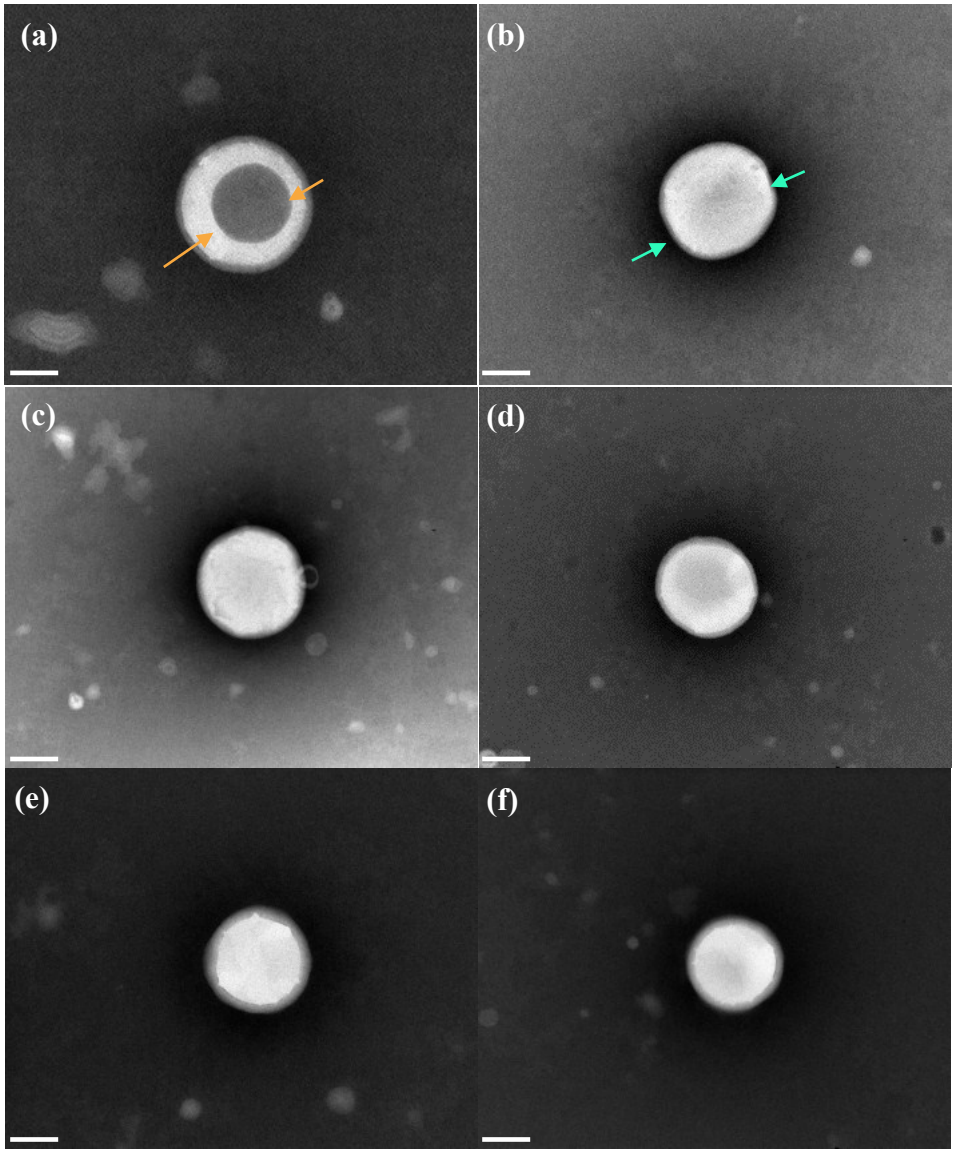

Figure 7.6: TEM images of single anthocyanin-loaded liposomes prepared with 10% anthocyanin and 20% cholesterol at 50°C and 300 bar at different depressurization rates: (a) 10 bar/min, (b) 20 bar/min, (c) 40 bar/min, (d) 60 bar/min, (e) 120 bar/min, (f) 200 bar/min. Scale bars in TEM images (a)-(f) represent 100 nm. Arrows indicate leakage (orange →) and irregularity (green →) induced by imperfect packing of phospholipid molecules.

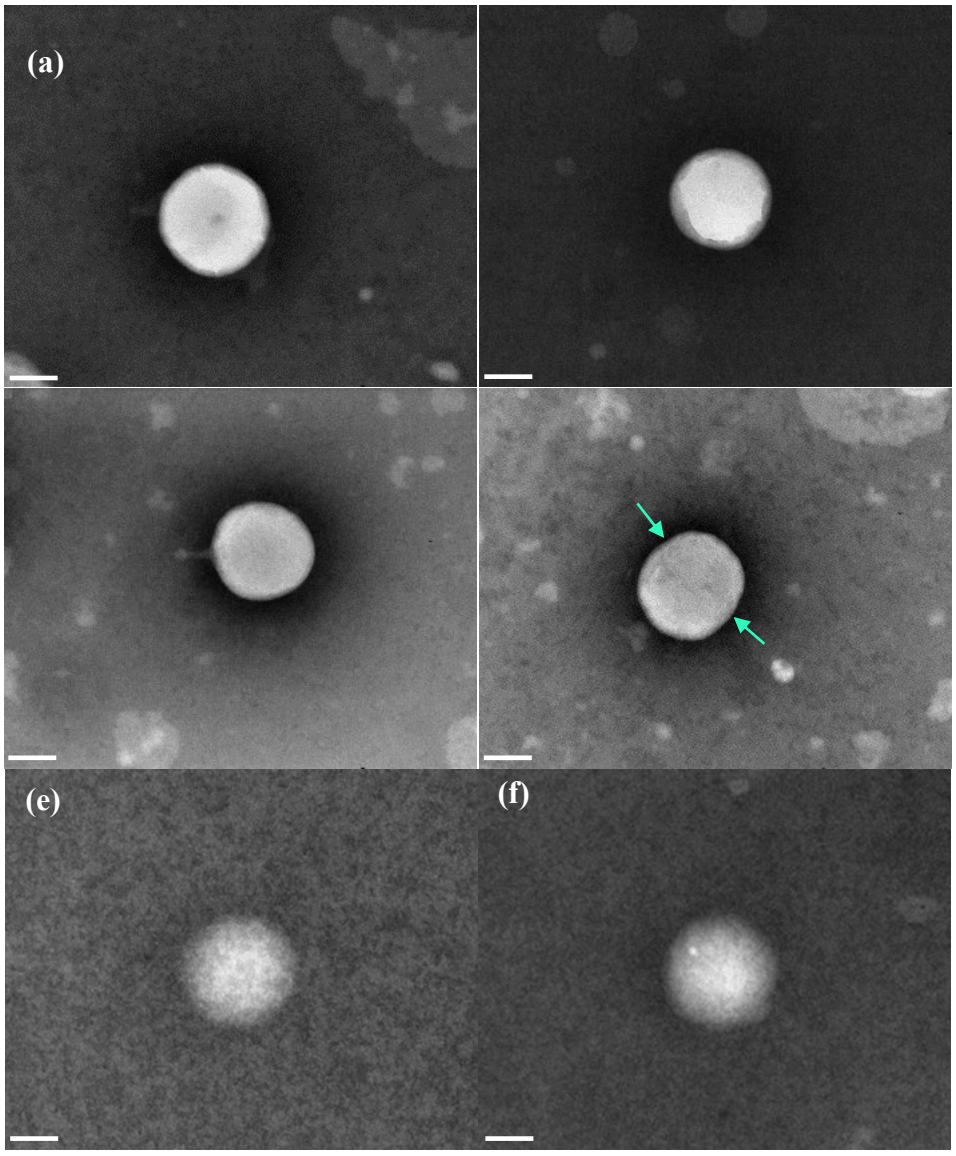

Figure 7.7: TEM images of (a-d) single anthocyanin-loaded liposomes and (e-f) external morphology prepared with 10% anthocyanin and 20% cholesterol at 300 bar and 90 bar/min at different temperatures: (a)(e) 40°C, (b) 55°C, (c) 60°C, (d)(f) 65°C. Scale bars in TEM images (a)-(f) represent 100 nm. Arrows indicate irregularity on liposomal surface induced by imperfect packing of phospholipid molecules.

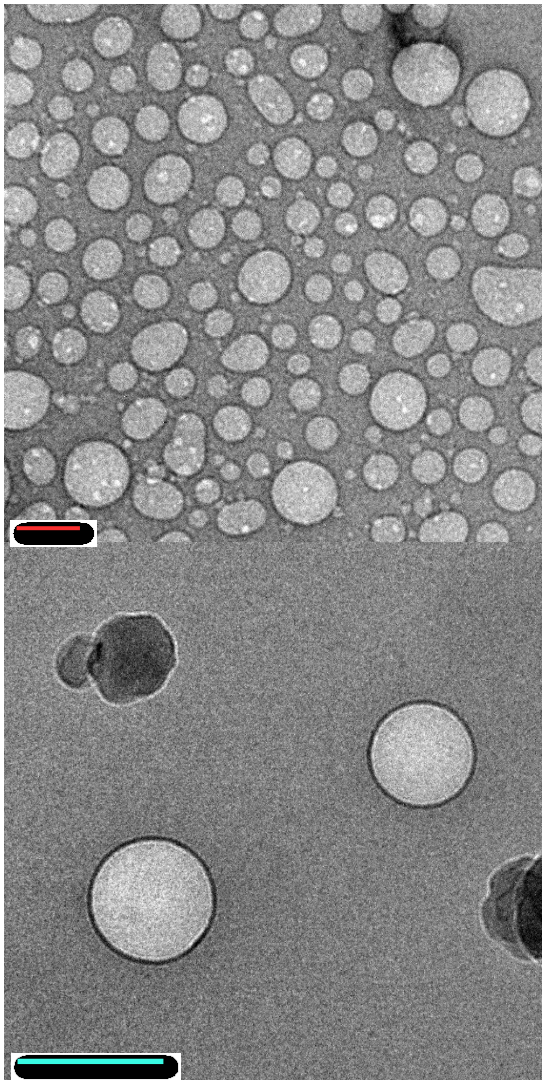

Figure 7.8: Cryo-TEM images of anthocyanin-loaded liposomes prepared with 10% anthocyanin and 20% cholesterol by the SC-CO_2 method at 50°C, 300 bar and 90 bar/min. Scale bars in red and green both represent 200 nm in the images obtained at different magnifications.

sphericity, which suggested that a strong dispersion of phospholipids caused by the release of a larger amount of solubilized CO_2 might lead to improved packing of liposome bilayers during their reassembly upon depressurization.

For the effect of depressurization rate (Fig. 7.6), relatively spherical vesicles without leakage were achieved at the high depressurization rate range (60-200 bar/min), whereas leakage was observed at a very low depressurization rate (10 bar/min) in the TEM image (Fig. 7.6(a)). This indicated that a slow release of CO_2 from the liquid phase might not be sufficient for the thorough dispersion of phospholipids and a higher depressurization rate is needed for the improved appearance of liposomes. Although a depressurization rate of 200 bar/min seemed to give the most spherical shape of liposomes, a lower depressurization rate (90-120 bar/min) is recommended for practical purposes as discussed in Section 7.3.2

For the effect of temperature on the morphology, the TEM images and external appearance of anthocyanin-loaded liposomes were shown in Fig. 7.7. Liposomes generated at lower temperatures (40-55°C) presented a relatively spherical appearance while those generated at higher temperatures (60-65°) showed reduced sphericity, becoming more cubic-like in appearance. According to the images of the external appearance (Fig. 7.7 (e-f)), liposomes obtained at 40°C were relatively more uniformly packed while those at 65°C exhibited significant vesicular asymmetry. This asymmetry may be attributed to the imperfect packing of phospholipids. High temperature could bring about improved fluidity of phospholipids owing to the high energy input and thereby reduced membrane stability of liposomes. Moreover, partitioning of anthocyanin into the liposomal bilayer membrane may be enhanced at high temperatures, which is favorable for hydrophobic interactions, meanwhile attenuating the water affinity and hydrophilic interactions (Anchordoguy, Carpenter, Crowe, & Crowe, 1992). With increased anthocyanin partitioning, the original packing order of phospholipids in the bilayers could be impaired and destabilized (Marsh, 2008). A temperature of 50 or 55 °C was selected for the optimal morphology considering the uniformity of vesicles.

The lamellarity of liposomes was assessed by cryo-TEM (Fig. 7.8). Anthocyanin-loaded liposomes displayed primarily unilamellar and spherical structures with a small number of oval or other irregular shaped vesicles. Multilamellar and multivesicular vesicles were rarely detected in any of the 48 images captured (complete data not shown). To sum up, the SC-CO_2 method could yield spherical and unilamellar liposomes with good intactness. These findings along with those on particle size discussed above suggested the possibility of regulating liposome characteristics by tuning processing parameters.

7.3.5. Comparison with the TFH method

The morphology of crude anthocyanin-lecithin suspension and bulk liposomes prepared by the SC-CO_2 and TFH methods was illustrated in Fig. 7.9 to assess the effectiveness of the SC-CO_2 method. Prior to high pressure treatment, large and heterogeneous phospholipid aggregates (mean diameter of 652±37 nm) in a variety of shapes were found in the anthocyanin-lecithin suspension. Single aggregates in the crude suspension showed a variety of multivesicular systems, but rarely any liposomal vesicles (Fig. 7.9(a)). However, after SC-CO_2 processing, spherical and unilamellar bulk liposomes in relatively high uniformity and high intactness were observed (Fig. 7.9(b)). This indicated the effectiveness of utilizing SC-CO_2 method for liposome production. In contrast, the TFH method yielded heterogeneous vesicles with unilamellar and multilamellar structures with dramatic leakage in vesicles (black region in the center of liposomes indicated dye entering the vesicle due to leakage) (Fig. 7.9(c)). Compared to those prepared by the SC-CO_2 method, liposomes obtained by the TFH method exhibited larger particle size (293±7 nm) and reduced uniformity (PdI of 0.44±0.01). Zeta potential results (Fig. 7.10) showed that liposomes prepared by the SC-CO_2 method had a relatively high zeta potential value of less than -44.3 ± 2.9 mV at different pressure levels ($p > 0.05$). Particles with an

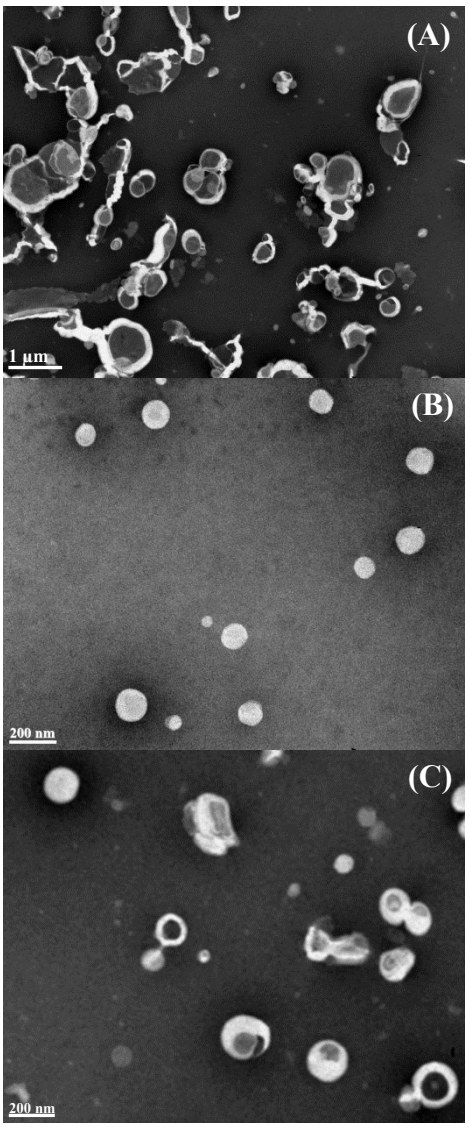

Figure 7.9: TEM images of anthocyanin-lecithin suspension and liposomes prepared by different methods: (a) crude anthocyanin-lecithin suspension used in SC-CO_2 preparation, and bulk liposomes prepared by the (b) SC-CO_2 and (c) TFH methods.

absolute zeta potential value greater than 30 mV have relatively high repulsive interaction and are considered to be stable (Jacobson & Papahadjopoulos, 1975). On the other hand, a higher surface charge was detected (zeta potential: -52.4±2.3 mV) for the liposomes prepared using the TFH method.

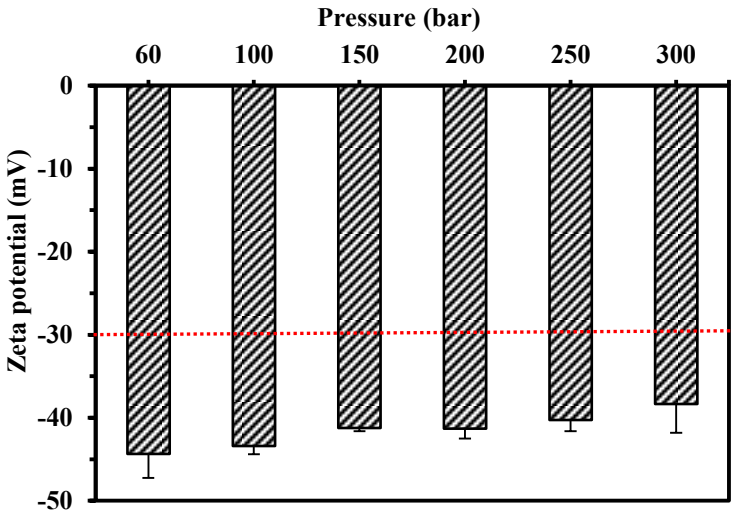

Figure 7.10: Zeta potential of anthocyanin-loaded liposomes as a function of pressure prepared with 10% anthocyanin and 20% cholesterol at 50°C and 90 bar/min.

The stability of anthocyanin-loaded liposomes prepared using the SC-CO_2 method was tested and the change in particle size at pH 3.5 over time is shown in Fig. 7.11. Liposomes remained stable for up to 3 weeks with minimal change in particle size (below 5%). Besides, the anthocyanin-loaded liposomes showed a narrow unimodal size distribution for up to 3 weeks and then switched to a polymodal and relatively broad distribution during the 4^{th} and 5^{th} week of storage. In comparison, the unloaded liposomes were stable for up to 6 weeks at pH 6.5 as reported previously in Chapter 4 (Fig. 4.10). The acidic pH condition was adopted in this study to maintain anthocyanin stability; however, phospholipids might undergo slow hydrolysis under this condition (pH 3.5) and partially form lysophospholipids and free fatty acids (Ickenstein, Sandström, Mayer, & Edwards, 2006), thereby reducing liposome stability compared to thosestored at neutral pH. On the other hand, the liposomes prepared using the TFH method had poor stability (less than 1 week) compared to those prepared by the SC-CO_2 method. This significant difference in the stability of liposomes prepared by the two methods cannot be

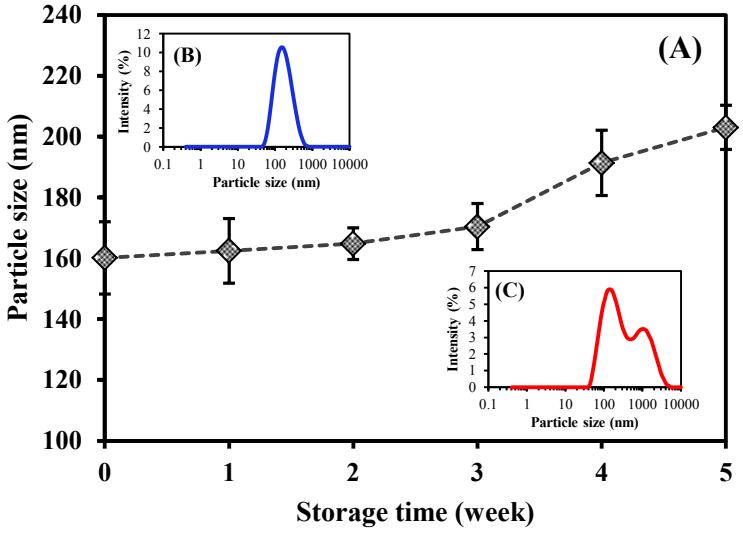

Figure 7.11: Storage stability of anthocyanin-loaded liposomes prepared by the SC-CO_2 method based on (A) particle size of liposomes as a function of time, and size distribution of (B) fresh liposomes and (C) liposomes stored for 4 weeks. The supercritical processing condition: 300 bar, 50°C and 90 bar/min. Storage condition: 4°C and pH of 3.5, under nitrogen and light proof.

explained by their zeta potentials since both had absolute zeta potentials above 30 mV. Although better understanding of stability differences requires further research, the cooling effect brought about by the release of CO_2 upon depressurization may contribute to the stability of liposomes. Due to the Joules-Thomson effect, rapid release of CO_2 withdraws heat from the liquid phase and induces a temperature drop in the liquid phase during depressurization, which may contribute to partial phase transition of phospholipids and stabilization of vesicles. This unique advantage is favorable for the protection of thermolabile compounds from heat damage while improving the membrane intactness of liposomes.

7.3.6. Proposed mechanism of liposome formation

The possible mechanism of liposome formation via the SC-CO_2 method was illustrated in Fig. 7.12, which is a modification of the mechanism proposed previously in Chapter 4 (Section 4.3.1, Fig. 4.2), considering the anthocyanin addition. Overall, the formation of anthocyanin-

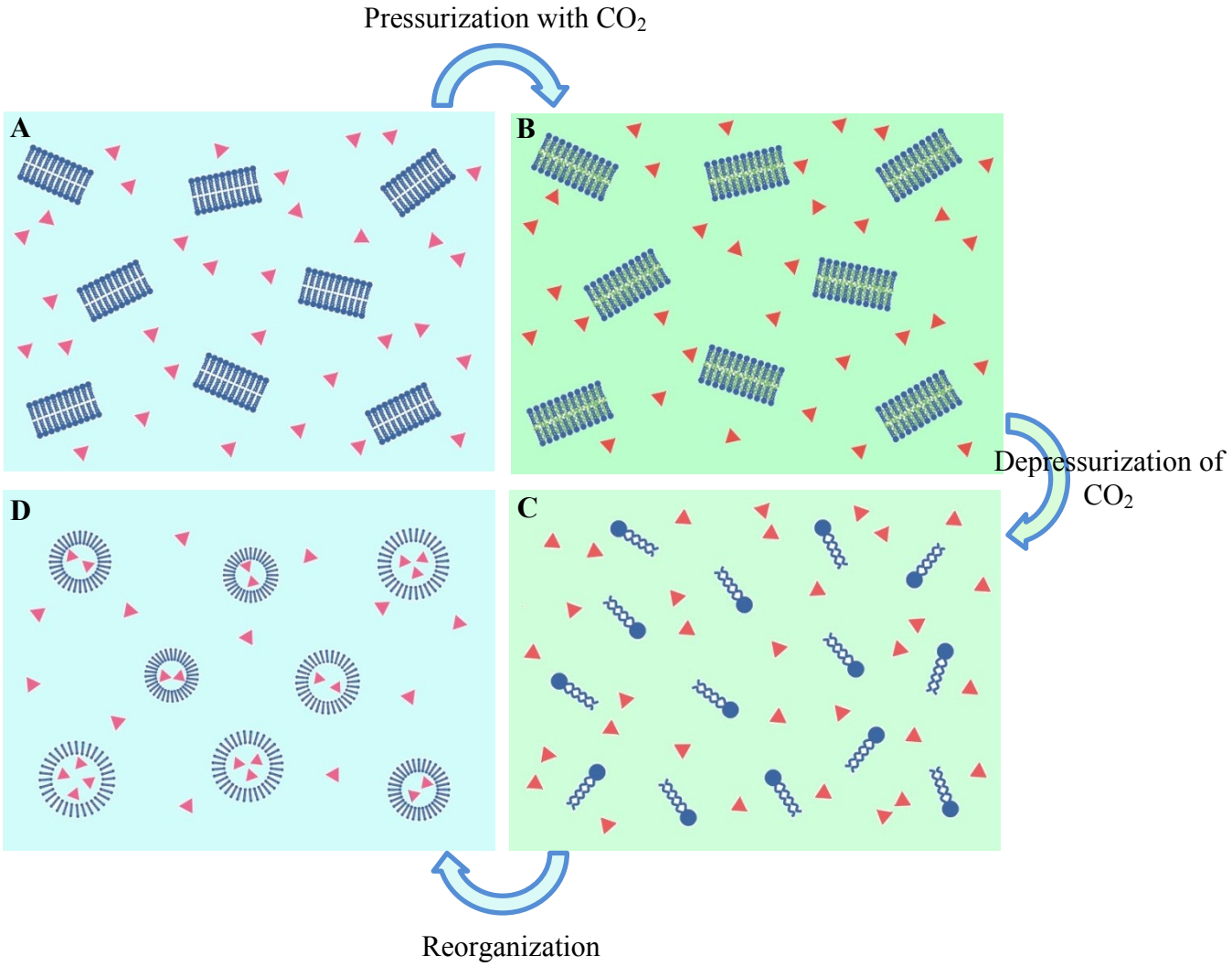

Figure 7.12: Schematic illustration of the proposed mechanism of liposome formation by the SC-CO_2 method: (A) Aqueous suspension of phospholipid bilayers and anthocyanin at ambient conditions, (B) CO_2-expanded phospholipid bilayers and anthocyanin suspension in equilibrium with high pressure CO_2, (C) Instantaneous solution of discrete phospholipid molecules and anthocyanin formed during depressurization of CO_2, (D) Anthocyanin-loaded liposome dispersion at ambient conditions.

loaded liposomes was achieved via a pressurization and depressurization process, which brought about a "dispersion and disruption effect" by the rapid release of CO_2 from the aqueous medium upon depressurization. The detailed mechanism includes four stages:

(A) At ambient conditions, phospholipid molecules were present primarily in the form of bilayer or curvature organized spontaneously in the aqueous medium. Cholesterol aggregates were randomly incorporated into the phospholipid bilayers. Anthocyanin was solubilized in the aqueous phase and was present in mixed forms at equilibrium, primarily in the form of flavylium cation and carbinol pseudobase, giving a pink-fuchsia color.

(B) Upon pressurization, CO_2 was rapidly solubilized in the aqueous phase, establishing the dissociation equilibrium, with a relatively small amount of CO_2 in carbonic acid form and the remaining amount in the unhydrated state (Erkmen, 2012). Dissociation of carbonic acid would result in more flavylium cations and color change into red due to increased acidity. Unhydrated CO_2 molecules would partially stay in between the hydrophobic fatty acyl chains of phospholipid bilayers and between the cholesterol molecules due to diffusion and solubilization and lead to an expansion in the length and thickness of bilayers. Finally, the equilibrium among CO_2, water, phospholipids, cholesterol and mixed forms of anthocyanin was established.

(C) Upon depressurization, CO_2 molecules would be rapidly released from the phospholipid bilayers to temporarily disrupt them into highly dispersed phospholipids. Similarly, cholesterol aggregates would also break up to form highly dispersed monomers. This strong dispersion would result in the formation of an instantaneous anthocyanin solution of discrete phospholipids and cholesterol. The pH value and anthocyanin in the aqueous phase would be transformed towards the original condition prior to pressurization as the CO_2 was released.

(D) After formation of the instantaneous solution, temporarily separated phospholipids and cholesterol would reorganize rapidly due to hydrophobic and van der Waals interactions and

finally assemble into anthocyanin-loaded liposomes. Anthocyanin would be transformed back to the pink-fuchsia color owing to the structural changes to the previous mixed forms and encapsulated into the aqueous core of liposomes, depending on the entrapped volume. Anthocyanin with less charged or hydroxyl groups may also partially penetrate into the bilayer membrane via the hydrophobic interaction between its hydrophobic portion and phospholipid fatty acyl chain. Determining the extent of anthocyanin partitioning into the bilayers requires further research.

7.4. Conclusions

Anthocyanin-loaded liposomes were produced utilizing an improved SC-CO_2 process, where the phospholipid/anthocyanin suspension was equilibrated with high pressure CO_2 and depressurized at a constant pressure and rate. Anthocyanin-loaded liposomes obtained at 300 bar, 90 bar/min and 50°C had a mean particle size of 160±2 nm, polydispersity index of 0.26±0.01, encapsulation efficiency of 52.2±2.1% and zeta potential of -44.3±2.9 mV. Increased pressure and depressurization rate resulted in reduced particle size and enhanced uniformity due to improved separation of phospholipids during depressurization. High temperature increased the fluidity of bilayer membrane but reduced the membrane stability of liposomes. Liposomes were stable for up to 3 weeks under nitrogen with a unimodal narrow size distribution. Liposomes produced by the SC-CO_2 method exhibited unilamellar and spherical shapes with minimal leakage and are free of organic solvent/surfactant compared with those prepared by the traditional thin film hydration method.

CHAPTER 8 – PREPARATION OF ANTHOCYANIN-LOADED LIPOSOMES USING SUPERCRITICAL CARBON DIOXIDE: EFFECTS OF COMPOSITIONAL PARAMETERS[6]

8.1. Introduction

Anthocyanin is a valuable plant-derived flavonoid bioactive with high antioxidant activity, which is present as the glycosides of polyhydroxy and polymethoxy derivatives of 2-phenyl-benzopyrylium. Anthocyanin has drawn great attention for its utilization in medical, food and nutraceutical fields due to its broad range of health benefits (Welch et al., 2008). Anthocyanin has been reported to be protective against neurological diseases, retard age-related decline in brain and cognitive functions (Ross, Winter, & Linseman, 2013; Subash et al., 2014) and was also associated with the reduced risks of cardiovascular disease, diabetes, cancer and inflammation (Wallace, 2011).

Despite all the health benefits, anthocyanin has been shown to have limited bioavailability (<6% of initial dose) since it readily undergoes rapid degradation due to different external conditions such as temperature, pH, light, oxygen, water activity and enzymes due to its high reactivity (Patras, Brunton, O'Donnell, & Tiwari, 2010; Xie et al., 2016). Current studies have focused on the encapsulation of unstable bioactives, like anthocyanin, into a polymeric matrix, which provides effective protection from external adverse conditions for enhanced stability and health benefits (Zhang et al., 2014). Different biopolymer matrices have been use to encapsulate anthocyanin, such as cross-linked β-glucan (Xiong, Melton, Easteal, & Siew, 2006), gum Arabic, pectin (Oidtmann et al., 2012), alginate (Belščak-Cvitanović et al., 2011), maltodextrin, ferritin

[6]A version of this chapter has been submitted for consideration for publication: Zhao, L., Temelli, F., & Chen, L. (2015). Encapsulation of anthocyanin in liposomes using supercritical carbon dioxide: effects of anthocyanin and sterols. *Journal of Functional Foods*.

(Zhang et al., 2014) and whey protein (Saravacos et al., 2011). Among these carriers, liposomes are promising and advanced encapsulation vehicles to protect anthocyanin from degradation. As biocompatible vesicles of a phospholipid bilayer, liposomes can not only provide protection of unstable and active compounds against environmental conditions but also enhance their absorption and bioavailability. Liposomes have gained increased interest in recent years for their versatile applications in the biomedical, food and cosmetic industries.

The most commonly used encapsulation method for anthocyanin protection is spray drying. Although rapid and inexpensive, the spray drying process has a few drawbacks in processing anthocyanin: (a) The high temperature required to evaporate the solvent may cause the degradation of anthocyanin; (b) a large particle size (usually within the micrometer range), heterogeneous size distribution as well as diverse morphology may limit the absorption and bioavailability of bioactives; and (c) loss of fine particulates in the exhaust air. To overcome these disadvantages, alternative encapsulation methods have been developed for improved particulate characteristics, such as freeze drying (Stoll, Costa, Jablonski, Flôres, & de Oliveira Rios, 2016), electrostatic extrusion (Belščak-Cvitanović et al., 2011) and thermal and ionic gelation (Ferreira, Faria, Grosso, & Mercadante, 2009). In the previous chapters, supercritical carbon dioxide (SC-CO_2) technology was introduced as a promising and novel alternative to overcome the drawbacks of traditional processing methods. SC-CO_2 is an inert, non-toxic and environmentally friendly solvent with great potential for encapsulation of various ingredients without thermal degradation and organic solvent residues.

Although with many merits, there are limited reports on liposomes loaded with anthocyanin, regardless of the preparation method employed. Hwang et al. (2013) used the thin film hydration method to produce anthocyanin-loaded liposomes and achieved a particle size of 158± 2 nm and

encapsulation efficiency of 55 ± 3% at 60°C. In Chapter 7, the encapsulation of anthocyanin with liposomes using the SC-CO_2 method was investigated and the effects of processing parameters were evaluated. Liposomes obtained with the SC-CO_2 method had a mean diameter of 160±2 nm, polydispersity index of 0.26±0.01 and encapsulation efficiency of 52.2±2.1%. In that study, the concentrations of anthocyanin and cholesterol were kept constant; however, they are also expected to have significant impacts on the liposomal characteristics and are therefore the subject of this study. Anthocyanin usually exists in a mixture of different forms in equilibrium, like flavylium cation, quinonoidal base and carbinol pseudobase, with one dominant form present at a specific pH condition (Welch et al., 2008). With hydroxyl groups and charged flavylium, anthocyanin may interact via hydrogen bonding and electrostatic interaction with the phospholipid membrane of liposomes (Ossman et al., 2016), which may affect the physicochemical properties of liposomes such as encapsulation efficiency, particle size and morphology. Cholesterol is incorporated into liposome membranes to reduce the membrane permeability and prevent the leakage of bioactives from liposomes (de Kruyff, Demel, & dan Deenen, 1972). Cholesterol can also be used to modulate and adjust the phospholipid packing, the membrane fluidity and surface charge of liposomes, which may further affect the particle size, encapsulation efficiency and morphology (Ohvo-Rekilä, Ramstedt, Leppimäki, & Peter Slotte, 2002). However, the literature lacks information in this regard.

The objective of this study was to evaluate the effects of anthocyanin and cholesterol concentrations on the characteristics of liposomes, including particle size distribution, morphology, encapsulation efficiency, bioactive loading, stability and *in vitro* release profiles. Utilization of liposome as an encapsulation medium for anthocyanin via the SC-CO_2 method may provide unique features to regulate the characteristics for its protection, oral administration

and delivery purposes. Such an approach is expected to be promising for applications in functional food, natural health products and medical fields.

8.2. Materials and methods

8.2.1. Materials

Soy lecithin obtained from Fisher Scientific (Ottawa, ON, Canada) was used for liposome formation. Anthocyanin from bilberry (*Vaccinium myrtillus*) was purchased from Hangzhou Ningsi Bio-tech (Hangzhou, China). Sodium citrate dehydrate (99%), citric acid monohydrate (99%), cholesterol, ethanol (99.8%) and methanol (99.9%) were purchased from Sigma-Aldrich (Oakville, ON, Canada). Porcine pepsin, pancreatin and bile salts (United States Pharmacopeia (USP) grade) were obtained from Sigma-Aldrich (Oakville, ON, Canada). Sodium hydroxide (>97%), dipotassium hydrogen phosphate (>98%), sodium chloride (99%) and hydrochloric acid (37%) were obtained from Fisher Scientific (Ottawa, ON, Canada). Liquid CO_2 (purity of 99.99%) supplied by Praxair Canada (Mississauga, ON, Canada) was used in the high pressure CO_2 processing. Water purified by a Milli-Q® ultrapure water purification system (EMD Millipore, Billerica, MA, USA) was used to prepare all aqueous agents.

8.2.2. Preparation of crude suspension

The crude lecithin/anthocyanin/cholesterol suspension was prepared in a similar manner as described in Section 7.2.2.

8.2.3. Preparation of liposomes by SC-CO_2

The preparation of anthocyanin-loaded liposomes was performed in a similar manner as described in Section 4.2.3. Crude lecithin/anthocyanin/cholesterol suspension (6 mL) was sealed in a high pressure vessel. Liposomes were formed as the CO_2-expanded suspension was depressurized at a constant pressure and depressurization rate. Different levels of anthocyanin

concentration (0-40%, mole % at fixed cholesterol concentration of 20%) and cholesterol concentration (0-40%, mole % at fixed anthocyanin concentration of 10%) were used to form liposomes at the pressure of 300 bar, depressurization rate of 90 bar/min and temperature of 50°C.

8.2.4. Particle size distribution

The particle size and size distribution of anthocyanin-loaded liposomes was measured in a similar manner as described in Section 3.2.7.

8.2.5. Zeta potential

The zeta potential of lutein-loaded liposomes was measured in a similar manner as described in Section 3.2.8.

8.2.6. Encapsulation efficiency and bioactive loading

The encapsulation efficiency (EE) and bioactive loading (BL) were determined in a similar manner as described in Section 7.2.7.

8.2.7. Morphology

The morphology of liposomes was measured via the TEM and cryo-TEM methods in a similar manner as described in Section 7.2.8.

8.2.8. Fourier transform infrared (FTIR) spectroscopy

Fourier transform infrared (FT-IR) spectra of anthocyanin, lecithin, their physical mixtures and anthocyanin-loaded liposomes were recorded using a Nicolet 6700 FTIR spectrophotometer (Thermo Fisher Scientific Inc., MA, USA). The samples were vacuum-dried for 24 h prior to the test to completely remove the water and then mixed with spectroscopic grade KBr and mulled to yield KBr pellets. Background spectra of blank wells were collected prior to each measurement.

A spectrum was recorded in the spectral range of 1800-600 cm^{-1} at 4 cm^{-1} resolution and room temperature (~23^{o}C) with 128 scans for each sample.

8.2.9. *In vitro* release assay

In vitro release profiles of anthocyanin from liposomes were studied by incubating anthocyanin-loaded liposomes in simulated gastric fluid (SGF) (pH 1.2) and simulated intestinal fluid (SIF) (pH 6.8) according to Oidtmann et al. (2012) and Li et al. (2015) with modification. SGF was composed of sodium chloride (2 g/L), hydrochloric acid 37% (0.008 L/L), and pepsin (3.2 g/L) at pH 1.2. SIF was prepared with sodium hydroxide (0.896 g/L), potassium dihydrogen phosphate (6.8 g/L), pancreatin (4.76 g/L), and bile salts (5.16 g/L). Digestion was performed in duplicate with unloaded liposomes at each condition as controls. Liposomes (1 mL) were mixed with 4 mL of release medium in individual tubes (separate tubes corresponding to each sampling time) and incubated at 37°C with continuous stirring at 100 rpm in a shaker bath. Following standard pharmacopoeia methods (USP 32), the mixed liposome-digestion media were incubated for 120 min in SGF and for 240 min in SIF. At each set time, tubes in duplicate were placed in a 95°C water bath for 3 min to inactivate enzymes completely. After cooling to room temperature, the pH of the liquid mixture was adjusted to 3.5 with sodium hydroxide solution (1 M, 0.2 M and 0.01 M) for SGF, and hydrochloric acid (1 M, 0.2 M and 0.01 M) for SIF. An aliquot (1 mL) of the mixture was then withdrawn from each tube and analyzed for free and encapsulated anthocyanin. The amount of released anthocyanin was determined in a similar manner as the determination of free anthocyanin described previously (Section 7.2.8). For the determination of retained anthocyanin, liposomes were first disintegrated using acidic methanol as described previously (Section 7.2.8) and subjected to ultracentrifugation at 50,000×g for 30 min to remove the inactivated enzymes, and then measured in a similar manner for the determination of

encapsulated anthocyanin (Section 7.2.8). The measurement for each tube was performed in duplicate. The total encapsulated anthocyanin was set as 100% of the bioactive to be released. The release and retention of anthocyanin were calculated as follows:

$$\text{Bioactive release (\%)} = \frac{\text{Released anthocyanin (mg)} - \text{initial free anthocyanin (mg)}}{\text{Total encapsulated anthocyanin (mg)}} \times 100\% \quad (8.1)$$

$$\text{Retained bioactive (\%)} = \frac{\text{Retained anthocyanin after certain digestion time (mg)}}{\text{Total encapsulated anthocyanin (mg)}} \times 100\% \quad (8.2)$$

8.2.10. Statistical analysis

Liposomes were prepared in triplicate at each processing condition. Particle size distribution, zeta potential, encapsulation efficiency and bioactive loading of liposomes were measured in triplicate while the release kinetics test was carried out in duplicate. Data analysis was performed using Minitab statistics software 16 (Minitab Inc., State College, PA, USA) and reported as the mean ± standard deviation (SD). One-way analysis of variance (ANOVA) was conducted and significant differences between means were obtained by Tukey's multiple comparison test at a significance level of $p < 0.05$.

8.3. Results and discussion

8.3.1. Particle size distribution

The mean hydrodynamic diameter and polydispersity index (PdI) of anthocyanin-loaded liposomes as influenced by the anthocyanin and cholesterol concentrations were shown in Fig. 8.1 (A) and (C), respectively. Particle size is a critical parameter closely associated with the aqueous solubility/dispersibility and aggregation as well as the biological performance such as absorption and fusion of nanoparticles (Jiang, Oberdörster, & Biswas, 2009), which can be used in different nutraceutical and food applications. PdI indicates the uniformity of the liposomes, which is related to the stability of the colloidal system. PdI values below 0.2 are usually

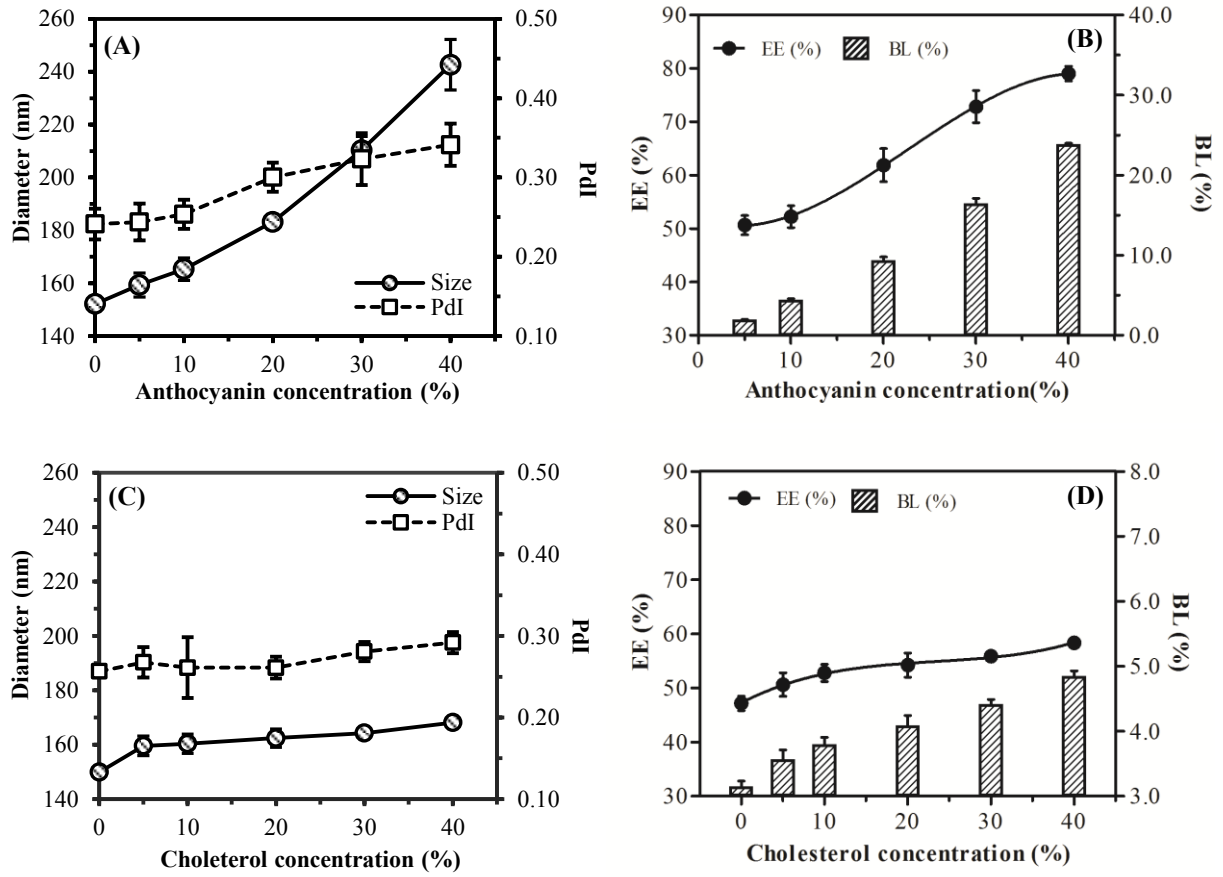

Figure 8.1: Effects of anthocyanin and cholesterol concentrations on the (A), (C) mean diameter and polydispersity index (PdI) and (B), (D) encapsulation efficiency (EE) and bioactive loading (BL) of liposomes prepared at 50°C, 300 bar and 90 bar/min using SC-CO_2. (A), (B) at 20% cholesterol and (C), (D) at 10% anthocyanin.

considered to be monodisperse, whereas values less than 0.3 are considered as ideal and indicate a narrow size distribution of particles (Furneri et al., 2000). As the anthocyanin concentration was increased, the particle size of liposomes significantly increased from 152±1 nm to 243±4 nm, while the PdI significantly increased from 0.241±0.019 to 0.342±0.027. The large vesicles caused by higher anthocyanin addition are associated with strengthened electrostatic interactions between the phosphate head groups of phospholipids and anthocyanin flavylium cations as well as hydrogen bonding associated with the hydroxyl groups of both species. These changes reduce the packing parameters of phospholipids associated with the expelled water molecules from the

phosphate head group and contribute to a larger liposomal size. Increased anthocyanin levels also bring about mixed component species in liposome formation and enhance the heterogeneity of particles. Particle size distribution of liposomes exhibited a narrow and unimodal size distribution but switched to a relatively wide and unimodal distribution with increased anthocyanin concentration (Fig. 8.2), which may have resulted from the enhanced heterogeneity due to the diversity of vesicular components. Elevated cholesterol concentration brought about a relatively small increase ($p<0.05$) in the particle size of liposomes compared to that induced by the increased anthocyanin concentration (Fig. 8.1 (a) and (c)). Sterol incorporation into the liposome bilayers weakened the van der Waals interactions between fatty acyl chains of phospholipids and altered the original packing of bilayers. Thus, the interactions between the anthocyanin and phosphate head groups may have a dominant effect on the packing and particle size compared to that of cholesterol.

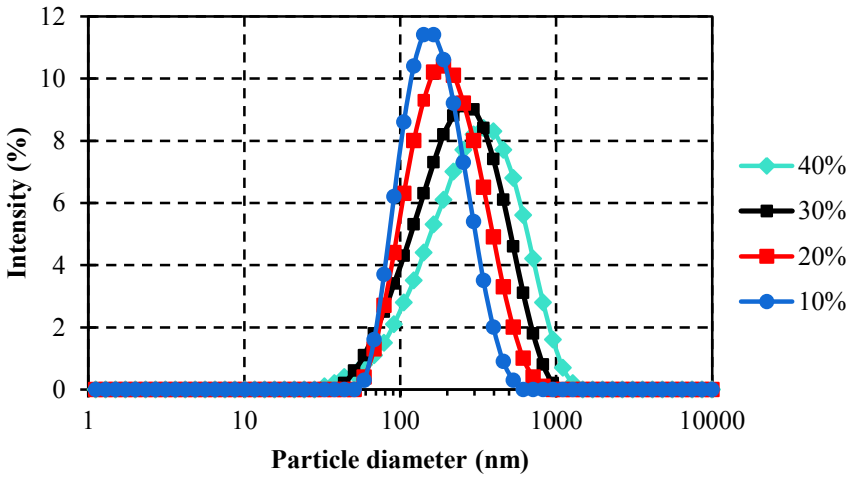

Figure 8.2: Size distribution of anthocyanin-loaded liposomes formed at different anthocyanin concentrations.

The possible mechanism of liposome formation via the SC-CO_2 technique was discussed in Chapter 7 (Section 7.3.6). Briefly, CO_2 solubilized into the phospholipid bilayers would yield an expanded lipid phase at the high pressure condition. Upon depressurization, CO_2 is released to thoroughly disrupt the phospholipid bilayers and disperse them into individual molecules, which would immediately reassemble to form liposomes via hydrophobic interactions. As indicated above, the anthocyanin-loaded liposomes were larger ($p<0.05$) than the unloaded liposomes (152 ±0.2 nm) prepared under similar conditions. It has been reported that anthocyanins with less charged or hydroxyl groups can partially penetrate into the hydrophobic region, which may modulate the membrane fluidity and enhance the particle size (Arora, Byrem, Nair, & Strasburg, 2000). In addition, anthocyanin may adsorb onto the liposomal surface, interacting with phosphate heads via electrostatic interaction and with cholesterol via hydrogen bonding simultaneously (Tarahovsky et al., 2014). This behavior may also increase the hydrodynamic diameter of liposomes since an increased number of water molecules would be interacting with the hydroxyl groups of anthocyanin via hydrogen bonding.

8.3.2. Encapsulation efficiency and bioactive loading

The EE and BL of anthocyanin-loaded liposomes as influenced by the anthocyanin and cholesterol concentrations were shown in Figs. 8.1 (B) and (D), respectively. Higher anthocyanin addition resulted in a significant increase ($p<0.05$) in the EE and BL of up to 78.2±1.4% and 23.8±0.2%, respectively. Higher cholesterol addition brought about a relatively small increase ($p<0.05$) in the EE and BL of up to 58.3±1.0% and 4.8±0.1%, respectively. These trends in EE and BL showed good consistency with those for the particle size of liposomes. Since EE and BL are proportional to the enclosed aqueous volume of liposomes, a large liposome yielded an enlarged enclosed aqueous core and therefore favored the improved encapsulation of bioactives.

The highest EE achieved in liposome preparation was 78.2±1.4% with 40% anthocyanin addition, which was higher than those reported for other hydrophilic compounds (Nii & Ishii, 2005). Such a high value may arise from the enhanced interactions between the flavylium cation of anthocyanin and the negatively charged phospholipid species as well as the partial partitioning of anthocyanin into the bilayers, with their hydrophobic portion interacting with the fatty acyl chain of phospholipids and hydroxyl groups interacting with phosphate heads. Higher addition of anthocyanin into the formulation enhances electrostatic interactions with phospholipids, which may be favorable for the encapsulation of anthocyanin into the vesicles. In addition, phospholipid molecules can be highly dispersed upon depressurization of CO_2, which also encourages the incorporation of anthocyanin into the bilayer membrane during their reassembly. Despite achieving the highest EE at the anthocyanin concentration of 40%, 10% is recommended as the optimal concentration, considering the uniformity of liposomes and their morphology as discussed in Section 8.3.3. For cholesterol addition, both 20% and 30% showed relatively spherical appearance in the liposomes. Since the EE values obtained at 20% and 30% of cholesterol were similar ($p>0.05$ based on t-test), 20% was selected as the optimal cholesterol concentration considering the lower PdI and better uniformity.

8.3.3. Morphology

The morphology of single and bulk liposomes based on the TEM and cryo-TEM characterization were displayed in Figs. 8.3-8.5. For each condition, one out of 30 TEM images was selected to typically represent a single vesicle. Anthocyanin-loaded liposomes primarily displayed spherical and near-spherical appearance at different anthocyanin and cholesterol concentrations. Compared to the unloaded liposomes in Fig. 8.3 (A), encapsulation of anthocyanin into the liposomes seems to yield less spherical vesicles with increased irregularity

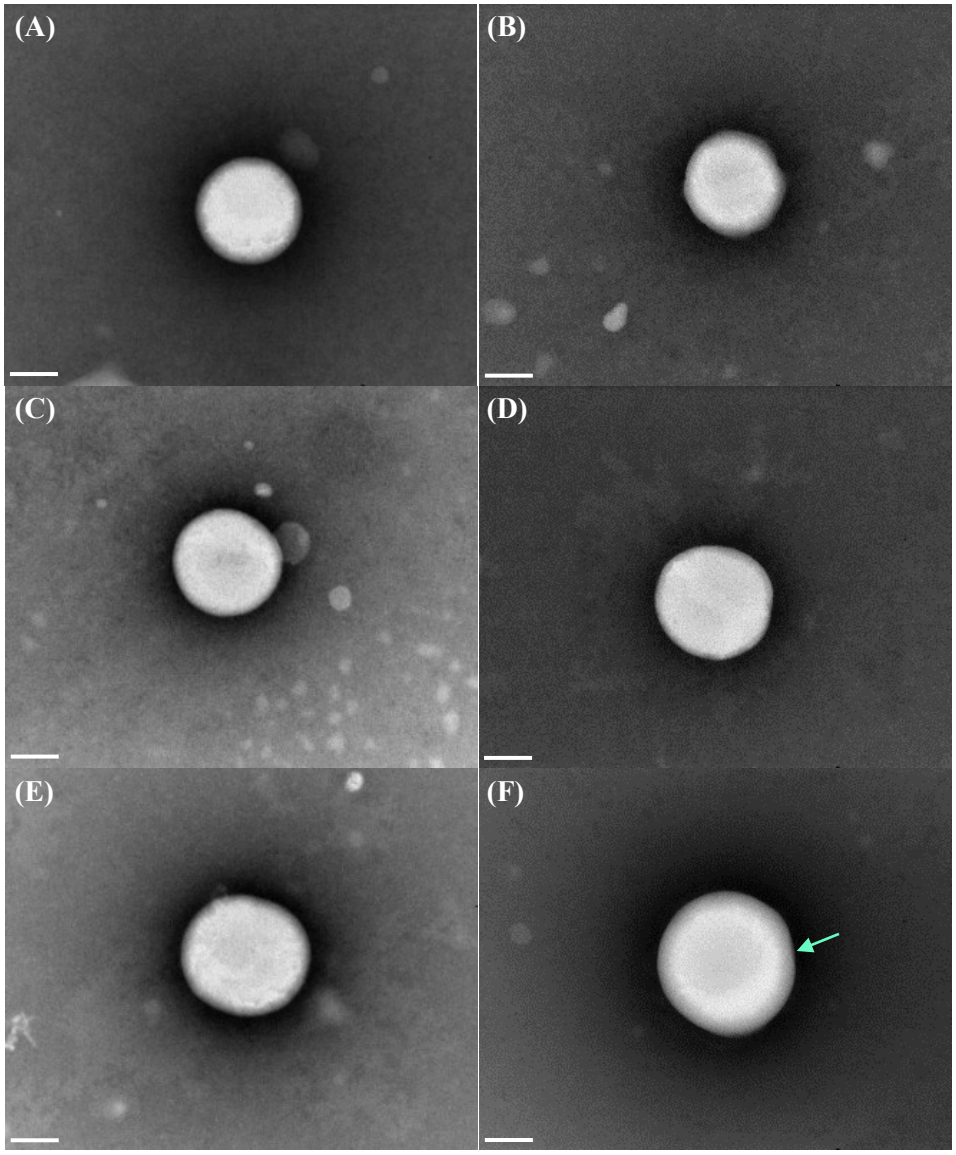

Figure 8.3: TEM images of anthocyanin-loaded liposomes with different levels of anthocyanin prepared at 20% cholesterol, 300 bar, 90 bar/min and 50°C: (A) 0%, (B) 5%, (C) 10%, (D) 20%, (E) 30%, (F) 40%. Scale bars in the images represent 100 nm.

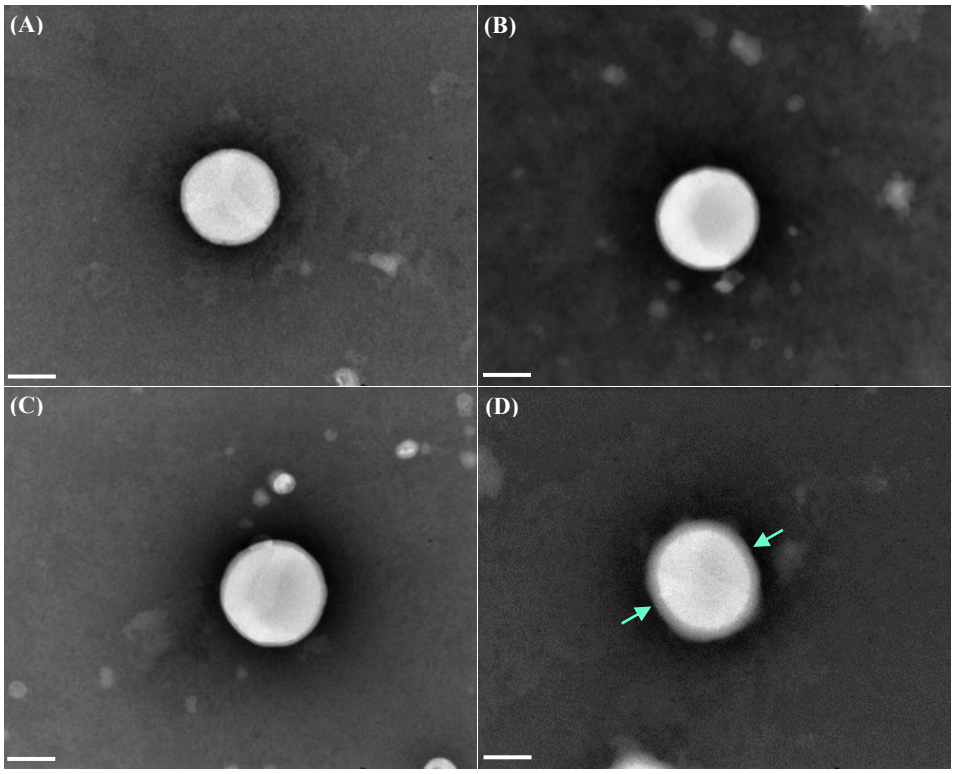

Figure 8.4: TEM images of anthocyanin-loaded liposomes with different levels of cholesterol addition prepared at 10% anthocyanin, 300 bar, 90 bar/min and 50°C: (A) 0%, (B) 5%, (C) 30%, (D) 40%. Scale bars in the images represent 100 nm.

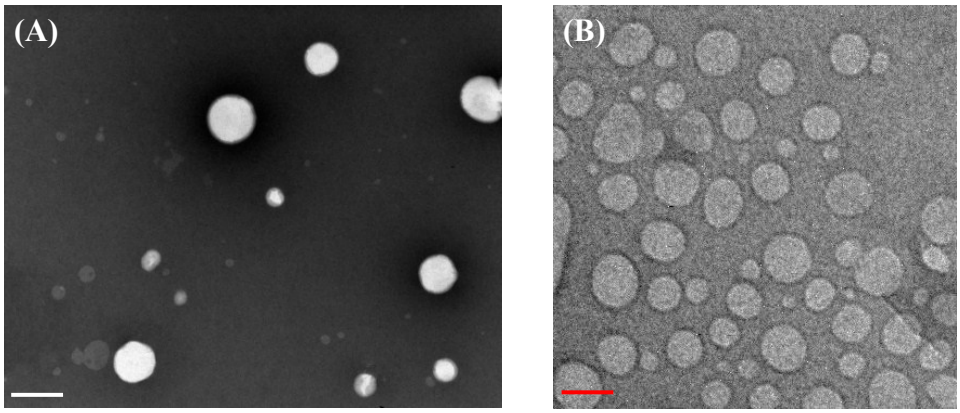

Figure 8.5: (A) TEM and (B) Cryo-TEM images of anthocyanin-loaded liposomes prepared at 10% anthocyanin and 20% cholesterol at 300 bar, 90 bar/min and 50°C. Scale bars in the images represent 200 nm.

and asymmetry with the increased level of anthocyanin addition (Fig. 8.3 (B-F)). This finding demonstrated that the relatively high level of anthocyanin addition could be unfavorable for the perfect packing of liposomal bilayers due to enhanced anthocyanin-phosphate interactions and partitioning of anthocyanin into the bilayer. In contrast, increasing the cholesterol level may have a relatively small impact on the membrane packing and liposomal shape since cholesterol levels of less than 40% yielded relatively spherical liposomes, as shown in Fig. 8.4. These findings regarding the morphology were consistent with those discussed in Section 8.3.1, regarding particle size and uniformity. The bulk liposomes observed by TEM (Fig. 8.5 (A)) had mostly spherical or near spherical shapes and intactness of bilayers (bright region indicates no dye entering the vesicles) without leakage of vesicles. Cryo-TEM images (Fig. 8.5 (B)) exhibited mostly unilamellar vesicles, without any multilamellar or multivesicular vesicles based on the 40 cryo-TEM images obtained for the bulk anthocyanin-loaded liposomes.

8.3.4. Zeta potential

Zeta potential of the anthocyanin-loaded liposomes as a function of the cholesterol concentration was shown in Fig. 8.6. Zeta potential indicates the surface charge of nanoparticles, which determines the repulsion among charged nanoparticles and in turn influences their storage stability. With 20% cholesterol addition, the zeta potential of liposomes was -40.2 mV at pH 3.5. As the cholesterol concentration was increased, the surface charge of liposomes was significantly reduced ($p<0.05$) due to the neutral nature of cholesterol. Particles with an absolute zeta potential value greater than 30 mV have relatively high repulsive interaction and are considered to be stable (Jacobson & Papahadjopoulos, 1975). At pH 3.5, anthocyanin-loaded liposomes had an absolute zeta potential value of higher than 30 mV at all cholesterol concentrations tested (Fig. 8.6), which suggested good storage stability. These high zeta potential values arise from the

presence of charged phospholipid species (phosphatidylinositol, phosphatidylglycerol and phosphatidic acid) in the soy lecithin used to form liposomes (Chapter 5). Anthocyanin-loaded liposomes remained stable for up to 3 weeks with less than 5% change in particle size, as reported previously in Chapter 7.

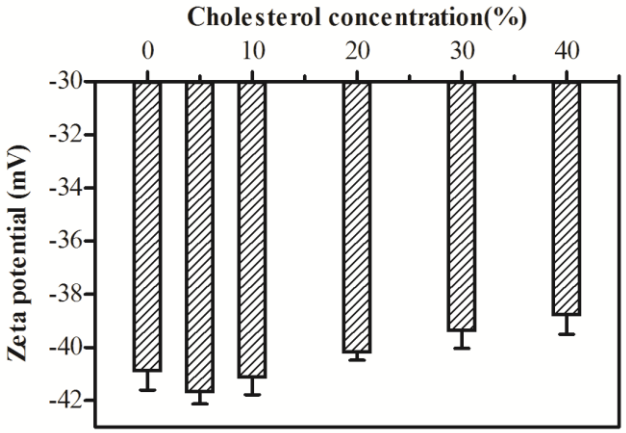

Figure 8.6: Zeta potential of anthocyanin-loaded liposomes as a function of cholesterol concentration with 10% anthocyanin addition at 300 bar, 90 bar/min and 50°C.

8.3.5. Structural features and anthocyanin-liposome interaction

The anthocyanin-phospholipid interactions were studied using FTIR spectroscopy for the anthocyanin, lecithin, physical mixtures and liposomes with different anthocyanin levels (Fig. 8.7). The infrared signal can indicate the molecular vibrations of functional groups and thus provide fingerprints for the characterization of encapsulated materials (Chang et al., 2013). At low anthocyanin concentration of 10% to 20%, the spectra of anthocyanin-loaded liposomes exhibited similarity to that of lecithin. However, with higher levels of anthocyanin addition (≥30%) some peak changes became apparent. The peak at the region of 1620 cm^{-1}, corresponding to the aromatic C=O bonds in the flavylium nucleus of anthocyanin and a peak shift at 1220-1250 cm^{-1} corresponding to P=O stretching may indicate a structural change in the

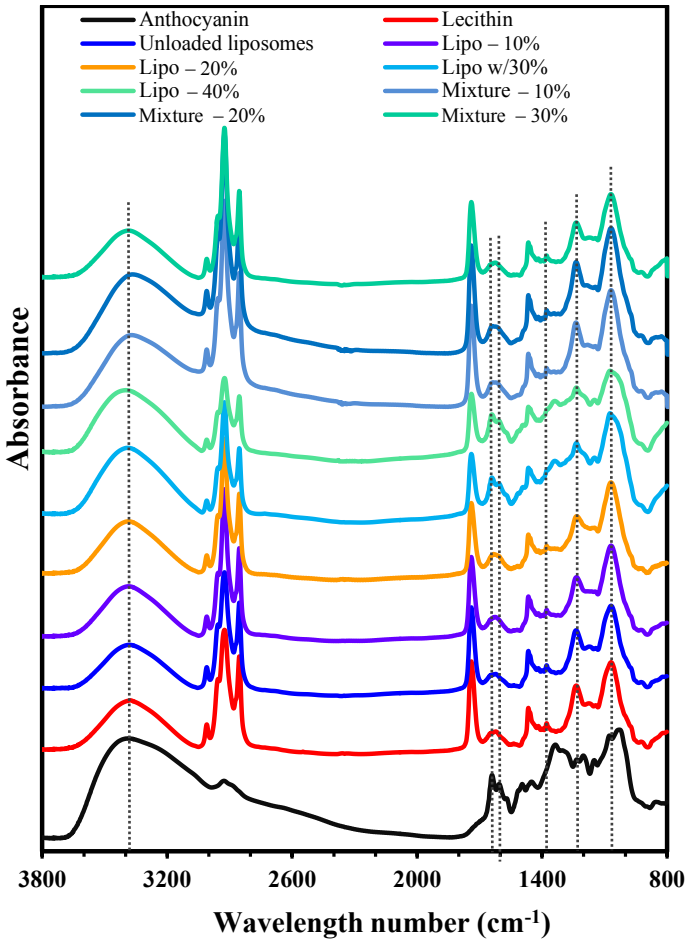

Figure 8.7: Fourier transform infrared spectroscopy (FTIR) spectra of lecithin, anthocyanin, their physical mixtures and anthocyanin-loaded liposomes obtained at different levels of anthocyanin addition (Lipo: liposomes). Liposomes were prepared using SC-CO_2 at 300 bar, 90 bar/min and 50°C.

liposomes as more anthocyanin was encapsulated into liposomes. The band observed at ~1070 cm^{-1} corresponds to the C–O–P stretching and the change in the shape of this peak for liposomes loaded with a high level of anthocyanin (30-40%) may be due to increased anthocyanin partitioning into bilayers. In addition, the peak shift at 1450 cm^{-1} to 1430 cm^{-1}, fingerprinting CH_2 in fatty acyl chains, may suggest a packing difference and disruption of bilayers at higher anthocyanin concentration (40%), which may be attributed to the elevated EE and partitioning of anthocyanin into the bilayers and thus affecting their phase transition (Chang, Alben, Wisner, &

Tsai, 1986). The peak at around 3,400 cm^{-1} corresponding to hydrogen bonding did not exhibit a significant change with elevated anthocyanin levels in the physical mixtures and liposomes. This finding is in agreement with the high EE discussed in Section 8.3.2. As some functional groups of anthocyanin and phospholipids showed overlapped peaks to some extent, interpretation of the full spectrum becomes challenging. However, the characteristic peaks at 1625 cm^{-1} and 1589 cm^{-1} associated with the anthocyanin flavylium and benzopyran indicated that there may a change in the chemical interactions and membrane composition of liposomes at anthocyanin concentrations higher than 30% due to the partitioning of bioactives into the bilayers.

8.3.6. *In vitro* release of bioactives

The release profiles of anthocyanin from the liposomes revealed sustained release of this bioactive at 37°C in the SGF and SIF (Fig. 8.8). Pepsin (a protease) and pancreatin (a mixture of amylase, lipases, trypsin and chymotrypsin) were used as enzyme sources for the hydrolysis of anthocyanin-loaded liposomes and release in the simulated gastrointestinal tract. Within 2 h of incubation, the release profile revealed a sustained release of anthocyanin of up to 35.9% in SGF (Fig. 8.8 (A)), which suggested a slow release of this bioactive from the liposomes under the stomach conditions. In contrast, the release trend was dramatically different in the SIF, which initially increased to 45.2% within 30 min but then decreased to 23.3% after 240 min (Fig. 8.8 (B)). Such a release behavior in SIF indicates rapid degradation of the bioactive at the near neutral pH, leading to an overall depression of the amount of bioactive as it is continuously released from the liposome matrix. Since the liposomes used for encapsulation are composed of phospholipids and sterols, a high bioactive release rate was anticipated in the simulated small intestinal tract conditions, because of the hydrolysis of lipids and degradation of the liposome matrix triggered by pancreatin, especially by the phospholipase A2, cholesterol esterase and bile

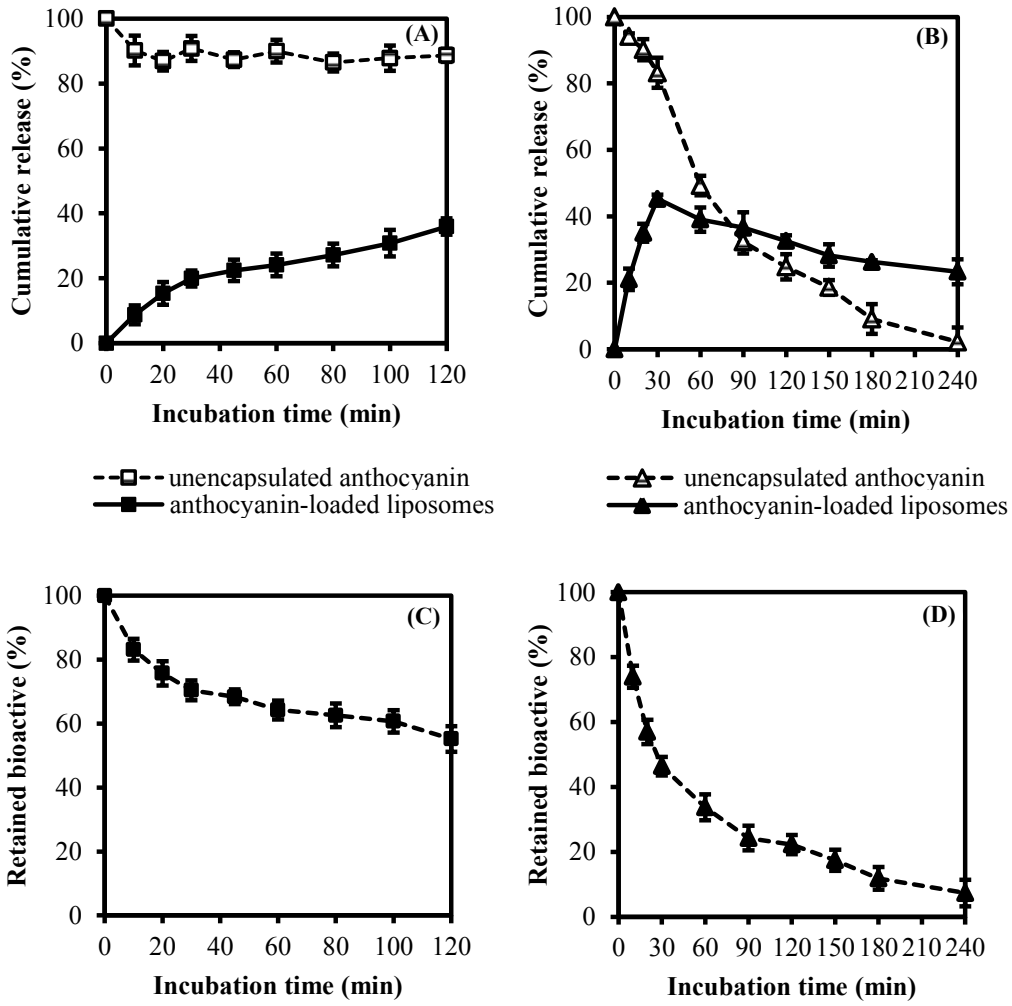

Figure 8.8: Bioactive release and retention profiles of anthocyanin-loaded liposomes and non-encapsulated anthocyanin under *in vitro* digestion conditions: (A), (C) anthocyanin in simulated gastric fluid (SGF) with incubation for 2 h; (B), (D) anthocyanin in simulated intestinal fluid (SIF) with incubation for 4 h. Liposomes were prepared using SC-CO_2 at 300 bar, 90 bar/min and 50°C.

salts secreted by the porcine pancreas. However, due to the instability of anthocyanin in the SIF medium and its degradation, the determination of the exact release rate of anthocyanin in the SIF medium is challenging when only based on the *in vitro* release profiles.

In order to understand the anthocyanin release rate in SIF better, the bioactive retention in the anthocyanin-loaded liposomes was further examined (Fig. 8.8 (C) and (D)). Liposomes

demonstrated a sustained release of bioactives in the SGF and retained 55.2% of the bioactive at the end of 2 h (Fig. 8.8 (C)), which was in agreement with the slow release rate as discussed above. In contrast, a dramatic decrease down to 7.3% was found in the anthocyanin retention in liposomes under the SIF condition (Fig. 8.8 (D)). With the total encapsulated anthocyanin set as 100%, theoretically a high release of over 90% of the bioactive was achieved in the SIF medium after 4 h. Although the retained anthocyanin in the liposomes was higher than the amount of non-encapsulated bioactive (2.2%) remaining after 4 h in SIF (Fig. 8.8 (B)), liposomal encapsulation provided relatively poor protection of anthocyanin in the SIF due to the rapid enzymatic hydrolysis of phospholipids. These findings confirmed the large extent of degradation of liposomes under the small intestinal tract conditions and that the anthocyanin released from the liposome was degraded quickly in the SIF medium. Based on these data, anthocyanin encapsulation in the liposomes may need further improvement, possibly by surface modification using an additional chitosan coating layer or multilamellar vesicle fabrication to enhance its stability in the small intestinal tract and thus potentially improve its absorption for the functional food and oral administration applications.

8.4. Conclusions

Anthocyanin-loaded liposomes prepared by the SC-CO_2 method were characterized in terms of the effects of anthocyanin and cholesterol concentrations. Anthocyanin-loaded liposomes obtained by the SC-CO_2 method had a particle size of 152±1 nm, PdI of 0.241±0.019, EE of 50.6% and zeta potential of -40.2 mV. High anthocyanin concentration resulted in a significant increase in particle size and PdI whereas the high cholesterol addition brought about a relatively small increase ($p<0.05$) compared to anthocyanin concentration. Higher anthocyanin and cholesterol addition also enhanced the EE and BL due to increased enclosed volume of the aqueous core.

Anthocyanin-loaded liposomes exhibited spherical and near-spherical appearance, which changed at high anthocyanin and cholesterol concentrations. Encapsulation of anthocyanin altered the packing of bilayer membranes and led to increased asymmetry in the morphology of liposomes. Higher anthocyanin concentration (30-40%) may contribute to structural and packing changes in loaded liposomes. Anthocyanin was released slowly from the liposomes in SGF while a rapid release and degradation was apparent in SIF, demonstrating the need for further protection for enhanced stability and bioavailability in functional food and oral administration applications.

CHAPTER 9 – CONCLUSIONS AND RECOMMENDATIONS

9.1. Summary and conclusions

Liposomes are versatile phospholipid vesicles with important applications in medical, food and nutraceutical areas. Encapsulated bioactive compounds can be isolated from the external conditions so that their chemical stability can be preserved for improved bioavailability and health benefits. Although there are a few conventional methods that can be employed to prepare liposomes, they have some drawbacks and thus supercritical carbon dioxide (SC-CO_2) techniques with unique advantages have drawn great attention. SC-CO_2 technique offers the possibility to eliminate the use of organic solvents and to achieve scale-up of the production of liposomes with controlled characteristics by fine tuning the processing parameters. In order to achieve improved liposome characteristics, two previously developed methods reported by Otake et al. (2006) and Cano-Sarabia et al. (2008) were used as the reference methods to design the improved version used in this research.

In the first study (Chapter 3), the feasibility and fundamentals of the improved supercritical reverse phase evaporation method (ISCRPE) reported by Otake et al. (2006) was studied. Unloaded liposomes were prepared via the depressurization of the supercritical phase. The relative volumetric expansion of water upon equilibrium with high pressure CO_2 reached a plateau at 14.36%, 12.28% and 10.24% at 40°C, 50°C and 60°C, respectively. Liposomes with a relatively large particle size (523±2 nm), high uniformity (polydispersity index (PdI): 0.198±0.016) and good stability (4 weeks with limited size change (below 5%)) were obtained by the ISCRPE method.

In the second study (Chapter 4), the improved SC-CO_2 method based on the combined features of the approaches reported by Otake et al. (2006) and Cano-Sarabia et al. (2008) was

developed and the preparation of unloaded liposomes as a function of different processing parameters was investigated. In this study, two protocols, including (I) depressurization at a constant rate and (II) depressurization at a constant rate and pressure were evaluated. Compared to the ISCRPE method employed in Chapter 3, the improved SC-CO_2 process yielded a substantial drop in liposome particle size (523 nm to 214 nm) by switching the depressurization from the supercritical phase to the liquid phase but with an increase in the heterogeneity of vesicles (PdI: 0.417±0.001 for protocol (II)). This improved method also enhanced the storage stability up to 8 and 6 weeks for protocols (I) and (II), respectively. Protocol (II) yielded smaller and more uniform particles. Therefore, this protocol was adopted for all the remaining studies.

In the third study (Chapter 5), the effects of compositional parameters on the characteristics of unloaded liposomes obtained using the improved SC-CO_2 method were studied. Upon modulation of the composition of liposomes, liposomes with sizes as small as 161±2 nm and improved uniformity (PdI decreased to 0.398±0.008) were achieved. The small particle size of <200 nm for the liposomes obtained in this study is advantageous for their intestinal transport and circulation in the human body, which may find applications in related nutraceutical and pharmaceutical fields. Increased phospholipid concentration was favorable for the formation of smaller size vesicles. However, increased chain length and degree of unsaturation of fatty acids in phospholipids was unfavorable and resulted in a larger particle size with enhanced asymmetry. Compared to the pure phospholipids tested, liposomes prepared with soy lecithin had the highest absolute zeta potential (-58.3±2.17 mV), resulting in the highest stability of the vesicular systems. Increased sterol concentration enlarged particle size but decreased zeta potential. The potential to use phytosterols in liposome formulations instead of the commonly used cholesterol was demonstrated.

In the fourth study (Chapter 6), a hydrophobic bioactive compound, lutein, was loaded into the liposomes. Although the effects of processing and compositional parameters impacting the physicochemical properties of unloaded liposomes were investigated in the previous studies, dramatically distinct trends were found after the bioactive compounds were encapsulated into the liposomes. Liposome characteristics were further improved compared to those of unloaded liposomes with a particle size of 155±1 nm, PdI of 0.28±0.02, encapsulation efficiency (EE) of 97.0±0.8% and zeta potential of -61.7±0.6 mV. The higher pressure (200-300 bar) and depressurization rate (90-200 bar/min) promoted a higher encapsulation of lutein whereas the lutein concentration had the dominant effect on the morphology of vesicles along with size distribution and EE. For the lutein-loaded liposomes, a broadened phase transition observed by differential scanning calorimetry and a substantial drop in the crystallinity indicated the disruption of the original packing of lipids and simultaneous rearrangement of lutein and phospholipid molecules into liposome membranes.

Next, a hydrophilic bioactive compound, anthocyanin, was loaded into the liposomes using the improved SC-CO_2 method. Similarly to the case of lutein addition, the effects of the processing (Chapter 7) and compositional (Chapter 8) parameters on the physicochemical properties of the anthocyanin-loaded liposomes were found to be different from those for the unloaded liposomes. Anthocyanin-loaded liposomes had a small particle size (160±2 nm) and high uniformity (PdI of 0.26±0.01); however, they exhibited a reduced EE (52.2±2.1%) and stability (for up to 3 weeks) in contrast with lutein-loaded liposomes owing to their reduced zeta potential (-41.3±1.2 mV). In terms of the compositional effects (Chapter 8), elevated anthocyanin concentration increased the particle size with reduced uniformity while the elevated cholesterol concentration depressed the surface charge of liposomes. Anthocyanin-loaded

liposomes exhibited unilamellar, spherical and near-spherical appearance with increased asymmetry and heterogeneity in the bilayer packing induced by increased anthocyanin and cholesterol addition. Higher levels of anthocyanin addition may contribute to structural and compositional changes in the bilayer membranes due to its partitioning into the bilayers. The *in vitro* release of the bioactive from the liposomes was slow with up to 35.9% in the simulated gastric fluid, whereas it was rapid in the simulated intestinal fluid induced by the degradation of the vesicles by pancreatin. Liposomes were effective for bioactive protection in the gastric tract but may require surface modification to maintain their integrity in the intestinal tract for enhanced stability.

In summary, an improved SC-CO_2 process was developed for liposome production, which could yield high quality liposomes loaded with bioactives with a relatively small particle size, high uniformity and free of organic solvents and other surfactants. A mechanism was proposed to describe liposome formation at the molecular level upon pressurization and depressurization of the lecithin suspension with SC-CO_2, which also included the addition of bioactives, like lutein and anthocyanin. The findings contribute to our fundamental understanding of liposome formation and how their characteristics can be controlled by fine tuning of different processing and compositional parameters. Despite being a complex mixture, soy lecithin derived from a natural source was used to replace the costly pure phospholipids commonly used for liposome formation, which were then characterized in detail using numerous techniques. In contrast to pure phospholipids, soy lecithin is promising in (a) modulating and increasing the surface charge of liposome bilayers and thus enhance particle stability, and (b) regulating the packing and phase behavior of the bilayer membranes, which may be beneficial for adjusting the *in vitro* and *in vivo* behavior such as modified bioactive release profiles but this aspect requires further research. In

addition, the use of phytosterols was demonstrated as a replacement for cholesterol commonly incorporated into liposome formulations. Even though the amount of cholesterol used for this purpose is relatively small, the use of phytosterols shows potential for the formulation of completely plant-based liposomal ingredients and avoid any adverse health effects attributed to high cholesterol intake. Although the improved SC-CO_2 method offers many advantages for the production of liposomes loaded with a variety of bioactives, this process may not be suitable for the encapsulation of certain bioactives that are sensitive to the low pH resulting from the pressurization with CO_2, such as proteins and peptides. Thus, careful selection of bioactives to be loaded into liposomes is needed before liposome preparation is undertaken using this method.

In conclusion, the improved SC-CO_2 method resulted in superior characteristics of liposomes that were highly associated with the ability of CO_2 to disperse phospholipids and hydrophobic bioactive molecules. This process shows great promise to homogenize a mixed system of amphiphilic molecules suspended in an aqueous medium into uniform nano/micro particles and to effectively encapsulate hydrophobic and hydrophilic bioactives. It was demonstrated that unloaded and bioactive-loaded liposomes displayed different behaviors upon variations of the processing parameters, especially pressure and depressurization rate, which indicated the unique features of liposomes brought about by the encapsulation of bioactives and the potential regulation of liposome properties via the fine tuning of processing and compositional parameters. This SC-CO_2 process is particularly advantageous and effective since it eliminates the use of organic solvents or other surfactants. Plus, the scale up of liposome production using this technique can be achieved with relative ease compared to the traditional thin film hydration method. This novel process shows great promise to yield liposomes

encapsulated with a variety of valuable bioactives and drugs for food, natural health product, cosmetic and medical applications.

9.2. Recommendations

Liposomes show great potential to encapsulate different types of valuable components. In the future, it would be worthwhile to study their surface modification and coating, functionality enhancement and encapsulation of several ingredients within one vesicle. Firstly, liposomes have been found to have a relatively poor *in vitro* stability due to their hydrolysis by pancreatin in the intestinal tract, which would reduce their protective effect on the bioactives. To improve their applications in oral administration, surface modification of liposomes can be performed, possibly by coating them with chitosan or polyethyleneglycol, to enhance the liposomal stability in the gastrointestinal tract.

Secondly, primary liposomes have been prepared in this research and by other researchers employing SC-CO_2 techniques. However, to date, the preparation of secondary, tertiary and quaternary liposomes, involving the addition of polyethyleneglycol, specific functional groups and antibodies, using the SC-CO_2 technique has not been investigated. If such functional structures can be generated using the SC-CO_2 process, investigation of their physicochemical properties, encapsulation features and phase behaviors under the supercritical conditions would be of great interest. This process can be further extended to encapsulate a number of different valuable compounds.

Thirdly, the encapsulation of more than one type of bioactive into single vesicles is recommended for investigation in the future. Although two model compounds (lutein and anthocyanin) were studied in this thesis project, encapsulation of two or more ingredients in one

liposome may save materials such as phospholipids as well as bring about boosted health benefits and efficacy.

Fourthly, it would be important to generate additional evidence to confirm the proposed mechanism of liposome formation using the improved SC-CO_2 method. The use of high pressure FTIR and confocal microscopy are recommended for this purpose. High pressure FTIR can monitor the interaction changes during the pressurization and depressurization steps while the confocal microscopy may be used to track the movement of phospholipids labeled with a fluorescent dye for clarifying the dispersion effect of CO_2. In addition, the entropy of the colloidal system may also be measured throughout the liposome formation process to assess the entropy changes in lipid or lutein aggregates.

Finally, scale-up of this improved SC-CO_2 process is recommended targeting potential production of liposomes in the industry. A continuous SC-CO_2 process can be developed based on the modification of the batch mode of operation reported in this research. During this process, streams of a crude phospholipid and bioactive suspension and SC-CO_2 can be homogenized by a static mixer prior to depressurization. Thus, thorough solubilization of CO_2 and a stable and equilibrated state between the SC-CO_2 and slurry can be achieved by adjusting the residence time in the static mixer.

REFERENCES

Ahmad, F. T., Asenstorfer, R. E., Soriano, I. R., & Mares, D. J. (2013). Effect of temperature on lutein esterification and lutein stability in wheat grain. *Journal of Cereal Science, 58*(3), 408-413.

Akbarzadeh, A., Rezaei-Sadabady, R., Davaran, S., Joo, S. W., Zarghami, N., Hanifehpour, Y., . . . Nejati-Koshki, K. (2013). Liposome: classification, preparation, and applications. *Nanoscale Research Letters, 8*(1), 102-102.

Alberts, D. S., Muggia, F. M., Carmichael, J., Winer, E. P., Jahanzeb, M., Venook, A. P., . . . Gabizon, A. A. (2004). Efficacy and safety of liposomal anthracyclines in Phase I/II clinical trials. *Seminars in Oncology, 31, Supplement 13*, 53-90.

Alexander, M., Lopez, A. A., Fang, Y., & Corredig, M. (2012). Incorporation of phytosterols in soy phospholipids nanoliposomes: encapsulation efficiency and stability. *LWT-Food Science and Technology*, *47*(2), 427-436.

Allen, T. M., & Cullis, P. R. (2013). Liposomal drug delivery systems: From concept to clinical applications. *Advanced Drug Delivery Reviews, 65*(1), 36-48.

Allen Zhang, J.-a., & Pawelchak, J. (2000). Effect of pH, ionic strength and oxygen burden on the chemical stability of EPC/cholesterol liposomes under accelerated conditions: Part 1: Lipid hydrolysis. *European Journal of Pharmaceutics and Biopharmaceutics, 50*(3), 357-364.

Almgren, M. (2000). Mixed micelles and other structures in the solubilization of bilayer lipid membranes by surfactants. *Biochimica et Biophysica Acta (BBA) - Biomembranes, 1508*(1–2), 146-163.

Anchordoguy, T. J., Carpenter, J. F., Crowe, J. H., & Crowe, L. M. (1992). Temperature-dependent perturbation of phospholipid bilayers by dimethylsulfoxide. *Biochimica et Biophysica Acta (BBA) - Biomembranes, 1104*(1), 117-122.

Anderson, M., & Omri, A. (2004). The effect of different lipid components on the in vitro stability and release kinetics of liposome formulations. *Drug Delivery, 11*(1), 33-39.

Anderson, N. A., Richter, L. J., Stephenson, J. C., & Briggman, K. A. (2007). Characterization and control of lipid layer fluidity in hybrid bilayer membranes. *Journal of the American Chemical Society, 129*(7), 2094-2100.

Andrieux, K., Forte, L., Lesieur, S., Paternostre, M., Ollivon, M., & Grabielle-Madelmont, C. (2009). Solubilisation of dipalmitoylphosphatidylcholine bilayers by sodium taurocholate: A model to study the stability of liposomes in the gastrointestinal tract and their mechanism of interaction with a model bile salt. *European Journal of Pharmaceutics and Biopharmaceutics, 71*(2), 346-355.

Arora, A., Byrem, T. M., Nair, M. G., & Strasburg, G. M. (2000). Modulation of liposomal membrane fluidity by flavonoids and isoflavonoids. *Archives of Biochemistry and Biophysics, 373*(1), 102-109.

Augustin, M. A., & Hemar, Y. (2009). Nano- and micro-structured assemblies for encapsulation of food ingredients. *Chemical Society Reviews, 38*(4), 902-912.

Augustin, M. A., & Sanguansri, L. (2012). 2 - Challenges in developing delivery systems for food additives, nutraceuticals and dietary supplements *Encapsulation Technologies and Delivery Systems for Food Ingredients and Nutraceuticals* (pp. 19-48): Woodhead Publishing.

Balaban, M. O., Arreola, A. G., Marshall, M., Peplow, A., Wei, C. I., & Cornell, J. (1991). Inactivation of pectinesterase in orange juice by supercritical carbon dioxide. *Journal of Food Science, 56*(3), 743-746.

Bangham, A. D., Hill, M. W., & Miller, N. G. A. (1974). Preparation and use of liposomes as models of biological membranes. In E. D. Korn (Ed.), *Methods in Membrane Biology: Volume 1* (pp. 1-68). Boston, MA: Springer US.

Bangham, A. D., Standish, M. M., & Watkins, J. C. (1965). Diffusion of univalent ions across the lamellae of swollen phospholipids. *Journal of Molecular Biology, 13*(1), 238-IN227.

Batzri, S., & Korn, E. D. (1973). Single bilayer liposomes prepared without sonication. *Biochimica et Biophysica Acta (BBA) - Biomembranes, 298*(4), 1015-1019.

Beh, C. C., Mammucari, R., & Foster, N. R. (2012). Lipids-based drug carrier systems by dense gas technology: A review. *Chemical Engineering Journal, 188*, 1-14.

Belščak-Cvitanović, A., Stojanović, R., Manojlović, V., Komes, D., Cindrić, I. J., Nedović, V., & Bugarski, B. (2011). Encapsulation of polyphenolic antioxidants from medicinal plant extracts in alginate–chitosan system enhanced with ascorbic acid by electrostatic extrusion. *Food Research International, 44*(4), 1094-1101.

Berson, E. L., Rosner, B., Sandberg, M. A., & et al. (2004). Further evaluation of docosahexaenoic acid in patients with retinitispigmentosa receiving vitamin a treatment: Subgroup analyses. *Archives of Ophthalmology, 122*(9), 1306-1314.

Berson, E. L., Rosner, B., Sandberg, M. A., Weigel-DiFranco, C., Brockhurst, R. J., Hayes, K. C., . . . Schaefer, E. J. (2010). Clinical trial of lutein in patients with retinitis pigmentosa receiving vitamin A. *Archives of Ophthalmology, 128*(4), 403-411.

Bhattacharya, S., & Haldar, S. (2000). Interactions between cholesterol and lipids in bilayer membranes. Role of lipid headgroup and hydrocarbon chain–backbone linkage. *Biochimica et Biophysica Acta (BBA) - Biomembranes, 1467*(1), 39-53.

Bhuvana, M., & Dharuman, V. (2014). Tethering of spherical DOTAP liposome gold nanoparticles on cysteamine monolayer for sensitive label free electrochemical detection of DNA and transfection. *Analyst, 139*(10), 2467-2475.

Bonarska-Kujawa, D., Pruchnik, H., Cyboran, S., Żyłka, R., Oszmiański, J., & Kleszczyńska, H. (2014). Biophysical mechanism of the protective effect of blue honeysuckle (lonicera caerulea l. var. kamtschatica sevast.) polyphenols extracts against lipid peroxidation of erythrocyte and lipid membranes. *The Journal of Membrane Biology, 247*(7), 611-625.

Bose, S., & Michniak-Kohn, B. (2013). Preparation and characterization of lipid based nanosystems for topical delivery of quercetin. *European Journal of Pharmaceutical Sciences, 48*(3), 442-452.

Bothun, G. D. (2008). Hydrophobic silver nanoparticles trapped in lipid bilayers: Size distribution, bilayer phase behavior, and optical properties. *Journal of Nanobiotechnology, 6*, 13-13.

Bozzuto, G., & Molinari, A. (2015). Liposomes as nanomedical devices. *International Journal of Nanomedicine, 10*, 975-999.

Brat, P., Tourniaire, F., & Amiot-Carlin, M. J. (2008). *Stability and analysis of phenolic pigments*. Boca Raton: CRC Press.

Bruno, M. J., Rusinova, R., Gleason, N. J., Koeppe, R. E., & Andersen, O. S. (2013). Interactions of drugs and amphiphiles with membranes: modulation of lipid bilayer elastic properties by changes in acyl chain unsaturation and protonation. Faraday Discussions, 161, 461–589.

Bryła, A., Lewandowicz, G., & Juzwa, W. (2015). Encapsulation of elderberry extract into phospholipid nanoparticles. *Journal of Food Engineering, 167, Part B*, 189-195.

Buckow, R., Kastell, A., Terefe, N. S., & Versteeg, C. (2010). Pressure and temperature effects on degradation kinetics and storage stability of total anthocyanins in blueberry juice. *Journal of Agricultural and Food Chemistry, 58*(18), 10076-10084.

Burling, H., & Graverholt, G. (2008). Milk – A new source for bioactive phospholipids for use in food formulations. *Lipid Technology, 20*(10), 229-231.

Burnett, E. S. (1923). Experimental study of the Joule-Thomson effect in carbon dioxide. *Physical Review, 22*(6), 590-616.

Cabrera, I., Elizondo, E., Esteban, O., Corchero, J. L., Melgarejo, M., Pulido, D., . . . Veciana, J. (2013). Multifunctional nanovesicle-bioactive conjugates prepared by a one-step scalable method using CO2-expanded solvents. *Nano Letters, 13*(8), 3766-3774.

Calvignac, B., Rodier, E., Letourneau, J.-J., Almeida dos Santos Pedro, M., & Fages, J. (2010). Cocoa butter saturated with supercritical carbon dioxide: measurements and modelling of solubility, volumetric expansion, density and viscosity. *International Journal of Chemical Reactor Engineering, 8*, pp.A73.

Campardelli, R., Espirito Santo, I., Albuquerque, E. C., de Melo, S. V., Della Porta, G., & Reverchon, E. (2016). Efficient encapsulation of proteins in submicro liposomes using a supercritical fluid assisted continuous process. *The Journal of Supercritical Fluids, 107*, 163-169.

Canelas, D. A., Herlihy, K. P., & DeSimone, J. M. (2009). Top-down particle fabrication: control of size and shape for diagnostic imaging and drug delivery. *Wiley Interdisciplinary Reviews: Nanomedicine and Nanobiotechnology, 1*(4), 391-404.

Cano-Sarabia, M., Ventosa, N., Sala, S., Patiño, C., Arranz, R., & Veciana, J. (2008). Preparation of uniform rich cholesterol unilamellar nanovesicles using CO_2-expanded solvents. *Langmuir, 24*(6), 2433-2437.

Cansell, M., Nacka, F., & Combe, N. (2003). Marine lipid-based liposomes increase in vivo FA bioavailability. *Lipids, 38*(5), 551-559.

Castangia, I., Nácher, A., Caddeo, C., Valenti, D., Fadda, A. M., Díez-Sales, O., . . . Manconi, M. (2014). Fabrication of quercetin and curcumin bionanovesicles for the prevention and rapid regeneration of full-thickness skin defects on mice. *Acta Biomaterialia, 10*(3), 1292-1300.

Cavalcanti, L. P., Konovalov, O., & Haas, H. (2007). X-ray diffraction from paclitaxel-loaded zwitterionic and cationic model membranes. *Chemistry and Physics of Lipids, 150*(1), 58-65.

Cavalcanti, R. N., Santos, D. T., & Meireles, M. A. A. (2011). Non-thermal stabilization mechanisms of anthocyanins in model and food systems—An overview. *Food Research International, 44*(2), 499-509.

Champion, J. A., Katare, Y. K., & Mitragotri, S. (2007). Particle shape: A new design parameter for micro- and nanoscale drug delivery carriers. *Journal of Controlled Release, 121*(1–2), 3-9.

Chan, Y.-H., Chen, B.-H., Chiu, C. P., & Lu, Y.-F. (2004). The influence of phytosterols on the encapsulation efficiency of cholesterol liposomes. *International Journal of Food Science & Technology, 39*(9), 985-995.

Chang, H., Kao, M.-J., Chen, T.-L., Chen, C.-H., Cho, K.-C., & Lai, X.-R. (2013). Characterization of natural dye extracted from wormwood and purple cabbage for dye-sensitized solar cells. *International Journal of Photoenergy, 2013*, 8.

Chang, S., Alben, J. O., Wisner, D. A., & Tsai, M. D. (1986). Phospholipids chiral at phosphorus: Fourier-transform infrared study on the gel-liquid crystalline transition of chiral thiophosphatidylcholine. *Biochemistry, 25*(11), 3435-3440.

Charcosset, C., Juban, A., Valour, J.-P., Urbaniak, S., & Fessi, H. (2006). Preparation of liposomes at large scale using the ethanol injection method: Effect of scale-up and injection devices. *Chemical Engineering Research and Design, 94*, 508-515.

Chen, C., Han, D., Cai, C., & Tang, X. (2010). An overview of liposome lyophilization and its future potential. *Journal of Controlled Release, 142*(3), 299-311.

Chia-Ming, C., & Weiner, N. (1987). Gastrointestinal uptake of liposomes. I. In vitro and in situ studies. *International Journal of Pharmaceutics, 37*(1), 75-85.

Chiu, G. N. C., Abraham, S. A., Ickenstein, L. M., Ng, R., Karlsson, G., Edwards, K., . . . Bally, M. B. (2005). Encapsulation of doxorubicin into thermosensitive liposomes via complexation with the transition metal manganese. *Journal of Controlled Release, 104*(2), 271-288.

Ciftci, O. N., & Temelli, F. (2014). Melting point depression of solid lipids in pressurized carbon dioxide. *The Journal of Supercritical Fluids, 92*, 208-214.

Cipolla, D., Wu, H., Eastman, S., Redelmeier, T., Gonda, I., & Chan, H. K. (2014). Development and characterization of an in vitro release assay for liposomal ciprofloxacin for inhalation. *Journal of Pharmaceutical Sciences, 103*(1), 314-327.

Coderch, L., Fonollosa, J., De Pera, M., Estelrich, J., De La Maza, A., & Parra, J. L. (2000). Influence of cholesterol on liposome fluidity by EPR: Relationship with percutaneous absorption. *Journal of Controlled Release, 68*(1), 85-95.

Colas, J.-C., Shi, W., Rao, V. S. N. M., Omri, A., Mozafari, M. R., & Singh, H. (2007). Microscopical investigations of nisin-loaded nanoliposomes prepared by Mozafari method and their bacterial targeting. *Micron, 38*(8), 841-847.

Corvo, M. L., Mendo, A. S., Figueiredo, S., Gaspar, R., Larguinho, M., Guedes da Silva, M. F. C., . . . Fernandes, A. R. (2016). Liposomes as delivery system of a Sn(IV) complex for cancer therapy. *Pharmaceutical Research, 33*(6), 1351-1358.

Cui, H., Zhao, C., & Lin, L. (2015). The specific antibacterial activity of liposome-encapsulated Clove oil and its application in tofu. *Food Control, 56*, 128-134.

Cullis, P. R., & De Kruyff, B. (1976). 31P NMR studies of unsonicated aqueous dispersions of neutral and acidic phospholipids. Effects of phase transitions, p2H and divalent cations on the motion in the phosphate region of the polar headgroup. *Biochimica et Biophysica Acta (BBA)-Biomembranes, 436*(3), 523-540.

Cygnarowicz, M. L., Maxwell, R. J., & Seider, W. D. (1990). Equilibrium solubilities of β-carotene in supercritical carbon dioxide. *Fluid Phase Equilibria, 59*(1), 57-71.

Das, S., & Chaudhury, A. (2011). Recent advances in lipid nanoparticle formulations with solid matrix for oral drug delivery. An Official Journal of the American Association of Pharmaceutical Scientists (AAPS PharmSciTech), 12(1), 62–76.

de Kruyff, B., Demel, R. A., & dan Deenen, L. L. M. (1972). The effect of cholesterol and epicholesterol incorporation on the permeability and on the phase transition of intact Acholeplasma laidlawii cell membranes and derived liposomes. *Biochimica et Biophysica Acta (BBA) - Biomembranes, 255*(1), 331-347.

de Melo, S. A. B. V., Danh, L. T., Mammucari, R., & Foster, N. R. (2014). Dense CO2 antisolvent precipitation of levothyroxine sodium: A comparative study of GAS and ARISE techniques based on morphology and particle size distributions. *The Journal of Supercritical Fluids, 93*, 112-120.

Demel, R. A., & De Kruyff, B. (1976). The function of sterols in membranes. *Biochimica et Biophysica Acta (BBA) - Reviews on Biomembranes, 457*(2), 109-132.

Desai, M. P., Labhasetwar, V., Amidon, G. L., & Levy, R. J. (1996). Gastrointestinal uptake of biodegradable microparticles: effect of particle size. *Pharmaceutical research, 13*(12), 1838-1845.

Ding, W., Palaiokostas, M., Wang, W., & Orsi, M. (2015). Effects of lipid composition on bilayer membranes quantified by all-atom molecular dynamics. *The Journal of Physical Chemistry B, 119*(49), 15263-15274.

Disalvo, E. A., Lairion, F., Martini, F., Tymczyszyn, E., Frías, M., Almaleck, H., & Gordillo, G. J. (2008). Structural and functional properties of hydration and confined water in membrane interfaces. *Biochimica et Biophysica Acta (BBA) - Biomembranes, 1778*(12), 2655-2670.

Dodds, W. S., Stutzman, L. F., & Sollami, B. J. (1956). Carbon dioxide solubility in water. *Industrial & Engineering Chemistry Chemical & Engineering Data Series, 1*(1), 92-95.

Duan, Z., & Sun, R. (2003). An improved model calculating CO_2 solubility in pure water and aqueous NaCl solutions from 273 to 533 K and from 0 to 2000 bar. *Chemical Geology, 193*(3–4), 257-271.

Egawa, H., & Furusawa, K. (1999). Liposome adhesion on mica surface studied by atomic force microscopy. *Langmuir, 15*(5), 1660-1666.

Elizondo, E., Larsen, J., Hatzakis, N. S., Cabrera, I., Bjørnholm, T., Veciana, J., . . . Ventosa, N. (2012). Influence of the preparation route on the supramolecular organization of lipids in a vesicular system. *Journal of the American Chemical Society, 134*(4), 1918-1921.

Elizondo, E., Moreno, E., Cabrera, I., Córdoba, A., Sala, S., Veciana, J., & Ventosa, N. (2011). Liposomes and other vesicular systems: structural characteristics, methods of preparation, and use in nanomedicine. In V. Antonio (Ed.), *Progress in Molecular Biology and Translational Science* (Vol. Volume 104, pp. 1-52): Academic Press.

Erdahl, W. L., Stolyhwo, A., & Privett, O. S. (1973). Analysis of soybean lecithin by thin layer and analytical liquid chromatography. *Journal of the American Oil Chemists Society, 50*(12), 513-515.

Erkmen, O. (2012). Effects of dense phase carbon dioxide on vegetative cells. In M. O. Balaban & G. Ferrentino (Eds.), *Dense phase carbon Dioxide: Food and Pharmaceutical Applications* (pp. 67-97). Chichester, UK: Wiley-Blackwell.

Fahr, A., & Liu, X. (2007). Drug delivery strategies for poorly water-soluble drugs. *Expert Opinion on Drug Delivery, 4*(4), 403-416.

Fang, Z., & Bhandari, B. (2010). Encapsulation of polyphenols – a review. *Trends in Food Science & Technology, 21*(10), 510-523.

Fenske, D. B., Chonn, A., & Cullis, P. R. (2008). Liposomal nanomedicines: an emerging field. *Toxicologic Pathology, 36*(1), 21-29.

Fernandez, E., Rodriguez, G., Cocera, M., Barbosa-Barros, L., Alonso, C., Lopez-Iglesias, C., . . . Lopez, O. (2015). Advanced lipid systems containing [small beta]-carotene: stability under UV-vis radiation and application on porcine skin in vitro. *Physical Chemistry Chemical Physics, 17*(28), 18710-18721.

Ferreira, D. S., Faria, A. F., Grosso, C. R. F., & Mercadante, A. Z. (2009). Encapsulation of blackberry anthocyanins by thermal gelation of curdlan. *Journal of the Brazilian Chemical Society, 20*, 1908-1915.

Ferrentino, G., Calix, T., Poletto, M., Ferrari, G., & Balaban, M. O. (2012). Experimental measurement of carbon dioxide solubility. *Dense Phase Carbon Dioxide* (pp. 37-66): Wiley-Blackwell.

Freitas, S., Merkle, H. P., & Gander, B. (2005). Microencapsulation by solvent extraction/evaporation: reviewing the state of the art of microsphere preparation process technology. *Journal of Controlled Release, 102*(2), 313-332.

Frenzel, M., Krolak, E., Wagner, A. E., & Steffen-Heins, A. (2015). Physicochemical properties of WPI coated liposomes serving as stable transporters in a real food matrix. *LWT - Food Science and Technology, 63*(1), 527-534.

Furneri, P. M., Fresta, M., Puglisi, G., & Tempera, G. (2000). Ofloxacin-loaded liposomes: In vitro activity and drug accumulation in bacteria. *Antimicrobial Agents and Chemotherapy, 44*(9), 2458-2464.

Garcia-Gonzalez, L., Geeraerd, A. H., Spilimbergo, S., Elst, K., Van Ginneken, L., Debevere, J., . . . Devlieghere, F. (2007). High pressure carbon dioxide inactivation of microorganisms in foods: The past, the present and the future. *International Journal of Food Microbiology, 117*(1), 1-28.

Garidel, P., Blume, A., & Hübner, W. (2000). A Fourier transform infrared spectroscopic study of the interaction of alkaline earth cations with the negatively charged phospholipid 1, 2-dimyristoyl-sn-glycero-3-phosphoglycerol. *Biochimica et Biophysica Acta (BBA)-Biomembranes, 1466*(1), 245-259.

Ghorbanzade, T., Jafari, S. M., Akhavan, S., & Hadavi, R. (2017). Nano-encapsulation of fish oil in nano-liposomes and its application in fortification of yogurt. *Food Chemistry, 216*, 146-152.

Gibis, M., Rahn, N., & Weiss, J. (2013). Physical and sxidative stability of uncoated and chitosan-coated liposomes containing grape seed extract. *Pharmaceutics, 5*(3), 421-433.

Gibis, M., Ruedt, C., & Weiss, J. (2016). In vitro release of grape-seed polyphenols encapsulated from uncoated and chitosan-coated liposomes. *Food Research International, 88, Part A*, 105-113.

Gibis, M., Zeeb, B., & Weiss, J. (2014). Formation, characterization, and stability of encapsulated hibiscus extract in multilayered liposomes. *Food Hydrocolloids, 38*, 28-39.

Gibson, L. (2007). Lipid-based excipients for oral drug delivery. *Oral Lipid-Based Formulations* (pp. 33-61): CRC Press.

Grit, M., & Crommelin, D. J. A. (1993). Chemical stability of liposomes: implications for their physical stability. *Chemistry and Physics of Lipids, 64*(1), 3-18.

Gruszecki, W. I., & Strzałka, K. (2005). Carotenoids as modulators of lipid membrane physical properties. *Biochimica et Biophysica Acta (BBA) - Molecular Basis of Disease, 1740*(2), 108-115.

Gülseren, İ., Guri, A., & Corredig, M. (2012). Encapsulation of tea polyphenols in nanoliposomes prepared with milk phospholipids and their effect on the viability of HT-29 human carcinoma cells. *Food Digestion, 3*(1), 36-45.

Guo, T., Zhang, Y., Zhao, J., Zhu, C., & Feng, N. (2015). Nanostructured lipid carriers for percutaneous administration of alkaloids isolated from Aconitum sinomontanum. *Journal of Nanobiotechnology, 13*, pp.47.

Hąc-Wydro, K., Wydro, P., Dynarowicz-Łątka, P., & Paluch, M. (2009). Cholesterol and phytosterols effect on sphingomyelin/phosphatidylcholine model membranes—Thermodynamic analysis of the interactions in ternary monolayers. *Journal of Colloid and Interface Science, 329*(2), 265-272.

Hadian, Z., Sahari, M. A., Moghimi, H. R., & Barzegar, M. (2014). Formulation, characterization and optimization of liposomes containing eicosapentaenoic and docosahexaenoic acids: a methodology approach. *Iranian Journal of Pharmaceutical Research : IJPR, 13*(2), 393-404.

Hasan, M., Belhaj, N., Benachour, H., Barberi-Heyob, M., Kahn, C. J. F., Jabbari, E., . . . Arab-Tehrany, E. (2014). Liposome encapsulation of curcumin: Physico-chemical characterizations and effects on MCF7 cancer cell proliferation. *International Journal of Pharmaceutics, 461*(1–2), 519-528.

Henry, C. R. (2005). Morphology of supported nanoparticles. *Progress in Surface Science, 80*(3–4), 92-116.

Hianik, T. (1999). Mechanical properties of lipid bilayers and protein-lipid interactions. In F. Bersani (Ed.), *Electricity and Magnetism in Biology and Medicine* (pp. 235-238). Boston, MA: Springer US.

Hirsch, M., Ziroli, V., Helm, M., & Massing, U. (2009). Preparation of small amounts of sterile siRNA-liposomes with high entrapping efficiency by dual asymmetric centrifugation (DAC). *Journal of Controlled Release, 135*(1), 80-88.

Hunter, R. J., Midmore, B. R., & Zhang, H. (2001). Zeta potential of highly charged thin double-layer systems. *Journal of Colloid and Interface Science, 237*(1), 147-149.

Hwang, J.-M., Kuo, H.-C., Lin, C.-T., & Kao, E.-S. (2013). Inhibitory effect of liposome-encapsulated anthocyanin on melanogenesis in human melanocytes. *Pharmaceutical Biology, 51*(8), 941-947.

Hwang, J. S., Tsai, Y. L., & Hsu, K. C. (2010). The feasibility of antihypertensive oligopeptides encapsulated in liposomes prepared with phytosterols-β-sitosterol or stigmasterol. *Food Research International*, *43*(1), 133-139.

Ickenstein, L. M., Sandström, M. C., Mayer, L. D., & Edwards, K. (2006). Effects of phospholipid hydrolysis on the aggregate structure in DPPC/DSPE-PEG2000 liposome preparations after gel to liquid crystalline phase transition. *Biochimica et Biophysica Acta (BBA) - Biomembranes, 1758*(2), 171-180.

Isailović, B. D., Kostić, I. T., Zvonar, A., Đorđević, V. B., Gašperlin, M., Nedović, V. A., & Bugarski, B. M. (2013). Resveratrol loaded liposomes produced by different techniques. *Innovative Food Science & Emerging Technologies, 19*(0), 181-189.

Isenschmid, A., Marison, I. W., & von Stockar, U. (1995). The influence of pressure and temperature of compressed CO_2 on the survival of yeast cells. *Journal of Biotechnology, 39*(3), 229-237.

Ito, Y., Wakai, K., Suzuki, K., Tamakoshi, A., Seki, N., Ando, M., . . . Group, J. S. (2003). Serum carotenoids and mortality from lung cancer: a case-control study nested in the Japan Collaborative Cohort (JACC) Study. *Cancer Science, 94*(1), 57-63.

Iwanaga, K., Ono, S., Narioka, K., Kakemi, M., Morimoto, K., Yamashita, S., . . . Oku, N. (1999). Application of surface-coated liposomes for oral delivery of peptide: Effects of coating the liposome's surface on the GI transit of insulin. *Journal of Pharmaceutical Sciences, 88*(2), 248-252.

Jacobson, K., & Papahadjopoulos, D. (1975). Phase transitions and phase separations in phospholipid membranes induced by changes in temperature, pH, and concentration of bivalent cations. *Biochemistry, 14*(1), 152-161.

Jenab, E., & Temelli, F. (2011). Viscosity measurement and modeling of canola oil and its blend with canola stearin in equilibrium with high pressure carbon dioxide. *Journal of Supercritical Fluids, 58*(1), 7-14.

Jenab, E., & Temelli, F. (2012). Density and volumetric expansion of carbon dioxide-expanded canola oil and its blend with fully-hydrogenated canola oil. *The Journal of Supercritical Fluids, 70*, 57-65.

Jesorka, A., & Orwar, O. (2008). Liposomes: Technologies and analytical applications. *Annual Review of Analytical Chemistry, 1*(1), 801-832.

Jiang, J., Oberdörster, G., & Biswas, P. (2009). Characterization of size, surface charge, and agglomeration state of nanoparticle dispersions for toxicological studies. *Journal of Nanoparticle Research, 11*(1), 77-89.

Johnson, N. R., Ambe, T., & Wang, Y. (2014). Lysine-based polycation:heparin coacervate for controlled protein delivery. *Acta Biomaterialia, 10*(1), 40-46.

Johnston, K. P., & Shah, P. S. (2004). Making nanoscale materials with supercritical fluids. *Science, 303*(5657), 482-483.

Jones, R. P., & Greenfield, P. F. (1982). Effect of carbon dioxide on yeast growth and fermentation. *Enzyme and Microbial Technology, 4*(4), 210-223.

Jose, S., Anju, S. S., Cinu, T. A., Aleykutty, N. A., Thomas, S., & Souto, E. B. (2014). In vivo pharmacokinetics and biodistribution of resveratrol-loaded solid lipid nanoparticles for brain delivery. *International journal of pharmaceutics*, *474*(1), 6-13.

Justo, O. R., & Moraes, Â. M. (2011). Analysis of process parameters on the characteristics of liposomes prepared by ethanol injection with a view to process scale-up: Effect of temperature and batch volume. *Chemical Engineering Research and Design, 89*(6), 785-792.

Kalepu, S., Manthina, M., & Padavala, V. (2013). Oral lipid-based drug delivery systems – an overview. *Acta Pharmaceutica Sinica B, 3*(6), 361-372.

Kamal, M. A., & Raghunathan, V. A. (2012). Phase behavior of phospholipid-phytosterol membranes. *Soft matter, 8*(34), 8952-8958.

Kamezaki, C., Nakashima, A., Yamada, A., Uenishi, S., Ishibashi, H., Shibuya, N., . . . Kogure, K. (2016). Synergistic antioxidative effect of astaxanthin and tocotrienol by co-encapsulated in liposomes. *Journal of Clinical Biochemistry and Nutrition, 59*(2), 100-106.

Kamihira, M., Taniguchi, M., & Kobayashi, T. (1987). Sterilization of microorganisms with supercritical carbon dioxide. *Agricultural and Biological Chemistry, 51*(2), 407-412.

Kaszuba, M., McKnight, D., Connah, M. T., McNeil-Watson, F. K., & Nobbmann, U. (2008). Measuring sub nanometre sizes using dynamic light scattering. *Journal of Nanoparticle Research, 10*(5), 823-829.

Keppler, K., & Humpf, H.-U. (2005). Metabolism of anthocyanins and their phenolic degradation products by the intestinal microflora. *Bioorganic & Medicinal Chemistry, 13*(17), 5195-5205.

Khan, A., & Marques, E. F. (1999). Synergism and polymorphism in mixed surfactant systems. *Current Opinion in Colloid & Interface Science, 4*(6), 402-410.

Kim, H., Kim, Y., & Lee, J. (2013). Liposomal formulations for enhanced lymphatic drug delivery. *Asian Journal of Pharmaceutical Sciences, 8*(2), 96-103.

Kopeć, W., Telenius, J., & Khandelia, H. (2013). Molecular dynamics simulations of the interactions of medicinal plant extracts and drugs with lipid bilayer membranes. *FEBS Journal, 280*(12), 2785-2805.

Kraft, J. C., Freeling, J. P., Wang, Z., & Ho, R. J. Y. (2014). Emerging research and clinical development trends of liposome and lipid nanoparticle drug delivery systems. *Journal of Pharmaceutical Sciences, 103*(1), 29-52.

Kučerka, N., Nieh, M.-P., & Katsaras, J. (2011). Fluid phase lipid areas and bilayer thicknesses of commonly used phosphatidylcholines as a function of temperature. *Biochimica et Biophysica Acta (BBA) - Biomembranes, 1808*(11), 2761-2771.

Kulkarni, S. B., Betageri, G. V., & Singh, M. (1995). Factors affecting microencapsulation of drugs in liposomes. *Journal of Microencapsulation, 12*(3), 229-246.

Lang, J. K. (1990). Quantitative determination of cholesterol in liposome drug products and raw materials by high-performance liquid chromatography. *Journal of Chromatography A, 507*(0), 157-163.

Laouini, A., Jaafar-Maalej, C., Limayem-Blouza, I., Sfar, S., Charcosset, C., & Fessi, H. (2012). Preparation, characterization and applications of liposomes: State of the art. *Journal of Colloid Science and Biotechnology, 1*(2), 147-168.

Laridi, R., Kheadr, E. E., Benech, R. O., Vuillemard, J. C., Lacroix, C., & Fliss, I. (2003). Liposome encapsulated nisin Z: optimization, stability and release during milk fermentation. *International Dairy Journal, 13*(4), 325-336.

Lasic, D. D. (1999). Spontaneous vesiculation and spontaneous liposomes. *Journal of Liposome Research, 9*(1), 43-52.

Lee, S., Lee, K., Kim, J., & Lim, S. (2005). The effect of cholesterol in the liposome bilayer on the stabilization of incorporated retinol. *Journal of Liposome Research, 15*(3-4), 157-166.

Lee, S. Y., Lee, S. J., Choi, D. S., & Hur, S. J. (2015). Current topics in active and intelligent food packaging for preservation of fresh foods. *Journal of the Science of Food and Agriculture, 95*(14), 2799-2810.

Leonenko, Z. V., Finot, E., Ma, H., Dahms, T. E. S., & Cramb, D. T. Investigation of temperature-induced phase transitions in DOPC and DPPC phospholipid bilayers using temperature-controlled scanning force microscopy. *Biophysical Journal, 86*(6), 3783-3793.

Lesoin, L., Boutin, O., Crampon, C., & Badens, E. (2011). CO_2/water/surfactant ternary systems and liposome formation using supercritical CO_2: A review. *Colloids and surfaces. A, Physicochemical and Engineering Aspects, 377*(1-3), 1-14.

Lesoin, L., Crampon, C., Boutin, O., & Badens, E. (2011). Preparation of liposomes using the supercritical anti-solvent (SAS) process and comparison with a conventional method. *The Journal of Supercritical Fluids, 57*(2), 162-174.

Lewis, R. N. A. H., & McElhaney, R. N. (1998). The structure and organization of phospholipid bilayers as revealed by infrared spectroscopy. *Chemistry and Physics of Lipids, 96*(1–2), 9-21.

Li, J., Wang, X., Zhang, T., Wang, C., Huang, Z., Luo, X., & Deng, Y. (2015). A review on phospholipids and their main applications in drug delivery systems. *Asian Journal of Pharmaceutical Sciences, 10*(2), 81-98.

Li, Z., Paulson, A. T., & Gill, T. A. (2015). Encapsulation of bioactive salmon protein hydrolysates with chitosan-coated liposomes. *Journal of Functional Foods, 19, Part A*, 733-743.

Lichtenberg, D., & Barenholz, Y. (2006). Liposomes: Preparation, characterization, and preservation. *Methods of Biochemical Analysis* (pp. 337-462): John Wiley & Sons, Inc.

Liolios, C. C., Gortzi, O., Lalas, S., Tsaknis, J., & Chinou, I. (2009). Liposomal incorporation of carvacrol and thymol isolated from the essential oil of Origanum dictamnus L. and in vitro antimicrobial activity. *Food Chemistry, 112*(1), 77-83.

Liu, D., Hu, H., Lin, Z., Chen, D., Zhu, Y., Hou, S., & Shi, X. (2013). Quercetin deformable liposome: Preparation and efficacy against ultraviolet B induced skin damages in vitro and in vivo. *Journal of Photochemistry and Photobiology B: Biology, 127*(0), 8-17.

Liu, J., & Conboy, J. C. (2004). Phase transition of a single lipid bilayer measured by sum-frequency vibrational spectroscopy. *Journal of the American Chemical Society, 126*(29), 8894-8895.

Liu, W., Ye, A., Liu, W., Liu, C., & Singh, H. (2013). Stability during in vitro digestion of lactoferrin-loaded liposomes prepared from milk fat globule membrane-derived phospholipids. *Journal of Dairy Science, 96*(4), 2061-2070.

Lu, Q., Li, D.-C., & Jiang, J.-G. (2011). Preparation of a tea polyphenol nanoliposome system and its physicochemical properties. *Journal of Agricultural and Food Chemistry, 59*(24), 13004-13011.

Maghraby, G. M. M., Williams, A. C., & Barry, B. W. (2005). Drug interaction and location in liposomes: correlation with polar surface areas. *International Journal of Pharmaceutics, 292*(1), 179-185.

Maki, K. C., Lawless, A. L., Reeves, M. S., Dicklin, M. R., Jenks, B. H., Shneyvas, E. D., & Brooks, J. R. (2012). Lipid-altering effects of a dietary supplement tablet containing free plant sterols and stanols in men and women with primary hypercholesterolaemia: a randomized, placebo-controlled crossover trial. *International Journal of Food Sciences and Nutrition, 63*(4), 476-482.

Malheiros, P. d. S., Sant'Anna, V., Barbosa, M. d. S., Brandelli, A., & Franco, B. D. G. d. M. (2012). Effect of liposome-encapsulated nisin and bacteriocin-like substance P34 on Listeria monocytogenes growth in Minas frescal cheese. *International Journal of Food Microbiology, 156*(3), 272-277.

Mannock, D. A., Lewis, R. N. A. H., McMullen, T. P. W., & McElhaney, R. N. (2010). The effect of variations in phospholipid and sterol structure on the nature of lipid–sterol interactions in lipid bilayer model membranes. *Chemistry and Physics of Lipids, 163*(6), 403-448.

Mansilla, M. C., Cybulski, L. E., Albanesi, D., & de Mendoza, D. (2004). Control of membrane lipid fluidity by molecular thermosensors. *Journal of Bacteriology, 186*(20), 6681-6688.

Marrink, S. J., & Mark, A. E. (2003). Molecular dynamics simulation of the formation, structure, and dynamics of small phospholipid vesicles. *Journal of the American Chemical Society, 125*(49), 15233-15242.

Marsanasco, M., Márquez, A. L., Wagner, J. R., del V. Alonso, S., & Chiaramoni, N. S. (2011). Liposomes as vehicles for vitamins E and C: An alternative to fortify orange juice and offer vitamin C protection after heat treatment. *Food Research International, 44*(9), 3039-3046.

Marsh, D. (2008). Energetics of hydrophobic matching in lipid-protein interactions. *Biophysical Journal, 94*(10), 3996-4013.

Marsh, D., & Smith, I. C. P. (1973). An interacting spin label study of the fluidizing and condensing effects of cholesterol on lecithin bilayers. *Biochimica et Biophysica Acta (BBA) - Biomembranes, 298*(2), 133-144.

McElhaney, R. N. (1976). The biological significance of alterations in the fatty acid composition of microbial membrane lipids in response to changes in environmental temperature. In Extreme environments: mechanisms of microbial adaptation (edited by M.R. Heinrich), pp 255-281, Academic Press, New York.

Mehta, R. T. (1996). Liposome encapsulation of clofazimine reduces toxicity in vitro and in vivo and improves therapeutic efficacy in the beige mouse model of disseminated Mycobacterium avium-M. intracellulare complex infection. *Antimicrobial Agents and Chemotherapy, 40*(8), 1893-1902.

Meledandri, C. J., Ninjbadgar, T., & Brougham, D. F. (2011). Size-controlled magnetoliposomes with tunable magnetic resonance relaxation enhancements. *Journal of Materials Chemistry, 21*(1), 214-222.

Meure, L. A., Foster, N. R., & Dehghani, F. (2008). Conventional and dense gas techniques for the production of liposomes: A Review. *AAPS PharmSciTech, 9*(3), 798.

Moeller, S. M., Parekh, N., Tinker, L., & et al. (2006). Associations between intermediate age-related macular degeneration and lutein and zeaxanthin in the carotenoids in age-related eye disease study (careds): Ancillary study of the women's health initiative. *Archives of Ophthalmology, 124*(8), 1151-1162.

Moghimi, S. M., Hunter, A. C., & Murray, J. C. (2001). Long-circulating and target-specific nanoparticles: theory to practice. *Pharmacological Reviews, 53*(2), 283-318.

Molavi, O., Xiong, X.-B., Douglas, D., Kneteman, N., Nagata, S., Pastan, I., . . . Lai, R. (2013). Anti-CD30 antibody conjugated liposomal doxorubicin with significantly improved therapeutic efficacy against anaplastic large cell lymphoma. *Biomaterials, 34*(34), 8718-8725.

Moldovan, B., David, L., Chişbora, C., & Cimpoiu, C. (2012). Degradation kinetics of anthocyanins from European cranberrybush (*Viburnum opulus* L.) fruit extracts. effects of temperature, pH and storage solvent. *Molecules, 17*(10), 11655.

Monteiro, N., Martins, A., Reis, R. L., & Neves, N. M. (2014). Liposomes in tissue engineering and regenerative medicine. *Journal of the Royal Society Interface, 11*(101), 20140459.

Mozafari, R. M., Johnson, C., Hatziantoniou, S., & Demetzos, C. (2008). Nanoliposomes and their applications in food nanotechnology. *Journal of Liposome Research, 18*(4), 309-327.

Nieto-Lozano, J. C., Reguera-Useros, J. I., Peláez-Martínez, M. d. C., & Hardisson de la Torre, A. (2006). Effect of a bacteriocin produced by Pediococcus acidilactici against Listeria monocytogenes and Clostridium perfringens on Spanish raw meat. *Meat Science, 72*(1), 57-61.

Nii, T., & Ishii, F. (2005). Encapsulation efficiency of water-soluble and insoluble drugs in liposomes prepared by the microencapsulation vesicle method. *International Journal of Pharmaceutics, 298*(1), 198-205.

Nomura, S.-i. M., Mizutani, Y., Kurita, K., Watanabe, A., & Akiyoshi, K. (2005). Changes in the morphology of cell-size liposomes in the presence of cholesterol: Formation of neuron-like tubes and liposome networks. *Biochimica et Biophysica Acta (BBA) - Biomembranes, 1669*(2), 164-169.

Nguyen Tuyet, M., De Vrieze, M., Van de Walle, D., Van Hoed, V., Lynen, F., & Dewettinck, K. (2014). Analysis of glycolipids in vegetable lecithin with HPLC-ELSD. *13th International symposium on Hyphenated Techniques in Chromatography and Separation Technology (HTC-13) and 3rd International symposium on Hyphenated Techniques for Sample Preparation (HTSP-3), Book of abstracts*. Presented at the 13th International symposium on Hyphenated Techniques in Chromatography and Separation Technology (HTC-13) ; 3rd International symposium on Hyphenated Techniques for Sample Preparation (HTSP-3).

Ohvo-Rekilä, H., Ramstedt, B., Leppimäki, P., & Peter Slotte, J. (2002). Cholesterol interactions with phospholipids in membranes. *Progress in Lipid Research, 41*(1), 66-97.

Oidtmann, J., Schantz, M., Mäder, K., Baum, M., Berg, S., Betz, M., . . . Richling, E. (2012). Preparation and comparative release characteristics of three anthocyanin encapsulation systems. *Journal of Agricultural and Food Chemistry, 60*(3), 844-851.

Olmedilla, B., Granado, F., Blanco, I., Vaquero, M., & Cajigal, C. (2001). Lutein in patients with cataracts and age-related macular degeneration: a long-term supplementation study. *Journal of the Science of Food and Agriculture, 81*(9), 904-909.

Omenn, G. S., Goodman, G. E., Thornquist, M. D., Balmes, J., Cullen, M. R., Glass, A., . . . Hammar, S. (1996). Effects of a combination of beta carotene and vitamin A on lung cancer and cardiovascular disease. *New England Journal of Medicine, 334*(18), 1150-1155.

Ossman, T., Fabre, G., & Trouillas, P. (2016). Interaction of wine anthocyanin derivatives with lipid bilayer membranes. *Computational and Theoretical Chemistry, 1077*, 80-86.

Otake, K., Imura, T., Sakai, H., & Abe, M. (2001). Development of a new preparation method of liposomes using supercritical carbon dioxide. *Langmuir, 17*(13), 3898-3901.

Otake, K., Shimomura, T., Goto, T., Imura, T., Furuya, T., Yoda, S., . . . Abe, M. (2006). Preparation of liposomes using an improved supercritical reverse phase evaporation method. *Langmuir, 22*(6), 2543-2550.

Palmer, A. F., Wingert, P., & Nickels, J. (2003). Atomic force microscopy and light scattering of small unilamellar actin-containing liposomes. *Biophysical Journal, 85*(2), 1233-1247.

Panwar, P., Pandey, B., Lakhera, P. C., & Singh, K. P. (2010). Preparation, characterization, and in vitro release study of albendazole-encapsulated nanosize liposomes. *International Journal of Nanomedicine, 5*, 101-108.

Pasenkiewicz-Gierula, M., Baczynski, K., Murzyn, K., & Markiewicz, M. (2012). Orientation of lutein in a lipid bilayer - revisited. *Acta Biochim Pol, 59*(1), 115-118.

Patel, H. M., & Ryman, B. E. (1976). Oral administration of insulin by encapsulation within liposomes. *FEBS Letters, 62*(1), 60-63.

Patras, A., Brunton, N. P., O'Donnell, C., & Tiwari, B. K. (2010). Effect of thermal processing on anthocyanin stability in foods; mechanisms and kinetics of degradation. *Trends in Food Science & Technology, 21*(1), 3-11.

Peschka, R., Purmann, T., & Schubert, R. (1998). Cross-flow filtration—an improved detergent removal technique for the preparation of liposomes. *International Journal of Pharmaceutics, 162*(1–2), 177-183.

Pham, T. T., Jaafar-Maalej, C., Charcosset, C., & Fessi, H. (2012). Liposome and niosome preparation using a membrane contactor for scale-up. *Colloids and Surfaces B: Biointerfaces, 94*, 15-21.

Picon, A., Serrano, C., Gaya, P., Medina, M., & Nuñez, M. (1996). The effect of liposome-encapsulated cyprosins on manchego cheese pipening. *Journal of Dairy Science, 79*(10), 1699-1705.

Pignatello, R., Musumeci, T., Basile, L., Carbone, C., & Puglisi, G. (2011). Biomembrane models and drug-biomembrane interaction studies: Involvement in drug design and development. *Journal of Pharmacy and Bioallied Sciences, 3*(1), 4-14.

Pintea, A., Diehl, H. A., Momeu, C., Aberle, L., & Socaciu, C. (2005). Incorporation of carotenoid esters into liposomes. *Biophysical Chemistry, 118*(1), 7-14.

Pohle, W., Gauger, D. R., Fritzsche, H., Rattay, B., Selle, C., Binder, H., & Böhlig, H. (2001). FTIR-spectroscopic characterization of phosphocholine-headgroup model compounds. *Journal of Molecular Structure, 563*, 463-467

Polidori, M. C., Cherubini, A., Stahl, W., Senin, U., Sies, H., & Mecocci, P. (2002). Plasma carotenoid and malondialdehyde levels in ischemic stroke patients: Relationship to early outcome. *Free Radical Research, 36*(3), 265-268.

QuÍlez, J., GarcÍa-Lorda, P., & Salas-Salvadó, J. (2003). Potential uses and benefits of phytosterols in diet: present situation and future directions. *Clinical Nutrition, 22*(4), 343-351.

Quinn, P. J. (1981). The fluidity of cell membranes and its regulation. *Progress in Biophysics and Molecular Biology, 38*, 1-104.

Ramasamy, S., Mazlan, N. A., Ramli, N. A., Rasidi, W. N. A., & Manickam, S. (2016). Bioactivity and stability studies of anthocyanin-Containing extracts from *Garcinia mangostana* L. and *Etlingera elatior* Jack. *Sains Malaysiana, 45*(4), 559-559.

Rao, D. R., Chawan, C. B., & Veeramachaneni, R. (1994). Liposome encapsulation of β-galactosidase: Comparison of two methods of encapsulation and *in vitro* lactose digestibility. *Journal of Food Biochemistry, 18*(4), 239-251.

Rashidinejad, A., Birch, E. J., Sun-Waterhouse, D., & Everett, D. W. (2014). Delivery of green tea catechin and epigallocatechin gallate in liposomes incorporated into low-fat hard cheese. *Food Chemistry, 156*, 176-183.

Rasti, B., Jinap, S., Mozafari, M. R., & Yazid, A. M. (2012). Comparative study of the oxidative and physical stability of liposomal and nanoliposomal polyunsaturated fatty acids prepared with conventional and Mozafari methods. *Food Chemistry, 135*(4), 2761-2770.

Ricci, M., Giovagnoli, S., Blasi, P., Schoubben, A., Perioli, L., & Rossi, C. (2006). Development of liposomal capreomycin sulfate formulations: Effects of formulation variables on peptide encapsulation. *International Journal of Pharmaceutics, 311*(1–2), 172-181.

Ross, E., Winter, A., & Linseman, D. (2013). Effects of anthocyanins on neuronal and cognitive brain functions. *Anthocyanins in Health and Disease* (pp. 279-308): CRC Press.

Rovoli, M., Gortzi, O., Lalas, S., & Kontopidis, G. (2014). β-Lactoglobulin improves liposome's encapsulation properties for vitamin E delivery. *Journal of Liposome Research, 24*(1), 74-81.

Ruozi, B., Belletti, D., Tombesi, A., Tosi, G., Bondioli, L., Forni, F., & Vandelli, M. A. (2011). AFM, ESEM, TEM, and CLSM in liposomal characterization: a comparative study. *International Journal of Nanomedicine, 6*, 557-563.

Sanguansri, P., & Augustin, M. A. (2006). Nanoscale materials development – a food industry perspective. *Trends in Food Science & Technology, 17*(10), 547-556.

Sant'Anna, V., Malheiros, P. d. S., & Brandelli, A. (2011). Liposome encapsulation protects bacteriocin-like substance P34 against inhibition by Maillard reaction products. *Food Research International, 44*(1), 326-330.

Saravacos, G., Taoukis, P., Krokida, M., Karathanos, V., Lazarides, H., Stoforos, N., . . . Kulozik, U. (2011). Microencapsulation of bioactive bilberry anthocyanins by means of whey protein gels.11th International Congress on Engineering and Food (ICEF11). *Procedia Food Science, 1*, 2047-2056.

Sebaaly, C., Greige-Gerges, H., Stainmesse, S., Fessi, H., & Charcosset, C. (2016). Effect of composition, hydrogenation of phospholipids and lyophilization on the characteristics of eugenol-loaded liposomes prepared by ethanol injection method. *Food Bioscience, 15*, 1-10.

Seelig, J., MacDonald, P. M., & Scherer, P. G. (1987). Phospholipid head groups as sensors of electric charge in membranes. *Biochemistry, 26*(24), 7535-7541.

Seifried, B., & Temelli, F. (2009). Density of marine lipids in equilibrium with carbon dioxide. *The Journal of Supercritical Fluids, 50*(2), 97-104.

Shafaa, M. W. I., Diehl, H. A., & Socaciu, C. (2007). The solubilisation pattern of lutein, zeaxanthin, canthaxanthin and β-carotene differ characteristically in liposomes, liver microsomes and retinal epithelial cells. *Biophysical Chemistry, 129*(2–3), 111-119.

Shahi, S., Sonwane, U., Zadbuke, N., & Tadwee, I. (2013). Design and development of diphenhydramine hydrochloride topical liposomal drug delivery system. *International Journal of Pharmacy and Pharmaceutical Sciences, 5*(3), 534-542.

Shang, L., Nienhaus, K., & Nienhaus, G. U. (2014). Engineered nanoparticles interacting with cells: size matters. *Journal of Nanobiotechnology, 12*, 5-5.

Shibata, H., Izutsu, K.-i., Yomota, C., Okuda, H., & Goda, Y. (2015). Investigation of factors affecting in vitro doxorubicin release from PEGylated liposomal doxorubicin for the development of in vitro release testing conditions. *Drug Development and Industrial Pharmacy, 41*(8), 1376-1386.

Smith, E. A., & Dea, P. K. (2013). *Differential Scanning Calorimetry Studies of Phospholipid Membranes: The Interdigitated Gel Phase*. INTECH Open Access Publisher.

Sparks, D. L., Davidson, W. S., Lund-Katz, S., & Phillips, M. C. (1993). Effect of cholesterol on the charge and structure of apolipoprotein A-I in recombinant high density lipoprotein particles. *Journal of Biological Chemistry, 268*(31), 23250-23257.

Stoll, L., Costa, T. M. H., Jablonski, A., Flôres, S. H., & de Oliveira Rios, A. (2016). Microencapsulation of anthocyanins with different wall materials and its application in active biodegradable films. *Food and Bioprocess Technology, 9*(1), 172-181.

Subash, S., Essa, M. M., Al-Adawi, S., Memon, M. A., Manivasagam, T., & Akbar, M. (2014). Neuroprotective effects of berry fruits on neurodegenerative diseases. *Neural Regeneration Research, 9*(16), 1557-1566.

Szoka, F., & Papahadjopoulos, D. (1978). Procedure for preparation of liposomes with large internal aqueous space and high capture by reverse-phase evaporation. *Proceedings of the National Academy of Sciences of the United States of America, 75*(9), 4194-4198.

Takahashi, M., Uechi, S., Takara, K., Asikin, Y., & Wada, K. (2009). Evaluation of an oral carrier system in rats: Bioavailability and antioxidant properties of liposome-encapsulated curcumin. *Journal of Agricultural and Food Chemistry, 57*(19), 9141-9146.

Takeuchi, H., Matsui, Y., Yamamoto, H., & Kawashima, Y. (2003). Mucoadhesive properties of carbopol or chitosan-coated liposomes and their effectiveness in the oral administration of calcitonin to rats. *Journal of Controlled Release, 86*(2–3), 235-242.

Tan, C., Xia, S., Xue, J., Xie, J., Feng, B., & Zhang, X. (2013). Liposomes as vehicles for lutein: Preparation, stability, liposomal membrane dynamics, and structure. *Journal of Agricultural and Food Chemistry, 61*(34), 8175-8184.

Tan, C., Xue, J., Lou, X., Abbas, S., Guan, Y., Feng, B., . . . Xia, S. (2014). Liposomes as delivery systems for carotenoids: comparative studies of loading ability, storage stability and in vitro release. *Food & Function, 5*(6), 1232-1240.

Tarahovsky, Y. S., Kim, Y. A., Yagolnik, E. A., & Muzafarov, E. N. (2014). Flavonoid–membrane interactions: Involvement of flavonoid–metal complexes in raft signaling. *Biochimica et Biophysica Acta (BBA) - Biomembranes, 1838*(5), 1235-1246.

Tegetmeier, A., Dittmar, D., Fredenhagen, A., & Eggers, R. (2000). Density and volume of water and triglyceride mixtures in contact with carbon dioxide. *Chemical Engineering and Processing: Process Intensification, 39*(5), 399-405.

Templeton, N. S., & Lasic, D. D. (1999). New directions in liposome gene delivery. *Molecular Biotechnology, 11*(2), 175-180.

Thompson, A. K., Couchoud, A., & Singh, H. (2009). Comparison of hydrophobic and hydrophilic encapsulation using liposomes prepared from milk fat globule-derived phospholipids and soya phospholipids. *Dairy Science & Technology, 89*(1), 99-113.

Tsuda, T. (2012). Dietary anthocyanin-rich plants: Biochemical basis and recent progress in health benefits studies. *Molecular Nutrition & Food Research, 56*(1), 159-170.

Ulrich, A. S., Sami, M., & Watts, A. (1994). Hydration of DOPC bilayers by differential scanning calorimetry. *Biochimica et Biophysica Acta (BBA) - Biomembranes, 1191*(1), 225-230.

van Meer, G., Voelker, D. R., & Feigenson, G. W. (2008). Membrane lipids: where they are and how they behave. *Nature reviews. Molecular cell biology, 9*(2), 112-124.

van Nieuwenhuyzen, W., & Tomás, M. C. (2008). Update on vegetable lecithin and phospholipid technologies. *European Journal of Lipid Science and Technology, 110*(5), 472-486.

Vanaja, K., Wahl, M. A., Bukarica, L., & Heinle, H. (2013). Liposomes as carriers of the lipid soluble antioxidant resveratrol: Evaluation of amelioration of oxidative stress by additional antioxidant vitamin. *Life Sciences, 93*(24), 917-923.

Vági, E., Simándi, B., Vásárhelyiné, K. P., Daood, H., Kéry, Á., Doleschall, F., & Nagy, B. (2007). Supercritical carbon dioxide extraction of carotenoids, tocopherols and sitosterols from industrial tomato by-products. *The Journal of Supercritical Fluids, 40*(2), 218-226.

Venkataram, S., Awni, W. M., Jordan, K., & Rahman, Y. E. (1990). Pharmacokinetics of two alternative dosage forms for cyclosporine: Liposomes and intralipid. *Journal of Pharmaceutical Sciences, 79*(3), 216-219.

Ventosa, N., Sala, S., Veciana, J., Torres, J., & Llibre, J. (2001). Depressurization of an expanded liquid organic solution (DELOS): A new procedure for obtaining submicron- or micron-sized crystalline particles. *Crystal Growth & Design, 1*(4), 299-303.

Vlaia, L., Coneac, G., Olariu, I., Vlaia, V., & Lupuleasa, D. (2016). Cellulose-derivatives-based hydrogels as vehicles for dermal and transdermal drug delivery. Emerging concepts in analysis and applications of hydrogels, Dr. Sutapa Biswas Majee (Ed.), InTech.

Wallace, S. J., Li, J., Nation, R. L., & Boyd, B. J. (2012). Drug release from nanomedicines: Selection of appropriate encapsulation and release methodology. *Drug Delivery and TranslationalRresearch, 2*(4), 284-292.

Wallace, T. C. (2011). Anthocyanins in cardiovascular disease. *Advances in Nutrition: An International Review Journal, 2*(1), 1-7.

Wang, D., Kong, L., Wang, J., He, X., Li, X., & Xiao, Y. (2009). Polymyxin E sulfate-loaded liposome for intravenous use: Preparation, lyophilization, and toxicity Assessment In Vivo. *PDA Journal of Pharmaceutical Science and Technology, 63*(2), 159-167.

Wang, T., Deng, Y., Geng, Y., Gao, Z., Zou, J., & Wang, Z. (2006). Preparation of submicron unilamellar liposomes by freeze-drying double emulsions. *Biochimica et Biophysica Acta (BBA) - Biomembranes, 1758*(2), 222-231.

Weiss, R. F. (1974). Carbon dioxide in water and seawater: the solubility of a non-ideal gas. *Marine Chemistry, 2*(3), 203-215.

Welch, C. R., Wu, Q., & Simon, J. E. (2008). Recent advances in anthocyanin analysis and characterization. *Current Analytical Chemistry, 4*(2), 75-101.

Wen, Z., You, X., Jiang, L., Liu, B., Zheng, Z., Pu, Y., & Cheng, B. (2011). Liposomal incorporation of rose essential oil by a supercritical process. *Flavour and Fragrance Journal, 26*(1), 27-33.

Wengeler, R., & Nirschl, H. (2007). Turbulent hydrodynamic stress induced dispersion and fragmentation of nanoscale agglomerates. *Journal of Colloid and Interface Science, 306*(2), 262-273.

Wisniewska, A., & Subczynski, W. K. (1998). Effects of polar carotenoids on the shape of the hydrophobic barrier of phospholipid bilayers. *Biochimica et Biophysica Acta (BBA) - Biomembranes, 1368*(2), 235-246.

Wisniewska, A., Widomska, J., & Subczynski, W. K. (2006). Carotenoid-membrane interactions in liposomes: effect of dipolar, monopolar, and nonpolar carotenoids. *Acta Biochim Pol, 53*(3), 475-484.

Wong, E. V. (2009). Cells: molecules and mechanisms: Axolotl Academic Publishing.

Woodbury, C. P. (2012). Biochemistry for the pharmaceutical sciences. Sudbury, MA: Jones & Bartlett Learning.

Xia, F., Hu, D., Jin, H., Zhao, Y., & Liang, J. (2012). Preparation of lutein proliposomes by supercritical anti-solvent technique. *Food Hydrocolloids, 26*(2), 456-463.

Xia, S., Tan, C., Zhang, Y., Abbas, S., Feng, B., Zhang, X., & Qin, F. (2015). Modulating effect of lipid bilayer–carotenoid interactions on the property of liposome encapsulation. *Colloids and Surfaces B: Biointerfaces, 128*, 172-180.

Xia, S., Xu, S., Zhang, X., & Zhong, F. (2007). Effect of coenzyme Q10 incorporation on the characteristics of nanoliposomes. *The Journal of Physical Chemistry B, 111*(9), 2200-2207.

Xie, L., Lee, S. G., Vance, T. M., Wang, Y., Kim, B., Lee, J.-Y., . . . Bolling, B. W. (2016). Bioavailability of anthocyanins and colonic polyphenol metabolites following consumption of aronia berry extract. *Food Chemistry, 211*, 860-868.

Xiong, S., Melton, L. D., Easteal, A. J., & Siew, D. (2006). Stability and antioxidant activity of black currant anthocyanins in solution and encapsulated in glucan gel. *Journal of Agricultural and Food Chemistry, 54*(17), 6201-6208.

Xiong, Y., Zhao, Y.-Y., Goruk, S., Oilund, K., Field, C. J., Jacobs, R. L., & Curtis, J. M. (2012). Validation of an LC–MS/MS method for the quantification of choline-related compounds and phospholipids in foods and tissues. *Journal of Chromatography B, 911*, 170-179.

Yaghmur, A., Azmi, I. D. M., Moghimi, S. M., & Helvig, S. (2015). Recent advances in cryo-TEM imaging of soft lipid nanoparticles. *AIMS Biophysics, 2*(2), 116-130.

Yang, Q., Guo, Y., Li, L., & Hui, S. W. (1997). Effects of lipid headgroup and packing stress on poly(ethylene glycol)-induced phospholipid vesicle aggregation and fusion. *Biophysical Journal, 73*(1), 277-282.

Yildiz, H. M., McKelvey, C. A., Marsac, P. J., & Carrier, R. L. (2015). Size selectivity of intestinal mucus to diffusing particulates is dependent on surface chemistry and exposure to lipids. *Journal of Drug Targeting, 23*(7-8), 768–774.

Yokota, D., Moraes, M., & Pinho, S. C. (2012). Characterization of lyophilized liposomes produced with non-purified soy lecithin: a case study of casein hydrolysate microencapsulation. *Brazilian Journal of Chemical Engineering, 29*, 325-335.

Yoshida, K., Mori, M., & Kondo, T. (2009). Blue flower color development by anthocyanins: from chemical structure to cell physiology. *Natural Product Reports, 26*(7), 884-915.

Yu, B., Lee, R. J., & Lee, L. J. (2009). Chapter 7 - Microfluidic methods for production of liposomes. *Methods in Enzymology* (Vol. Volume 465, pp. 129-141): Academic Press.

Zák, A., Zeman, M., Vítková, D., Hrabák, P., & Tvrzická, E. (1990). Beta-sitosterol in the treatment of hypercholesterolemia. *Casopis lekaru ceskych, 129*(42), 1320-1323.

Zhang, J. (2003). Self-assembled nanostructures (Vol. 2). Springer Science & Business Media.

Zhang, T., Lv, C., Chen, L., Bai, G., Zhao, G., & Xu, C. (2014). Encapsulation of anthocyanin molecules within a ferritin nanocage increases their stability and cell uptake efficiency. *Food Research International, 62*, 183-192.

Zhao, C., Cheng, H., Jiang, P., Yao, Y., & Han, J. (2014). Preparation of lutein-loaded particles for improving solubility and stability by Polyvinylpyrrolidone (PVP) as an emulsion-stabilizer. *Food Chemistry, 156*, 123-128.

Zhao, L., Xiong, H., Peng, H., Wang, Q., Han, D., Bai, C., . . . Deng, B. (2011). PEG-coated lyophilized proliposomes: preparation, characterizations and in vitro release evaluation of vitamin E. *European Food Research and Technology, 232*(4), 647-654.

Zhigaltsev, I. V., Maurer, N., Akhong, Q.-F., Leone, R., Leng, E., Wang, J., . . . Cullis, P. R. (2005). Liposome-encapsulated vincristine, vinblastine and vinorelbine: A comparative study of drug loading and retention. *Journal of Controlled Release, 104*(1), 103-111.

Zook, J. M., & Vreeland, W. N. (2010). Effects of temperature, acyl chain length, and flow-rate ratio on liposome formation and size in a microfluidic hydrodynamic focusing device. *Soft matter, 6*(6), 1352-1360.

Zuidam, N. J., Gouw, H. K. M. E., Barenholz, Y., & Crommelin, D. J. A. (1995). Physical (in) stability of liposomes upon chemical hydrolysis: the role of lysophospholipids and fatty acids. *Biochimica et Biophysica Acta (BBA) - Biomembranes, 1240*(1), 101-110.

Zvonar, A., Berginc, K., Kristl, A., & Gašperlin, M. (2010). Microencapsulation of self-microemulsifying system: Improving solubility and permeability of furosemide. *International Journal of Pharmaceutics, 388*(1–2), 151-158.